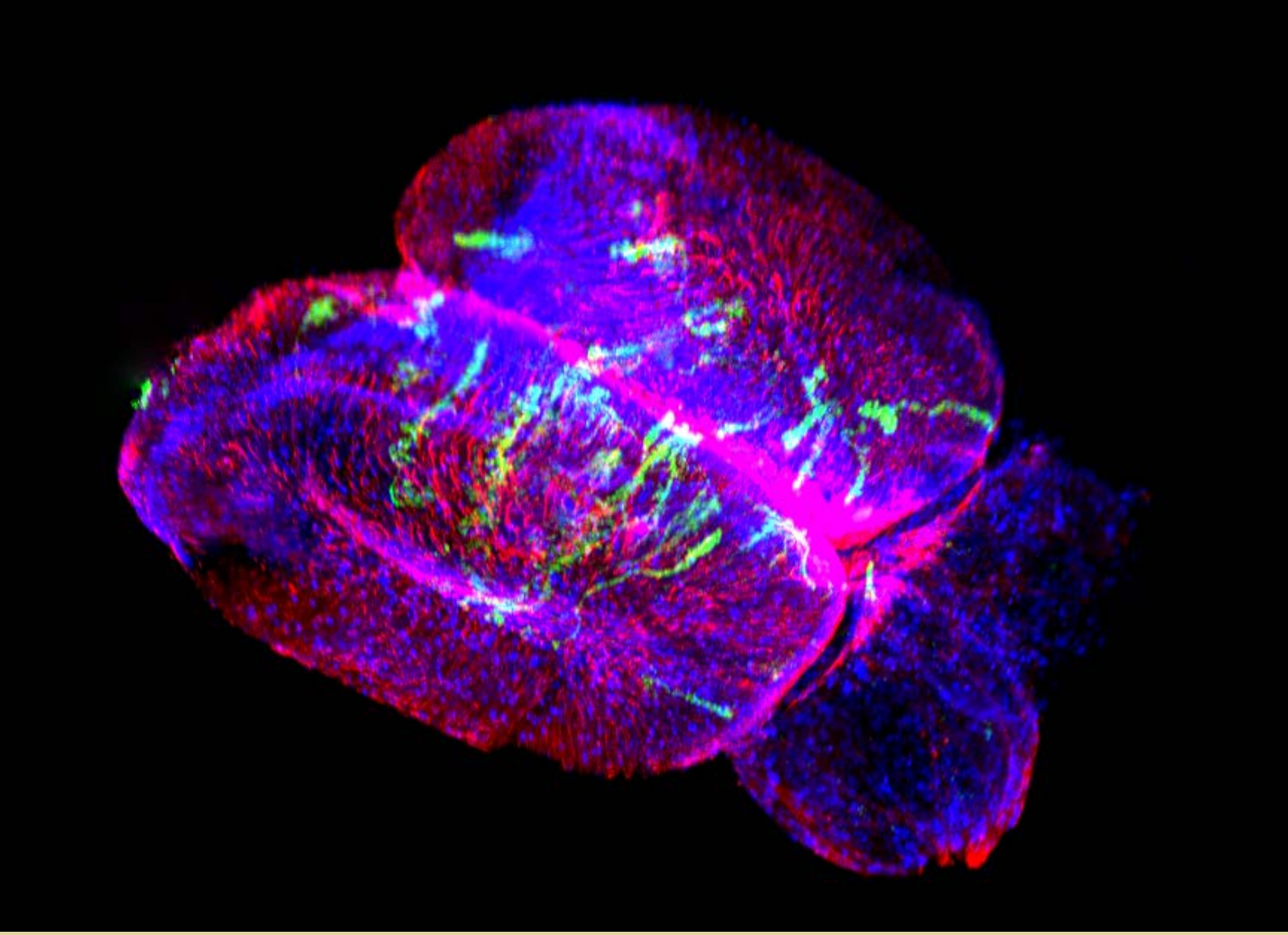

Joana Santos Barbosa

In vivo single cell analysis reveals distinct behavior of neural stem and progenitor cells in homeostasis and regeneration in the adult brain

Tese de Doutoramento em Ciências da Saúde (Pré-Bolonha), ramo de Ciências Biomédicas, orientada pelo Doutor João José Oliveira Malva da Faculdade de Medicina da Universidade de Coimbra e pela Professora Doutora Magdalena Götz do Helmholtz-Zentrum München (Munique, Alemanha) e entregue à Faculdade de Medicina da Universidade de Coimbra

Julho de 2014

· U C ·

Universidade de Coimbra

· U C · FMUC FACULDADE DE MEDICINA
UNIVERSIDADE DE COIMBRA

In vivo single cell analysis reveals distinct behavior of neural stem and progenitor cells in homeostasis and regeneration in the adult brain

Análise *in vivo* de células individuais revela o comportamento distinto das células estaminais e progenitoras neurais na homeostase e regeneração do cérebro adulto

Joana Santos Barbosa

Thesis submitted to the Faculty of Medicine of University of Coimbra, for fulfillment of the requirements for the doctoral degree in Health Sciences, subfield of Biomedical Sciences.

Tese apresentada à Faculdade de Medicina da Universidade de Coimbra, para prestação de provas de doutoramento em Ciências da Saúde, no ramo de Ciências Biomédicas.

Trabalho efectuado sob a orientação de

Doutor João José Oliveira Malva
Faculdade de Medicina | Universidade de Coimbra | Coimbra | Portugal

Professora Doutora Magdalena Götz
Institute of Stem Cell Research | Helmholtz Zentrum München | Munique | Alemanha
Institute of Physiology | Ludwig-Maximilians-Universität | Munique | Alemanha

Front cover image

Whole-mount staining of an adult zebrafish telencephalon electroporated with a Green Fluorescence Protein (GFP)-expressing plasmid to label individual Radial Glia cells. The brain is stained for DAPI (4',6' Diamidino-2-phenylindole) in blue, glial fibrillary acidic protein (GFAP, red) and GFP (green).

UNIVERSIDADE DE COIMBRA

Thesis presented to obtain the PhD degree in Health Sciences at the Faculty of Medicine, University of Coimbra. This work was carried out under the tutorage of the Center for Neuroscience and Cell Biology of Coimbra, in the context of the PhD program for Experimental Biology and Biomedicine (2008), under the supervision of Doctor João Malva. The practical work was performed under the supervision of Professor Doctor Magdalena Götz at the Institute of Stem Cell Research, Helmholtz Zentrum München. This work was supported by the doctoral grant SFRH / BD / 33469 / 2008 from Fundação para a Ciência e Tecnologia.

Tese apresentada para obtenção do grau de Doutoramento em Ciências da Saúde pela Faculdade de Medicina da Universidade de Coimbra. Este trabalho foi efectuado sob a tutela do Centro de Neurociências e Biologia Celular de Coimbra ao abrigo do Programa Doutoral de Biologia Experimental e Biomedicina (2008), sob supervisão do Doutor João Malva. O trabalho prático foi realizado sob a orientação da Professora Doutora Magdalena Götz, no Institute of Stem Cell Research, Helmholtz Zentrum München. Este trabalho foi financiado pela bolsa SFRH / BD / 33469 / 2008 da Fundação para a Ciência e Tecnologia.

Within the scope of the present PhD thesis, the following original articles have been published or submitted for publication in an international peer reviewed journal:

Appendix I

Baumgart, E.V., Barbosa, J.S., Bally-Cuif, L., Götz, M., and Ninkovic, J. (2012). Stab wound injury of the zebrafish telencephalon: a model for comparative analysis of reactive gliosis. Glia 60, 343-357.

Barbosa, J.S., Götz, M., and Ninkovic, J. *In vivo* single cell analysis reveals distinct behavior of neural stem and progenitor cells in homeostasis and regeneration in the adult brain. [Submitted to Science].

Acknowledgments

Without any question, this work was only accomplished with the precious help of many people, in many different ways. These years of PhD work in the Götz lab were essential for my education as a scientist and to develop many important skills that prepared me for future challenges in my career.

I am very grateful to my supervisors, Jovica Ninkovic and Magdalena Götz, for giving me the great opportunity to perform my PhD in this outstanding lab and to work on this very exciting and challenging project that made me overcome my limits and beliefs. It was a pleasure to work with such amazing scientists. Thank you very very much, Jovica, for the great supervision, for the endless time we spent discussing my project, for the close guidance and support, for sharing your knowledge and for keeping my motivation high with your enthusiasm. Without you, I would definitely not have made it and I am extremely grateful for that. I am also very grateful to you Magdalena for your useful ideas, suggestions and your constant, very inspiring optimism and love for science. Thank you also for creating a great scientific environment with outstanding scientists, a lot of knowledge exchange and the accessible state-of-the-art technologies, without which this work would not have been possible.

I would also like to acknowledge the help from the members of my thesis committee, João Malva and Laure Bally-Cuif, for the important comments and suggestions on my project, and especially to João for being my co-supervisor at the University of Coimbra.

I am also thankful to the PhD Program BEB for giving me the opportunity to do a PhD, and also the BEB colleagues for their companionship during the first year.

Thank you also to all members of the Götz lab and particularly those of the adult neurogenesis club, for active discussions and intelligent comments during my presentations. I would also like to thank specifically the “fish group”, Rossella and Rosario, for nice discussions and ideas.

I am also very thankful to the present and former technical assistants in the lab: Emily, Timo, Julia, Sarah, Angelika and Andrea, who always made sure everything in the lab ran smoothly and nothing was missing. A very special thank you to Emily, for all her patience and help in the beginning of my work, for sharing with me all the knowledge she has on zebrafish, and for the important contribution on my clonal analysis experiments. A particular thanks also to Timo for the maxi-preps and virus production, and to Julia and Sarah for help with immunostainings.

Very importantly, the years in this lab wouldn’t have been as pleasant if I hadn’t met fantastic people, who contributed to a warm working atmosphere, and always made me feel less lonely in this foreign country. Muito obrigada Elsinha pela tua ajuda preciosa desde o início até ao fim, pelas inúmeras conversas, imenso apoio e principalmente pela tua amizade, que eu espero manter para sempre. I’d also like to show my gratitude to other lab members, in particular Vidya, Lena, Franzi, Emily, Gregor, Timo, Tessa, Francesca, Silvia, Ruth, Rossella, Stefi, Pia and Judith, for the amazing happy occasions we enjoyed together during these years, especially outside the lab. Meeting you was really a pleasure and it really helped in my adaptation to Munich!

Apesar de não estarem em Munique, eu tenho de agradecer aos meus queridos amigos portugueses, que sempre me fizeram sentir acarinhada, e contribuíram para encurtar a distância que nos separa com emails, conversas no Skype e até visitas a Munique. Muito muito obrigada às minhas Marias de Biologia Aplicada, especialmente à minha mana do coração, Diana, que esteve sempre perto mesmo longe e foi incansável na ajuda que me prestou durante o doutoramento, em especial na fase final, e ao Hugo que também me ouviu sempre e motivou com as conversas de Skype. Obrigada também aos amigos de Nine: Patrícia, Diogo, Catarina, Neuza e Luísa por me apoiarem sempre e me fazerem sentir especial.

I am also very grateful that this adventure in Munich to perform my PhD also offered me an unexpected gift: love. Thank you, Philipp, for your love, patience, unconditional support and for making me feel happy all this time. Ich liebe dich!

Por fim, tenho de agradecer às pessoas mais importantes, não só deste doutoramento e início de carreira, mas da minha vida em geral: os meus pais. Muito obrigada pelo vosso apoio constante, por acreditarem em mim e tudo fazerem para eu poder concretizar os meus objectivos. Sem a vossa inspiração, espírito de sacrifício e apoio incondicional eu não teria chegado até aqui. Obrigada também ao meu irmão e aos restantes membros da minha família, Santos e Barbosas, sei que estiveram sempre a torcer por mim.

Abstract

During embryonic neural development, Radial Glia (RG) cells act as Neural Stem Cells (NSCs), generating neurons and glial cells that constitute the central nervous system. Interestingly, neurogenesis and gliogenesis in the adult brain are also mediated by NSCs with RG characteristics. Despite the increasing interest in adult NSCs and their putative application in regenerative therapies, the cellular behavior of adult NSCs underlying the live-long neurogenesis in the vertebrate brain has never been observed *in vivo*. In the present work, due to its widespread adult neurogenesis, tremendous regenerative capacity and feasibility for *in vivo* imaging, zebrafish (*Danio rerio*) was used as a model organism to investigate NSC behavior during constitutive neurogenesis and regeneration. Additionally, the distinct contribution of the ventricular zone (VZ) progenitor types (RG and non-glial progenitors) to regeneration was dissected.

In a first set of experiments, I demonstrated that a subset of non-glial progenitors (the neuroblasts) does not change its proliferation status after injury in the telencephalon. However, differential labeling of RG cells and non-glial progenitors by transfection and retroviral transduction, respectively, revealed that the non-glial progenitors react quickly after injury by generating progeny that migrates from the VZ and contributes with new neurons to the regenerating telencephalon.

To investigate the behavior of NSCs, I developed an *in vivo* imaging technique, that allowed the continuous monitoring of NSCs over time in their natural niche. The observation of NSCs in the adult zebrafish telencephalon revealed that during homeostasis they are essentially quiescent and only a small subset is enrolled in neurogenesis. This subset was composed of either dividing cells or cells undergoing direct conversion into neurons without proliferation (direct neurogenesis). Dividing NSCs in the intact brain always self-renewed, dividing either symmetrically to generate two RG-like NSCs (symmetric gliogenic division) or asymmetrically, giving rise to a NSC and a non-glial cell, that presumably further generates neurons.

After injury, the proportion of dividing NSCs increased and there was a shift in the mode of cell division, with the occurrence of terminal differentiating, symmetric non-gliogenic divisions and an absence of symmetric gliogenic divisions. The terminal differentiating type of division leads to a net increase in the production of non-glial cells, important to reconstitute this progenitor cell population that is lost by migration after injury. Interestingly, the occurrence of direct neurogenesis events after injury was very rare.

In conclusion, this work revealed for the first time the *in vivo* behavior of neural stem/progenitor cells in the adult vertebrate brain and how it changes after injury. The results obtained herein highlight the role of non-glial progenitors in reconstituting the injury site with newborn neurons, and the role of NSCs in re-establishing the progenitor zone. Additionally, the *in vivo* imaging technology developed in this thesis may be a valuable tool to further investigate mechanisms controlling the behavior of NSCs in the healthy and injured adult vertebrate brain.

Resumo

Durante o desenvolvimento neural embrionário, as células da Glia Radial (GR) atuam como Células Estaminais Neurais (CENs), dando origem aos neurónios e células da glia que constituem o sistema nervoso central. Curiosamente, a neurogénese e a gliogénese no cérebro adulto também são mediadas por células com características da GR. Apesar do elevado interesse em CENs e da sua possível aplicação em terapias regenerativas, o comportamento celular das CENs adultas, que está na base da neurogénese adulta contínua em organismos vertebrados, nunca foi observado *in vivo*. No presente trabalho, devido à sua neurogénese adulta difundida por várias regiões do cérebro, à tremenda capacidade regenerativa e à facilidade para *imaging in vivo*, o peixe-zebra (*Danio rerio*) foi usado como modelo para investigar o comportamento de células estaminais/progenitoras neurais durante a neurogénese constitutiva e a regeneração. Adicionalmente, a contribuição dos diferentes tipos de progenitores da zona ventricular (ZV) (GR e progenitors não-gliais) no processo de regeneração foi distinguida.

Num primeiro conjunto de experiências, eu observei que um sub-tipo de progenitores não-gliais (os neuroblastos) não altera a sua proliferação após lesão do telencéfalo. No entanto, a marcação diferencial de GR e progenitores não-gliais através de transfecção ou transdução com retrovirus, respetivamente, revelou que os progenitores não-gliais respondem rapidamente após a lesão, dando origem a descendência que migra da ZV e contribui com novos neurónios para a regeneração do telencéfalo.

Para investigar o comportamento das CENs, eu desenvolvi uma nova técnica de *imaging in vivo*, que permitiu a monotorização contínua de CENs ao longo do tempo no seu nicho natural. A observação de CENs no telencéfalo adulto de peixe-zebra revelou que, em condições homeostáticas, estas células são essencialmente quiescentes, e só uma pequena subpopulação está envolvida na neurogénese. Esta subpopulação é composta por células que se dividem ou células que se convertem diretamente em neurónio sem proliferação (neurogénese direta). As CENs que se dividem no cérebro intacto renovam-se sempre em cada divisão, quer de forma simétrica dando origem a duas CENs com características de GR (divisão simétrica gliogénica), quer de forma assimétrica, dando origem a uma GR e a uma célula não-glial, que presumivelmente originará neurónios.

Após lesão a proporção de CENs que se divide aumenta e parece haver uma alteração no modo de divisão das células, com a ocorrência de divisões diferenciativas terminais (divisão simétrica não-gliogénica) e a ausência de divisões simétricas gliogénicas. As divisões

diferenciativas terminais levam a um aumento da produção bruta de células não-gliais, importante para reconstitutir esta população de progenitores que desaparece com a migração após lesão. Curiosamente, a ocorrência de eventos de neurogénese direta é muito rara após lesão.

Em conclusão, este trabalho revelou pela primeira vez o comportamento *in vivo* de células estaminais/progenitores neurais no cérebro adulto de um organismo vertebrado e como este comportamento se altera após lesão. Os resultados obtidos no presente trabalho realçam o papel dos progenitores não-neurais na reconstituição do local da lesão com novos neurónios, e o papel das CENs no restabelecimento da zona de progenitores. Adicionalmente, a técnica de *imaging in vivo* desenvolvida nesta tese pode ser uma ferramenta valiosa para investigar mecanismos que controlam o comportamento de CENs no cérebro saudável e lesionado de organismos vertebrados adultos.

Contents

Abbreviations

2pLSM	2photon Laser Scanning Microscopy
%	percent
°C	degrees Celsius
µ	micro
ACSF	Artificial Cerebrospinal Fluid
aPKC	atypical Protein Kinase C
BABB	Benzyl Alcohol/ Benzyl Benzoate
BBB	Blood brain barrier
BLBP	Brain Lipid-Binding Protein
BrdU	Bromo-deoxy-uridine
CMV	Cytomegalovirus
CNS	Central Nervous System
CSF	Cerebrospinal Fluid
CXCR4/5	C-X-C Chemokine Receptor Type 4/5
Cystlr1	Cysteinyl Leukotriene Receptor 1
DAPI	4',6' Diamidino-2-phenylindole
DEL	Dorsal Ependymal Lining
DG	Dentate Gyrus
DMEM	Dulbecco's Modified Eagle Medium
DMSO	Dimethyl Sulfoxide
DNA	Deoxyribonucleic Acid
dpi	Days post-injury
dpl	Days post-labeling
ECM	Extracellular Matrix
EDTA	Ethylenediaminetetraacetic Acid
EF1α	Elongation Factor-1α
e.g.	exempli gratia
FCS	Fetal Calf Serum
FGF	Fibroblast Growth Factor
g	Gram(s)
g	Gravitational Acceleration
GABA	γ-aminobutyric acid

GAD	Glutamic Acid Decarboxylase
GCL	Granule Cell Layer
GFAP	Glial Fibrillary Acidic Protein
GFP	Green Fluorescent Protein
GLAST	Glutamate-Aspartate Transporter
h	Hour(s)
hpf	Hours post-fertilization
i.e.	id est
IHC	Immunohistochemistry
l	Liter
LB	Lysogeny Broth
LSM	Laser Scanning Microscopy
LTC4	Leukotriene C4
m	Meter
M	Molar
Mash1	Mammalian Achaete Scute Homolog
min	Minute
ML	Molecular Layer
ms	mili-second
n	Nano
N	Normality
NDS	Normal Donkey Serum
NE	Neuroepithelial
NSC	Neural Stem Cell
OB	Olfactory Bulb
OPC	Oligodendrocyte Progenitor Cell
Par3	Partitioning defective 3 Homolog
Pax6	Paired BoX gene 6
PBS	Phosphate Buffered Saline
PCNA	Proliferating Cell Nuclear Antigen
PCR	Polymerase Chain Reaction
PFA	Paraformaldehyde
Prox1	Prospero homeobox protein 1

PSA-NCAM	Polysialic Acid-Neural Cell Adhesion Molecule
RFP	Red Fluorescent Protein
RG	Radial Glia
RMS	Rostral Migratory Stream
RT	Room Temperature
s	Second
S100β	β-subunit of S100 protein
SAP	Sub-Apical Progenitor
Sdf1α	Stromal-Derived Factor 1α
SEM	Standard Error of the Mean
SGZ	Sub-Granular Zone
SHH	Sonic Hedgehog
Sox2	SRY (sex determining region Y)-box 2
SVZ	Sub-Ventricular Zone
TAE	TRIS acetate EDTA
TAP	Transit Amplifying Cell
Tbr 1/2	T-box brain protein 1/2
TH	Tyrosine Hydroxylase
TRIS	Tris-(hydroxymethyl)-aminomethane
V	Volts
VSV-g	Vesicular Stomatitis Virus Glycoprotein
VZ	Ventricular Zone
ZO-1	Zonula Occludens 1

1 Introduction

Neural stem cells (NSCs) are self-renewing and multipotent cells in the nervous system that, directly or indirectly (via intermediate progenitor states), generate neurons, astrocytes and oligodendrocytes (Weiner, 2008). The process by which these cells give rise to neurons is called neurogenesis. For many years, neurogenesis was thought to be restricted to the animals' developmental and perinatal period, but in the 1960s, Altman provided the first evidence that neurogenesis also exists in the post natal brain of rats and cats (Altman, 1963; Altman, 1969b; Altman and Das, 1965b).

The discovery of neurogenesis in adult brains, including humans (Eriksson et al., 1998), raised the hope of applying the adult NSCs as potential therapy for brain pathologies (Aboody et al., 2011). Therefore, revealing the basic biology of adult NSCs is a major step towards their application in regenerative therapies. In this regard, the main topic to be addressed in this thesis is the investigation of the cellular behavior of adult NSCs at the single cell level in the intact brain (homeostasis) and after injury (regeneration) in zebrafish (*Danio rerio*).

1.1 Adult neural stem cells and neurogenesis

The existence of adult neurogenesis has been described in many different species, being conserved in insects (Cayre, 1994; Fernández-Hernández et al., 2013), non-mammalian vertebrates (Adolf et al., 2006; Birse et al., 1980; Goldman and Nottebohm, 1983; Grandel et al., 2006; López-Garcia, 1984; Simmons et al., 2008; Zupanc and Zupanc, 1992) and nearly all mammals analyzed so far, including primates and humans (Barker et al., 2011; Eriksson et al., 1998; Ernst et al., 2014; Gould et al., 1998; Kornack and Rakic, 1999; Spalding et al., 2013) (Figure 1.1).

A common characteristic of adult NSCs in different animal species studied is their similarity to the neuroepithelial (NE) and radial glial (RG) cells, the NSCs during brain development (reviewed in (Kriegstein and Alvarez-Buylla, 2009)). NE cells exhibit true epithelial characteristics, such as apical-basal polarity, connection to neighboring cells via adherens and tight junctions at the most apical end of their lateral plasma membrane (Aaku-Saraste et al., 1996; Chenn et al., 1998; Götz and Huttner, 2005; Manabe et al., 2002; Weigmann et al., 1997) and attachment to the basement membrane via integrins (Haubst et al., 2006; Hirsch et al., 1994). Additionally, NE cells express the intermediate filament nestin and the transcription factor SRY (sex determining region Y)-box 2 (known as Sox2) (Dimou and Götz, 2014; Götz and Huttner, 2005). As neurogenesis starts, NE cells loose some of their

epithelial hallmarks and concurrently acquire features of astroglial cells, such as the expression of brain lipid-binding protein (BLBP), vimentin, glial fibrillary acidic protein (GFAP) and Glutamate-aspartate transporter (GLAST) (Aaku-Saraste et al., 1996; Aaku-Saraste et al., 1997; Feng et al., 1994; Götz and Huttner, 2005; Hartfuss et al., 2001; Shibata et al., 1997). This distinct, but related cell type, comprising both epithelial and astrocytic hallmarks, is the RG cell. Characteristics of NE inherited by RG are the expression of Sox2 and nestin (Hartfuss et al., 2001), the maintenance of an apical-basal polarity (Aaku-Saraste et al., 1996; Chenn et al., 1998; Weigmann et al., 1997) and their role as NSC (Malatesta et al., 2000; Noctor et al., 2001).

Like embryonic NSCs, most adult NSCs in different organisms express proteins such as Prominin1, BLBP, nestin, vimentin, GFAP, and Sox2 (Beckervordersandforth et al., 2010; Chapouton et al., 2006; Dimou and Götz, 2014; Doetsch et al., 1997; Ganz et al., 2010; Gubert et al., 2009; Jászai, 2013; Lam et al., 2009; März et al., 2010a; Pellegrini et al., 2007; Shen et al., 2008). Additionally, they also possess a radial process and have epithelial characteristics (Alvarez-Buylla et al., 1990; Berg et al., 2010; García Verdugo, 1981; Grupp et al., 2010; Mirzadeh et al., 2008; Stensaas and Stensaas, 1968).

During evolution, the sites of persistence of these RG-like NSCs in the adult brain became more and more restricted, for instance, fishes have several constitutive neurogenic sites widespread along the rostro-caudal axis (Adolf et al., 2006; Grandel et al., 2006; Zupanc, 1999), whereas rodents have only three accepted neurogenic niches: the sub-ventricular zone (SVZ) of the lateral ventricles, the sub-granular zone (SGZ) of the hippocampus and the hypothalamus (Altman, 1969a; Altman and Das, 1965a; Kaplan and Bell, 1984; Lois and Alvarez-Buylla, 1994; Robins et al., 2013). Surprisingly, from the mammalian species analyzed so far, only the bats seem to lack neurogenesis in the hippocampus (Amrein et al., 2007). Interestingly, the abundance of RG-like adult NSCs niches also seems to correlate with the capacity for a species to regenerate the central nervous system (CNS) after an insult (reviewed in (Grandel and Brand, 2013) and see section 1.2).

In the sections below, NSCs and adult neurogenesis are described and compared in more detail in the better characterized rodent model and in zebrafish, the animal model used in the present work.

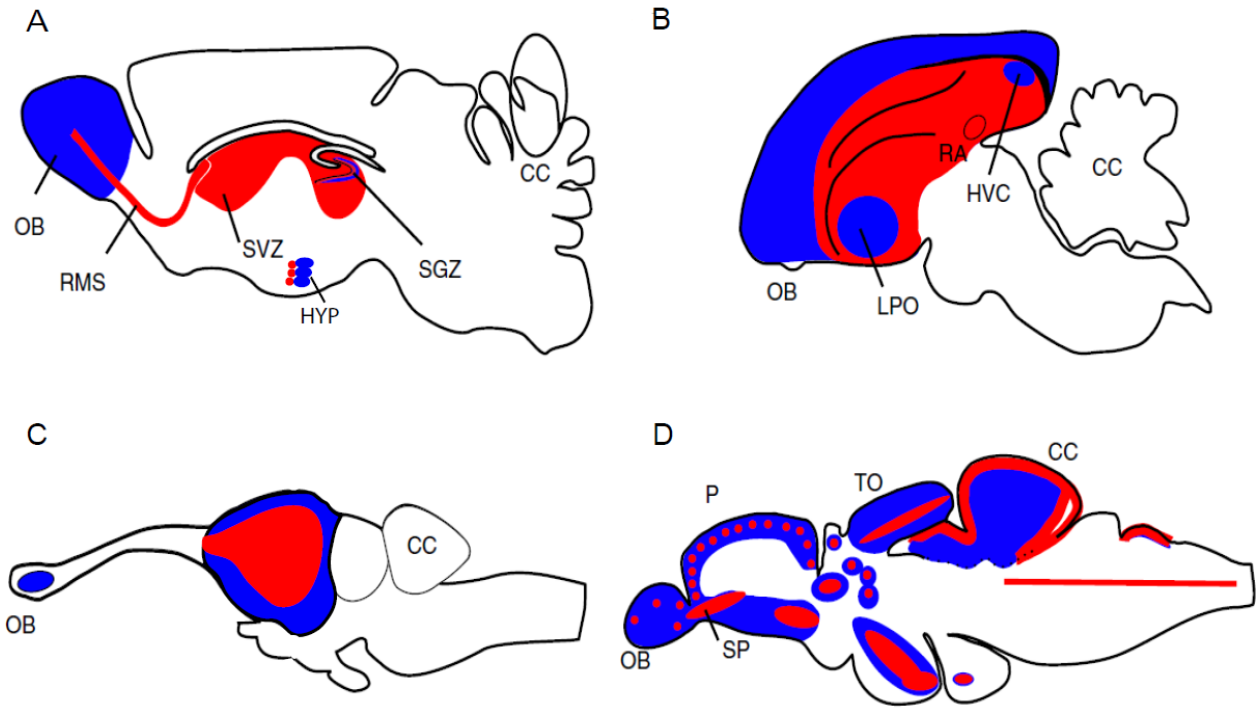

Figure 1.1: Adult neurogenesis is a conserved feature in vertebrates and became more restricted spatially during evolution. Sagittal brain sections representing the sites of constitutive proliferation (red) and neurogenesis (blue) in the brains of adult mice (A), canaries (B), lizards (C) and zebrafish (D). Abbreviations: CC-corpus cerebelli, HVC-high vocal center (nucleus engaged in song learning and production), HYP-hypothalamus, LPO-lobus parolfactorius, OB-olfactory bulb, P-pallium (dorsal telencephalon), RA-robust nucleus of the archistriatum, RMS-rostral migratory stream, SGZ-sub-granular zone, SP-subpallium (ventral telencephalon), SVZ-sub-ventricular zone, TO-optic tectum. Modified from (Grandel and Brand, 2013).

1.1.1 Adult neural stem cells and neurogenesis in rodents

As mentioned above adult neurogenesis occurs in three restricted brain regions in rodents: the SVZ of the lateral ventricles, the SGZ in the hippocampus and the hypothalamus (Altman, 1969b; Altman and Das, 1965c; Kaplan and Bell, 1984; Lois and Alvarez-Buylla, 1994; Robins et al., 2013).

The SVZ is composed of several cell types belonging to the neurogenic lineage: the adult NSCs (or type B cells), the transit amplifying progenitors (TAPs, or type C cells) and the neuroblasts (or type A cells) (Doetsch et al., 1997; Mirzadeh et al., 2008) (Figure 1.2). Additionally, different cell types not directly belonging to the neurogenic lineage co-exist in this niche: ependymal cells, endothelial cells and astrocytes (Beckervordersandforth et al., 2010; Doetsch et al., 1997; Miller and Gauthier-Fisher, 2009; Shen et al., 2008; Tavazoie et al., 2008)

Ependymal cells are multi-ciliated, cuboidal cells that form a single cell layer lining the ventricle, with tight junctions between cells (Mirzadeh et al., 2008). This epithelium controls the exchange of molecules between the cerebrospinal fluid (CSF) and the brain tissue

(reviewed in (Del Bigio, 1995)). Under normal physiological conditions, these cells are quiescent *in vivo* (Carlen et al., 2009; Spassky et al., 2005). The beating activity of the motile cilia was shown to regulate the flow of the CSF and to contribute to the migration of neuroblasts to the Olfactory Bulb (OB), by the creation of gradients of guidance molecules (Sawamoto et al., 2006). Moreover, the ependymal organization and niche structure were shown to be important for control of neurogenesis (Paez-Gonzalez et al.).

In the SVZ niche, the adult NSCs with somata located below the ependymal layer, contact the lateral ventricle through an apical process that extends through the ependymal cell layer and contains a Promini1-positive primary cilium at its extremity (Figure 1.2B). The structure at the ventricle, formed by the apical membrane of the adult NSC that contains the cilium, surrounded by a rosette of ependymal cells is called “pin-wheel” (Mirzadeh et al., 2008). On the basal side, adult NSCs contact the basement membrane surrounding the neighboring blood vessels (Shen et al., 2008; Tavazoie et al., 2008).

Adult NSCs divide slowly (Doetsch et al., 1999; Doetsch et al., 1997) and give rise to TAPs that are fast cycling intermediate progenitors that amplify the neuronal output of a single stem cell (Doetsch et al., 1997). TAPs further differentiate into doublecortin- and Polysialic Acid-Neural Cell Adhesion Molecule (PSA-NCAM)-positive neuroblasts, which also proliferate and migrate tangentially in chains towards the OB, where they differentiate into neurons (Coskun and Luskin, 2002; Lois and Alvarez-Buylla, 1994) (Figure 1.2C). These rostrally migratory chains of cells are referred to as Rostral Migratory Stream (RMS) and are ensheathed by astrocytes (Lois et al., 1996; Peretto et al., 1997). Notably, blood vessels running parallel in the RMS serve as scaffold to the moving neuroblasts (Bovetti, 2007). The new neurons added to the adult OB are important to odor learning and/or discrimination, and their survival is affected by exposure to olfactory learning tasks (reviewed in (Lazarini and Lledo, 2011)). Throughout this thesis, this complete neurogenic system, composed of the proliferative zone (SVZ), the neuroblast migratory behavior (in the RMS) and the neuron deposition and differentiation (at the OB) is named SVZ/RMS/OB system.

In addition to producing neurons, adult NSCs from the SVZ were also shown to generate oligodendrocytic cells that migrate to the corpus callosum (Jackson et al., 2006; Menn et al., 2006).

Several studies have demonstrated that the adult SVZ is regionally specified along the dorso-ventral, rostro-caudal axis, with progenitors from different areas giving rise to distinct sub-types of OB neurons (Brill et al., 2009; De Marchis et al., 2007; Merkle et al., 2007; Young et al., 2007).

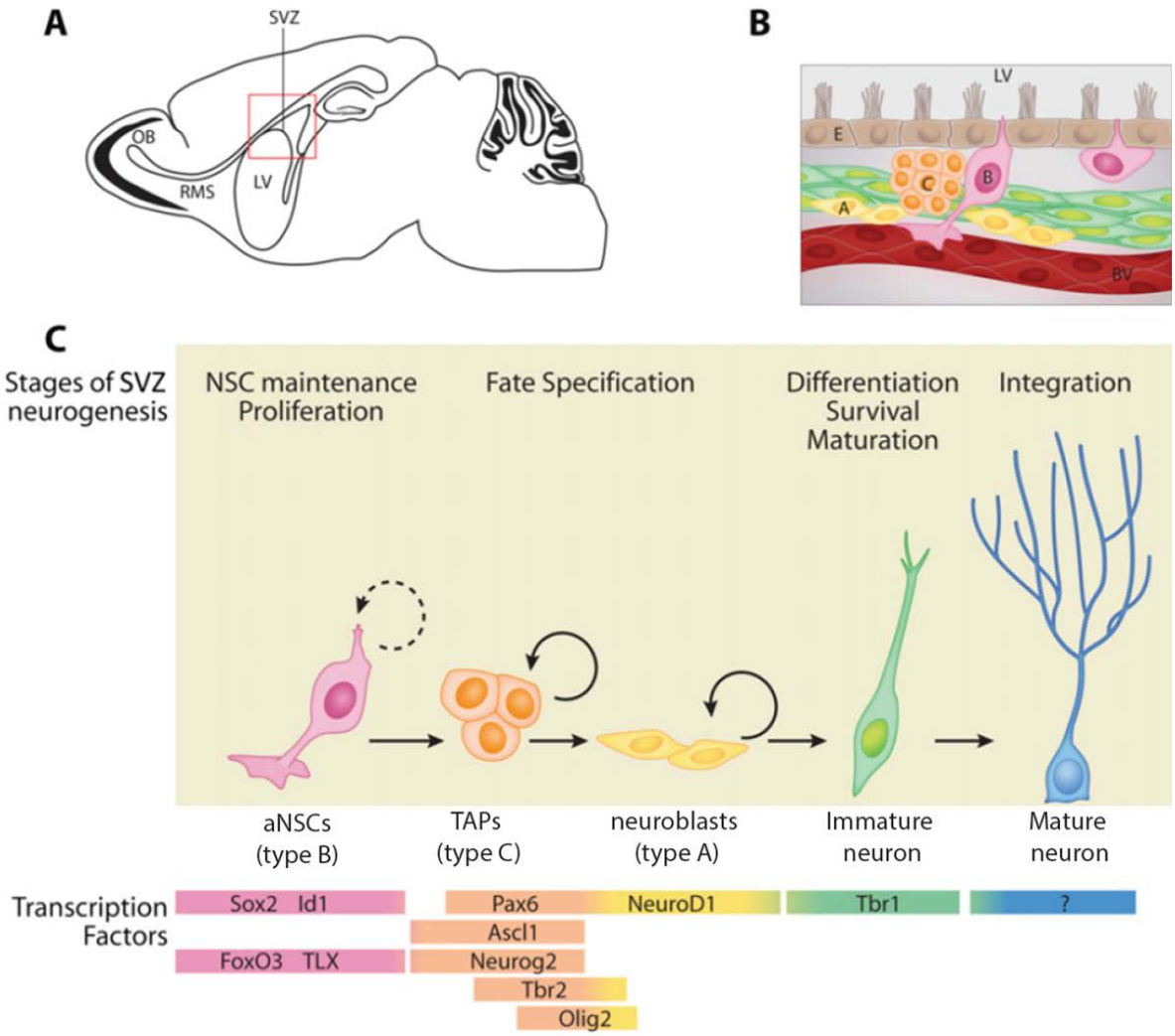

Figure 1.2: Adult neurogenesis in the SVZ/RMS/OB system. (A) Sagittal view of the adult rodent brain, with the red box outlining the SVZ region next to the lateral ventricle (LV). (B) Schematic of the SVZ with ependymal cells (E), blood vessel cells (BV), and distinct stem/progenitor cell types (types B, C, and A). (C) In the SVZ niche, type B adult NSCs (pink) generate type C TAPs (orange) that divide fast and amplify the progeny from single NSCs. TAPs give rise to type A neuroblasts (yellow), that migrate via the RMS to the OB where they differentiate into immature neurons (green), and later integrate in the circuit (mature neurons (blue)). Bellow each cell type is presented the specific expression of some transcription factors important to control the different steps of lineage progression (bottom colored panels). Adapted from (Hsieh, 2012).

Despite the vast knowledge on the SVZ/RMS/OB neurogenic system, the behavior of single adult NSCs at the SVZ has not been assessed *in vivo.* A question that remains to be answered is whether there is multipotency at the single cell level, or instead there are several populations of progenitor cells with restricted potency. Insights from population analysis suggest that after an initial division of adult NSCs, TAPs divide approximately 3 times and a lower degree of amplification (1-2 divisions) occurs at the neuroblasts level (Ponti et al., 2013). Remarkably, this data is supported by *in vitro* imaging of adult NSCs in a primary culture system (Costa et al., 2011). Other evidences from the same *in vitro* culture system revealed that oligodendrogenic and neurogenic lineages are independent, with the same adult

NSCs never generating the two differentiated cell types (Ortega, 2013). Nevertheless, clonal analysis and imaging *in vivo* are still lacking to clarify the exact lineage generated from single adult NSCs in their niche.

Neurogenesis in the SVZ/OB system has been shown to decline with age (Enwere et al., 2004; Maslov et al., 2004; Shook et al., 2012; Tropepe et al., 1997). Interestingly, a recent study revealed that the total number of NSCs per area is reduced with age, but the number of mitotically active adult NSCs is maintained in old mice (Shook et al., 2012), suggesting that the decreased production of neurons might be due to changes at the TAP and neuroblast levels.

In contrast to the adult NSCs in the SVZ, stem cells in the SGZ of the hippocampal dentate gyrus (DG) are not in contact with the ventricle (Figure 1.3A). Two different populations constitute the adult NSCs in this region: one with a radial process penetrating through the granule cell layer (GCL) and branching in the molecular layer (ML) (Type 1 radial astrocytes), and another with branched processes, parallel to the SGZ (Type 1 horizontal astrocytes) (Lugert et al., 2010; Seri et al., 2004; Seri, 2001). Even though both populations have in common the expression of several astroglial/RG markers, like GFAP, vimentin, nestin, BLBP or Sox2, they seem to differ in the mitotic activity and in the response to different stimuli (Lugert et al., 2010).

Type 1 cells give rise to Type2a cells that lose or down-regulate the expression of glial/RG markers but express Sox2 and mammalian achaete-scute homolog-1 (Mash1) (Seri, 2001; Suh et al., 2007). Type 2a cells divide once, originating type 2b cells, which start expressing T-box brain protein 2 (Tbr2) and doublecortin (Lugert et al., 2012) and undergo multiple rounds of divisions, acting as the main transit amplifying progenitor population of the DG. Type 2b cells give rise to type3 cells (neuroblasts), that can further divide and acquire granule cell identity, gradually maturating and integrating in the hippocampal circuitry (Figure 1.3C) (Lugert et al., 2012). Different from the SVZ/RMS/OB system, in which γ-aminobutyric acid (GABA)ergic, dopaminergic and glutamatergic neurons are generated (Batista-Brito et al., 2008; Brill et al., 2009; Lledo et al., 2008; Young et al., 2007), neurons formed in the SGZ have a glutamatergic identity and the progeny of NSCs does not migrate far from the mother cells. The adult NSCs in the DG (type 1 cells) do not generate oligodendrocytes (Bonaguidi et al., 2011), which seem to be generated in this region by neural/glial antigen 2 (NG2)-positive progenitors (Kang et al., 2010).

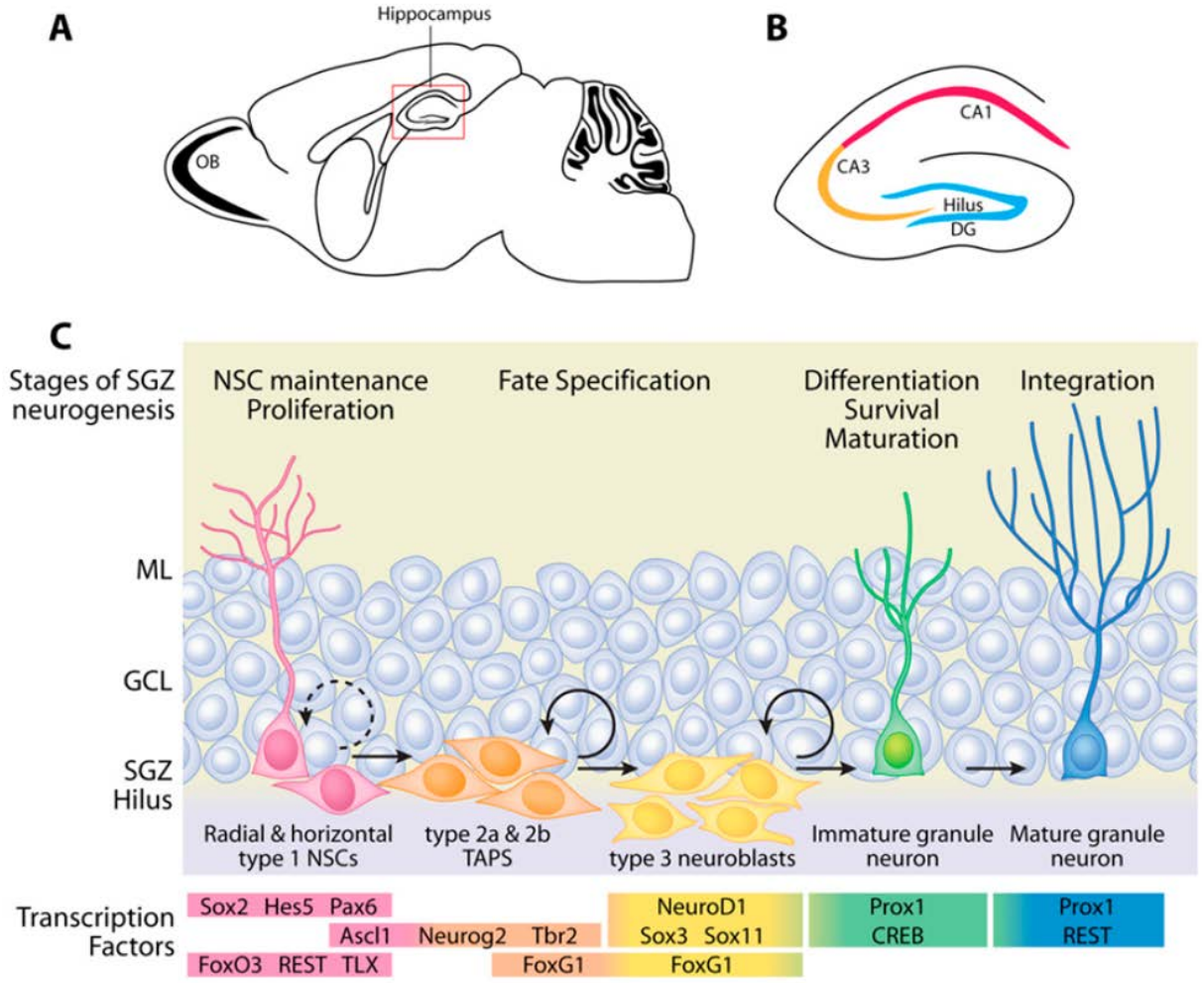

Figure 1.3: Adult neurogenesis in the SGZ of the DG. (A) Sagittal view of the adult rodent brain with the boxed region outlining the hippocampus. (B) Schematic of the hippocampus with the CA1, CA3, dentate gyrus (DG), and hilus regions. Adult newborn granule neurons are formed in the DG. (C) The SGZ niche is constituted of radial and horizontal type 1 NSCs (pink), type 2 TAPs (orange), type 3 neuroblasts (yellow), immature granule neurons (green), and mature granule neurons (blue). The progression from type 1 NSCs to mature granule neurons in adult SGZ is controlled by the sequential expression of transcription factors (bottom colored panels). Abbreviations: GCL-granule cell layer; ML-molecular layer; SGZ-sub-granular zone. Adapted from (Hsieh, 2012).

The reduced migration of the NSC progeny in the hippocampus has allowed the investigation of the progeny of single adult NSCs by clonal analysis (Bonaguidi et al., 2011; Encinas et al., 2011). Type 1 cells seem to undergo different types of self-renewal divisions (symmetric, generating two Type 1 cells, or asymmetric, generating one Type 1 and differentiated cell types), and some of them were shown to be bi-potent, giving rise to both neurons and astrocytes (Bonaguidi et al., 2011; Suh et al., 2007). Interestingly, the self-renewal capacity seems to be limited to few divisions, and upon the last division the NSC terminally differentiates into an astrocyte (Encinas et al., 2011). With aging, due to these terminal differentiation events, the number of adult NSCs diminishes, which results in a decrease of neurogenesis.

Neurogenesis in the hippocampus has been shown to be important for learning and memory, and to respond to external stimuli, like physical exercise or complex environments (reviewed in (Deng, 2010)).

In the other, less characterized, neurogenic niche in the adult mouse brain, the hypothalamus, RG-like cells (referred to as tanycytes) line the third ventricle and were recently shown to generate glial cells and neurons *in vivo* in physiological conditions (Robins et al., 2013). Tanycytes seem to differ regarding their dorso-ventral position and the expression of some proteins: β-tanycytes are located ventrally and express fibroblast growth factor 10 (FGF10) but not GFAP or GLAST, whereas α-tanycytes are more dorsally located, express GFAP and GLAST but lack FGF10 (Haan, 2013; Robins et al., 2013). While β-tanycytes generate neurons within the first two-postnatal months and upon high-fat diet (Haan, 2013), α-tanycytes generate few neurons and glia in normal adult animals (Robins et al., 2013). Very importantly, only the later sub-population shows NCS properties *in vitro* (Robins et al., 2013). Even though hypothalamic neurogenesis is rather low, it can be activated by metabolic stimuli (Haan, 2013; Lee et al., 2012; Pierce, 2010).

In spite of the insights obtained with clonal analysis in the hippocampus and *in vitro* imaging of SVZ-derived cells, the single cell potency and behavior of adult NSCs in their niche is still not completely understood, and the field would greatly benefit from the establishment of *in vivo* imaging techniques in mammals that allow the visualization of adult NSCs behavior.

1.1.2 Adult neural stem cells and neurogenesis in zebrafish

In contrast to mammals, fish, amphibian and reptiles have many more proliferative/neurogenic areas in adult brains (Figure 1.1). Studying these animals with widespread adult neurogenesis may reveal important features of the biology and niche of adult NSCs, that could provide clues for the existence of restricted neurogenic sites in mammals and help improving adult neurogenesis in these species. Teleost fishes, a taxonomic group to which the zebrafish belongs, are amongst the species with the most widespread adult neurogenesis (Kaslin et al., 2008). In addition to the widespread adult neurogenesis, the many advantages of using zebrafish as a model organism (such as its good characterization and the availability of genetic tools) contributed to the choice of using this species as the model to pursue this study.

Adult neurogenesis in zebrafish takes place in all the brain sub-divisions along the rostro-caudal axis (Adolf et al., 2006; Grandel et al., 2006). This increased neurogenesis in

fish allows the continuous brain growth throughout life, and may be associated with the life-long growth of the body and input from sensory organs (Brandstätter and Kotrschal, 1990; Marcus et al., 1999). Despite the generalized existence of neurogenic zones, there are some differences between the various niches, namely with respect to the identity of the stem cells and the fate of the progeny.

In the zebrafish optic tectum and cerebellum, adult NSCs seem to be NE-like, as they bear apical-basal polarity and adherens junctions, but don't express glial hallmarks. In these regions, RG-like cells exist but do not proliferate and may serve as a scaffold for newborn neuron migration (Ito et al., 2010; Kaslin et al., 2009).

Another neurogenic site is located in the boundary between the midbrain and the hindbrain. In this region, *her5:*GFP-positive cells located at the ventricle seem to fulfill several hallmarks of adult NSCs: slow cycle, expression of GFAP, BLBP and Sox2, and capability of generating both neurons and glia (Chapouton et al., 2006).

The neurogenic niches of the adult zebrafish telencephalon are amongst the better characterized adult NSC niches in zebrafish (Adolf et al., 2006; Ganz et al., 2010; Grandel et al., 2006; März et al., 2010a; Pellegrini et al., 2007). Due to the homology of this brain area with the telencephalon in mammals (the only brain sub-division in which adult neurogenesis occurs in this Class), studying this region is of particular interest from a comparative point of view. On one hand, like in rodents, there is addition of new neurons to the OB and the region equivalent to the hippocampus; on the other hand there are additional neurogenic zones in the zebrafish telencephalon that are not present in rodents: the dorsal telencephalon proper and the ventral telencephalon (homologous to the striatum) (Mueller and Wullimann, 2009; Wullimann and Rink, 2002). Studying these new regions is important because it can reveal specific mechanisms of stem cell behavior and regulation not present in mammals. Moreover, several areas of the telencephalon in humans are affected by neurological diseases (eg. striatum, hippocampus), and the knowledge on stem cell activity obtained from studying the highly neurogenic- and regeneration-competent zebrafish might be of help in the search for a cure of such pathologies.

1.1.2.1 Constitutive neurogenesis in the adult zebrafish telencephalon

As the zebrafish telencephalon develops by evagination, the ventricular zone (VZ) is located not only internally but also at the outer surface of the telencephalon, below the brain pia (Northcutt and Braford, 1980), contrasting with its position in rodents (Figure 1.4A). In the adult zebrafish telencephalon there is no ependymal cell layer separating the zone of

proliferation from the ventricular lumen, so the adult NSCs are directly lining the ventricle. However, a dorsal ependymal lining (DEL) exists, covering the entire rostro-caudal aspect of the dorsal telencephalon, bridging the two hemispheres dorsally. The DEL is composed of a single cell layer of classical ependymal cells with cuboidal shape and several cilia projecting to the ventricular lumen (Lindsey et al., 2012).

In the telencephalon two proliferative zones can be distinguished: the dorsal/pallial (Figure 1.4B) and the ventral/subpallial proliferative zone (Figure 1.4D) (Adolf et al., 2006; Ganz et al., 2010; März et al., 2010a).

In the dorsal VZ, newborn neurons are continuously generated and deposited immediately below the proliferative zone, in a fashion reminiscent of hippocampal neurogenesis in mammals (Adolf et al., 2006; Grandel et al., 2006). In fact, based both on neuroanatomical evidence (Butler, 2000; Northcutt and Braford, 1980; Vargas et al., 2000; Wullimann and Rink, 2002) and functional studies (Portavella et al., 2004; Rodríguez et al., 2002), the lateral and posterior zones of the zebrafish pallium are thought to be homologous to the mammalian hippocampus. The neurons generated in this region express parvalbumin, NeuroD, prospero homeobox protein 1 (Prox1) and Tbr1 (Ganz et al., 2012; Kroehne et al., 2011).

The cells that constitute this proliferative zone are RG cells and non-glial progenitors. As their name implies, RG have a cell body located at the ventricle and extend a radial process towards the basement membrane. As RG during mammalian development, these cells express GFAP, the β-subunit of S100 protein (S100β), nestin, BLBP and Sox2 (Adolf et al., 2006; Ganz et al., 2010; Kroehne et al., 2011; März et al., 2010a) (Figure 1.4B-C). Additionally, they were also shown to express high levels of aromatase B, a key enzyme in estrogen biosynthesis (Pellegrini et al., 2007). Label retaining experiments and clonal analysis have shown that RG have characteristics of adult stem cells, such as slow cell cycle, self-renewal and multipotency (Adolf et al., 2006; Ganz et al., 2010; März et al., 2010a; Rothenaigner et al., 2011). One important study using clonal analysis with lentivirus revealed the single cell lineage of RG cells, demonstrating that they always self-renew, dividing either symmetrically to generate two RG, or asymmetrically to generate one RG and a non-glial cell (Figure 1.4C) (Rothenaigner et al., 2011). This constant self-renewal, without depletion of the RG stem cell pool, may be on the basis for the continuous neurogenesis and brain growth throughout the fish's life. Even though RG cells are the adult NSCs in this region, the majority of them at a given time is not in a proliferative state (Chapouton et al., 2010). Quiescence of RG was shown to be maintained by Notch signaling from neighboring

proliferating cells via the notch3 receptor. The blockade of this signaling pathway strongly induces proliferation of RG cells (Alunni et al., 2013; Chapouton et al., 2010).

In addition to RG, also more committed, non-glial progenitor cells have been observed in the dorsal VZ. These cells are in close proximity to RG cells, immediately below the most apical surface, do not have a radial morphology and are negative for the glial or NSC markers mentioned above (Figure 1.4B-C) (Ganz et al., 2010; März et al., 2010a). Some of these progenitors express Sox2 and PSA-NCAM and, due to their similarity to the type 3 cells in the hippocampus, they have been named Type III (or neuroblasts) in the zebrafish adult telencephalon (März et al., 2010a). Other progenitors observed in the pallial VZ are negative for PSA-NCAM (Baumgart et al., 2012), and probably constitute an intermediate step between RG cells and the more differentiated neuroblasts (Figure 1.4C). These non-glial progenitors that don't express PSA-NCAM have been named throughout this thesis as sub-apical progenitors (SAPs). Non-glial progenitors are thought to cycle faster than RG (Adolf et al., 2006; März et al., 2010a; Rothenaigner et al., 2011), and to divide once or twice before terminally differentiating into neurons in the dorsal telencephalon (Rothenaigner et al., 2011).

The ventral proliferation zone is homologous to the SVZ in mammals and generates GABA-ergic or tyrosine hydroxylase (TH)-positive interneurons to the OB (Adolf et al., 2006; Grandel et al., 2006). These cells migrate from their place of origin to the OB in a structure similar to the RMS, with chains of PSA-NCAM-positive cells guided by aligned blood vessel structures, but in the case of zebrafish without an astrocyte enwrapping sheet (Adolf et al., 2006; Grandel et al., 2006; Kishimoto et al., 2011). In contrast to mammals, the proliferation zone of the subpallium also generates neurons that settle in the adjacent parenchyma, an area homologous to the mammalian striatum (Mueller and Wullimann, 2009). These neurons can be Paired box protein 6a (*pax6a*)-, TH- or glutamic acid decarboxylase (*gad67*)-positive (Adolf et al., 2006).

Similarly to the stem cells in the cerebellum and optic tectum, some progenitors of the subpallial region exhibit features of NE cells, such as nestin and apical marker (Zonula occludens (ZO)-1) expression, and are characterized by lack of expression of glial markers (Ganz et al., 2010; März et al., 2010a). Thus, typical RG cells are not present in this ventral VZ (Figure 1.4D-E). Also very abundant in this region are the more committed progenitor types, SAPs and neuroblasts (Figure 1.4D-E). Proliferation in the subpallial region seems to be dependent on FGF signaling, as blockage of FGF-receptor 1 leads to a strong decrease in the number of dividing cells (Ganz et al., 2010).

As mentioned so far, the proliferating cells of the telencephalic VZ only generate neurons or RG cells. Additional proliferating cells in the intact telencephalic parenchyma are the oligodendrocyte progenitor cells (OPCs) that generate oligodendrocytes in the adult telencephalon (März et al., 2010b).

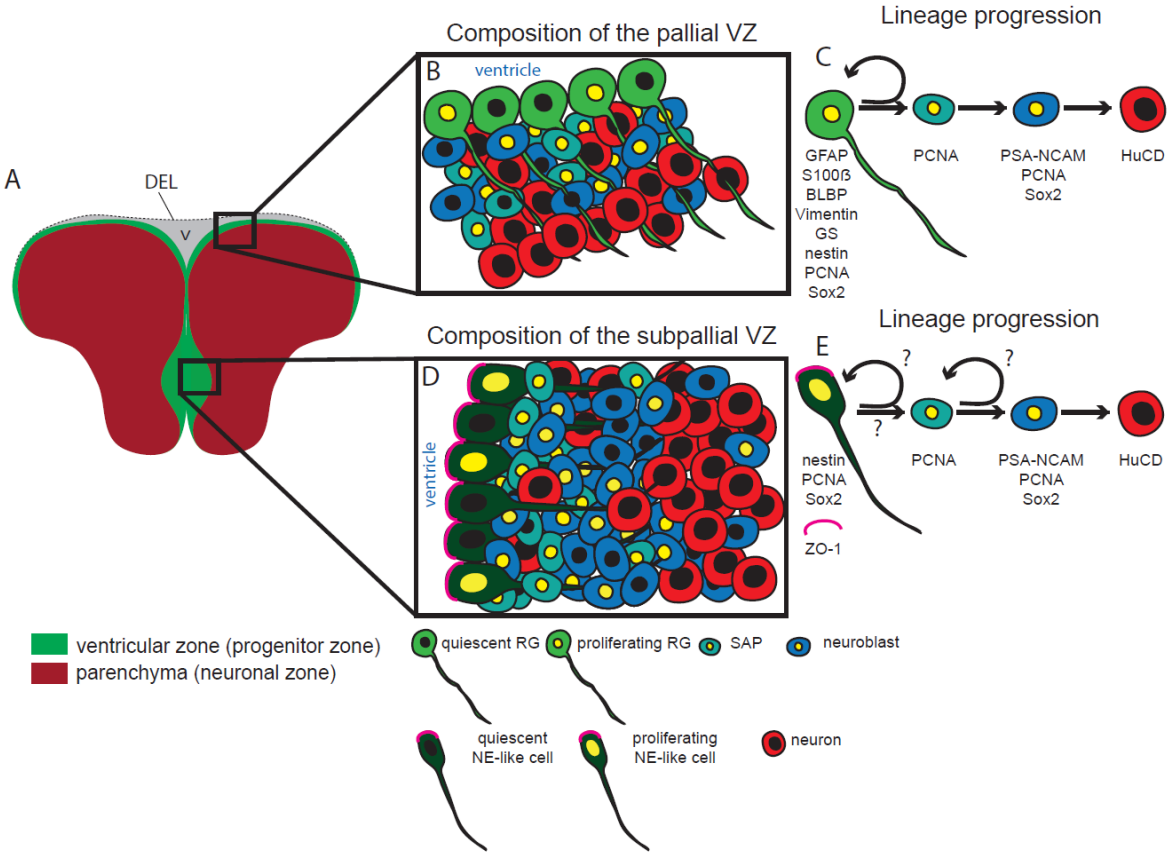

Figure 1.4: Composition of the VZ and neurogenic lineage in the zebrafish adult pallium and subpallium. (A) Scheme of a coronal section of the everted adult zebrafish telencephalon highlighting the VZ (green) and the parenchyma (red), mostly composed of progenitors and neurons, respectively. Newborn neurons in the adult telencephalon are deposited immediately adjacent to the VZ, and not in the deep parenchyma. A dorsal ependymal lining (DEL) bridges the two hemispheres and closes the ventricle (v). (B) Illustration of the dorsal VZ, composed of 3 types of progenitors: RG cells lining the ventricle, SAPs and neuroblasts. (C) Representation of the lineage progression in the dorsal VZ and the markers expressed by each cell type. (D) Illustration of the ventral VZ, composed of 3 types of progenitors: NE-like cells, SAPs and neuroblasts. (E) Representation of the putative lineage progression in the ventral VZ and the markers expressed by each cell type. Question marks indicate that the real lineage relationship between the different progenitor types has never been proved. Note that there are also PSA-NCAM-positive neuroblasts that do not proliferate (Baumgart et al., 2012) and could likewise generate neurons. Dimensions are not to scale.

Similarly to mammalian neurogenesis, adult neurogenesis in the zebrafish telencephalon also decreases with age. This decline was recently found to be due to a decrease in the recruitment of RG cells to division, with the progeny generated per RG cell being maintained (Edelmann et al., 2013). Curiously, this mechanism of age-related decrease in neurogenesis is more similar to the one occurring in the rodent DG, rather than in the SVZ/OB system (Encinas et al., 2011; Shook et al., 2012).

Despite the increasing knowledge on the telencephalic neurogenesis in zebrafish, as well as on the different progenitor cell types at the VZ, several questions remain unanswered: How do individual RG cells and their progeny behave during constitutive neurogenesis? Are RG cells a homogenous population of cells, with the same potency and cell cycle characteristics, or are there different sub-populations, restricted in their lineage? The best way to unravel these and other questions is the direct observation of the behavior of adult NSC in their niche *in vivo*, by means of imaging techniques. Due to the particularly privileged position of the RG cells of the pallial VZ directly at the outer surface of the telencephalon (Figure 1.4A), the adult zebrafish is an attractive model system to establish the non-invasive imaging technique necessary to reveal the behavior of adult NSCs in a vertebrate model during homeostasis.

1.2 *In vivo* imaging in the brain

Laser scanning microscopy (LSM) is a very widely used technique for fluorescence imaging. In confocal microscopy, samples are illuminated throughout their depth, but only the fluorescence from a certain optical plane is detected, due to the existence of a pinhole that excludes the out-of-focus emitted light. This technical feature provides a greater contrast than simple fluorescence microscopy and allows three-dimensional reconstructions by combining a series of optical planes from a stack (Conchello and Lichtman, 2005). The development of two-photon LSM (2pLSM) brought further improvement to the fluorescence microscopy field. By combining a near infrared laser with a precise spatial and temporal concentration of the excitation light, 2-photon microscopy greatly increased the tissue penetration depth and reduced the photo-damage to the imaged specimen, being for this reason a very popular method for long term *in vivo* imaging (Helmchen and Denk, 2005).

The establishment of 2pLSM in the adult mouse brain has potentiated the investigation on several research areas, such as neuronal circuits (Keck, 2008), synaptic plasticity (Trachtenberg, 2002), cerebral vasculature (Blinder et al., 2010) and acute and chronic CNS pathologies (Misgeld, 2006). However, despite the great advantages of this technology, the visualization of individual adult NSCs in mammalian models in their intact niche has not been achieved so far, mainly due to the large distance at which these niches are located relative to the brain surface.

In the everted adult zebrafish telencephalon, however, RG cells are located at the outer surface of the brain (Adolf et al., 2006; Ganz et al., 2010; März et al., 2010a). Due to this superficial position, RG cells in this model are a more feasible adult NSC population to be

investigated using optical imaging approaches. *In vivo* imaging in the adult zebrafish brain has not been extensively reported, probably due to the technical challenges related to the animal's survival. Nevertheless, in one single instance adult zebrafish were used for short term imaging of calcium responses in optic tectum neurons using epifluorescence illumination (Kassing et al., 2013).

On the other hand, zebrafish embryos have long been used for confocal and 2pLSM *in vivo* imaging studies due to their transparency and easy handling during embryonic and larval stages (Clarke, 2009; Megason and Fraser, 2003; W. Köster and Fraser, 2004). This combination allowed the visualization of several cell behaviors in young animals, such as microglia digestion of neurons (Peri and Nüsslein-Volhard, 2008), establishment of neuronal connections (Mumm et al., 2006), disease mechanisms (Paquet et al., 2009) and NSC activity (Alexandre, 2010; Buckley et al., 2013; Dong et al., 2012; Lyons et al., 2003; Tawk, 2007).

1.3 Modes of neural stem cell division: insights from imaging during development

Despite the lack of adequate, high resolution, *in vivo* imaging techniques in adult vertebrates, that prevented so far the observation of adult NSCs behavior, much information on NSC modes of division and potency has emerged from imaging in zebrafish embryos and in embryonic slice cultures in rodents or chicken.

In the early mouse embryo, NE cells forming the neural tube mostly undergo fast symmetric proliferative divisions to amplify the NSC pool (Cayouette and Raff, 2003; Saito et al., 2003; Sauer, 1935); a minority of these cells however divides asymmetrically to generate one NE cell and a more differentiated cell type (neuron or intermediate progenitor) (Haubensak et al., 2004; Kowalczyk et al., 2009; Williams and Price, 1995). With time, NE cells gradually lose some epithelial features and start expressing glial markers, giving rise to RG cells (Aaku-Saraste et al., 1996; Aaku-Saraste et al., 1997), the other NSCs during development (Malatesta et al., 2000; Noctor et al., 2001). RG cells in the mouse dorsal telencephalon were shown to undergo different modes of asymmetric cell division to generate neurons: in the direct neurogenesis mode, RG generates another RG and directly one neuron; in the indirect neurogenesis mode they produce one RG and an intermediate progenitor that can undergo one or two rounds of division before generating neurons, further amplifying the neuronal output (Haubensak et al., 2004; Miyata et al., 2004; Noctor et al., 2004; Noctor et al., 2007; Wu et al., 2005).

In the ventral mouse telencephalon, there is a higher heterogeneity of progenitor cells, with apical RG being the only self-renewing type of stem cell that divides asymmetrically and generates a wide diversity of sub-apical or basal progenitors that further divide and greatly contribute to lineage amplification (Pilz et al., 2013). Therefore, in this region the direct mode of neurogenesis from apically located RG cells never occurs. Interestingly, this is the region that gives rise to the adult lateral wall of the SVZ, where most adult NSCs are located (Pilz et al., 2013).

In the zebrafish developing forebrain, *in vivo* imaging revealed that a majority of RG cells undergo asymmetric cell divisions, of which 50% directly generate one neuron, whereas the other half generate neurons indirectly via intermediate progenitors (Dong et al., 2012). These direct and indirect neurogenesis modes are reminiscent of the division types observed in the mouse developing cortex. The remaining stem cells in the embryonic zebrafish telencephalon divide in a symmetric way, generating either 2 neurons or 2 progenitors (Dong et al., 2012). Importantly, many of these intermediate progenitors could undergo more than one round of division to generate neurons, increasing the lineage amplification (Dong et al., 2012).

Surprisingly, however, in the embryonic zebrafish hindbrain progenitor cells seem to rarely undergo self-renewing divisions, with the majority of neurons being originated from terminal symmetric divisions. Therefore, direct neurogenesis is the most abundant mechanism of neuron generation in this system (Lyons et al., 2003). Peculiarly, a subset of these progenitors labeled at the neural rod stage directly converted into one neuron, without undergoing division (Lyons et al., 2003).

In contrast, imaging of spinal cord slices from chicken showed that the majority of NSCs divide in a symmetric proliferative way, generating more progenitors. Thus, few progenitors generate neurons directly in this particular system (Wilcock et al., 2007).

In conclusion, it seems that neural stem and progenitor cells from different species and CNS regions exhibit different capacities regarding self-renewing and neuron formation. Ultimately, the establishment of tools to image NSCs with high resolution in the adult vertebrate brain would be of extreme relevance to investigate the behavior of individual adult NSCs during homeostasis and in the context of regeneration.

1.4 Adult neural stem cells and brain regeneration

The ability of a vertebrate to successfully regenerate a brain damage seems to correlate with its phylogenetic position and appears to be related to the prevalence of constitutive

neurogenesis in that particular species. Accordingly, different teleost fishes, as well as reptiles and amphibians were shown to regenerate several areas within the CNS (Ayari et al., 2010; Berg et al., 2010; Font et al., 1991; Reimer et al., 2008; Richter, 1965, 1970; Zupanc, 1999; Zupanc and Ott, 1999b) by recruitment of ventricular progenitors that constitutively proliferate in the adult brain (Berg et al., 2010; Font et al., 1991; Kroehne et al., 2011). In contrast, neuronal regeneration seems to be impaired in the mammalian brains (reviewed in (Barkho, 2011)).

With the innumerous existing neurodegenerative diseases in humans, and the traumatic brain injuries resulting from accidents, there is an urgent demand for brain repair therapies. Therefore it is of great importance to study species that have the ability to endogenously regenerate the CNS, in order to use this knowledge to improve regeneration in the mammalian system, namely in humans.

1.4.1 Adult neural stem cells and brain regeneration in rodents

After injury in the mammalian brain, the adult NSCs present in the constitutive neurogenic niches increase their proliferation and generate neuroblasts that migrate to the injury site (Arvidsson et al., 2002; Kim and Szele, 2008; Nakatomi et al., 2002; Ohab, 2006; Rice et al., 2003; Zhang et al., 2004). Moreover, some of these cells seem to differentiate into the correct neuron type of the damaged area (Arvidsson et al., 2002; Brill et al., 2009; Chen et al., 2004; Collin et al., 2005; Magavi et al., 2000; Ohab, 2006; Sundholm-Peters et al., 2005). SVZ-derived neuroblasts were shown to replace damaged neurons after brain injury within different brain areas, such as the hippocampus, striatum and neocortex (Jin et al., 2003; Kuge et al., 2009; Yamashita et al., 2006). Disappointingly however, the number of neurons generated from endogenous NSCs is extremely low (Arvidsson et al., 2002), and the survival and integration of these new neurons in the lesioned areas is minimal (Arvidsson et al., 2002; Takasawa, 2002; Thored et al., 2006; Thored et al., 2007; Tonchev et al., 2005). From these findings, it seems that endogenous adult NSCs in mammalian models have some intrinsic capacity of responding to the injury signals and initiating a regenerative reaction but somehow the environment in these animals is rather inhibitory of neuronal integration and survival.

Interestingly, it was shown that ependymal cells can be activated from their quiescent state to generate neuroblasts and astrocytes after stroke (Carlen et al., 2009). However, also in this case, most of the neuroblasts generated died and no mature neurons were formed in these conditions (Carlen et al., 2009).

The reasons for the detrimental environment that does not allow successful neuronal regeneration may rely in part on the reactive gliosis process, mediated by the action of glial cells to the injury, such as microglia, astrocytes and OPCs (reviewed in (Robel et al., 2011)).

Microglia, the resident macrophage population of the brain, are the first cells to react to injury, rapidly proliferating and migrating to the injury site where they clear damaged cells and cellular debris (Hanisch and Kettenmann, 2007).

Astrocytes react by hypertrophy, with swelling of their cell somata and primary processes, polarization (establishment of elongated processes towards the injury), up-regulation of intermediate filaments (like GFAP, vimentin) and increasing proliferation close to the injury site (Bardehle et al., 2013; Buffo et al., 2008). Even though reactive astrocytes do not generate neurons *in vivo*, they were shown to have the potential to do so *in vitro* (Buffo et al., 2008), and Sonic hedgehog (shh) seems to be necessary and sufficient to elicit these responses *in vivo* and *in vitro* (Sirko et al., 2013). Astrocytes are important to limit the size of injury and inflammation, and are thought to play a role in re-establishing the blood brain barrier (BBB) (Buffo et al., 2010; Robel et al., 2011; Sofroniew, 2009).

OPCs reactions to injury include hypertrophy, cell division and migration to the injury site ((Hughes et al., 2013; Simon et al., 2011), von Streitberg and Dimou, unpublished data).

Despite the intense reaction of glial cells to the injury, all of them fail to generate neurons *in vivo* (Buffo et al., 2008; Kang et al., 2010; Tatsumi et al., 2008). Instead, the combined action of these glial cells, together with fibroblasts and endothelial cells and a change in the composition of the extracellular matrix (ECM) components, creates a scar at the site of lesion (Stichel and Müller, 1998). This scar is initially beneficial, since it reestablishes the integrity of the CNS by sealing it off, but it also prevents axonal growth (Stichel and Müller, 1998) and neuronal regeneration (Li et al., 2008; Widestrand et al., 2007).

Interestingly, in lesion models in which neurons die by apoptosis, reactive gliosis is minimized and newborn neurons manage to survive (Chen et al., 2004).

In summary, despite the attempts of adult NSCs (and ependymal cells) to regenerate damaged brain areas in mammalian models, the non-permissive environment created after an injury strongly prevents successful neuronal regeneration. Moreover, this environment seems to instruct mostly the generation of glial cells from parenchymal proliferating cells (Buffo et al., 2008; Kang et al., 2010; Tatsumi et al., 2008), even though astrocytes from injured brains have the potential to generate neurons *in vitro* (Buffo et al., 2008).

1.4.2 Adult neural stem cells and brain regeneration in zebrafish

In zebrafish, on the other hand, the situation seems to be different. Efficient neuronal regeneration in adult zebrafish (and other fishes) has been documented in the telencephalon, cerebellum, spinal cord and retina (Ayari et al., 2010; Baumgart et al., 2012; Kishimoto et al., 2012; Kroehne et al., 2011; März et al., 2011; Mensinger and Powers, 1999; Reimer et al., 2008; Sherpa et al., 2008; Zupanc and Ott, 1999a).

In different lesioned areas, inflammatory reaction seems to be the initial response (Baumgart et al., 2012; Hui et al., 2010; Kroehne et al., 2011; Kyritsis et al., 2012). Very importantly, and in contrast to the mammalian response to brain injury, in zebrafish there is no massive astrogliosis, except in white matter regions of the cerebellum and optic nerve (Clint and Zupanc, 2001; Koke et al., 2010). This reduced astrogliosis can be at least partially explained by the general absence of typical stellate-shaped astrocytes in the brain of teleosts (Kálmán, 1998). Additionally, only a mild or no reaction of cells of the oligodendrocyte lineage was observed in the zebrafish brain (Baumgart et al., 2012; März et al., 2011), strongly differing from their response to injury in mammals (Hughes et al., 2013; Simon et al., 2011). In agreement with the reduced astrogliosis and oligodendrocyte reaction, there is also no scar formation in zebrafish, which could be one reason for the successful neuronal regeneration (Ayari et al., 2010; Baumgart et al., 2012; Kroehne et al., 2011; März et al., 2011).

Common to some injured areas, RG-like cells increase proliferation at the ventricle (Baumgart et al., 2012; Kroehne et al., 2011; Reimer et al., 2008). Interestingly, even when these RG-like cells do not normally proliferate in the intact adult CNS, they resume proliferation and contribute to neurogenesis after injury. This is the case for Müller glia in the retina and ependymal cells in the spinal cord (Fausett and Goldman, 2006; Reimer et al., 2008).

As mentioned in the previous sections, the zebrafish telencephalon was selected as the animal model to study adult NSCs in this thesis. In the next section, a more detailed description of regeneration in this area in presented.

1.4.2.1 Regeneration in the adult zebrafish telencephalon

The regeneration of the zebrafish adult telencephalon has recently been the focus of many different studies (Ayari et al., 2010; Baumgart et al., 2012; Kishimoto et al., 2012; Kroehne et al., 2011; März et al., 2011). One reason to choose this area is the possibility to

compare the regeneration process and the cellular players in zebrafish with the regenerative responses in the mammalian telencephalon, hoping to get insights into possible ways of improving this process in the later species. A more technical reason is that, since in normal conditions there is no neurogenesis in the zebrafish telencephalic parenchyma (only in the layers adjacent to the VZ-see Figure 1.5A) (Adolf et al., 2006; Grandel et al., 2006), when a lesion is performed in this neuron-rich parenchyma, it is easy for the observer to distinguish between constitutive and regenerative neurogenesis.

Injury models established in the zebrafish telencephalon so far differ in the size and the approach to provoke the damage. Common to all the models, the injury triggers an increase in the proliferation of different cell types at the injury site and at the VZ, and most importantly *de novo* neurogenesis and tissue repair (Ayari et al., 2010; Baumgart et al., 2012; Kishimoto et al., 2012; Kroehne et al., 2011; März et al., 2011).

In this thesis, injury was performed as previously described (Baumgart et al., 2012), by insertion of a thin glass capillary through the fish nostrils, causing damage in the telencephalic parenchyma throughout the whole rostral-caudal axis of the telencephalon, and avoiding the VZ. In this particular model, complete tissue restoration is apparent already at 7 days post-injury (dpi) and no scar was observed (Baumgart et al., 2012).

Similarly to the situation in mice, the first cells reacting to injury are microglia. These cells have a peak of proliferation already at 2dpi, both in the parenchyma and in the VZ, and their morphology changes from ramified to a phagocytic type (Figure 1.5B). At 7dpi, proliferation returns to baseline levels. Endothelial cell proliferation also peaks at 2dpi (Baumgart et al., 2012).

In striking contrast to the response in the mammalian brain, *olig2:*GFP-positive cells, that usually proliferate and generate mature oligodendrocytes in the uninjured zebrafish parenchyma (März et al., 2010b), do not change their proliferation status after injury (Figure 1.5B) (Baumgart et al., 2012). This observation, together with the fact that the zebrafish telencephalon does not possess typical stellate astrocytes (März et al., 2010a), may be part of the reason for the absence of scar in this model.

The NSCs, on the other hand, respond to injury by an increase in proliferation at 2dpi, that further peaks at 7dpi (Figure 1.5B-C) (Baumgart et al., 2012). Remarkably, at this time point the injury is not visible anymore and the tissue appears fully restored. The delayed response of RG cells is reminiscent of the late increase in astrocytes proliferation in the rodent brain (Buffo et al., 2008; Simon et al., 2011). However, in contrast to the rodent, there is no up-regulation of *gfap:*GFP expression and no *gfap:*GFP-positive cell bodies were observed in

the zebrafish injured parenchyma (Baumgart et al., 2012), suggesting that the absence of strong astrogliosis could also contribute for a more successful regeneration. Interestingly, however, when a bigger injury was made, some *gfap:*GFP-positive somata could be found at the injury site, indicating that only the bigger lesions are able to produce enough signals to recruit RG cells (Baumgart et al., 2012). Additional studies in which the lesion size was bigger and/or the BBB was disrupted also showed migration of VZ-derived cells and/or up-regulation of GFAP, reinforcing the idea that the injury size regulates the extent to which RG cells respond (Ayari et al., 2010; Kishimoto et al., 2012; Kroehne et al., 2011; März et al., 2011).

Very importantly, and independently of the injury size, the damage elicited *de novo* neurogenesis in the telencephalic parenchyma, where newborn neurons are normally not deposited during constitutive neurogenesis, and these new neurons were able to survive for up to 2.5 months after injury (Baumgart et al., 2012) (Figure 1.5D).

In conclusion, different cell types seem to react to injury and a successful regenerative neurogenesis occurs (see summary in Figure 1.5).

Nevertheless, several points in this model need to be further elucidated. Many BrdU-positive cells were observed at the injury site, that were negative for the immunohistochemistry markers used, suggesting the participation of additional cell types in the process. Possible candidates are the SAPs and/or the neuroblasts, which participate normally in constitutive neurogenesis (Rothenaigner et al., 2011). It would be therefore important to examine the reaction of these non-glial progenitors to this injury model.

Additionally, the cellular origin of the newborn neurons was not assessed in this study. The RG cells would be one conceivable candidate, but no *gfap:*GFP-positive cells were observed at the injury site (except when the injury was larger) (Baumgart et al., 2012). Nevertheless, it is possible that these cells rapidly down-regulate *gfap:*GFP expression upon differentiation, and for this reason the GFP signal does not appear in the injured parenchyma. Additionally, the peak of RG cell proliferation in this model is at 7dpi, a time point at which the tissue appears already restored (Baumgart et al., 2012), prompting the question of why do RG cells need to proliferate at this late time point.

Another reasonable candidate to generate the new neurons in the parenchyma would be the BrdU-positive, marker-negative cells (SAPs); they accumulate at the injury site at 2dpi and, since the long-term surviving newborn neurons were generated at this time (before the peak of RG cell proliferation) (Baumgart et al., 2012), it is plausible that the newborn neurons could be derived from these SAPs.

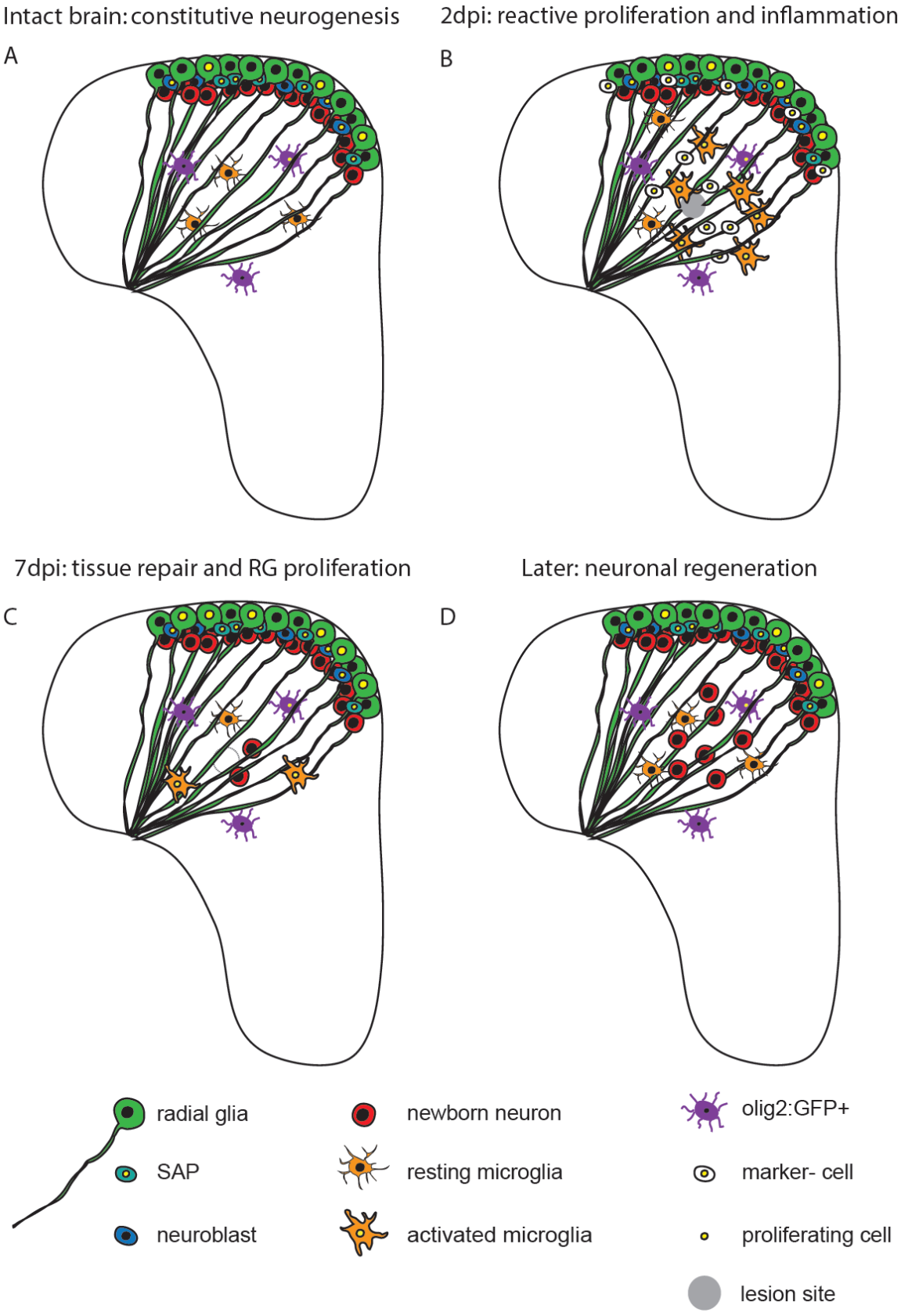
Intact brain: constitutive neurogenesis
A
2dpi: reactive proliferation and inflammation
B
7dpi: tissue repair and RG proliferation
C
Later: neuronal regeneration
D
radial glia
SAP
neuroblast
newborn neuron
resting microglia
activated microglia
olig2:GFP+
marker- cell
proliferating cell
lesion site

Figure 1.5: Steps of the regenerative response to injury in the adult zebrafish telencephalon. (A) Illustration of an intact telencephalon, with the neuronal progenitor types located at the VZ and the newborn neurons deposited immediately adjacent to them. Parenchymal cells are neurons, oligodendrocytes and OPCs (both *olig2:GFP*-positive). Some resting microglia also populate the telencephalon. (B) Dramatic increase in proliferating cells in the injured parenchyma at 2dpi, many of them being activated microglia and marker-negative cells. Note the absence of response of *oli2:GFP*-positive cells. At this time-point, also a mild increase in proliferating RG cells at the VZ occurs. (C) At 7dpi, general proliferation returns to normal and the wound is closed, but the number of proliferating RG cells at the VZ is further increased. (D) With time, proliferation returns to normal, and newborn neurons contribute to regenerate the parenchyma. The apparent lack of response of SAPs and neuroblasts does not necessarily mean they did not react, but rather that their reaction was not thoroughly investigated. Figure made based on data from (Baumgart et al., 2012). Dimensions of cells and telencephalic hemisphere are not to scale.

In fact, in an injury model in which a larger damage was induced, lineage tracing of RG cells using a *her4.1:*Cre inducible zebrafish line, which recombines in RG cells, showed the accumulation of reporter-positive neurons in the parenchyma exclusively after injury, indicating that cells within the RG lineage do contribute to the additional neurogenesis (Kroehne et al., 2011). Nonetheless, with this technology it is not possible to distinguish between the response of RG cells and their immediate progeny, the SAPs and/or neuroblasts, since these can still inherit sufficiently high levels of the Cre recombinase and therefore also be reporter positive.

Interestingly, another study proposed the migration of post mitotic neuronal precursors expressing *ngn1:*GFP from the VZ to the injury site, providing further support to the involvement of VZ-derived progenitors in the neuronal regeneration process (Kishimoto et al., 2012).

As a result of these considerations, it is important to examine and discriminate the exact contribution of each progenitor type to the formation of new neurons in response to injury. Towards this purpose, a differential labeling of each progenitor type would be fundamental to elucidate the specific response and the individual role of each progenitor type. Moreover, the characterization of adult NSCs and progenitors reaction to injury has only been done at the population level, in analysis that do not take into account possible heterogeneity within the stem cell population. Therefore, for a better characterization of the single cell reaction to injury, the best approach is the continuous single cell imaging of adult NSCs in their niche *in vivo*.

2 Aims of this study

The major aim of this study was to investigate the behavior of adult NSCs *in vivo*, during constitutive neurogenesis and after an injury. Towards this aim, an *in vivo* imaging technique was established using the adult zebrafish as a model. The choice of this model organism was based on the accessible location of adult NSCs in the dorsal telencephalon (allowing a better visualization of the cells), the constitutive neurogenesis ongoing in this area, and the efficient neuronal regeneration observed after injury in this species. Within this goal, several aspects of stem cell behavior should be unraveled: NSC quiescence/ recruitment to cell cycle, mode of division, stem cell potency and migration. Very importantly, the continuous observation of single cells over time should allow the examination of whether the pool of adult NSCs in the zebrafish telencephalon is a homogeneous cell population or is constituted of distinct cell sub-populations. Additionally, the roles of the different VZ progenitor types in the neuronal regeneration process were dissected, by comparing the specific contributions of RG cells and the sub-apically located non-glial progenitors to the formation of newborn neurons in the injured telencephalic parenchyma.

3 Experimental procedures

3.1 Commonly used solutions

Phosphate-buffered saline (PBS)

NaCl 137mM (Cat. Nr. BP358-212, Fisher Bioreagents)

KCl 2.7mM (Cat. Nr. 104936, Merck)

$Na_2HPO_4 \cdot 7H_2O$ 8.3mM (Cat. Nr. 106574, Merck)

KH_2PO_4 1.4mM (Cat. Nr. 104873, Merck)

Artificial cerebrospinal fluid (ACSF)

NaCl 100mM (Cat. Nr. BP358-212, Fisher Bioreagents)

KCl 2.46mM (Cat. Nr. 104936, Merck)

$NaH_2PO_4 \cdot H_2O$ 0.44mM (Cat. Nr. 106346, Merck)

$MgCl_2.6H_2O$ 1mM (Cat. Nr. A537, Roth)

$CaCl_2$ 1.13mM (Cat. Nr. 102378, Merck Millipore)

$NaHCO_3$ 5mM (Cat. Nr. 106323, Merck)

Glucose 10mM (Cat. Nr. G7021, Sigma)

10x PO_4 buffer (pH 7.2-7.4)

$NaH_2PO_4 \cdot H_2O$ 2.5M (Cat. Nr. 106346, Merck)

NaOH 1.9M (Cat. Nr. 9356, Roth)

Storage buffer

Glycerol 30 ml (Cat. Nr. 3783, Sigma)

Poly (ethylene glycol) 30 ml (Cat. Nr. 202398, Sigma)

10x PO_4 Buffer 10 ml

Distilled H_2O 30 ml

3.2 Fish maintenance and strains

Zebrafish were maintained under standard conditions (Westerfield, 2000) in the Helmholtz Zentrum fish facility. For *in vivo* imaging animals used were between 2.5 and 3 months old to make sure the skull and skin were not too thick (maximizing imaging quality); in all the other experiments the animals were between 3 and 5 months old. The

strains/transgenic lines used were wild-type AB/EK hybrid, *brassy* (Kelsh et al., 1996), *Tg(gfap:gfp)mi2001* (Bernardos and Raymond, 2006) crossed with *brassy*, *Tg(HuC:GFP)* (Park et al., 2000) crossed with *brassy* and *Tg(-3.5ubi:loxP-EGFP-loxP-mCherry)* (*ubi:Switch*) (Mosimann et al., 2011). To identify transgenic animals, embryos at 24 hours post-fertilization (hpf) or 48hpf were screened for positive fluorescent signal under a stereomicroscope (Stereo Lumar.V12, Zeiss). All experiments were performed according to the handling guidelines and regulation of Bavaria.

3.3 Plasmids

Plasmids used for clonal analysis were pCS-GFP (cytoplasmic localization), pCS-lynGFP (membrane localization) and pCS-H2B-eYFP (nuclear localization), generous gifts from Reinhard Köster. For *in vivo* imaging the plasmids pCS-GFP, pCS-lynGFP, pCS-TagRFP-GI (cytoplasmic localization), pCS-tdtomatoGI (all gifts from Reinhard Köster), pCS-H2B-mRFP (Sean Megason) and pCS2-tdTomatomem (cloned in-house) were used. In all the above constructs the expression of reporter fluorescent protein was driven by the Cytomegalovirus (CMV) promoter and the antibiotic resistance gene was ampicillin. In some *in vivo* imaging experiments, the construct pCM221\pDestTol2pA2ubi2320_mCherry (for simplification ubi:mCherry) (Mosimann et al., 2011) was used, in which the ubiquitin promoter drives mCherry expression. A pCS-Cre plasmid (cloned in-house) was used for lipofections in the transgenic line *Tg(-3.5ubi:loxP-EGFP-loxP-mCherry)* (*ubi:Switch*) (Mosimann et al., 2011).

3.4 Cloning

The pCS2-tdTomatomem construct was obtained by polymerase chain reaction (PCR) of the tdTomato sequence (Shaner et al., 2008) fused to the H-ras farnesylation site from the construct pRRL.PPT.SF.TdTomatomem (HrasF) (Shroeder group) using the forward primer TATGGATCCATGGTGAGCAAGGGCGAGGAG, containing a restriction site for the enzyme *BamHI* (New England Biolabs) and the reverse primer GACTCGAGTCAGGAGAGCACACACTTGCAG, which comprises a restriction site for the restriction enzyme *XhoI* (New England Biolabs). The fragment was then cloned into a pCSII vector backbone.

For lipofections in the *ubi:Switch* transgenic line, Cre recombinase sequence from a pLV-CMV-Cre plasmid (Pfeifer et al., 2001) was inserted into a pCSII vector backbone using

the forward primer CGAATTCGACCCTCGACCATGCCC, containing a *EcoRI* restriction site and the reverse primer CCCTCGAGCCCCGCGTTAATGGCTA, comprising a *XhoI* (New England Biolabs) restriction site. Incubations with restriction enzymes were done according to the manufacturer's instruction (New England Biolabs).

3.4.1 Polymerase chain reaction (PCR)

PCR primers were designed using the online platform Primer 3 (http://biotools.umassmed.edu/bioapps/primer3_www.cgi). Annealing temperature was chosen according to the software. PCR was carried out according to manufacturer's instruction using *Taq* DNA polymerase from Qiagen (Cat. Nr. 201203, Qiagen). PCR products were purified with the QIAquick PCR Purification Kit (Cat. Nr. 28104, Qiagen).

3.4.2 Agarose gel

DNA (deoxyribonucleic acid) fragments from restriction digests and PCR products were separated on 1.5% agarose (Cat. Nr. 840004, Biozym) gels prepared in TAE-buffer composed of 40 mM tris-(hydroxymetyhl)-aminomethane (TRIS) (Cat. Nr.5429.3, Roth), 20 mM acetic acid (Cat. Nr. 1000632511, Merck) and 1 mM ethylenediaminetetraacetic acid (EDTA) (Cat. Nr. 8043.2, Roth). Agarose gels were stained with 1% ethidium bromide solution (Cat. Nr. 2218.2, Roth) at a concentration of 5 µl per 100 ml of agarose solution. DNA fragments were separated with voltages between 100 V and 150 V in TAE-buffer.

3.4.3 Purification of DNA fragments

DNA fragments were cut out from agarose gels using a scalpel and purified with the QIAEX II Gel Extraction Kit (Cat. Nr. 20021, Qiagen), according to the manufacturer's instructions. DNA fragments were resuspended in H_2O and DNA concentration was measured on a NanoDrop spectrophotometer nd-1000 (Thermo Scientific, Waltham, USA).

3.4.4 Ligations

Ligations were performed with T4 ligase (Cat. Nr. #EL0011, Thermo Scientific), according to the manufacturer's instructions.

3.4.5 Transformation of bacteria

Transformation was started by thawing competent DH5α *Escherichia coli* bacteria frozen at – 80 °C for 15 minutes (min) on ice. Up to 100 ng of plasmid or ligation cocktail were added to the bacteria suspension and incubated 30 min on ice. After heat-shock treatment of bacteria for 90 s at 42 °C, the suspension was cooled 2 min on ice. Afterwards, 1 ml lysogeny broth (LB)-medium (Cat. Nr. 12780-029, Invitrogen) was added to the cells and these were incubated 1 h at 37 °C with strong agitation. Then, bacteria suspension was plated on LB agar (Cat. Nr. 244520, Becton Dickinson) with adequate antibiotic for selection of successfully transformed bacteria. LB agar plates were incubated overnight at 37 °C.

3.4.6 Isolation of plasmid DNA

High copy plasmids from DH5α bacteria were purified from 5 ml overnight cultures using the QIAprep Spin Miniprep Kit (Cat. Nr. 27104, Qiagen). Purification from 200 ml overnight cultures was performed using the Endofree Plasmid Maxi Kit (Cat. Nr. 12362, Qiagen).

3.4.7 Sequencing

To confirm the successful cloning, sequencing was performed in the in-house sequencing facility using the BigDye Terminator v3.1 Cycle Sequencing Kit (Cat. Nr. 4337455, Applied Biosystems) and the DyeEx 2.0 Spin kit (Cat. Nr. 63204, Qiagen) on a 3730 DNA Analyzer (both Applied Biosystem, Foster City, USA).

3.5 Generation of retrovirus

3.5.1 Retrovirus production

Vesicular stomatitis virus glycoprotein (VSV-g) pseudotyped retrovirus (elongation factor-1α (EF1α)-GFP (Rothenaigner et al., 2011)) was produced in 293GPG cells, that constantly express genes encoding for viral proteins (Ory et al., 1996). Cells were cultured in medium A: Dulbecco's modified Eagle medium (DMEM) (Cat. Nr. 61965-026, Life Technologies) containing 10% heat inactivated fetal calf serum (FCS) (Cat. Nr. 2602-P250316, Pan Biotech), 1mg/ml penicillin/streptomycin (Cat. Nr. 15140-122, Life Technologies), 2µg/ml puromycin dihydrochloride (Cat. Nr. A11138-03, Life Technologies), 1µg/ml tetracyclin (Cat. Nr. Cat. Nr. 02194542, MPvBiomedicals Inc.) and 0.3mg/ml geneticin (Cat. Nr. 10131-027, Life Technologies).

For viral production, cells were plated into 10cm dishes (Cat. Nr. 353003, Falcon™) in medium A without tetracycline. The next day, when cells reached 80-90% confluence, they were washed in PBS to remove all traces of antibiotics and incubated for 1h at 37ºC in DMEM containing 10% FCS and penicillin/streptomycin. In the meantime, the transfection mix was prepared. For each 10cm plate, 60µl Lipofectamine® Reagent 2000 (Cat. Nr. 11668-019, Life Technologies) were diluted in 1,5ml Opti-MEM® I Reduced Serum Medium (Cat. Nr. 51985-026, Life Technologies). In parallel, 24µg of retroviral plasmid DNA were diluted in 1,5ml Opti-MEM® and both solutions were incubated at 5min at room temperature (RT). Afterwards, the lipofectamine and DNA solutions were combined and incubated for 30min at RT while shaking. Medium was then removed from the cells and the 3ml of transfection mix were added and incubated overnight at 37ºC.

The next day, transfection medium was replaced by DMEM supplemented with 10% FCS and 1mg/ml penicillin/streptomycin. First viral harvest was done 48h after transfection, followed by as second harvest at 96h. The virus containing medium was filtered through a pre-wetted 0.45µm PVDF filter (Cat. Nr. SLHV033RS, Merck Millipore) and centrifuged at 48000 x *g* for at least 90min at 4ºC. The medium was discarded and viral pellets were resuspended in a buffer containing 50mM Tris-HCl pH 7.8, 130mM NaCl, 10mM KCl and 5mM $MgCl_2$. Aliquots of 5µl or 10µl were stored at -80ºC.

3.5.2 Retrovirus titration

Virus titer was determined by transducing primary embryonic cortical cell cultures from mice with serial dilutions of viral solution. After 2 days *in vitro*, cells were fixed in 4% paraformaldehyde (PFA) diluted in PBS for 15min at RT, and processed for green fluorescent protein (GFP) immunohistochemistry. The calculation of the virus titer was based on the number of GFP-positive colonies counted per coverslip and the known applied dilution of the viral solution to each coverslip.

3.6 Ventricular injections and electroporations

Fish were anaesthetized in 0.02% Tricaine (Cat. Nr. A5040-25G, Sigma) and held in a wet sponge. A small hole in the skull was made in the region between the telencephalon and the optic tectum using a micro-knife (Cat. Nr. 10056-12, Fine Science Tools). The solutions were mixed with 4.5% fast green (stock solution 1mg/ml) (Cat. Nr. F7258-25G, Sigma) for

better visualization, loaded into a glass capillary (Cat. Nr. 30-0016, Harvard Apparatus) and injected with a pressure injector (Femtojet®, Eppendorf).

For lipofections, 2.5µl of Lipofectamine® 2000 Transfection Reagent (Cat. Nr. 11668-019, Life Technologies) were mixed with 1µl of ACSF, vortexed and added to 3µl of solution containing 4-5µg of plasmid. After 20min of incubation at RT the solution was injected into the telencephalic ventricle, approximately 300-400ng of plasmid per fish.

For electroporations, 300-400 ng of plasmid diluted in ACSF were injected in the ventricle and electroporated using a TSS20 Ovodyne electroporator (Intracel), applying 5 pulses at 40V during 50ms each and at 1s intervals. The positive electrode was placed in the ventral side of the animal´s head.

For retrovirus injections, a retrovirus expressing GFP under the EF1α promoter (Rothenaigner et al., 2011) was used, at a titer between 4 x 10^5 and 3 x 10^6, and approximately 0.5µl were injected per fish. After injection fish were placed in penicillin-streptomycin containing water (100U/ml) for 3h at 37°C to allow proper activity of the virus.

3.7 Injury

Stab wound injury was performed in both telencephalic hemispheres as described previously (Baumgart et al., 2012). Briefly, animals were anesthetized in 0.02 % Tricaine and held on a wet sponge. A glass capillary (Cat. Nr. KG01, A.Hartenstein) pulled and cut to have a 100µm width was inserted in both hemispheres through the nose apertures until the most caudal part of the telencephalon. Afterwards the animals were allowed to recover in fresh water.

3.8 Bromo-deoxy-uridine (BrdU) labeling

To label proliferating cells in the S-phase of the cell cycle for the analysis of proliferating neuroblasts reacting to injury (Figure 4.1), fish were injected intraperitoneally with 50 µl/g body weight of the thymidine analogue bromo-deoxy-uridine (BrdU, Cat. Nr 16880, Sigma) diluted in 110 mM NaCl pH 7.0 at a concentration of 5 mg/ml (250µg BrdU/g fish). Since the clearance of BrdU in adult fish was estimated to be approximately 4h (Zupanc and Ott, 1999a), animals were given 2 injections with a 2h interval followed by a survival time of 2h after the last injection. Animals were sacrificed at different time points after injury and BrdU injections were performed 4h before the sacrifice.

For long term labeling of proliferating cells, fish were placed in a tank with 10mM BrdU for 6h every second day during 2 weeks. During the remaining time animals were swimming in normal water.

3.9 Immunohistochemistry

3.9.1 Tissue preparation and immunohistochemistry in sections

To process brains for sectioning and immunohistochemistry, animals were sacrificed with 0.2% of Tricaine. Brains were fixed with 4%PFA (in PBS) at 4ºC for 1h in the skull to facilitate dissection, and dissected brains were further fixed for 2h. After fixation, brains were embedded in 3% agarose (dissolved in PBS) and 100µm coronal slices were cut in a vibration microtome (Microm HM 650V, Thermo Scientific). If necessary, slices were kept at -20ºC in storage buffer until further processing.

In general, antibodies were diluted in PBS containing 0.5% Triton-X-100 (Cat. Nr. 3051, Roth) and 10% normal goat serum (Cat. Nr. S1000, Vector Laboratories). Primary antibody incubation was done overnight at 4°C, followed by 3 washes of 10min each in PBS. Afterwards samples were exposed to subclass specific goat secondary antibodies conjugated to Alexa 488, Alexa 546 or Alexa 647 (Life Technologies) for 2h at RT. For nuclear staining DAPI (4',6' Diamidino-2-phenylindole, Cat. Nr. D8417, Sigma, 20mg/ml) was added to the secondary antibody solution. All the Alexa-conjugated secondary antibodies and DAPI were applied at a concentration of 1:1000. After complete labeling, slices were washed 3 times in PBS and mounted in Aqua Poly/Mount (Cat. Nr. 18606, Polyscience Inc.). In Table 3-1, a list of all the primary antibodies used is presented, with the respective dilution and pre-treatments applied.

In the specific staining of retrovirus injected brains, amplification of the GFP signal was needed. After incubation with the chicken anti-GFP antibody, a solution of biotinylated anti-chicken antibody (Cat. Nr. BA-9010, Vector Laboratories, dilution 1:250) was added to the sections and let act for 1h at RT. Subsequently, three washes of 10min in PBS were done and sections were incubated in secondary antibody solution containing Streptavidin conjugated with Alexa Fluor 488 (Cat. Nr. S11223, Life Technologies, dilution 1:500) for 2h at RT.

Table 3-1: List of all the primary antibodies used in this study, and the correspondent information about each antibody.

Antigen	Source	Dilution	Host, isotype	Pre-treatment
BrdU	*Serotec (MCA2060)*	*1:200*	*Rat, IgG2a*	*2N HCl 30min*
GFAP	*DAKO (Z0334)*	*1:200*	*rabbit*	-
GFP	*Aves lab (GFP-1020)*	*1:700*	*chicken, IgY*	-
HuCD	*Molecular probes (A-21271)*	*1:500*	*Mouse, IgG2b*	-
PCNA	*DAKO (M0879)*	*1:500*	*Mouse, IgG2a*	*3%H_2O_2 30min*
PSA-NCAM	*Millipore, MAB5324*	*1:100*	*IgM*	*No triton*
RFP	*Rockland (600-401-379)*	*1:1000*	*rabbit*	-

3.9.1.1 Special treatments

For immuno-staining against BrdU, slices were pre-incubated for 30min at RT in 2N HCl (Cat. Nr. 100319, Merck Millipore) to denaturate DNA and washed two times for 15min each in 0.1M sodium tetraborate buffer (pH 8.5, Cat. Nr. 106306, Merck Millipore) before addition of the primary antibody. When samples were co-stained with additional antibodies, BrdU labelling was done after completing the labelling with other antibodies.

To expose the epitope to which the anti-proliferating cell nuclear antigen (PCNA) antibody binds, slices were beforehand incubated in 3% H_2O_2 (Cat. Nr. 8070, Roth) diluted in PBS for 30min at RT.

In the case of PSA-NCAM staining, since the epitope is located on the surface of the cells, the antibody was diluted in PBS containing 10% normal goat serum, but without detergent to avoid damage of the plasma membrane. When co-stained with other antibodies, PSA-NCAM labelling was performed first, followed by the labelling for the other proteins.

3.9.2 Tissue preparation, immunohistochemistry and clearing in whole-mount brains

The whole brain staining and clearing after *in vivo* imaging was based on the protocol from Huber *et al* (Huber et al., 2005). Briefly, brains were fixed in 4% PFA (in PBS) at 4°C either in the skull overnight or after dissection for 3h. Then they were bleached in a solution

containing H_2O_2, methanol (Cat. Nr. 1.06007, Merck) and dimethyl sulfoxide (DMSO, Cat. Nr. D-2438, Sigma) for 24h at 4°C, rinsed five times in 100% methanol and further fixed in methanol and DMSO for at least 24h. Sometimes brains were stored in this solution for few days until further processing. Afterwards brains were washed three times for 1h each in PBS and incubated in primary antibody solution (containing 5% heat-inactivated normal donkey serum (NDS), 75% PBS, 20% DMSO) for 2 days at 4°C. Subsequently samples were washed five times for 1h in PBS and exposed to secondary antibody solution for 24h also at 4°C. After five washes in PBS, brains were permeabilized in methanol (incubation three times for 20min) and cleared/mounted in 100% BABB (1 part benzyl alcohol (Cat. Nr. 8.22259, Merck) and 2 parts benzyl benzoate (Cat. Nr. 8.18701, Merck)). The mounting chambers were prepared with a 0.5µm thick silicone sheet (Cat. Nr. P-24745, Life technologies) shielded on both sides with a glass coverslip. All washes and incubations were done in a rotating/shaking device to allow better permeabilization of the different solutions.

3.9.3 Image acquisition and processing

Immunohistochemistry images were acquired with an Olympus FV1000 cLSM system (Olympus), using the FW10-ASW 4.0 software (Olympus). The system was equipped with laser diodes 405nm, 559nm and 635nm and a multi-line Argon laser (458nm, 488nm, 515nm, Showa Optronics Co.). Color adjustments were performed in the acquisition software, or using Image J or Adobe Photoshop.

3.10 Quantifications

Unless otherwise stated in the figure legends, all the quantifications from fixed analysis were done in a minimum of three animals per experimental condition, four sections per animal. Assessment of co-staining for two or more markers was done using the FW10-ASW 4.0 software, by analyzing all the individual z-planes of a z-stack. To quantify distances of cells to the telencephalic VZ, also with the FW10-ASW 4.0 software, a line was traced and measured between the cell and the closest point at the VZ. In the quantifications of proliferating PSA-NCAM cells after injury, all the PSA-NCAM/BrdU-double positive cells in a section were counted. In the analysis of cell-cycle re-entry the total number of double- or triple-positive cells was counted only in the pallial VZ. Quantifications are presented as the mean +/- standard error of the mean (SEM).

3.11 *In vivo* imaging

3.11.1 Animals and cell labeling

For *in vivo* imaging only animals in the *brassy* background were used, to avoid the interference of the auto-fluorescence from the pigment cells existing in wild type strains. Zebrafish lines used were *brassy, Tg(gfap:gfp)mi2001* crossed with *brassy* or *Tg(HuC:GFP)* crossed with *brassy*. Imaged cells were labeled by electroporation of a plasmid (or combination of plasmids) listed in section 3.3. Animals started to be imaged between 3 and 7 days after electroporation. To improve the visibility of the imaged cells, the skin was removed and the skull was thinned above the telencephalon area, using a micro-driller (Cat. Nr. K.1070, Foredom), once per week.

3.11.2 Experimental set up

Fish were anesthetized in 0.015% Tricaine and moved to the microscope stage where they were immobilized with a custom made holder (see Figure 4.6) and oxygenated water containing 0.012% Tricaine was pumped into the animal's mouth.

Imaging was performed with an Olympus FV1000 cLSM/MPE system, composed of a BX-61WI upright microscope (Olympus), laser diodes 405nm, 559nm and 635nm and a multi-line Argon laser (458nm, 488nm, 515nm, Showa Optronics Co.) and internal photomultiplier tube detectors. The system was also equipped with a multi-photon, near-infrared, pulsed MaiTai HP DeepSee laser, tunable from 690nm to 1020nm (Spectra Physics) and a FV10-MRG filter (barrier filter = 495–540 nm, dichromatic mirror = 570 nm, BA 575–630 nm). A water immersion objective (XL Plan N, 25x, 1.05NA, Olympus) was used. In the case of the multi-photon laser, an excitation wavelength of 935nm was used to excite the different fluorophores: GFP and Red Fluorescent Protein (RFP)-derived fluorophores. The optical sections were acquired with a resolution in the *x-y* dimension between 512 x 512 and 800 x 800 pixels and in the *z*-dimension at 2µm interval between single sections.

Areas to be imaged were chosen based on intensity of the fluorescent signal (which directly correlates with the distance of cells to the most dorsal part of the telencephalon), with brighter signal being preferred to fainter one. After each session, animals were allowed to recover in an aquarium with aerated water and placed in the normal aquarium until the following imaging session, two days later. The imaged area in each fish was reliably identified in the following imaging session based on the general distribution pattern of electroporated cells and/or pigment cells.

Both when animals died during the imaging procedure or after the completion of all the imaging sessions, the brains were dissected and treated according to section 3.9.2 for a confirmation of cells' identity.

3.11.3 Imaging analysis

Imaging analysis was performed in the FW10-ASW 4.0 software (Olympus) by careful examination through each individual z-plane of cells' identity (being *gfap:*GFP- or *HuC:*GFP-positive or negative), cells' morphology (with the presence or absence of a defined cellular process typical of RG cells), number of cells and distribution pattern of the analyzed and neighboring cells. In some cases, Imaris V6.3 software (Bitplane) was used to better visualize the three-dimensional aspect of the cells and confirm cell identity or number. When image quality was not satisfactory, animals or areas were excluded from the analysis. To classify the types of division, the identity of the daughter cells was assigned in the first time point when division was noticed.

3.12 Clonal analysis

Clonal analysis criteria were based on a previous publication (Rothenaigner et al., 2011). To ensure clonality, only brains with 5 or less clones per hemisphere (located in the pallium) were considered for quantifications. The analysis was performed in clones located exclusively in the dorsal telencephalon because in this region the migration of progeny is thought to be minimal and proliferating cells are sparsely located (Adolf et al., 2006; Grandel et al., 2006), which facilitates the distinction between individual clones and therefore improves the reliability of the analysis. A clone was considered a single cell or a group of cells within 10µm distance. Clones were classified as glial when all the cells presented a RG morphology, as non-glial when none of the cells had RG morphology and as mixed if there was at least one cell with RG morphology and one without. Immunostaining against GFAP, and in some cases the neuronal marker HuCD, was used to additionally assess cells' identity.

3.13 Statistical analysis

Statistical significance was tested with the Graphpad Prism software. A nonparametric Mann-Whitney test was used when the mean of only two groups was compared (e.g. for comparison of cells' distance from the VZ after electroporation, percentages of cells re-entering the cell cycle with and without injury). A nonparametric Kruskal-Wallis test was

used when the mean of more than two experimental groups was compared (eg. proliferating PSA-NCAM-positive cells at different time-point after injury). For *in vivo* imaging analysis, a Chi-squared test was used, to evaluate the differences in the relative proportion of several categorical variables (e.g. types of cell behavior) between different groups (control versus injury).

4 Results

4.1 Analysis of neuroblast proliferation after injury

Due to the continuous life-long and widespread adult neurogenesis and the high regenerative capacity, zebrafish is an attractive model to study mechanisms of NSC regulation and proliferation in homeostasis and regeneration.

Some pioneering work (Ayari et al., 2010; Baumgart et al., 2012; Kroehne et al., 2011) has established an injury model that damages the telencephalic parenchyma (composed mostly of neurons, see Figure 1.4A), with minimal damage in the ventricular proliferative zones containing neural stem/progenitor cells. Common to all the studies, the injury was followed by increased proliferation of cells in the VZ and the telencephalic parenchyma, generation of new neurons in the injured parenchyma and remarkable tissue restoration (Ayari et al., 2010; Baumgart et al., 2012; Kroehne et al., 2011). To better understand the regeneration process at the cellular level, these studies characterized the cell types that proliferated in response to injury. Generally, in the telencephalic parenchyma most of the proliferating cells included immune cells (4C4- or L-plastin-positive), cells in the oligodendrocyte lineage and endothelial cells, probably engaged in the angiogenesis process (Baumgart et al., 2012; Kroehne et al., 2011). At the VZ, on the other hand, many of the proliferating cells were *gfap:*GFP-positive RG cells (Baumgart et al., 2012; Kroehne et al., 2011).

However, a detailed quantification of all these types of proliferating cells revealed that additional BrdU-positive cells exist, that are negative for all the previously used markers. (Baumgart et al., 2012). This observation suggested the existence of additional cell populations that might be engaged in the regenerative process. Therefore it was important to evaluate the proliferative response of other cells. An obvious candidate population was the neuroblasts population, expressing PSA-NCAM (see section 1.1.2.1 and Figure 1.4)

To assess the proliferation rate of neuroblasts in response to injury, animals received two intraperitoneal injections of the DNA-base analogous, BrdU, 4h prior to sacrifice to label PSA-NCAM-positive neuroblasts in the S-phase. BrdU- and PSA-NCAM-positive cells were counted at different time-points after injury (Figure 4.1). Curiously, even after injury, these cells were found exclusively at the VZ and never in the telencephalic parenchyma (Figure 4.1A-B and (Baumgart et al., 2012)). Even though PSA-NCAM-positive cells constituted the majority of BrdU-positive cells at all time-points verified, when compared to the other cell

types investigated (Baumgart et al., 2012), there was no significant difference in the absolute number of PSA-NCAM and BrdU double-positive cells between the intact and the injured animals (Figure 4.1C). This observation indicates that PSA-NCAM-positive neuroblasts do not increase their proliferation in response to injury.

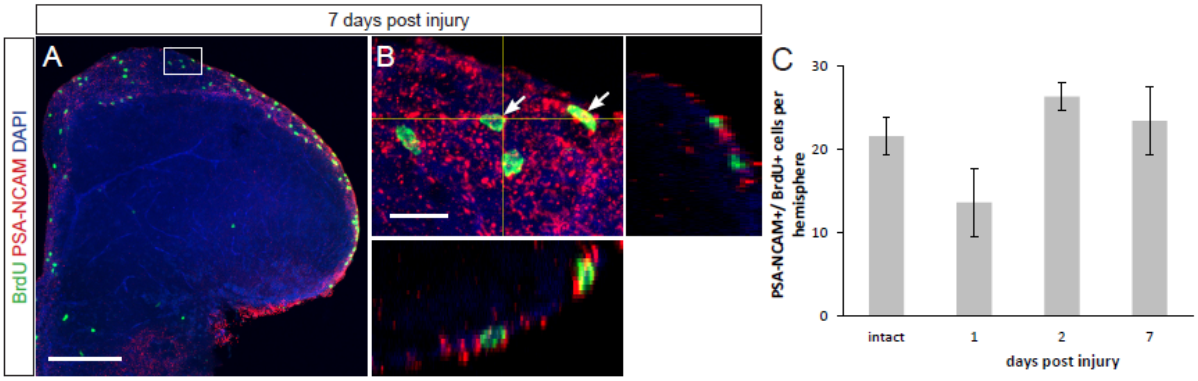

Figure 4.1: Proliferation of PSA-NCAM-positive neuroblasts does not significantly change after injury. (A) Confocal picture of a coronal hemi-section of the telencephalon of an adult zebrafish at 7 dpi, labeled for PSA-NCAM, BrdU and DAPI to identify proliferating neuroblasts. (B) Magnification of the boxed area in A, depicting an orthogonal projection of a confocal z-stack to highlight a cell positive for both PSA-NCAM and BrdU. White arrows point to double-positive cells. In both panels A and B dorsal is up. Scale bars: A-100µm, B-10µm. (C) Quantification of the total number of double-positive cells per section per hemisphere in intact brains and at different time points after injury. Data are shown as mean +/- SEM; n=3 animals; $p>0.05$ (non-significant), Mann-Whitney test. [Data published in (Baumgart et al., 2012)].

The absence of increase in neuroblasts proliferation after injury raised the question of how is the neuronal replacement achieved in this particular model.

One possibility is that these cells contribute with new neurons to the injured parenchyma without undergoing proliferation but simply by migrating to the injury site and differentiating. Indeed, PSA-NCAM-positive cells that were negative for the S-phase marker BrdU could be observed (Figure 4.1B), and the reaction of these cells was not analyzed in this study (Baumgart et al., 2012). Additionally it is possible that the SAPs, another non-glial progenitor type at the VZ that is PSA-NCAM-negative (see Figure 1.4), could play a role in the regenerative process. Finally, RG cells can also have a pivotal function in the neuronal regeneration process, since they were shown to increase proliferation after injury and, in the case of larger injuries, to generate progeny that contributes with new cells to the parenchyma (Baumgart et al., 2012; Kroehne et al., 2011). Interestingly, in the injury model by Baumgart and colleagues the maximum of RG cells' increase in proliferation was at 7dpi, when the tissue already appears completely restored (Baumgart et al., 2012), raising the additional question of what is the role of this delayed reaction of RG. In the larger injury model by Kroehne and colleagues, newborn neurons in the injured parenchyma were shown to derive

from *her4.1*:GFP-positive cells, which belong to the RG lineage (Kroehne et al., 2011). However this genetic lineage tracing technique did not allow the distinction between RG cells and their progeny (SAPs and neuroblasts), since both the RG cells (upon Cre-mediated recombination) and their progeny (upon generation from RG cells) are GFP-positive.

To clarify these questions and distinguish the roles of RG and non-glial progenitors in neuronal regeneration, it is important to differentially label these progenitor cell types for a better analysis of their individual response to injury.

4.2 Differential labeling of RG and non-glial progenitors

To access the role of the different progenitors in the regeneration process, a differential labeling of RG cells and SAPs was implemented.

RG cells in the adult zebrafish pallium are directly contacting the ventricle and, at a given time, the vast majority of them is in a quiescent, non-proliferative state (Adolf et al., 2006; Chapouton et al., 2010; Rothenaigner et al., 2011) (Figure 1.4B). Due to their location at the brain surface, it is predictable that transfection of a reporter plasmid using lipofectamine (lipofection) is an adequate technique to label RG cells.

Indeed, when a construct expressing GFP was injected together with lipofectamine (see methods, section 3.6) in the telencephalic ventricle of adult fish, 91% of the labeled cells at 2days post-labeling (dpl) were GFAP+ (n=191 cells), indicating their RG phenotype (Figure 4.2). Importantly, the majority of RG cells were distributed as single cells (Figure 4.2F).

To label the sub-apically located non-glial progenitors (SAPs and neuroblasts), a retrovirus expressing GFP under the control of the Ef1α promoter was injected into the telencephalic ventricle, as in a previous publication (Rothenaigner et al., 2011). The rational to use this technique is that SAPs and neuroblasts proliferate faster than RG cells (Adolf et al., 2006; Ganz et al., 2010; März et al., 2010a; Rothenaigner et al., 2011), and therefore, since the retrovirus only transduces dividing cells, the probability of being targeted by retrovirus is increased. In agreement with this prediction, the analysis of 11 animals at 2dpl showed five GFP-positive cells (Figure 4.3), three of which were PCNA-positive/GFAP-negative (Figure 4.3C) and two had glial identity (Figure 4.3D), further supporting the idea that retrovirus preferentially targets SAPs/neuroblasts.

Despite the low number of cells observed at this short time-point following injection, these observations are in line with the quantifications at 7dpl from Rothenaigner and colleagues (Rothenaigner et al., 2011).

This analysis demonstrates that RG cells are specifically labeled by lipofection, while retroviral transduction permanently labels both RG and non-glial progenitors (that can be SAPs or neuroblasts). Therefore, the comparison of the reaction of cells labelled with these two different techniques allows the dissection of the individual reaction of RG and non-glial progenitors to the injury.

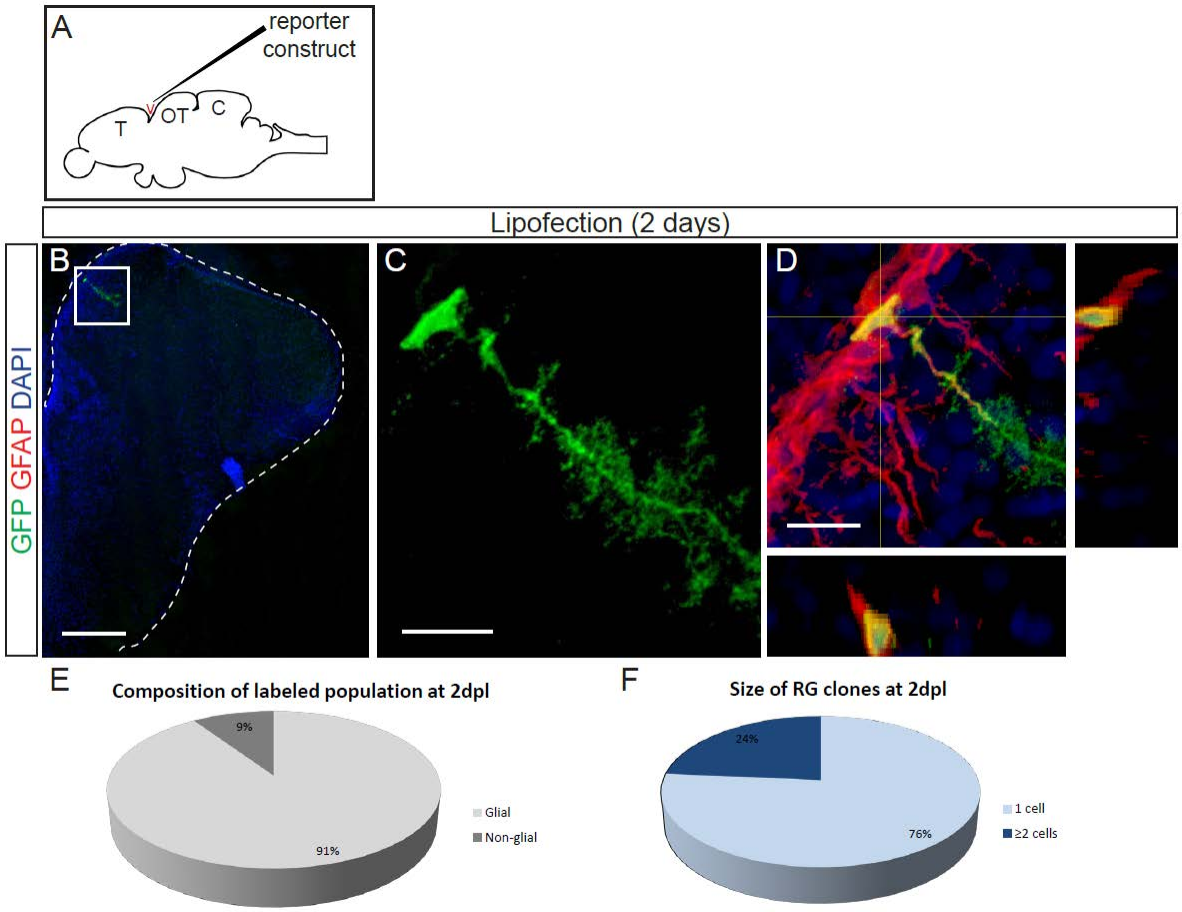

Figure 4.2: The vast majority of cells targeted by lipofection are RG cells. (A) Sagittal view of the zebrafish brain, exemplifying the site of plasmid injection, at the telencephalic ventricle (v). (B) Confocal picture of a coronal hemi-section of an adult zebrafish telencephalon, two days after lipofection of a pCS-GFP plasmid, stained for GFP and DAPI. The dashed line marks the limits of the hemisphere. (C) High magnification of the boxed area in B, showing a single RG cell. (D) Orthogonal projection of the cell in C, highlighting the co-localization of GFP and GFAP immunostaining. In all panels dorsal is up. Scale bars: A-100µm, B and C-10µm. (E) Pie chart depicting the proportion of GFP-positive cells at two days post lipofection that are co-labeled with GFAP (glial) or are GFAP-negative (non-glial); n=191cells from 10 animals. (F) Pie chart depicting the proportion of RG cell clones composed of a single RG or more than two RG cells; n=110clones from 10 animals. Abbreviations: C-cerebellum, OT-optic tectum, T-telencephalon, v-ventricle.

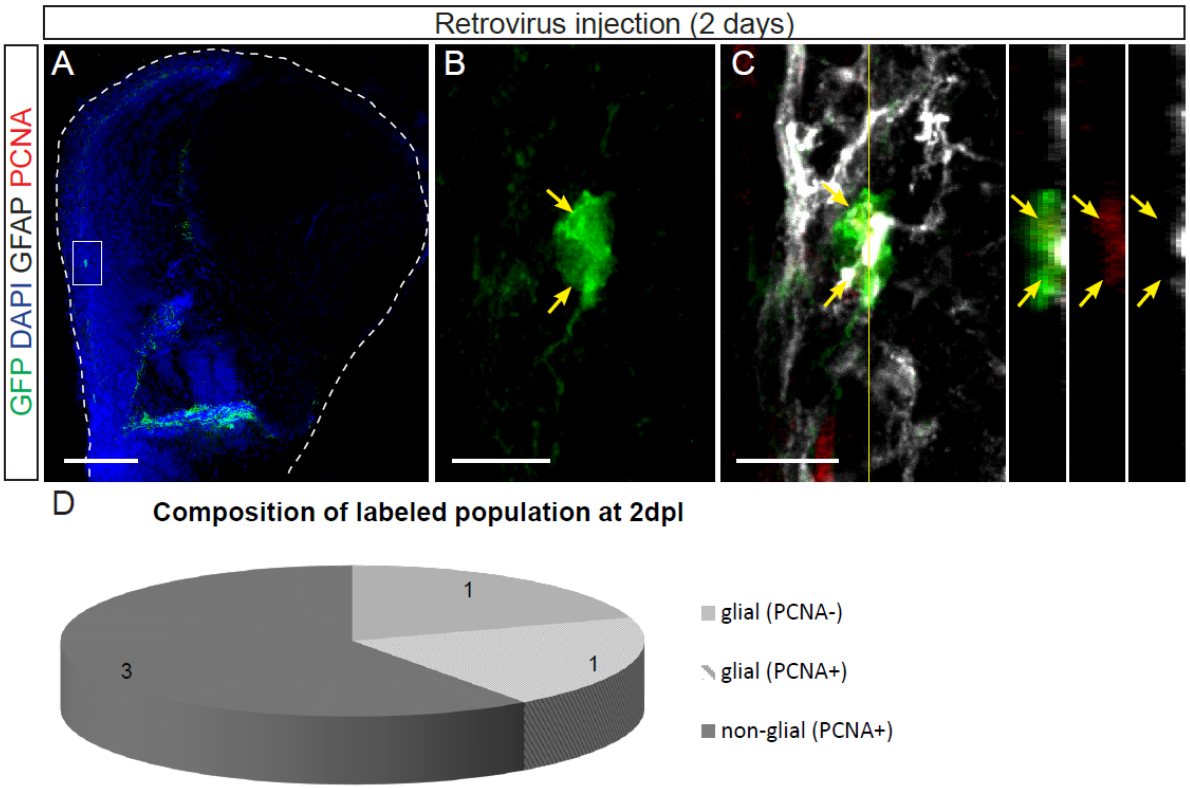

Figure 4.3: Retrovirus transduction preferentially targets non-glial cells. (A) Confocal picture of a coronal hemi-section of an adult zebrafish telencephalon, two days after retrovirus injection, stained for GFP and DAPI. (B) High magnification of the boxed area in A, displaying two GFP-positive cells (yellow arrows). (C) Orthogonal projection of the cells in B, showing co-localization of GFP and PCNA immunostaining, but absence of GFAP labeling. In all panels dorsal is up. Scale bars: A-100µm, B and C-10µm. (D) Pie chart depicting the identity of GFP-positive cells at 2dpl; n=5cells from 11animals.

4.3 Identification of the progenitor cell type generating new neurons in the brain parenchyma after injury

During constitutive neurogenesis, the neurons generated from the progenitors at the VZ are deposited immediately adjacent to this proliferative zone, and do not migrate to the parenchyma. After injury of the telencephalic parenchyma, however, newborn neurons are deposited far from the VZ, at the injury site (see Figure 1.5).

To investigate the specific contribution of the different progenitor cell types to the neuronal repair, lipofection and retroviral transduction were used to differentially label RG or non-glial progenitors, and to follow the position and fate of their progeny over time (Figure 4.4). Injury was performed one day after the labeling and analysis was done at 14dpi (Figure 4.4B). The migration of neuronal progeny to the parenchyma was assessed by measuring the distance of single non-glial cells to the closest point of the VZ. These cells were identified by being negative for the RG marker GFAP. To set the baseline migration of neuronal progeny

from the VZ during constitutive neurogenesis (red line in the graph in Figure 4.4M), the distances of neuronal progeny to the VZ were also measured in control brains (Figure 4.4M).

When retrovirus labeling was used, non-glial cells were found not only close to the VZ, as occurs during constitutive neurogenesis, but also in the previously injured parenchyma, distant from the VZ where they originated (Figure 4.4C-E). In the cases when HuCD staining was performed, the neuronal identity of the parenchymal cells was confirmed (Figure 4.4D). These observations indicate that cells labeled by this technique respond to injury and contribute to replace the neurons in the damaged area. Nonetheless, since retrovirus can also label RG cells (Figure 4.3), it is only possible to discriminate between the response of non-glial progenitors and RG by comparing these results to the ones obtained with labeling by lipofection, which specifically targets RG (Figure 4.2).

When cells were labeled by lipofection, all the GFP-positive, non-glial cells at 14dpi were restricted to the first 15 μm away from the VZ (Figure 4.4F-H,M), which is within the distance of migration of progeny during constitutive neurogenesis (red line in Figure 4.4M). These results indicate that within this time frame, there is no migration of RG-derived cells to the injured parenchyma. This difference in non-glial cell location suggests a distinct behavior of RG cells and non-glial progenitors, in which the later cell type reacts to injury by generating progeny that migrates to the parenchyma, contributing to the regenerative neurogenesis.

In homeostasis, RG cells generate non-glial progenitors that are involved in constitutive adult neurogenesis (Figure 1.4C and Figure 4.4A) (Rothenaigner et al., 2011). However, when lipofection was used to label RG cells, no RG-derived progeny was observed in the previously injured telencephalic parenchyma (Figure 4.4F-H). The reason for this lack of migration could be that the labeled RG cells take time to generate the non-glial progenitors and after their production, the instructive signals from the injury site are not present anymore to induce their migration. In the retrovirus labeling paradigm non-glial progenitors are already present when the injury is performed, and therefore can immediately respond to the signals.

To test this possibility, a delayed injury paradigm was implemented (Figure 4.4I), in which RG cells labeled by lipofection were given time to generate SAPs and neuroblasts for a week. Seven days after labeling, the injury was performed and the position of GFP-positive, non-glial cells relative to the VZ was measured. Similar to the observations made with the retrovirus labeling technique, some neurons (GFP-positive, GFAP-negative, HuCD-positive) were found in the telencephalic parenchyma using this delayed-paradigm (Figure 4.4J-M),

having migrated a larger distance than they normally do during constitutive neurogenesis (Figure 4.4M)

All together these results suggest that non-glial progenitors (SAPs and neuroblasts) present at the VZ directly contribute to regenerative neurogenesis and that their reaction occurs shortly after injury, probably while the instructive signals from the injury site are still present. On the other hand, these signals seem to not last long enough to instruct the migration of late-generated, RG-derived non-glial cells.

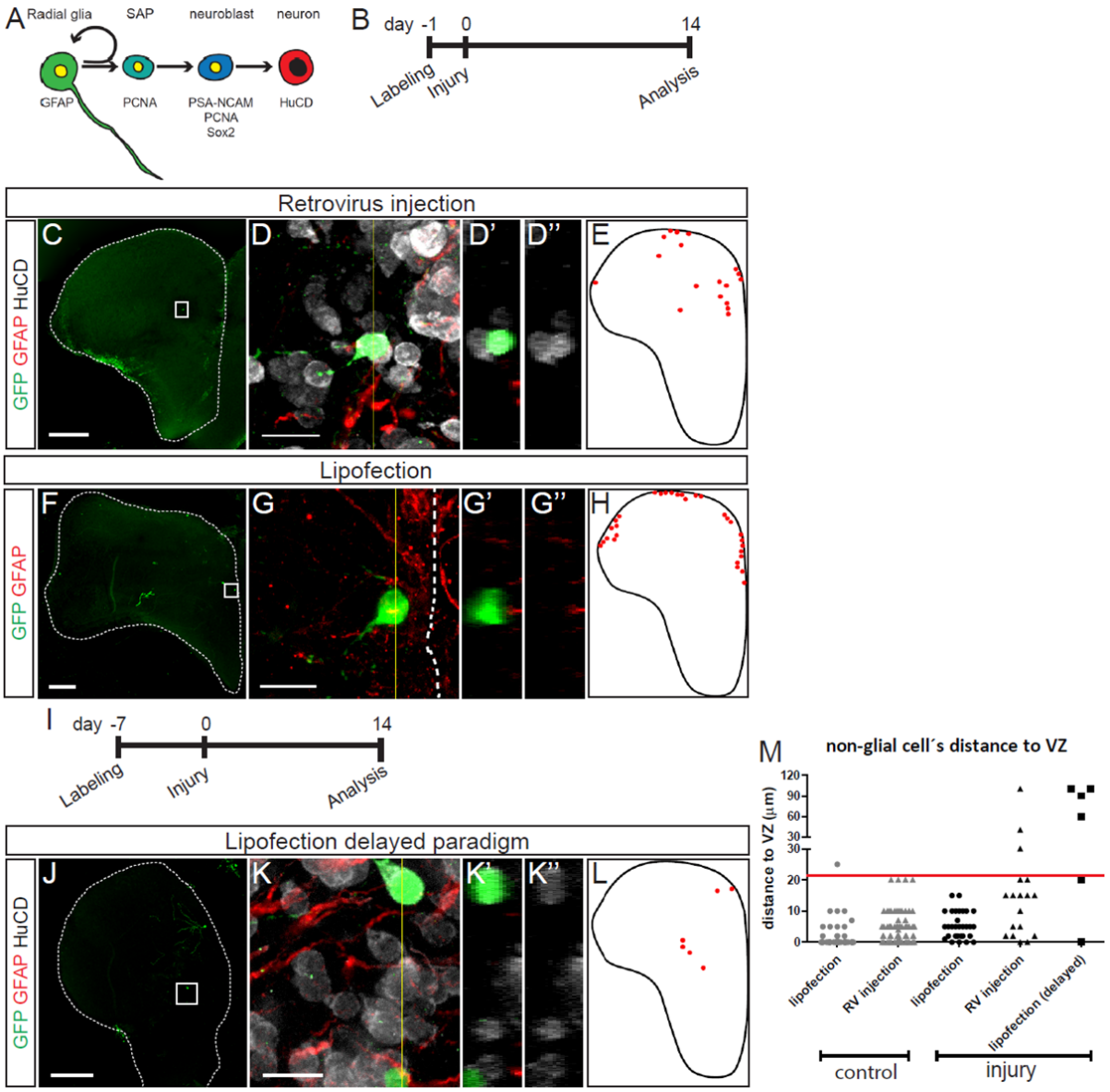

Figure 4.4: Non-glial progenitors react to injury by migrating to the parenchyma and contributing to neuronal replacement. (A) Simplified illustration of the neuronal lineage progression in the dorsal VZ and some markers expressed by each cell type. Note that there are also PSA-NCAM-positive neuroblasts that do not proliferate (Baumgart et al., 2012) and could likewise generate neurons. (B) Scheme of the time schedule implemented for analysis of cell location after injury. (C) Confocal image of an injured telencephalic section 14dpi after RV labeling. (D) Magnification of the boxed area in C, depicting a reporter-positive non-glial cell in the parenchyma. D' and D'' are orthogonal projections to certify the non-glial identity of the cell (GFAP-negative and HuCD-positive). (E) Scheme representing the location of individual non-glial cells labeled with retrovirus injection at 14 dpi. (F) Confocal image of an injured telencephalic section after labeling with lipofection at 14dpi. (G) Magnification of the boxed area in F, depicting a non-glial cell close to the VZ. The dashed line marks the VZ. G' and G'' are orthogonal projections to certify the non-glial identity of the cell (GFAP-negative). (H) Scheme representing the location of individual non-glial cells labeled with lipofection at 14 dpi. (I) Scheme of the time schedule implemented for analysis of cell location after injury in the "delayed paradigm". (J) Confocal image of an injured telencephalic section, 14dpi after labeling with lipofection in the delayed paradigm. (K) Magnification of the box in J, depicting non-glial cells in the parenchyma. K' and K'' are orthogonal projections to certify the non-glial identity of the cells (GFAP-negative and HuCD-positive). (L) Scheme representing the location of individual non-glial cells labeled in the lipofection delayed paradigm. In all panels dorsal is up. Scale bars: C,F,J-100µm; D,G,K-10µm. (M) Graph depicting the distances of individual non-glial cells to the VZ, in all the labeling paradigms used, in control conditions and after injury. Each symbol represents one cell. The red line marks the limit of non-glial cell deposition during constitutive neurogenesis, as observed in control conditions. Note that with retrovirus (RV) injections and in the lipofection delayed paradigm, some non-glial cells migrate far beyond this limit.

4.4 *In vivo* imaging of RG cell behavior

The results presented above show the role of non-glial progenitors in migrating and re-populating the telencephalic parenchyma after injury (Figure 4.4C-E,M). Nevertheless, it is known that RG cells do react to injury by increasing proliferation (Baumgart et al., 2012; Kroehne et al., 2011) and that during homeostasis they are the NSCs in the adult zebrafish telencephalon (Adolf et al., 2006; Rothenaigner et al., 2011).

Consequently, it is important to further explore the behavior of these cells in order to understand how the NSCs in the adult zebrafish brain contribute to the regeneration process.

The best approach to investigate how a cell behaves *in vivo* is to directly observe it in a continuous mode, by means of imaging techniques. Towards this aim, RG cells in the adult zebrafish telencephalon were labeled (section 4.4.1) and an *in vivo* imaging technique was established to follow these cells in adult animals (section 4.4.2), taking advantage of the location of RG at the outer surface of the telencephalon in this animal model (Figure 1.4). For a good understanding of how the behavioral pattern of RG cells changes in response to injury compared to non-injury conditions, *in vivo* imaging was also performed in intact animals (section 4.4.3). In fact, the characterization of RG cells during homeostasis so far had only been done at the population level (Adolf et al., 2006; Ganz et al., 2010; März et al., 2010a) and by using clonal analysis in fixed brain sections (Rothenaigner et al., 2011), thus a visualization of the behavior of the adult NSCs in the intact vertebrate brain was still lacking. Therefore, this imaging technique could be used to observe for the first time the activity of

adult NSCs in their niche *in vivo* in a vertebrate brain, not only during constitutive neurogenesis but also as part of an efficient regenerative response (section 4.4.3).

4.4.1 Cell labeling for *in vivo* imaging

To mark cells for *in vivo* imaging, a strong fluorescent signal is needed, that is constitutively expressed in different cell types (so that it is kept in case of cell changes its fate). Additionally, cell fate should be easily assessed by morphology and/or co-expression of cell-specific markers. Lastly, cell labeling should be sparse enough to allow identification of the same cells over time, but dense enough to ensure there is a considerable number of cells to be followed.

Considering these criteria, transfection of RG cells by injection of a plasmid into the telencephalic ventricle can be an adequate method (Figure 4.5). When using lipofection, the number of labeled cells was reasonably small, a limitation that would make the whole imaging protocol very inefficient (Figure 4.5A).

To overcome this problem, transfection was performed by electroporation. As observed in Figure 4.5B-C, the number of labeled cells by electroporation was considerably higher than with lipofection, making this an appropriate transfection method for *in vivo* imaging. The plasmids used drove the expression of fluorescent proteins (GFP, TdTomato, mCherry) under the control of the ubiquitous promoters CMV or ubiquitin (see section 3.3). No differences in expression or cell behavior were observed between these two promoters (data not shown).

In order to characterize the population of cells labeled with this transfection technique, the identity of electroporated cells was assessed at two days following electroporation by immunohistochemistry against GFAP, to identify RG cells, and HuCD, to mark neurons (Figure 4.5D). As shown in Figure 4.5E, 48% of the cells were GFAP-positive, being this the major population labeled by this method. In contrast to lipofection (Figure 4.2D), electroporation additionally targets a considerable proportion of HuCD-positive cells (27%), 26% of marker-negative cells (which can be SAPs or neuroblasts), and an unexpected small population (5%) of GFAP/HuCD double positive cells (Figure 4.5E), which could be fast differentiating glial cells that had not yet time to down-regulate GFAP.

Since the major goal was to follow the behavior of RG cells *in vivo*, attention was focused on cells with RG morphology, i.e., with cell body located at the VZ and a process extending into the telencephalic parenchyma. The identification of cells with RG morphology at 2dpl (Figure 4.5F) showed that the vast majority (85%) of cells with RG morphology are indeed GFAP-positive, validating the morphological criteria as an acceptable criteria to

identify RG cells. On the other hand, cells without RG morphology were mostly non-glial cells (73%, Figure 4.5G), further certifying this criteria as a faithful indicator of cell identity.

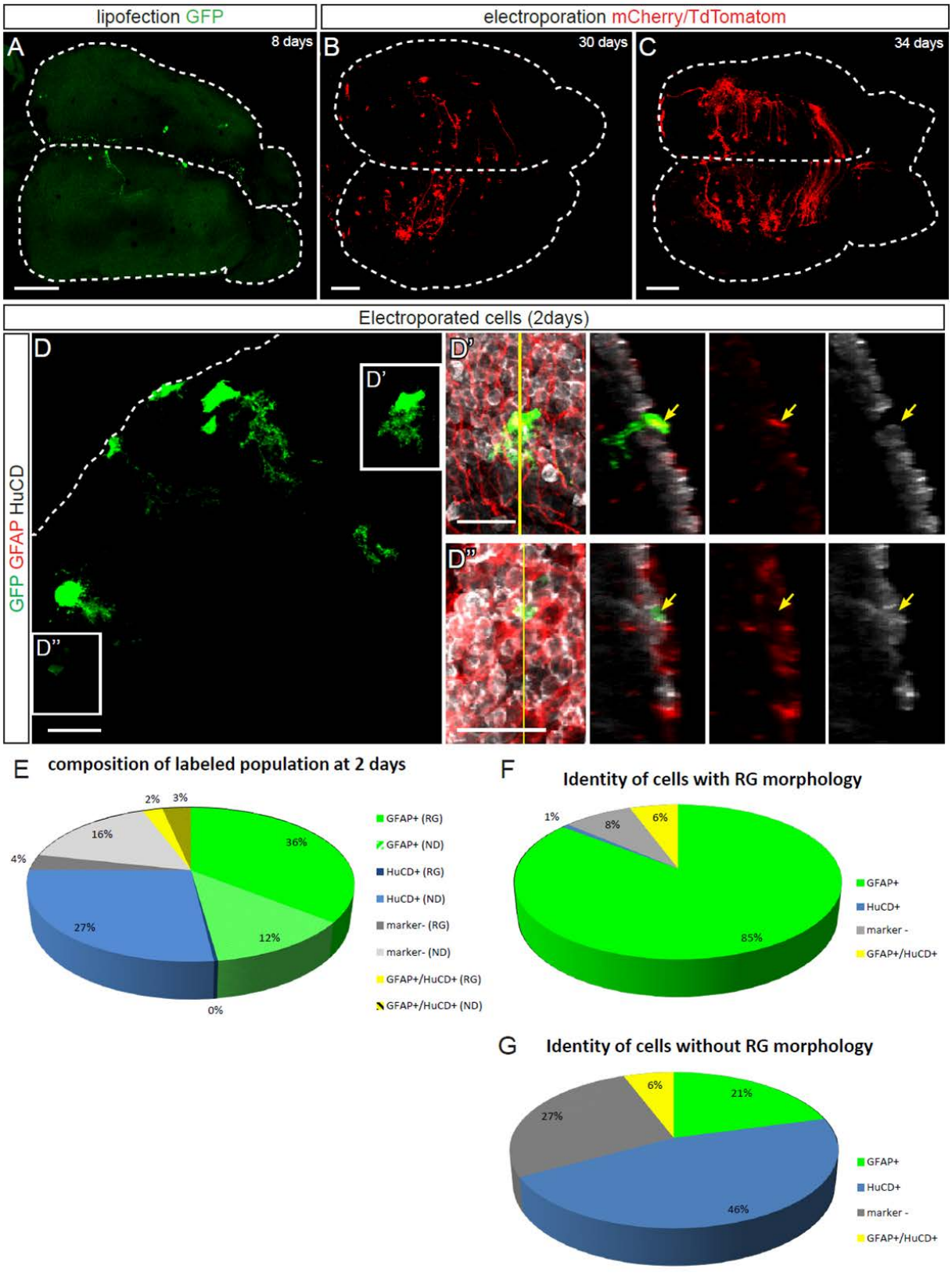

Figure 4.5: Electroporation is an adequate method to label RG cells for *in vivo* imaging. (A) Confocal picture of a whole zebrafish telencephalon at 8 days after labeling with lipofection of a pCS-GFP reporter construct. Note the presence of few labelled cells. (B) and (C) Confocal pictures of whole telencephali 30 (B) and 34 (C) days after labeling with electroporation of a ubi:mCherry (B) or a pCS-TdTomatom (C) construct. Note the high number of RG cells marked. A, B and C-Dorsal view, rostral is right and caudal is left. (D) Example of different cells labelled by electroporation of a pCS-GFP construct (2days), in a telencephalic section stained for GFP, GFAP and HuCD. The dashed line marks the limit of the telencephalic section. (D') Magnification of the boxed area in D, depicting an example of RG cell (GFAP-positive and HuCD-negative). (D'') Magnification of the boxed area in D showing an example of non-glial cell (GFAP-negative and HuCD-positive). Scale bars: A, B, C-100µm D, D' and D''-20µm. (E) Pie chart depicting the proportion of each cell type labeled by electroporation, at 2 dpl; n=297 cells. (F) Identity of cells with RG morphology, observed at 2 days after electroporation; n=124 cells. (G) Identity of cells without RG morphology, observed at 2 days after electroporation; n=173 cells. Abbreviations: RG-cells with RG morphology, ND-cells without RG morphology.

Based on the above quantifications (Figure 4.5F-G), cells followed by *in vivo* imaging were classified as RG when they had a RG-like morphology, whereas cells without a clear cellular process were classified as non-glial. In most *in vivo* imaging experiments, the reporter construct was injected in the transgenic fish *Tg(gfap:gfp)mi2001* (Bernardos and Raymond, 2006) crossed with *brassy* (Kelsh et al., 1996), which expresses GFP under the control of the zebrafish *gfap* upstream regulatory elements, and therefore labels RG cells. The pattern of *gfap:*GFP-positive cells was used to help in the identification of the same reporter-positive cells in different imaging sessions.

4.4.2 Establishment of the *in vivo* imaging set up

Despite being a widely used procedure in the developing zebrafish, *in vivo* imaging is a more demanding technique in the adult animal, since the adult zebrafish are not transparent and cannot be immobilized by embedding in agarose like the embryos and larvae. Therefore, to establish the *in vivo* imaging method in adult zebrafish (Figure 4.6), several challenges needed to be overcome:

-The skin area above the telencephalon should be as transparent as possible;

-The animals should be kept completely immobilized during the imaging session;

-The animals should be kept alive during and over many different imaging sessions.

The first requirement was achieved by using fish in the genetic background *brassy* (Kelsh et al., 1996), which lack melanin and have dull iridophores. Additionally, to reduce the thickness that the light has to penetrate until it reaches the target cells, the skull area above the telencephalon was mildly thinned with a micro-driller. This skull-thinning procedure was preferred to the implantation of a cranial window in order to avoid the immune response of

microglia, as reported in rodents (Xu, 2007). Moreover, since the RG cells are located immediately underneath the meninges, they would be easily damaged during such a procedure.

To keep the fish immobilized during the imaging session, a low concentration (0.015%) of Tricaine was used and they were introduced in a holding device that keeps their body immobilized while leaving the head free to be accessed by the imaging objective. In order to maintain the animals alive, oxygenated water containing 0.012% of Tricaine was constantly pumped into the fish's mouth, to assure the high oxygen levels at the gills (see Figure 4.6C).

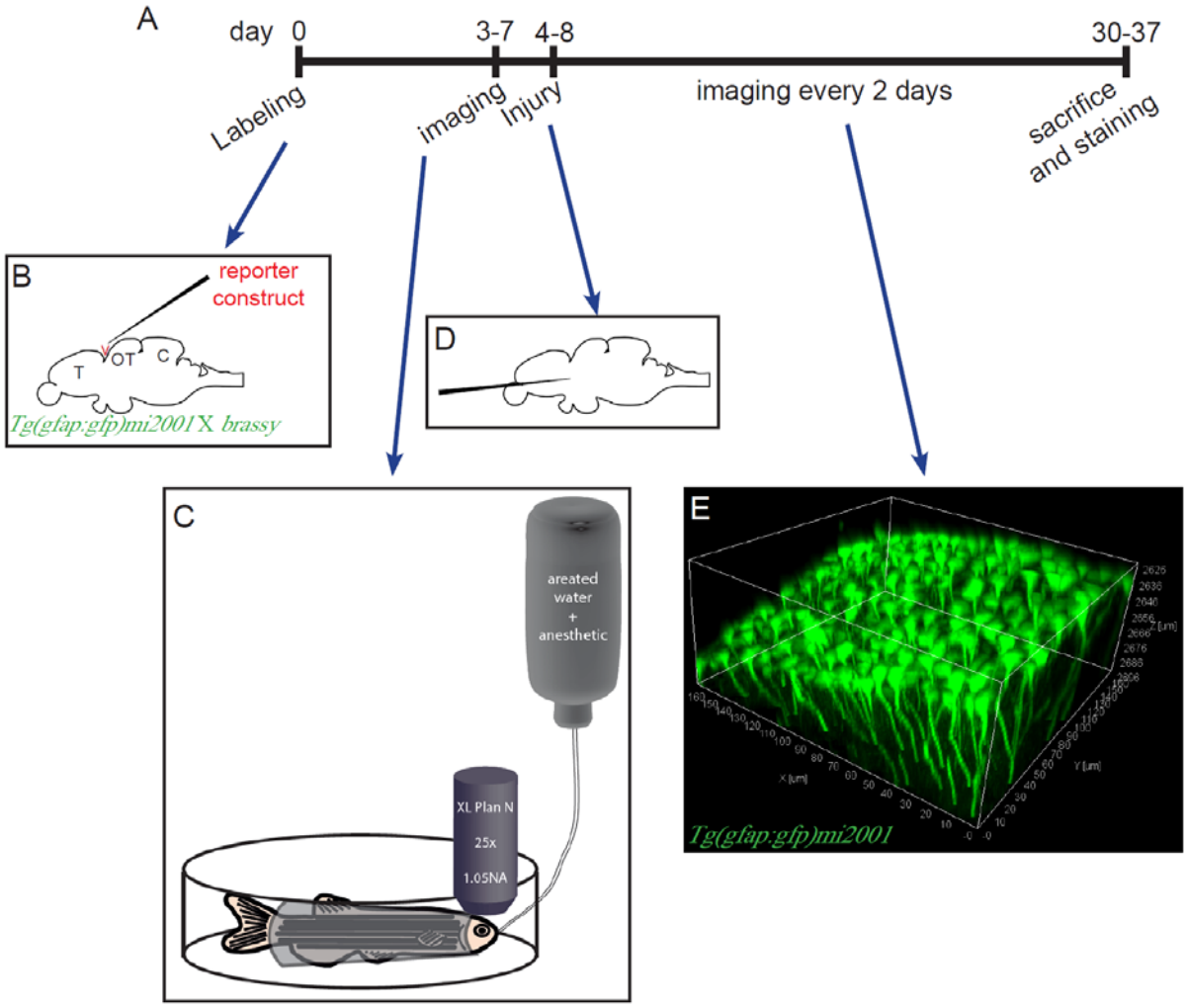

Figure 4.6: Scheme of the experimental set up used for *in vivo* imaging. (A) Representation of the time schedule implemented for *in vivo* imaging. (B), (C), (D) Illustrations of the procedures for cell labeling (B), imaging the adult zebrafish (C) and injuring the telencephalon (D). (E) Three-dimensional view of RG cells in the telencephalon of a live adult zebrafish from the *Tg(gfap:GFP)* line, obtained in an *in vivo* imaging session with 2-photon laser. Abbreviations: C-cerebellum, OT-optic tectum, T-telencephalon, V-ventricle.

Using this procedure, it was possible to keep the adult zebrafish alive, for at least the time necessary to image one area in the telencephalon per session. The usage of the *brassy*

fish and the skull thinning procedure made it possible to obtain pictures with a satisfactory resolution, either using the multi-photon (Figure 4.6E) or confocal microscopy.

4.4.3 Behavior of RG cells during constitutive neurogenesis and regeneration

To analyze the continuous behavior of RG *in vivo*, animals were electroporated to label single cells feasible to be followed (as explained in section 4.4.1) and immobilized under the microscope (section 4.4.2). The cells selected to be imaged were chosen based on the RG morphology (having a cell body at the VZ and extending a process deep to the parenchyma) and on the closest location to the most dorsal surface of the telencephalon, which contributes to a stronger fluorescent signal, more easily observable. Afterwards, one single picture per area was taken, and the animals were allowed to freely swim until the following imaging session. The same area was found in every session based on the general distribution pattern of electroporated cells. The morphology and the number of cells were registered at each session, allowing the continuous monitoring of RG cell behavior over time. After the last imaging session, animals were sacrificed, and the whole brains were cleared (see experimental procedures section 3.9.2) and stained for GFAP and/or HuCD to confirm the identity of the imaged cells.

In the present and in the following sections, the different types of behaviors of RG cells are described and exemplified with figures taken either in control or injured animals. Since each individual behavior looked the same in control or injury, only one example of each behavior is presented, regardless of its brain of origin.

Over the imaging time, RG cells exhibited different types of behavior: quiescence (Figure 4.7), division (Figure 4.8), direct neurogenesis (Figure 4.9 and Figure 4.10), death (Figure 4.11) and migration (Figure 4.12). The relative proportion of each behavior in control or injury conditions is shown in Figure 4.13.

Quiescent RG cells maintained their morphology, identity and position over the imaging time (Figure 4.7). In control conditions, cell quiescence was the most frequently observed behavior of RG cells (60.5%, Figure 4.13), demonstrating the highly quiescent nature of RG cells, in agreement with previous observations (Rothenaigner et al., 2011). After injury, however, cell quiescence represented only 16.5% of the observed cell behaviors (Figure 4.13).

In control conditions, 12.8% of RG cells divided during the observation period (Figure 4.8, Figure 4.13), a percentage that is comparable with previous studies (Chapouton et al., 2010; Rothenaigner et al., 2011). Remarkably, this proportion increased to 25.8% after injury

(Figure 4.13), confirming that RG cells at the VZ get activated by the injury-induced signals from the parenchyma and increase proliferation.

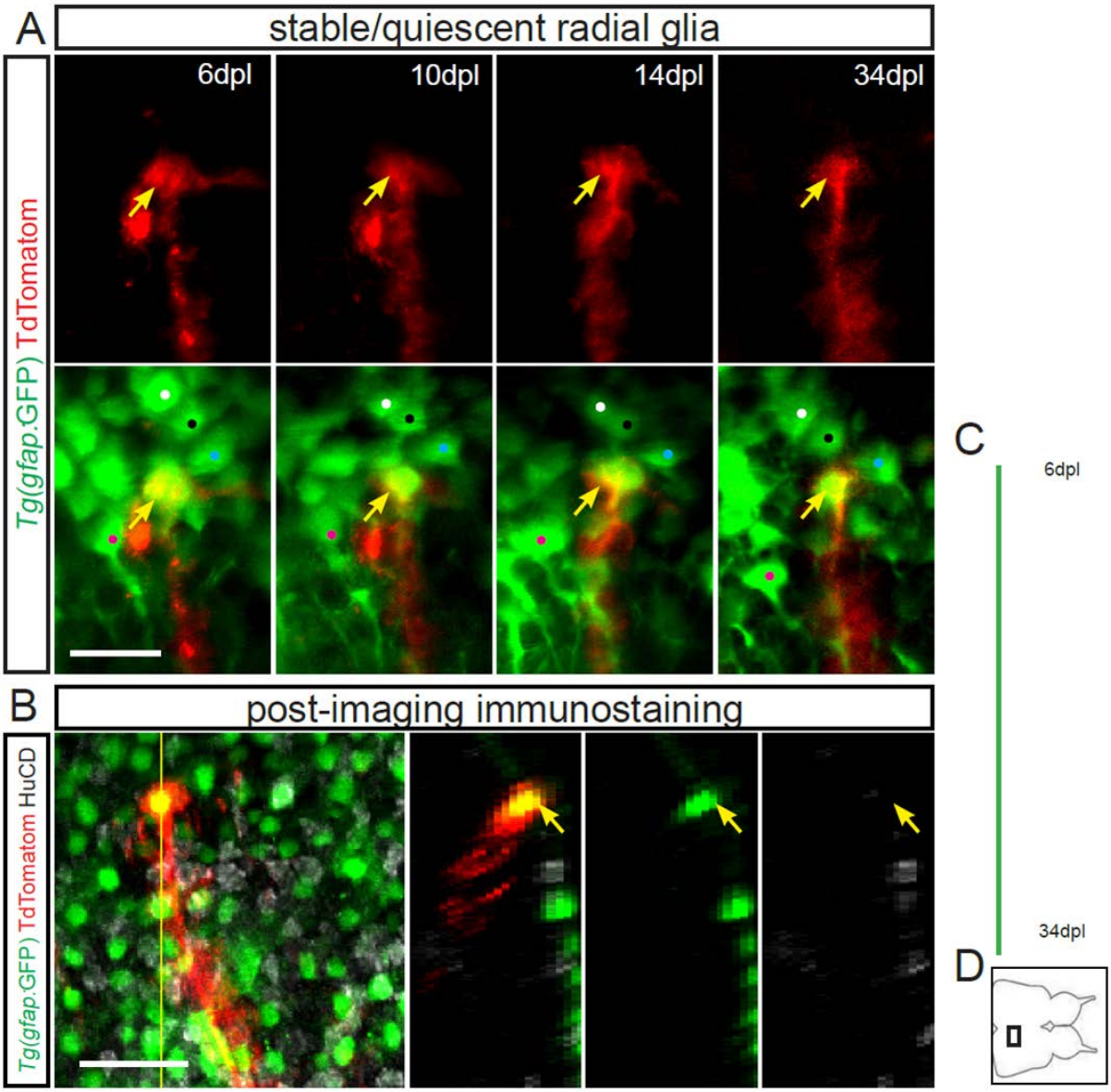

Figure 4.7: Example of a quiescent RG cell observed *in vivo* in a non-injured zebrafish. (A) Confocal images of the same TdTomatom-labeled RG cell at different time-points after labeling in the *Tg(gfap:GFP)* line. Yellow arrows point at the cell followed. Dorsal view, midline is up. The colored dots in the lower panels mark the same *gfap:*GFP-positive cells over the different time-points, and were used to help in the orientation and reliably find the same position. (B) Immunostaining in the whole brain for GFP, TdTomatom and HuCD at 34dpl, to confirm the cell's identity. Scale bars: A,B-20µm. (C) Lineage tree of the cell. Green line represents a RG identity (morphology and *gfap:*GFP expression). (D) Representative scheme of the telencephalon viewed from top. The black rectangle marks the area where this cell was imaged. Abbreviations: dpl-days post-labeling.

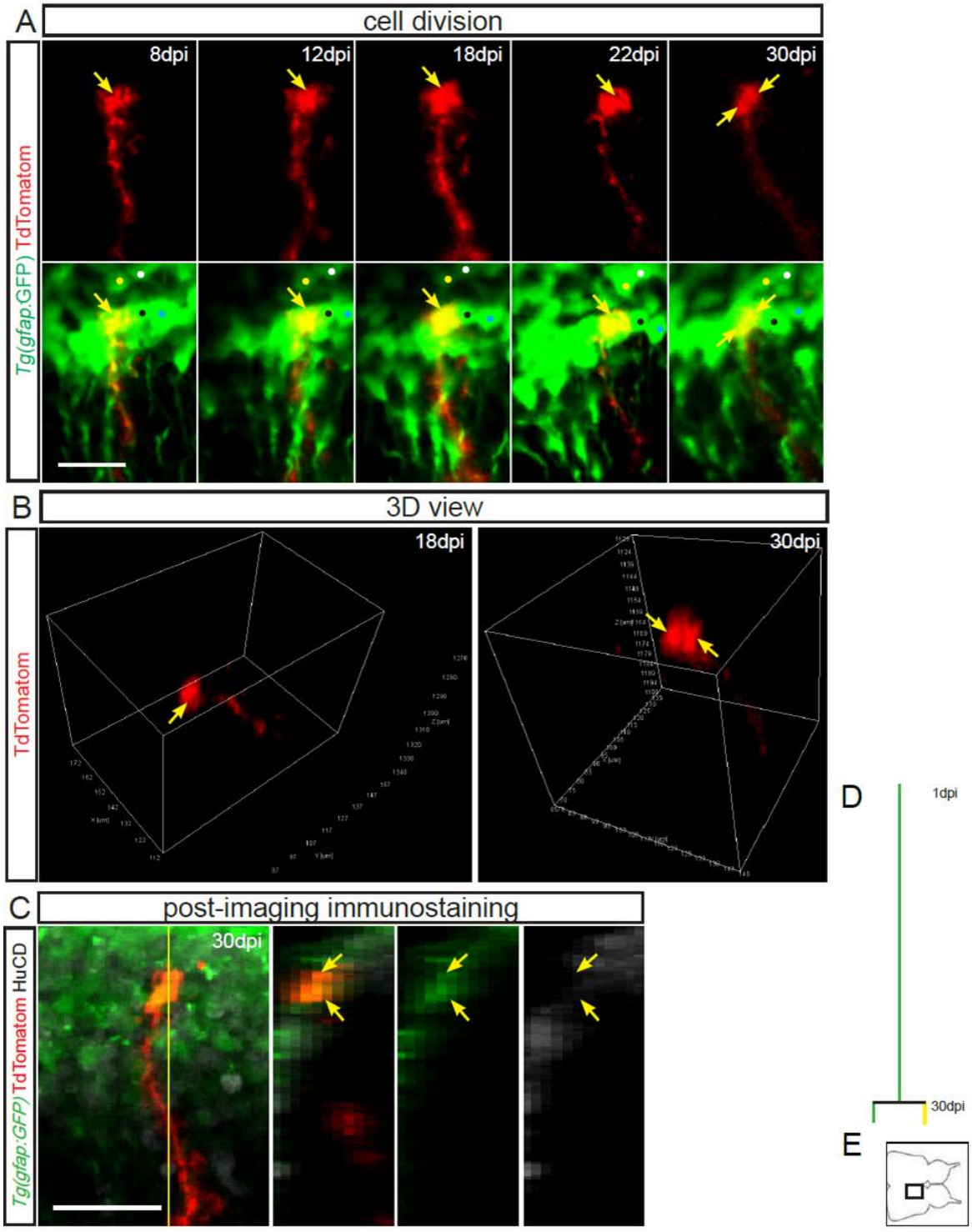

Figure 4.8: Example of a division of a RG cell observed *in vivo* in an injured zebrafish. (A) Confocal images of the same TdTomatom-labeled RG cell at different time-points after injury in the *Tg(gfap:GFP)* line. Yellow arrows point at single cells. Note that only one RG cell is present at 8, 12, 18 and 22dpi, but two cells are present at 30dpi. Dorsal view, midline is up. The colored dots in the lower panels mark the same *gfap:*GFP-positive cells over the different time-points, and were used to help in the orientation and reliably find the same position. (B) Three-dimensional views of the cells at two different time-points, used for a better visualization of the number of cells. (C) Immunostaining in the whole brain for GFP, TdTomatom and HuCD at 30dpi, to confirm the identity of the cells. Scale bars: A,C-20µm. (D) Lineage tree of the cell. Green line represents a RG identity (morphology and *gfap*:GFP expression) and yellow line represents a non-glial identity (no RG morphology and *gfap*:GFP expression). (E) Representative scheme of the telencephalon viewed from top. The black rectangle marks the area where this cell was imaged. Abbreviations: dpi-days post-injury.

A remarkable behavior exhibited by 17.4% of control RG cells and 3.2% of the cells after injury (Figure 4.13), was the direct neurogenesis, in which RG cells directly converted/differentiated into non-glial cells without undergoing cell division (Figure 4.9). In these events, cells gradually lost the RG morphology (and the *gfap:*GFP expression when the *Tg(gfap:GFP)* fish line was used), and the neuronal identity of the cell at the end of this process could even be confirmed in some cases after whole-brain immunostaining (Figure 4.9F).

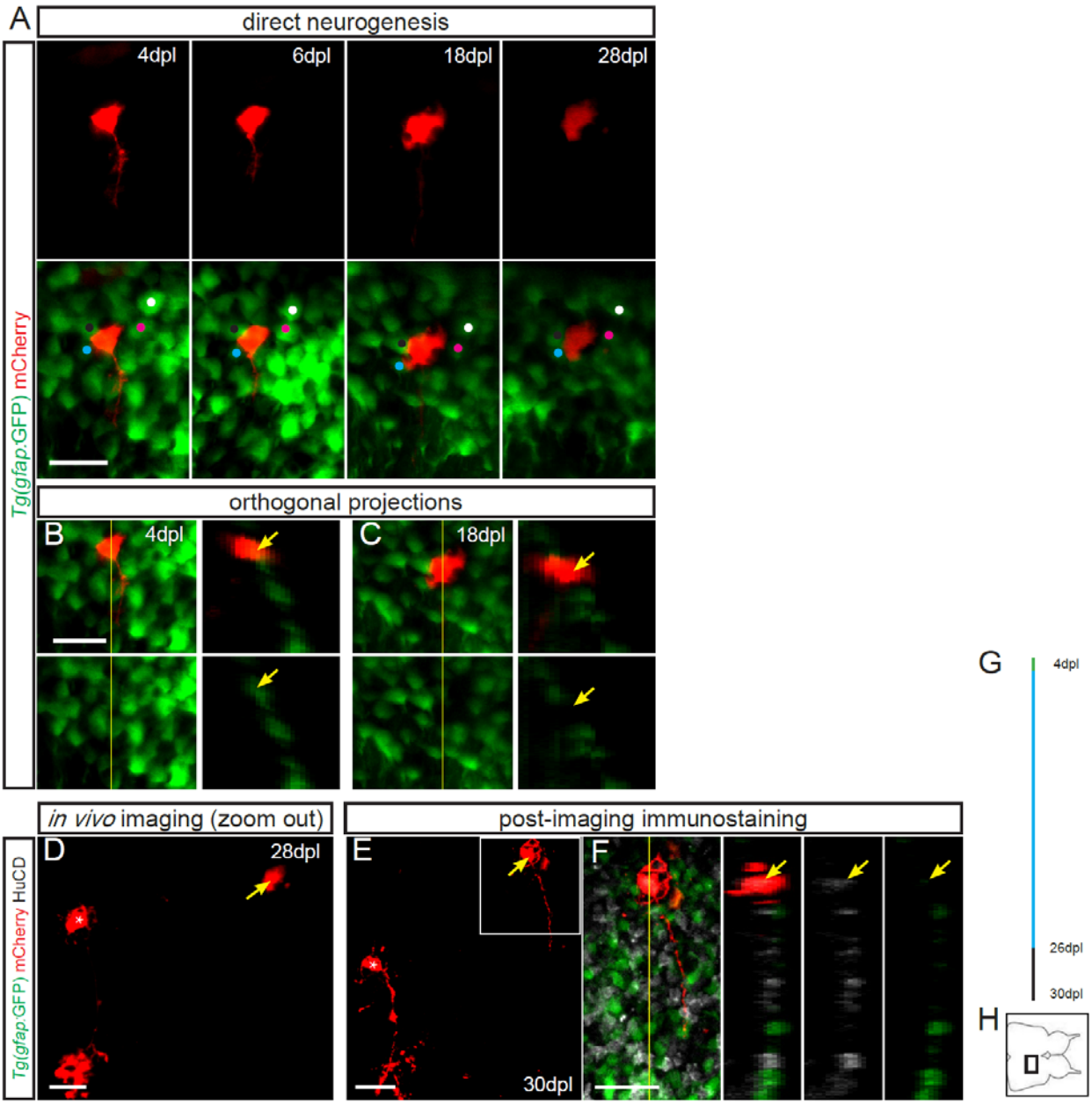

Figure 4.9: Example of a RG cell observed *in vivo* undergoing direct neurogenesis in a non-injured brain. (A) Confocal images of the same mCherry-labeled cell at different time-points after labeling in the *Tg(gfap:GFP)* line. Note that at 4dpl the cell is *gfap:*GFP-positive and has a RG morphology, whereas at later time points (e.g., 18dpl, 28dpl) the cell loses these RG characteristics. Dorsal view, midline is up. The colored dots in the lower panels mark the same *gfap:*GFP-positive cells over the different time-points, and were used to help in the orientation and reliably find the same position. (B) and (C) Orthogonal views of the cell at two different time-points, used for a better visualization of the cells' identity. Yellow arrows point at the location of the cell. Note the co-localization with *gfap*:GFP at 4dpl (B) but not at 18dpl (C). (D) Confocal image of the same cell (yellow arrow) observed *in vivo* at a lower magnification, for a better visualization of the surrounding area. Asterisk marks a neighboring cell used to find the same position after post-imaging staining. (E) Immunostaining in the whole brain for GFP, mCherry and HuCD at 30dpl, to confirm the identity of the cell. Yellow arrow and asterisk mark the same cells as in D. (F) Orthogonal projections of the differentiating cell to confirm its non-glial identity (HuCD-positive). Scale bars: A to F-20µm. (G) Lineage tree of the cell. Green line represents a RG identity (morphology and *gfap:GFP* expression); blue line represents a RG identity (morphology) and black line represents a non-glial identity (no RG morphology and no *gfap*:GFP expression). (H) Representative scheme of the telencephalon viewed from top. The black rectangle marks the area where this cell was imaged. Abbreviations: dpl-days post-labeling.

To further confirm *in vivo* the neuronal identity of the cells undergoing direct neurogenesis, imaging was performed in the *Tg(HuC:GFP)* line (Park et al., 2000) crossed with *brassy* (Figure 4.10). In this line, GFP is expressed under the control of the neuron specific promoter HuC, reporting the entry in the neuronal differentiation process. Also in this line, RG cells that initially were *HuC*:GFP-negative, gradually started to express GFP, revealing their conversion into the neuronal fate and supporting the analysis done in the *Tg(gfap:GFP)* line.

The direct generation of neuronal progeny from RG cells without undergoing a cell division step had never been reported so far in the adult vertebrate brain. This observation reveals an important new feature of the adult constitutive neurogenesis in the zebrafish telencephalon, in which a considerable sub-population of RG cells terminally differentiates, depleting itself and generating one neuron. Notably, this behavior is almost not present after injury (Figure 4.13), suggesting that instead cells divide to produce neuronal progeny while maintaining the stem cell pool that might be needed in these hostile conditions.

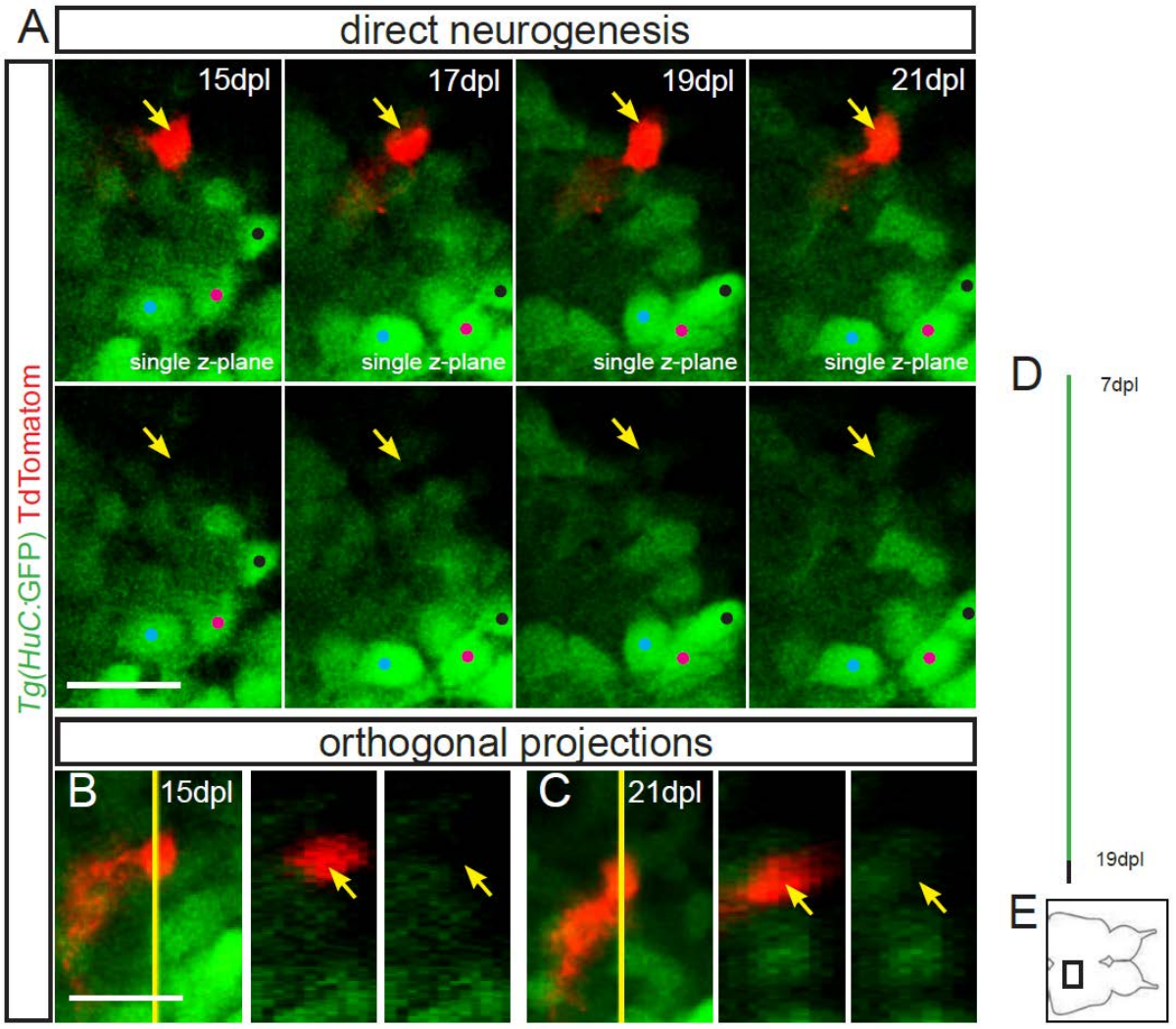

Figure 4.10: Example of a RG cell observed *in vivo* undergoing direct neurogenesis in a non-injured brain. (A) 2-photon images of the same TdTomatom-labeled cell at different time-points after labeling in the *Tg(HuC:GFP)* line. Each image is a single z-plane. Note that at 15dpl the cell is *HuC*:GFP-negative and has a RG morphology, whereas at later time points (e.g., 19dpl, 21dpl) the cell starts to express the neuronal reporter transgene *HuC:*GFP. Dorsal view, midline is up. The colored dots in the lower panels mark the same *HuC*:GFP-positive cells over the different time-points, and were used to help in the orientation and reliably find the same position. (B) and (C) Orthogonal views of the cell at two different time-points, used for a better visualization of the cells' identity. Yellow arrows point at the location of the cell. Note the absence of co-localization with *HuC*:GFP at 15dpl (B) and the co-expression at 21dpl (C). Images B and C are partial projections. Scale bars: A, B-20µm. (D) Lineage tree of the cell. Green line represents a RG identity (RG morphology and no *HuC:*GFP expression) and black line represents a non-glial identity (*HuC*:GFP expression). (E) Representative scheme of the telencephalon viewed from top. The black rectangle marks the area where this cell was imaged. Abbreviations: dpl-days post-labeling.

A rare observation made with this technique was the shrinkage and fragmentation, and the subsequent disappearance of the cell (Figure 4.11), characteristics that are consistent with the cell death process. This event occurred in a control animal (Figure 4.13) and within a two days period of time (Figure 4.11).

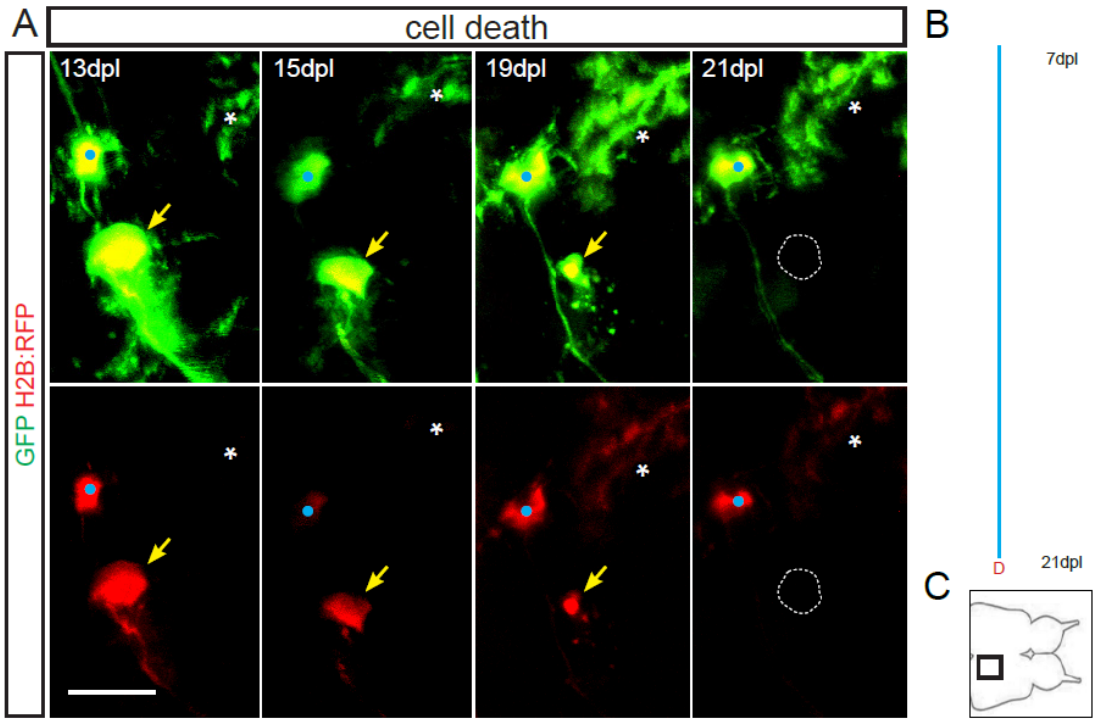

Figure 4.11: Example of a dying RG cell observed *in vivo* in a non-injured zebrafish. (A) Confocal images of the same GFP/H2B:RFP-labeled RG cell at different time-points after labeling in the *brassy* line. Yellow arrows point at the followed cell. Note that a RG cell is present at 13 and 15dpl but at 19dpl it presents a morphology of dying cell, with shrinkage of the nucleus. At 21dpl the cell is not present anymore (white dashed circle). Dorsal view, midline is up. The blue dots mark the same GFP-positive cell and the asterisks mark the processes of another cell (not seen here) over the different time-points; both landmarks were used to help in the orientation and reliably find the same position. Scale bar: 20µm. (B) Lineage tree of the cell. Blue line represents RG identity (morphology); D-cell death. (C) Representative scheme of the telencephalon viewed from top. The black rectangle marks the area where this cell was imaged. Abbreviations: dpl-days post-labeling.

Another cell behavior observed *in vivo* was the disappearance of cells from the imaging plane (Figure 4.12). Interestingly, these events were observed in the majority of RG cells imaged after injury (54.8%) whereas it constituted only 8.3% of cell behaviors in control animals (Figure 4.13).

Cell disappearance could be due to several reasons: silencing of the reporter plasmid during cell differentiation into neurons, cell death or cell migration. The first possibility is not very likely, since in static analysis of electroporated brains (Figure 4.5) non-glial cells were observed (some confirmed to be neurons), labeled with the reporter plasmids, showing that there are non-glial cells in which the reporter expression is not silenced. The hypothesis of cell death cannot be discarded, since it could happen in the 2-days interval between different imaging sessions. However, morphological characteristics that would suggest this behavior were not observed in the examples of cells that disappeared (Figure 4.12 and data not shown).

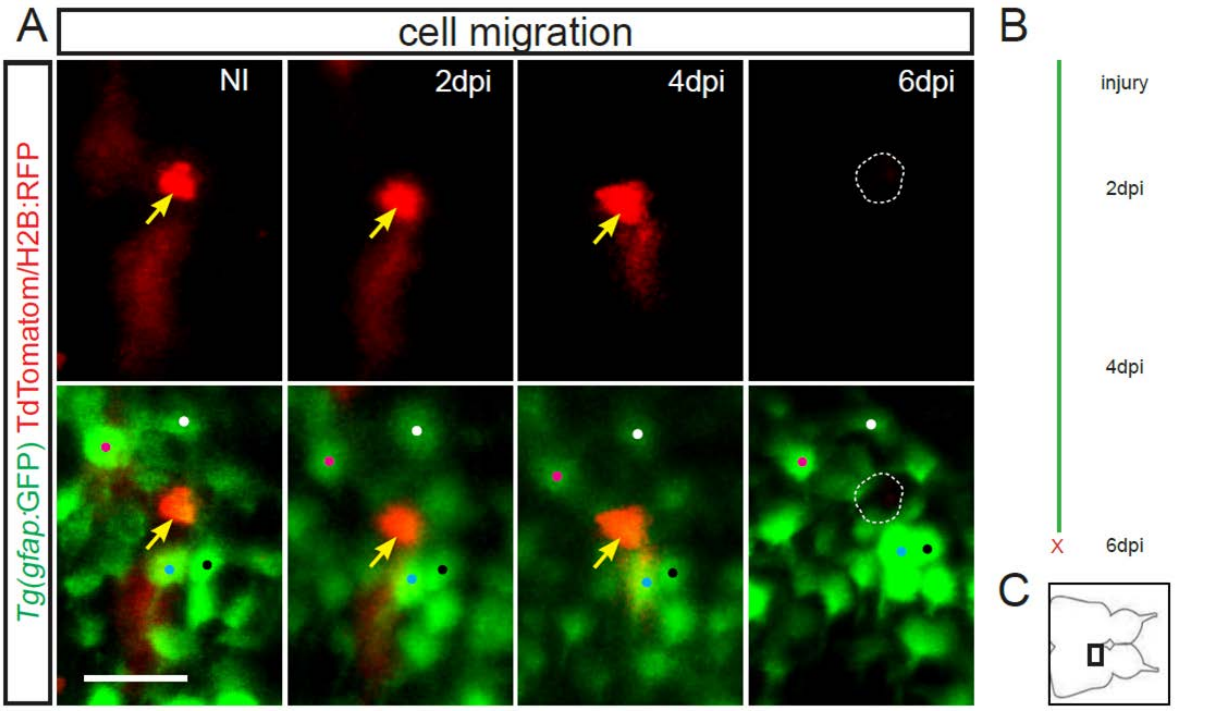

Figure 4.12: Example of a RG cell observed *in vivo* that disappeared from the imaging plane in an injured zebrafish, probably migrated to the parenchyma. (A) Confocal images of the same TdTomatom-labeled RG cell at different time-points after electroporation in the *Tg(gfap:GFP)* line. Yellow arrows point at single cells. Note that one RG cell is present before injury (NI), at 2 and 4dpi, but the cell is not present anymore at 6dpi in the same area. Dorsal view, midline is up. The colored dots in the lower panels mark the same *gfap*:GFP-positive cells over the different time-points, and were used to help in the orientation and reliably find the same position. Scale bar: 20µm. (B) Lineage tree of the cell. Green line represents a RG identity (RG morphology and *gfap*:GFP expression); X-cell disappearance. (E) Representative scheme of the telencephalon viewed from top. The black rectangle marks the area where this cell was imaged. Abbreviations: NI-non-injured; dpi-days post-injury.

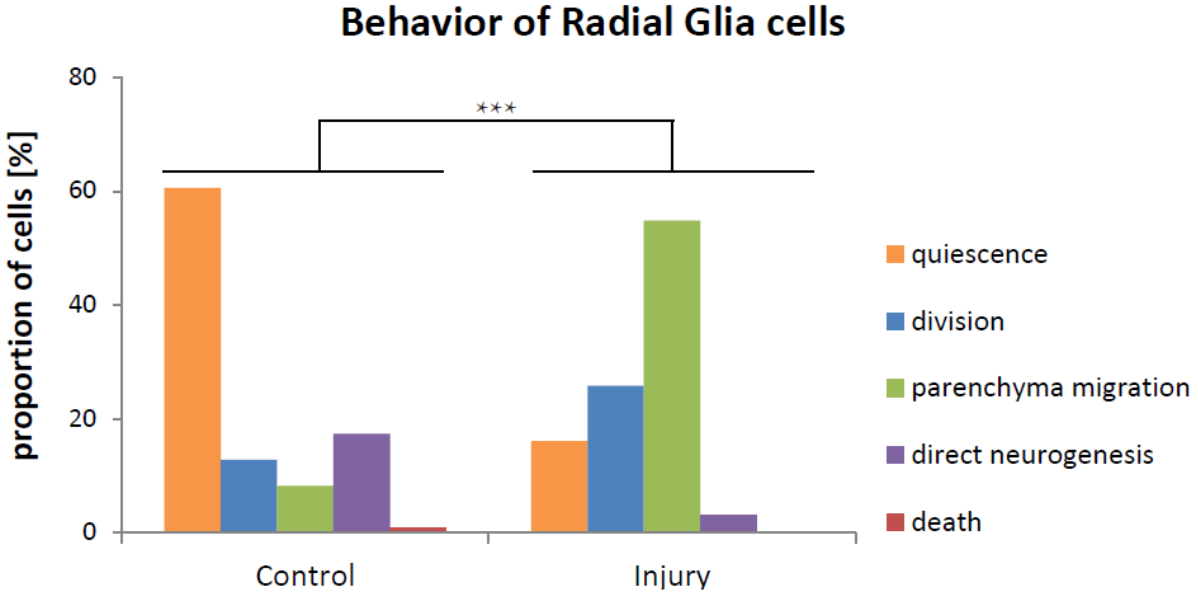

Figure 4.13: RG cells behave differently in intact and injured telencephali. Percentage of each type of behavior observed in control conditions and after injury. The behaviors from all cells analyzed from one condition were pooled in the same group. Control: n=109cells; injury: n=31cells. $p<0.001$, Chi-squared test, comparing the relative proportion of the different behaviors in the two populations (control and injury).

Another, more likely, possibility is the migration of cells away from the imaging plane (supported by the data in Figure 4.4). Due to the limit of depth penetration of the lasers used for the *in vivo* imaging experiments, it is possible that cells cannot be observed anymore if they migrate to the deeper parenchyma.

Since the hypothesis of cell migration cannot be confirmed by *in vivo* imaging due to the technical limitations of laser penetration, this hypothesis was tested in an alternative experiment: the same cell labeling technique (electroporation) was used for analysis of cell position in telencephalic sections, with and without injury (Figure 4.14). Labeling was performed 7 days prior to injury and the distance of non-glial cells to the VZ was measured 7 days after injury (Figure 4.14A). In control animals only RG cell processes (Figure 4.14B-C) and very rarely non-glial cells (Figure 4.14F) were found in the parenchyma; almost all cells remained close to the ventricle. In contrast, after injury more HuCD-positive electroporated cells were found at big distances from the VZ (Figure 4.14D-F), proving the increased migration of non-glial cell progeny to the parenchyma after an injury and explaining the disappearance of cells in the *in vivo* imaging experiments (Figure 4.12).

In summary, the *in vivo* imaging data reveals that during homeostasis, most RG cells remain quiescent and a small percentage undergoes cell division. Interestingly, a considerable proportion of RG cells undergoes direct neurogenesis, generating one neuron without proliferation, uncovering a new way of generating neurons in the adult vertebrate brain. After injury, the proportion of cells undergoing direct neurogenesis is greatly reduced, and RG cells react mostly by dividing and generating progeny that migrates to the parenchyma.

Since *in vivo* imaging is not a trivial technique, it is challenging to obtain a high number of cells for analysis. Moreover, during the imaging procedure, animals are taken from their normal environment and subjected to anesthesia every second day during a month, conditions that could eventually influence the behavior of cells. Therefore, to strengthen the results obtained by this method, *in vivo* clonal analysis was performed in animals that were maintained in their normal environment until sacrifice. To label sparse RG cells, animals were injected at the ventricle with a reporter construct together with Lipofectamine. As shown before, this technique labels mostly RG cells (Figure 4.2). Injury was done one day after labeling and fish were sacrificed either one or four weeks following injury (Figure 4.15A) to evaluate clone size and composition. Based on previous clonal analysis performed with viruses (Rothenaigner et al., 2011), a clone was defined as a cell or a group of cells within 10 µm distance.

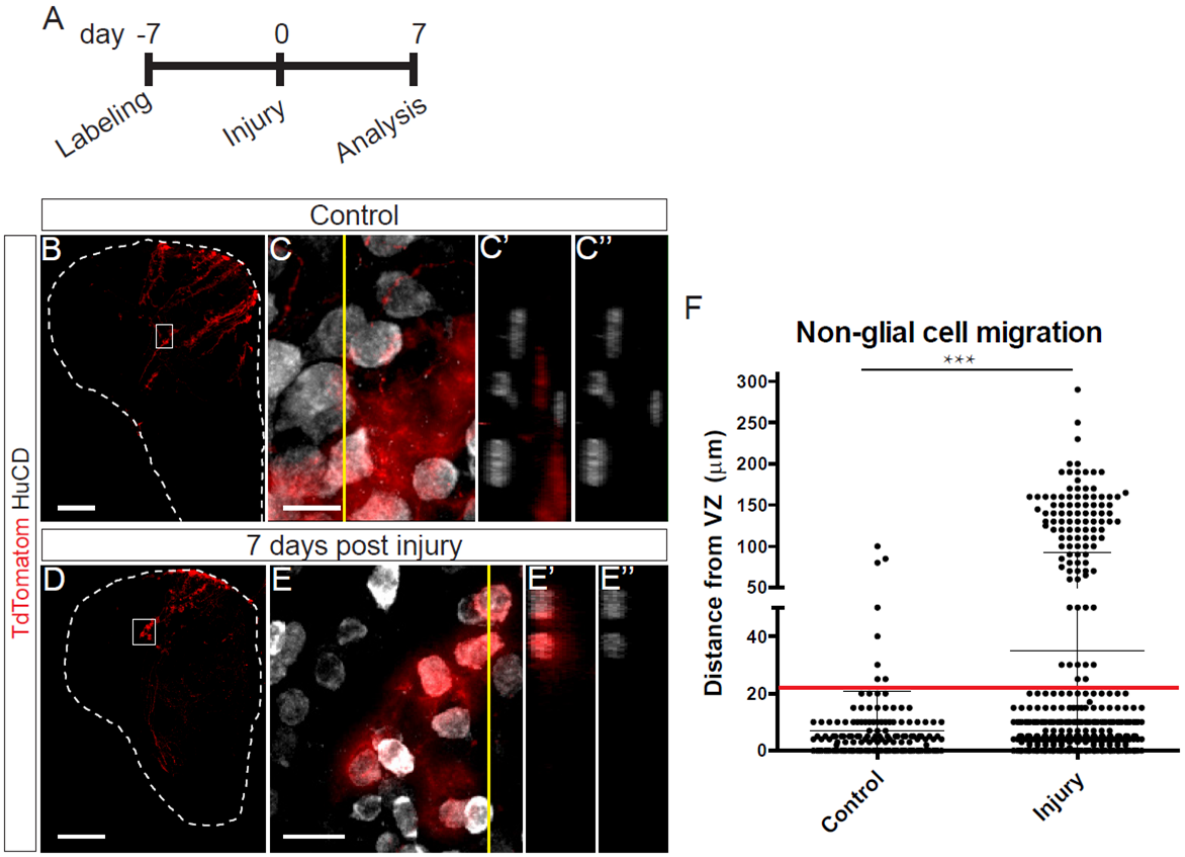

Figure 4.14: Non-glial cells labeled by electroporation at the VZ migrate bigger distances into the parenchyma after injury. (A) Scheme of the time schedule implemented for analysis of cell migration after injury. (B) Confocal image of a control telencephalic section 14 days after labeling by electroporation of a TdTomatom construct. The dashed line marks the limits of the hemisphere. (C) Magnification of the boxed area in B, depicting only RG cell processes between HuCD-positive neurons. C' and C'' are orthogonal projections of the image in C. (D) Confocal image of an injured telencephalic section at 7 dpi, after labeling by electroporation of a TdTomatom construct. The dashed line marks the limits of the hemisphere. (E) Magnification of the boxed area in D, depicting HuCD-positive neurons in the parenchyma. E' and E'' are orthogonal projections of the image in E to certify the neuronal identity of the cells in the parenchyma. Scale bars: B,D-100µm; C,E-10µm. (F) Graph depicting the distances of individual non-glial cells to the VZ, in control and injured animals. Each symbol represents one cell. Horizontal black lines represent the mean +/- SEM. The red line marks the limit of non-glial cell deposition during constitutive neurogenesis, based on the upper limit of the SEM bar in control conditions; n=152 cells in control and n=414 cells injured (6 animals per condition were analyzed); $p<0.001$, Mann-Whitney test.

As observed in Figure 4.15, close to 80% of the analyzed clones in control animals were composed of a single cell (Figure 4.15D), consistent with previous findings (Rothenaigner et al., 2011) and with the idea that RG cells are mostly quiescent. Surprisingly, this percentage was similar in injured animals at 7 days. At 28 dpi the percentage of bigger clones (2 or more cells) is slightly increased, indicating that more RG divided in this period (Figure 4.15E). The increase in clone size is mostly due to the increase in clones composed of 2 cells, suggesting that even though more RG cells divided at these late time-point after injury, the proliferative capacity of each dividing RG was not changed, since most of them generated only two cells.

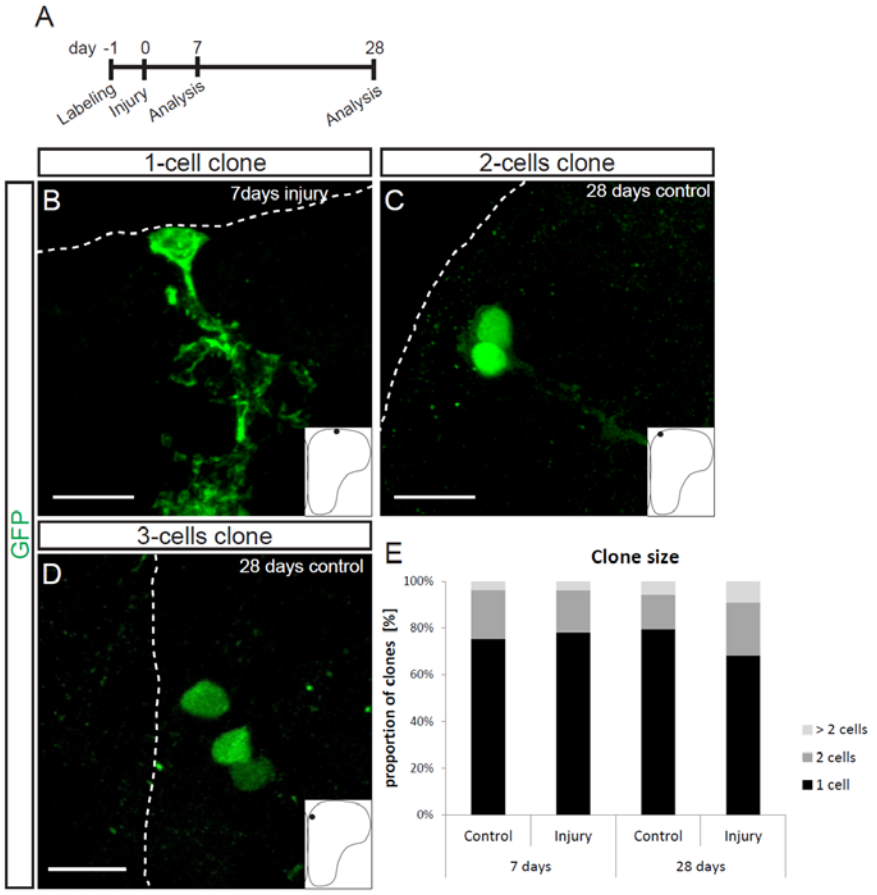

Figure 4.15: Clonal analysis with lipofection validates the highly quiescent behavior of RG cells. (A) Scheme of the time schedule implemented for clonal analysis. (B) to (D) Confocal images of one- (B), two- (C) and three-cells (D) clones labeled with pCS-GFP plasmid. The dashed lines indicate the surface of the hemisphere. Schemes on the right lower corner of the images represent the position of each clone in the telencephalon. Scale bars: 10µm. (E) Proportion of each clone size at 7 days and 28 days, in control and injury conditions. Total number of clones: control 7 days-183; injury 7 days-207; control 28 days-34; injury 28 days-22.

A possible concern with the use of transfection to label cells is that, due to the fact that the plasmid does not integrate in the cell genome, there might be dilution of the construct when the cell undergoes multiple rounds of division and consequently the daughter cells might lose the fluorescent signal. To exclude the possibility that the small clone size observed (Figure 4.15E) is derived from plasmid dilution, a control lipofection was done in a Cre-reporter line, *Tg(-3.5ubi:loxP-EGFP-loxP-mCherry)*(Mosimann et al., 2011), by injection of a pCS-CMV:Cre construct to label RG cells genetically, and therefore permanently (Figure 4.16). As expected, mCherry-positive cells were observed only after Cre injection, but not in non-injected animals (Figure 4.16B-E), suggesting that there is no leakiness in the expression of the transgene in this line. Also in this set of experiments with permanent genetic labeling, no large clones were observed (Figure 4.16G), excluding that plasmid dilution contributed to the small RG-derived clone size observed with lipofection (Figure 4.15E).

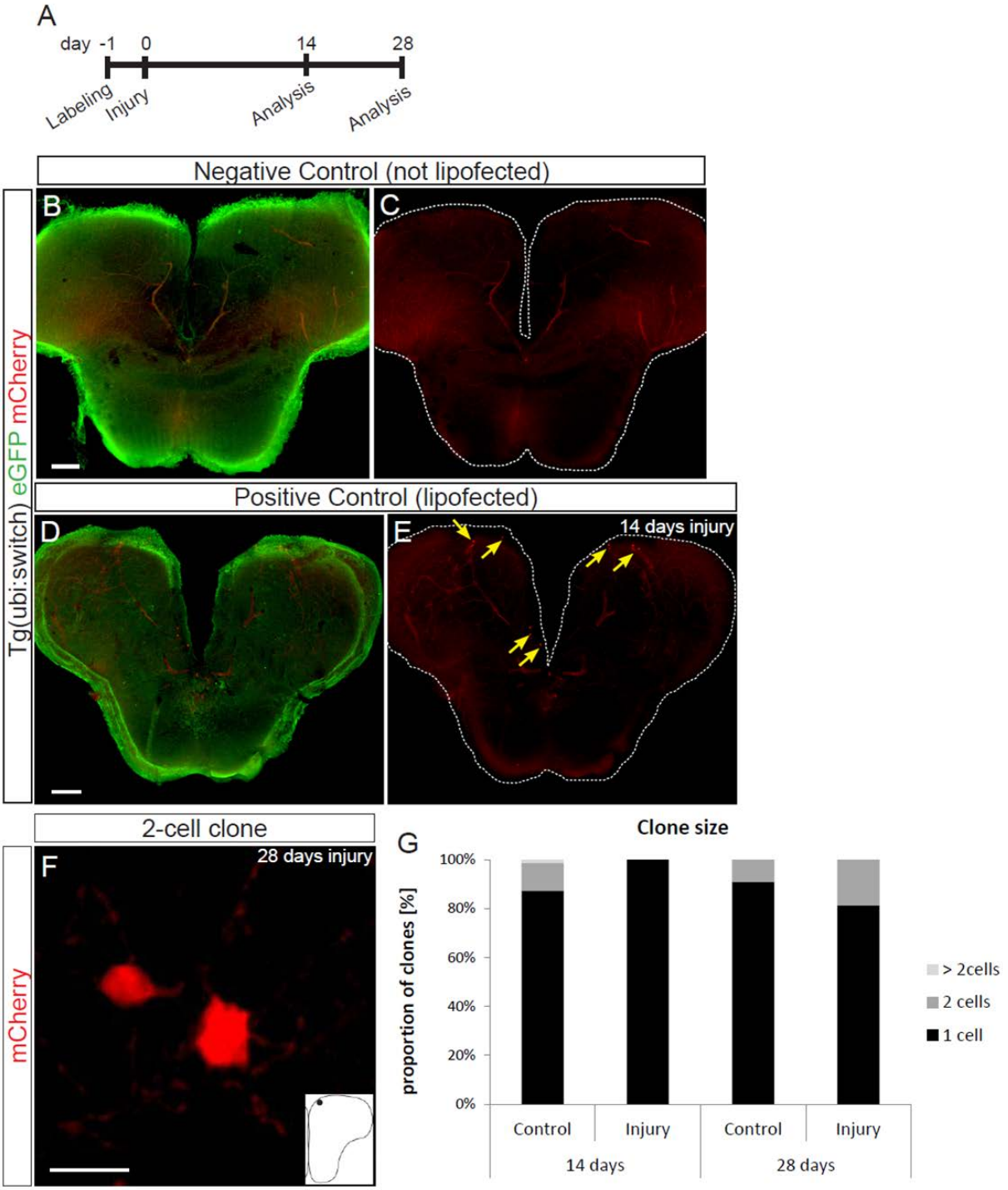

Figure 4.16: Clonal analysis in the *Tg(-3.5ubi:loxP-EGFP-loxP-mCherry)* line confirms small size of RG-derived clones. (A) Scheme of the time schedule implemented for clonal analysis. (B) and (C) Confocal images of a telencephalic section from the *Tg(-3.5ubi:loxP-EGFP-loxP-mCherry)* line without lipofection of Cre. Note on (C) the absence of recombined mCherry-positive cells. (D) and (E) Confocal images of a telencephalic section from the *Tg(-3.5ubi:loxP-EGFP-loxP-mCherry)* line at 14dpi, lipofected with a Cre-expressing construct. Note on (E) the presence of recombined mCherry-positive cells (yellow arrows). (F) Example of a 2-cell clone observed at 28dpi in a lipofected brain. Scheme on the right lower corner represents the position of the clone in the telencephalon. Scale bars: B and D-100µm, F-10µm. (G) Proportion of each clone size at 14 days and 28 days, in control and injury conditions. Total number of clones: control 14 days-71; injury 14 days-77; control 28 days-22; injury 28 days-64.

This *in vivo* clonal analysis approach was also used to verify the direct neurogenesis behavior of RG cells, by examining the percentages of single non-glial cells over time (Figure 4.17). Since 91% of the cells targeted by lipofection are RG (Figure 4.2), only a small proportion of non-glial cells are labeled with this method. However, if direct conversion occurs, the percentage of single non-glial cells generated from RG should increase over time.

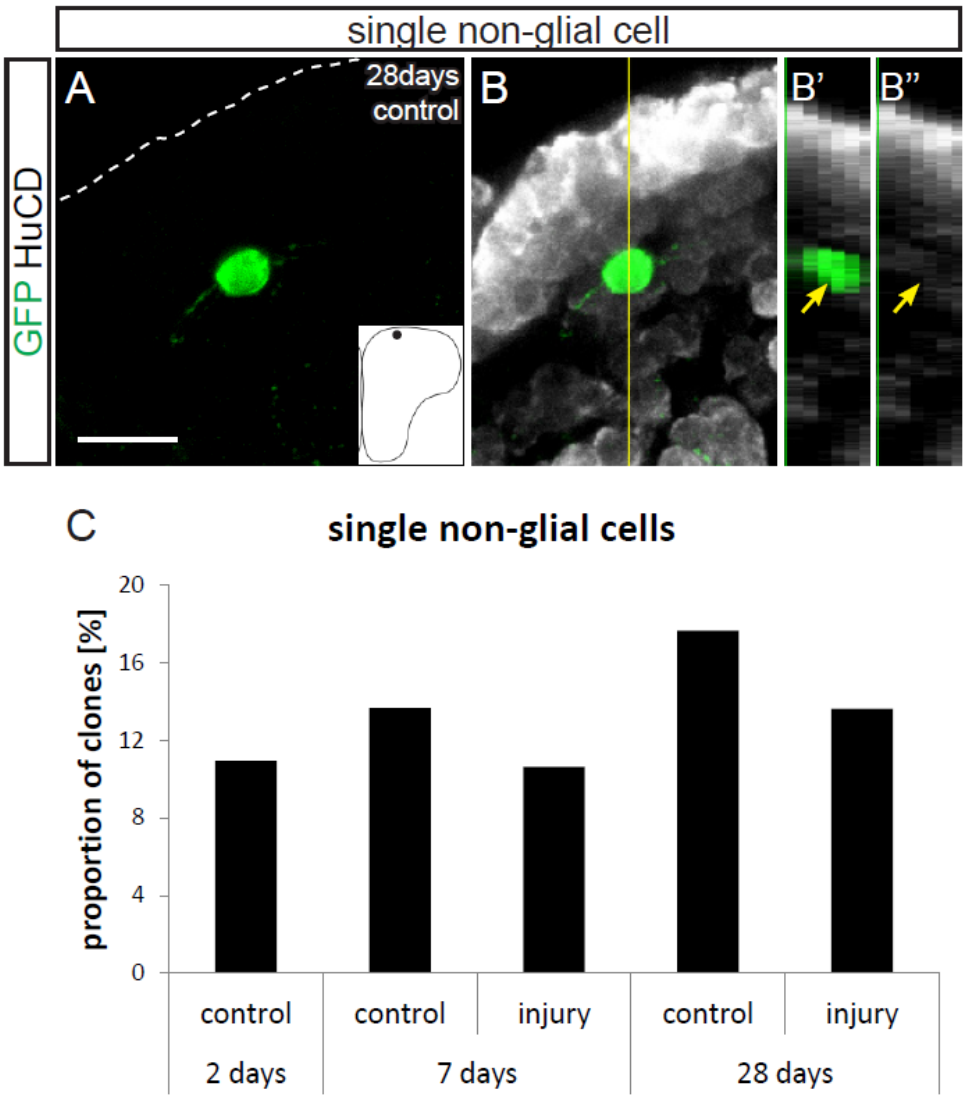

Figure 4.17: The quantification of single non-glial cells over time by clonal analysis supports the direct neurogenesis observations *in vivo*. (A) Confocal image of a single non-glial cell 28days after labeling. Scheme on the right lower corner of the image represents the position of the cell in the telencephalon. The dashed lines indicate the limit of the section. (B') and (B'') are orthogonal projections of the cell in (B) (yellow arrows), for a better visualization of the co-localization with HuCD. Scale bar: 10µm. (C) Percentage of single non-glial cell clones over the total amount of clones observed at 2, 7 and 28 days, in control and injured animals. Total number of clones per condition: 2days control-128; 7days control-183; 7days injury-207; 28days control-34; 28days injury-22.

In fact, this was the case in control conditions, where the percentage of single non-glial cells increased from 2dpl to 7dpl and even further at 28dpl (Figure 4.17C). Interestingly, the

percentage was smaller in the injured animals (Figure 4.17C), corroborating the observations made with the *in vivo* imaging method that the direct neurogenesis behavior is less frequent after injury (Figure 4.13).

Taken together, the clonal analysis data strongly supports the *in vivo* imaging observations that during homeostasis RG cells are mostly quiescent and contribute to constitutive neurogenesis by division or direct differentiation, whereas after injury they divide more and less of them undergo direct neurogenesis.

4.4.3.1 Modes of division of RG cells observed *in vivo*

The *in vivo* imaging technique revealed an increase in the proportion of dividing RG cells after injury (Figure 4.13), in agreement with previous data (Baumgart et al., 2012; Kroehne et al., 2011). A question that was not addressed by these studies was whether these proliferating RG cells divide in the same way during constitutive neurogenesis and during regeneration. To investigate this issue, the mode of cell division was analyzed using the *in vivo* imaging procedure. Single RG cells were followed over time and, based on morphological criteria, three types of cell divisions were classified: symmetric gliogenic division (when both daughter cells presented a typical RG morphology, Figure 4.18), asymmetric division (when one daughter cell had RG morphology and the other not, Figure 4.19) and symmetric non-gliogenic division (when none of the daughters showed RG morphology, Figure 4.20). Based on the analysis of the identity of electroporated cells presented in Figure 4.5, the cells without RG morphology were considered to be non-glial. The classification of the mode of cell division was done at the first time point when the two daughter cells were observed.

Both in control and in injured animals, the most frequently observed mode of division was the asymmetric (Figure 4.21), which results in the self-renewal of the RG cell concomitantly with the generation of more differentiated progeny. Interestingly, however, the symmetric gliogenic mode of division was observed exclusively during homeostasis, whereas the symmetric non-gliogenic mode occurred only after injury (Figure 4.21).

These results indicate that, during homeostasis, dividing RG cells always self-renew, generating either one or two new RG cells. After injury, however, some RG generate only non-glial progeny, depleting themselves, but increasing the net production of non-glial cells. These non-glial cells are likely to generate neurons, but this assumption remains to be directly confirmed by post-imaging immunostaining for the neuronal marker HuCD or by *in vivo* imaging of RG cell divisions in the *Tg(HuC:GFP)* line. Nevertheless, the analysis of

electroporated cells at 2 days demonstrated that a considerable proportion of cells without RG morphology are indeed HuCD-positive (Figure 4.5), strengthening the idea that non-glial cells might be or become neurons.

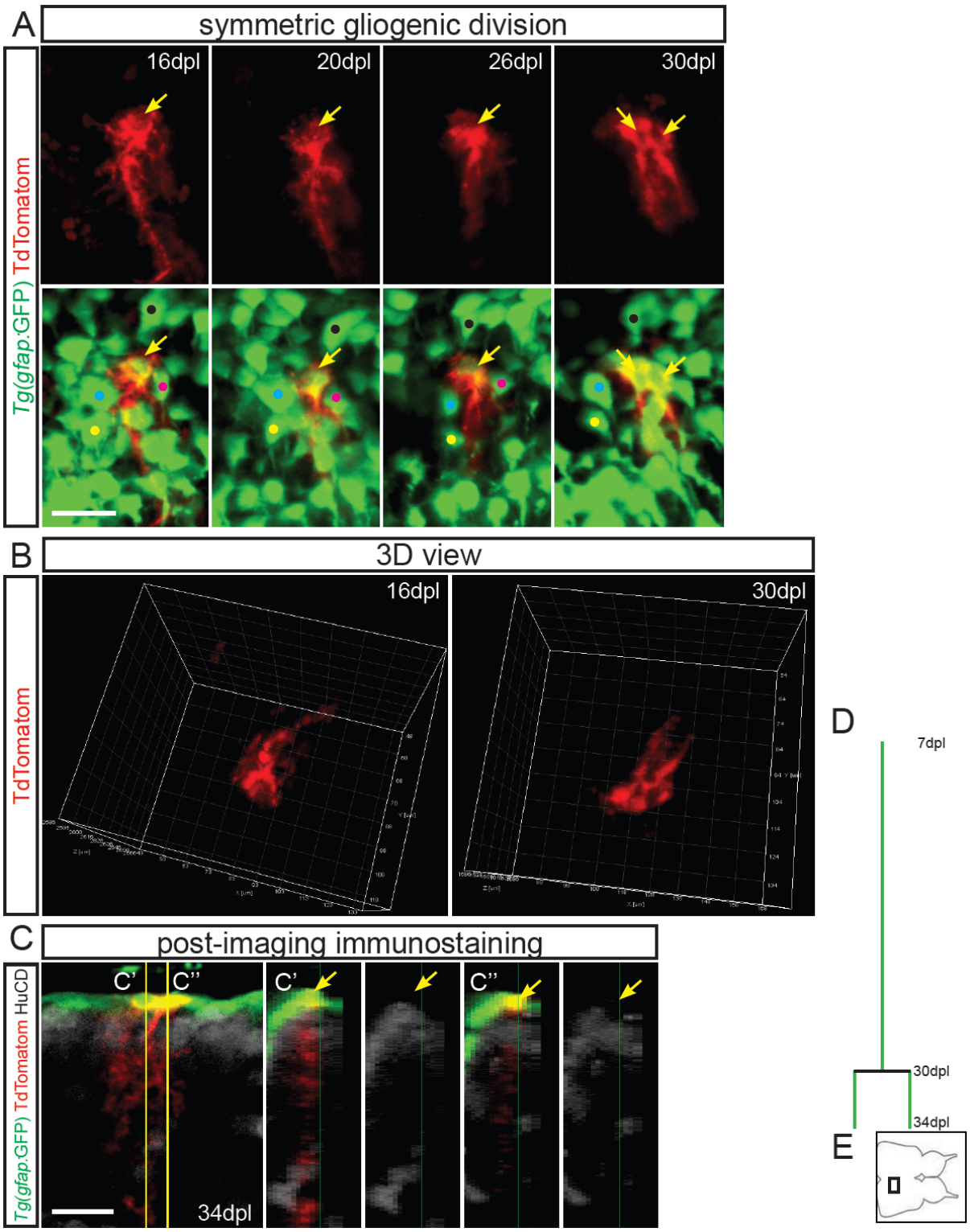

Figure 4.18: Example of a symmetric gliogenic division of a RG cell observed *in vivo* in a non-injured brain. (A) Confocal images of the same TdTomatom-labeled RG cell at different time-points after labeling in the *Tg(gfap:GFP)* line. Yellow arrows point at single cells. Note that only one RG cell is present at 16, 20 and 26dpl, but two cells with RG morphology are present at 30dpl. Dorsal view, midline is up. The colored dots in the lower panels mark the same *gfap:*GFP-positive cells over the different time-points, and were used to help in the orientation and reliably find the same position. (B) Three-dimensional views of the cells at two different time-points, used for a better visualization of the number of cells. (C) Immunostaining in the whole brain for GFP, TdTomatom and HuCD at 34dpl, to confirm the identity of the cells. Panels C' and C'' correspond to the two different cells in C. Scale bars: A,C-20µm. (D) Lineage tree of the cell. Green line represents a RG identity (RG morphology and *gfap*:GFP expression). (E) Representative scheme of the telencephalon viewed from top. The black rectangle marks the area where this cell was imaged. Abbreviations: dpl-days post-labeling.

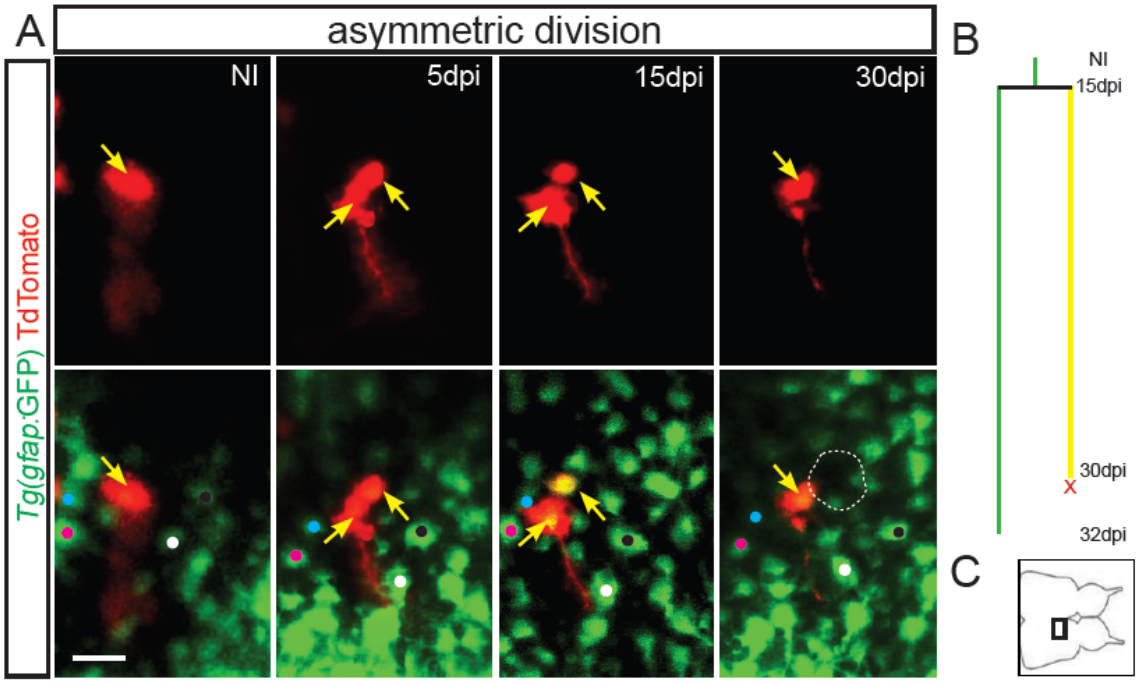

Figure 4.19: Example of an asymmetric division of a RG cell observed *in vivo* in an injured zebrafish. (A) Confocal images of the same TdTomato-labeled RG cell at different time-points after labeling in the *Tg(gfap:GFP)* line. Yellow arrows point at single cells. Note that only one RG cell is present before injury (NI), but two cells are present at 5dpi, one with (left) and one without (right) RG morphology. At 30dpi, only the cell with RG morphology is observed. Dorsal view, midline is up. The colored dots in the lower panels mark the same *gfap:*GFP-positive cells over the different time-points, and were used to help in the orientation and reliably find the same position. The dashed circle at 30dpi represents the location of the lost non-glial cell. Scale bar: 20µm. (B) Lineage tree of the cell. Green line represents a RG identity (RG morphology and *gfap*:GFP expression) and yellow line represents a non-glial identity (no RG morphology and *gfap*:GFP expression); X-cell disappearance. (C) Representative scheme of the telencephalon viewed from top. The black rectangle marks the area where this cell was imaged. Abbreviations: NI-non-injured; dpi-days post-injury.

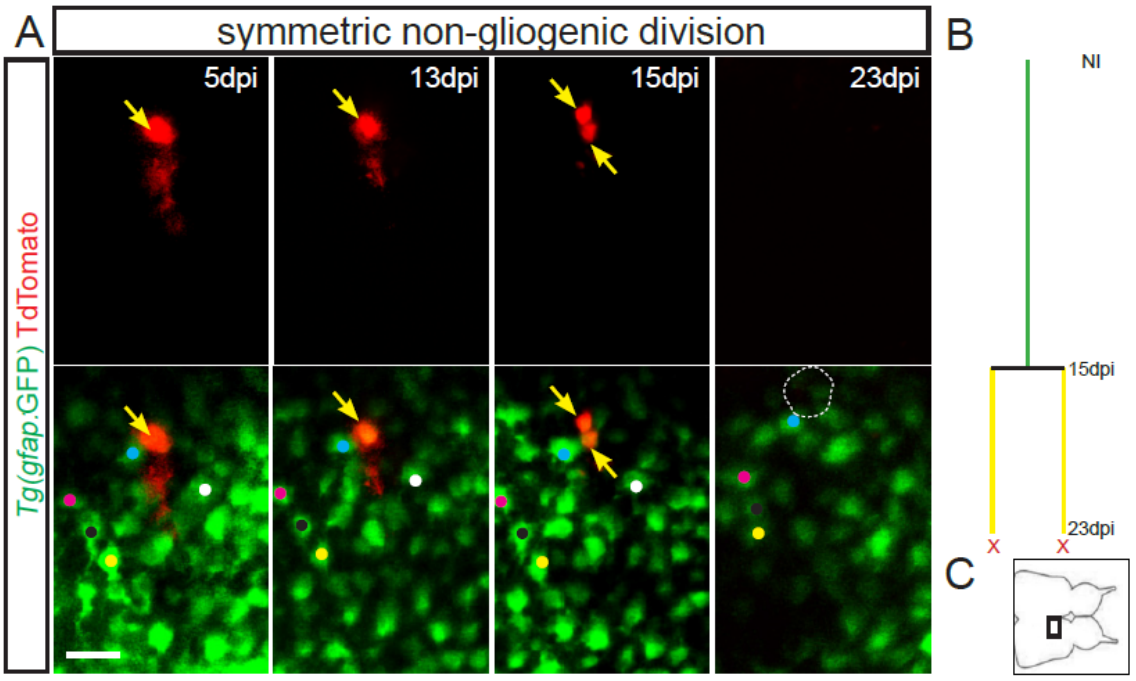

Figure 4.20: Example of a symmetric non-gliogenic division of a RG cell observed *in vivo* in an injured zebrafish. (A) Confocal images of the same TdTomato-labeled RG cell at different time-points after labeling in the *Tg(gfap:GFP)* line. Yellow arrows point at single cells. Note that only one RG cell is present at 5dpi and 13dpi, but two cells are present at 15dpi, both without RG morphology. At 23dpi, both cells disappeared from the imaging plane. Dorsal view, midline is up. The colored dots in the lower panels mark the same *gfap:*GFP-positive cells over the different time-points, and were used to help in the orientation and reliably find the same position. The dashed circle at 23dpi represents the location of the lost non-glial cells. Scale bar: 20µm. (B) Lineage tree of the cell. Green line represents a RG identity (RG morphology and *gfap*:GFP expression) and yellow line represents a non-glial identity (no RG morphology and *gfap*:GFP expression); X-cell disappearance. (C) Representative scheme of the telencephalon viewed from top. The black rectangle marks the area where this cell was imaged. Abbreviations: dpi-days post-injury.

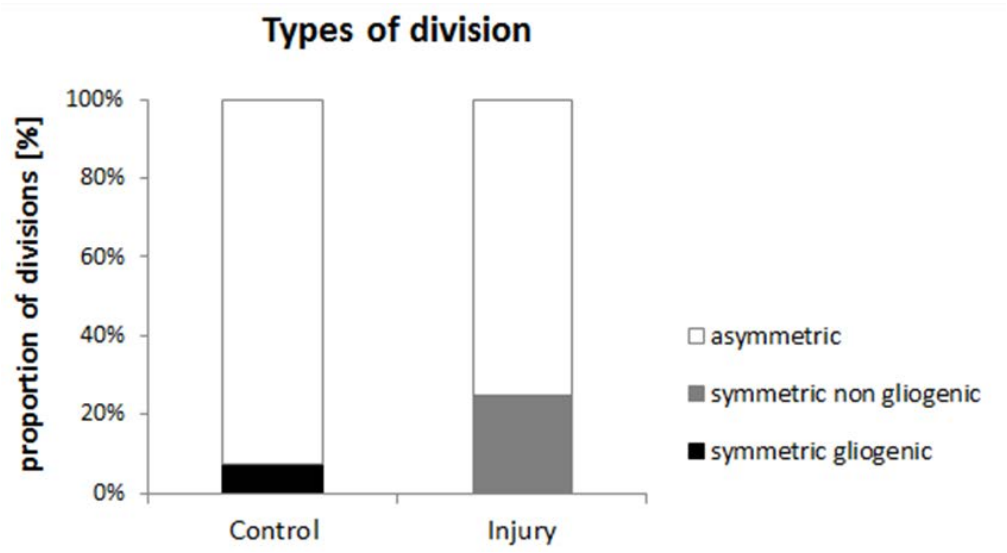

Figure 4.21: *In vivo* imaging reveals different modes of division of RG cells in control and injured animals. Proportion of each type of division observed in control conditions and after injury. The divisions from all cells analyzed were pooled in the same experimental group. Control: n=14 cells; injury: n=8 cells.

To confirm the shift in the mode of division of RG cells by the complementary clonal analysis technique, the composition of clones containing 2 or more cells was examined. The experimental procedure was the same as in Figure 4.15A. Based on the same criteria used for *in vivo* imaging (cell morphology), three types of clones were classified: glial (containing 2 or more cells with RG morphology, Figure 4.22A), mixed (containing at least one RG and a non-glial cell, Figure 4.22B) and non-glial clones (containing 2 or more cells without RG morphology, Figure 4.22C) reflecting the symmetric gliogenic, asymmetric and symmetric non-gliogenic divisions, respectively.

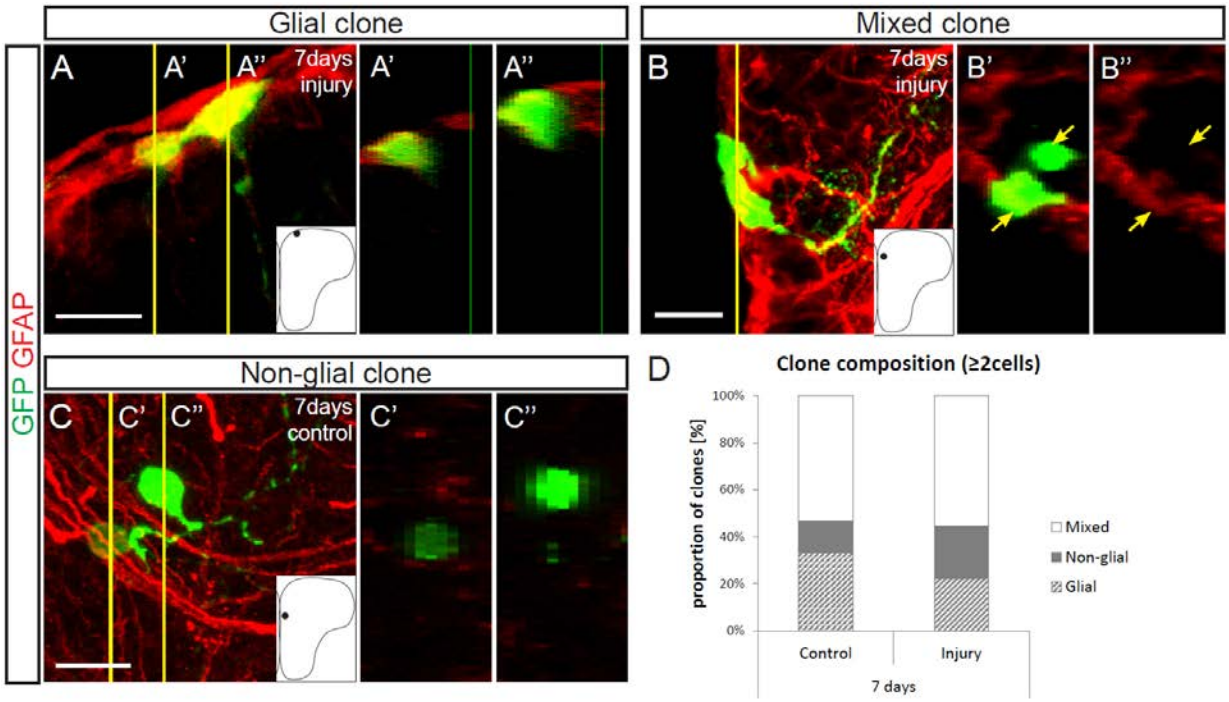

Figure 4.22: Clonal analysis of RG cells reveals a shift towards an increased production of non-glial cells after injury. (A) to (C) Confocal images of a glial (A), mixed (B) and a non-glial (C) clone labeled with pCS-GFP plasmid in sections stained for GFAP. A' and A'' are orthogonal projections of the cells in A marked with A' and A'', respectively. B' and B'' are orthogonal projections of the cells in B. C' and C'' are orthogonal projections of the cells in C marked with C' and C'', respectively. Schemes on the right lower corner of the images represent the position of each clone in the telencephalon. Scale bars: 10µm. (D) Proportion of each clone type at 7days, in control and injury conditions. Total number of clones: control-45; injury-45.

In both conditions, the vast majority of clones were mixed (Figure 4.22D), suggesting a prevalence of asymmetric cell divisions of RG. In control animals, the second most observed clone type was composed only of RG cells, indicating that the symmetric gliogenic mode of division is also frequent during homeostasis (Figure 4.22D). However, in regenerative conditions, the proportion of glial clones decreased, concomitantly with an increase in the proportion of non-glial clones (Figure 4.22D), revealing the bias towards more symmetric

non-gliogenic divisions after injury. Therefore, clonal analysis data provides strength to the *in vivo* imaging data, revealing a shift in the mode of cell division that results in a net increase in the generation of non-glial progeny in response to injury.

For a more comprehensive understanding of the behavior of single dividing cells, the lineage trees of each cell followed with the *in vivo* imaging procedure were examined (Figure 4.23-control and Figure 4.24-injury).

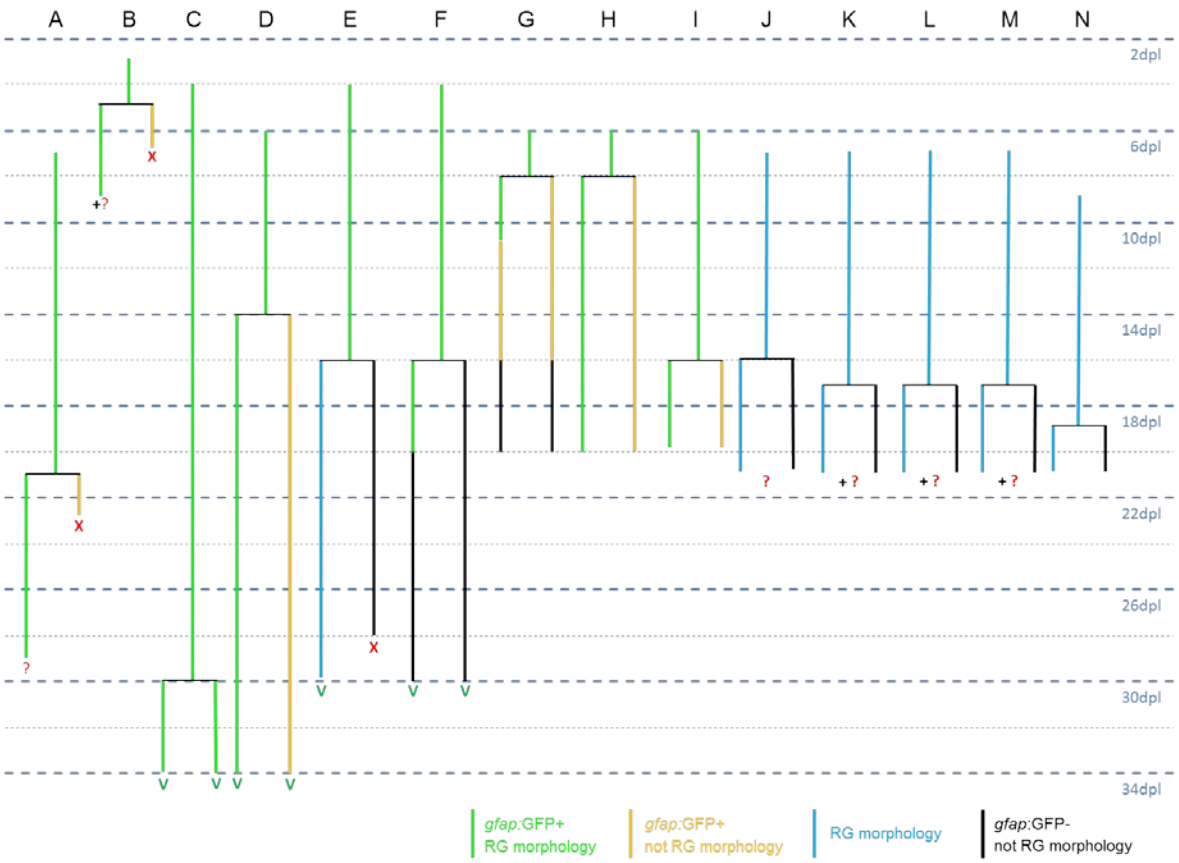

Figure 4.23: Lineage trees of dividing cells in control animals. Trees A-I were obtained in the *Tg(gfap:GFP)* zebrafish line, and trees J-N in the *brassy* line. Abbreviations: dpl-days post-labeling. Symbols: **?**-cell not found after staining, **V**-cell identity confirmed after staining, **X**-cell disappeared, **+**- animal died.

One important observation from the analysis of the lineage trees is that the proliferative capacity of single RG cells seems not to change after injury, since during the time of observation only one division per RG cell was detected both in control (Figure 4.23) and in injury situations (Figure 4.24). This limited proliferative capacity per cell indicates that the injury-induced increase in proliferation is based on the recruitment of more cells to division, rather than the increase in the number of rounds of division per RG cell. In one single

example of RG cell division after injury a second round of division occurred (cell E in Figure 4.24), but was performed by the non-glial daughter cell (probably a SAP or neuroblast) (example in Figure 4.25). This low proliferative capacity per cell was also evident in the *in vivo* analysis of clone size (Figure 4.15E).

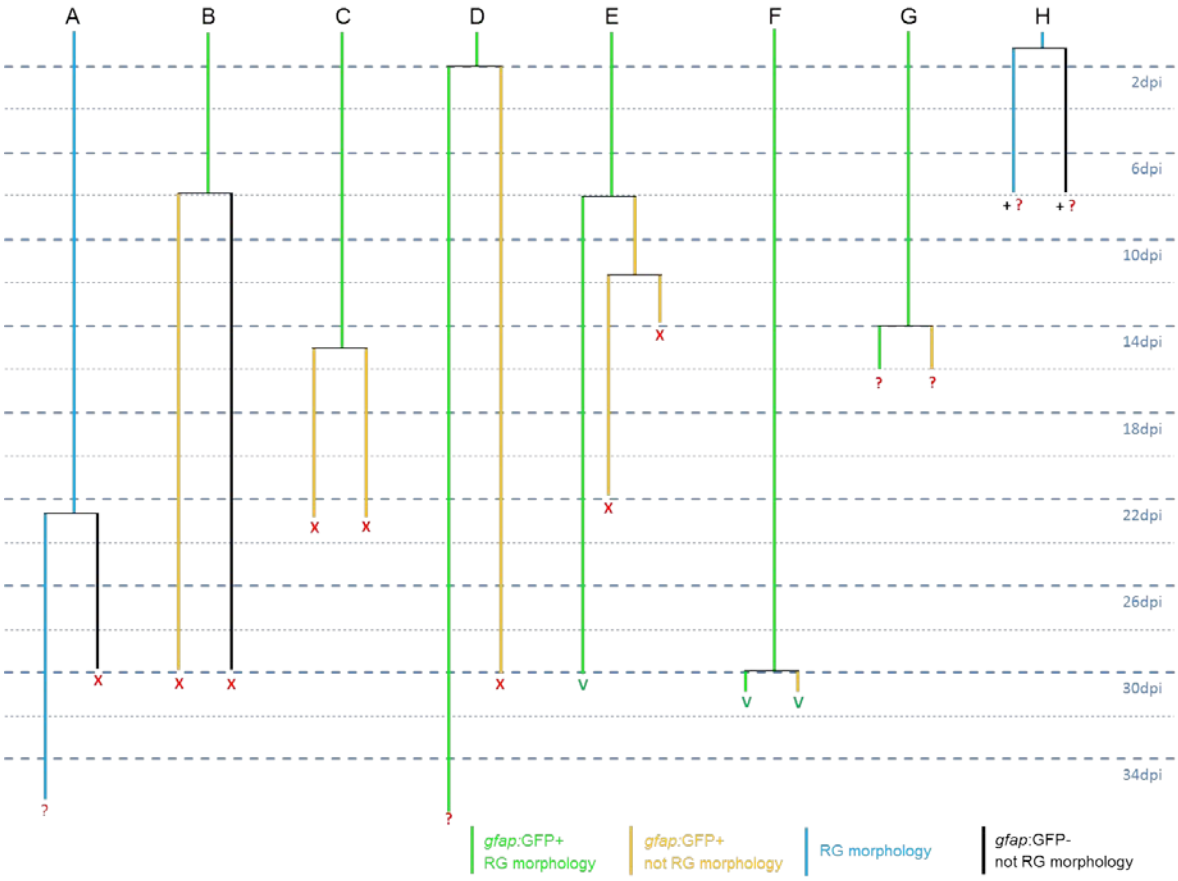

Figure 4.24: Lineage trees of dividing cells in injured animals. Trees A and H were obtained in the *brassy* line, and trees B-G in the *Tg(gfap:GFP)* line. Abbreviations: dpi-days post-injury. Symbols: **?**-cell not found after staining, **V**-cell identity confirmed after staining, **X**-cell disappeared, **+**- animal died.

The analysis of the lineage trees of dividing cells further allowed to recognize that after injury the majority of non-glial cells generated migrated away from the imaging plane (eg. trees A, B, C, D and E in Figure 4.24), whereas they remained "stable" at the VZ in control conditions (eg. trees D, F-N in Figure 4.23). The information on the fate of daughter cells after division is summarized in Figure 4.26, and further reinforces the idea of non-glial cell migration to contribute to regenerate the parenchyma after injury.

Taken together, the observation of cell divisions *in vivo* indicate that after injury, not only more RG cells divide, but also their mode of division is shifted towards an increase in the production of non-glial progeny, most of which migrates to the parenchyma. Interestingly however, the proliferative capacity of single cells seems not to be altered.

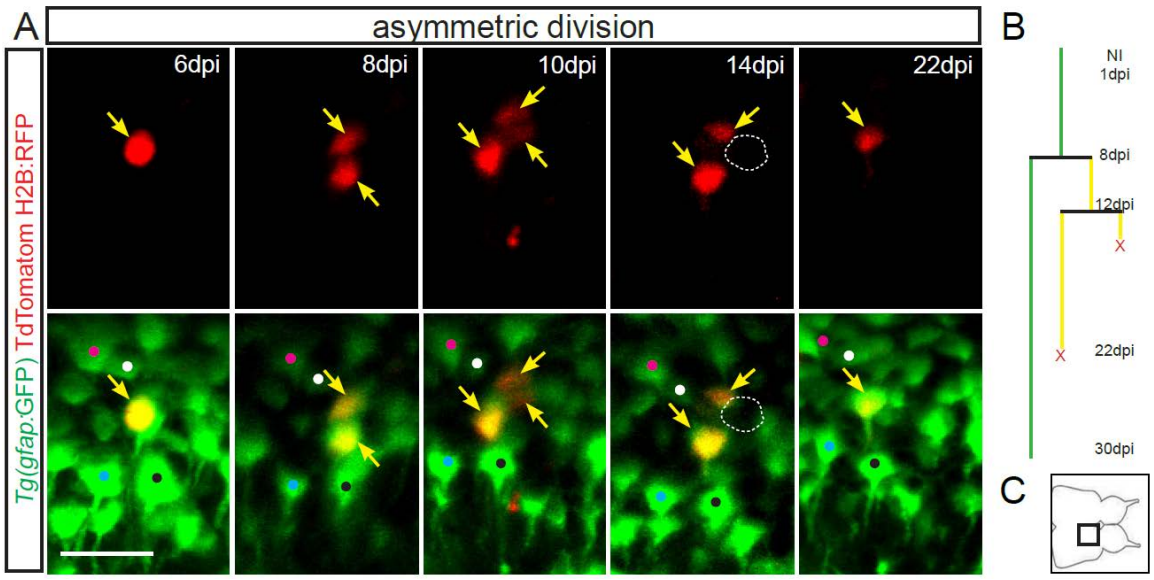

Figure 4.25: Example of an asymmetric division of a RG cell followed by another division of the non-glial cell daugther. (A) Confocal images of the same H2B:RFP-labeled RG cell at different time-points after labeling in the *Tg(gfap:GFP)* line. Yellow arrows point at single cells. Note that only one cell is present at 6dpi, two at 8dpi and three at 10dpi. At later stages (22dpi) only the RG cell daughter remains. Dorsal view, midline is up. The colored dots in the lower panels mark the same *gfap:GFP*-positive cells over the different time-points, and were used to help in the orientation and reliably find the same position. Scale bar: A -20µm. (B) Lineage tree of the cell. Green line represents a RG identity (RG morphology and *gfap*:GFP expression) and yellow line represents a non-glial identity (no RG morphology and *gfap*:GFP expression); **X**-cell disappearance. (C) Representative scheme of the telencephalon viewed from top. The black rectangle marks the area where this cell was imaged. Abbreviations: NI- non-injured, dpi-days post-injury.

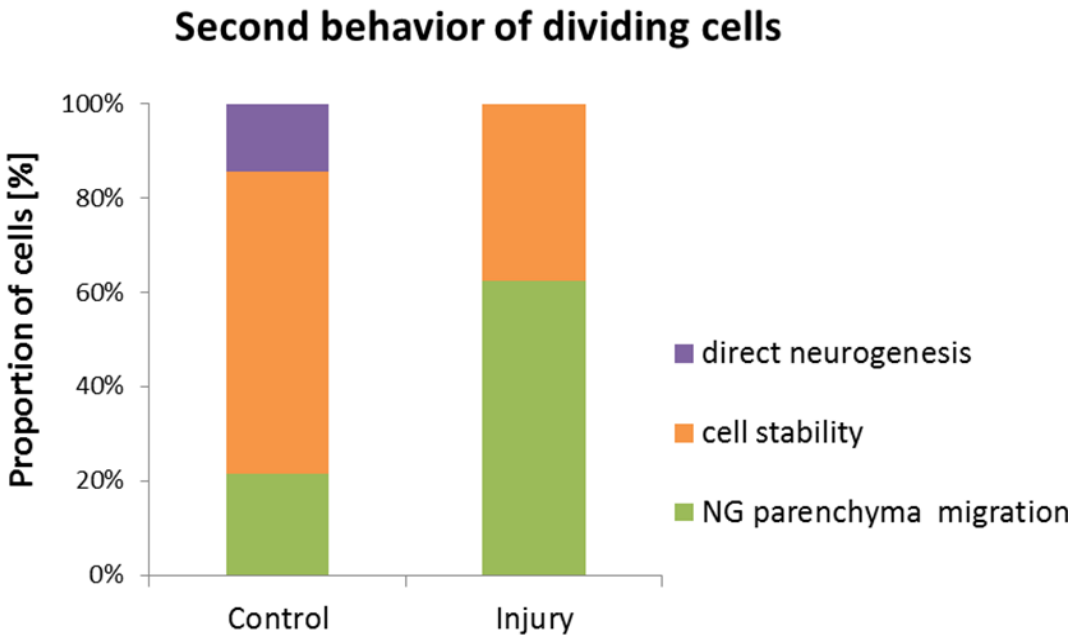

Figure 4.26: After division daughter cells behave differently in control and injured animals. Proportion of each type of daughter cell behavior observed after division in control conditions and after injury. The behaviors from all cells analyzed were pooled in the same experimental group. Control: n=14cells; injury: n=8cells.

4.5 Analysis of progenitor cell re-entry in cell cycle after injury

An important question prompted by the previous results is whether the cells proliferating after injury are part of the same sub-population of cells that divide during constitutive neurogenesis, or whether they constitute a distinct subset of progenitors that reacts specifically after the injury stimulus. To investigate this issue, an additional experiment was performed taking advantage of the BrdU labeling technology (Figure 4.27). BrdU was given to the animals for two weeks to label as many dividing cells as possible, followed by a 10 days chase to make sure that the fast proliferating cells dilute the thymidine analog or differentiate into neurons. In this paradigm, cells located at the VZ that keep the BrdU labeling should be slow dividing cells (and therefore NSCs). The injury was performed after the chase period and animals were killed at the peak of RG cell proliferation (7 dpi) and labeled for a proliferation marker (PCNA) to mark cells entering the cell cycle after injury. The animals used were from the *Tg(gfap:GFP)* line, to facilitate the identification of GFP-positive RG cells. However, since GFP can still be inherited by the SAPs and neuroblasts generated from RG, a certain amount of GFP-positive cells might also belong to these non-glial populations. In this experiment, three types of cells were taken into consideration: cells that divided before but didn't do so after the injury (*gfap:*GFP+/BrdU+/PCNA-, Figure 4.27C), cells that were not dividing before injury but were recruited to the cell cycle afterwards (*gfap*:GFP+/BrdU-/PCNA+, Figure 4.27D) and cells that divided before and after injury (*gfap*:GFP+/BrdU+/PCNA+, Figure 4.27E).

The analysis of the percentage of previously proliferating RG cells (*gfap*:GFP+/BrdU+) that re-entered the cell cycle after injury (*gfap*:GFP+/BrdU+/PCNA+) revealed no difference between control and injury groups (Figure 4.27G), indicating that RG cells dividing after injury are not preferentially part of the normal "quiescent" or "dividing" sub-population. In other words, this cell cycle re-entry analysis revealed that the population of cells proliferating during constitutive neurogenesis is not more prone to respond to injury than the cells that are normally quiescent. In the future, single cell *in vivo* imaging of the different populations of RG cells during homeostasis and after injury could be useful to further understand the heterogeneity within the RG cell population.

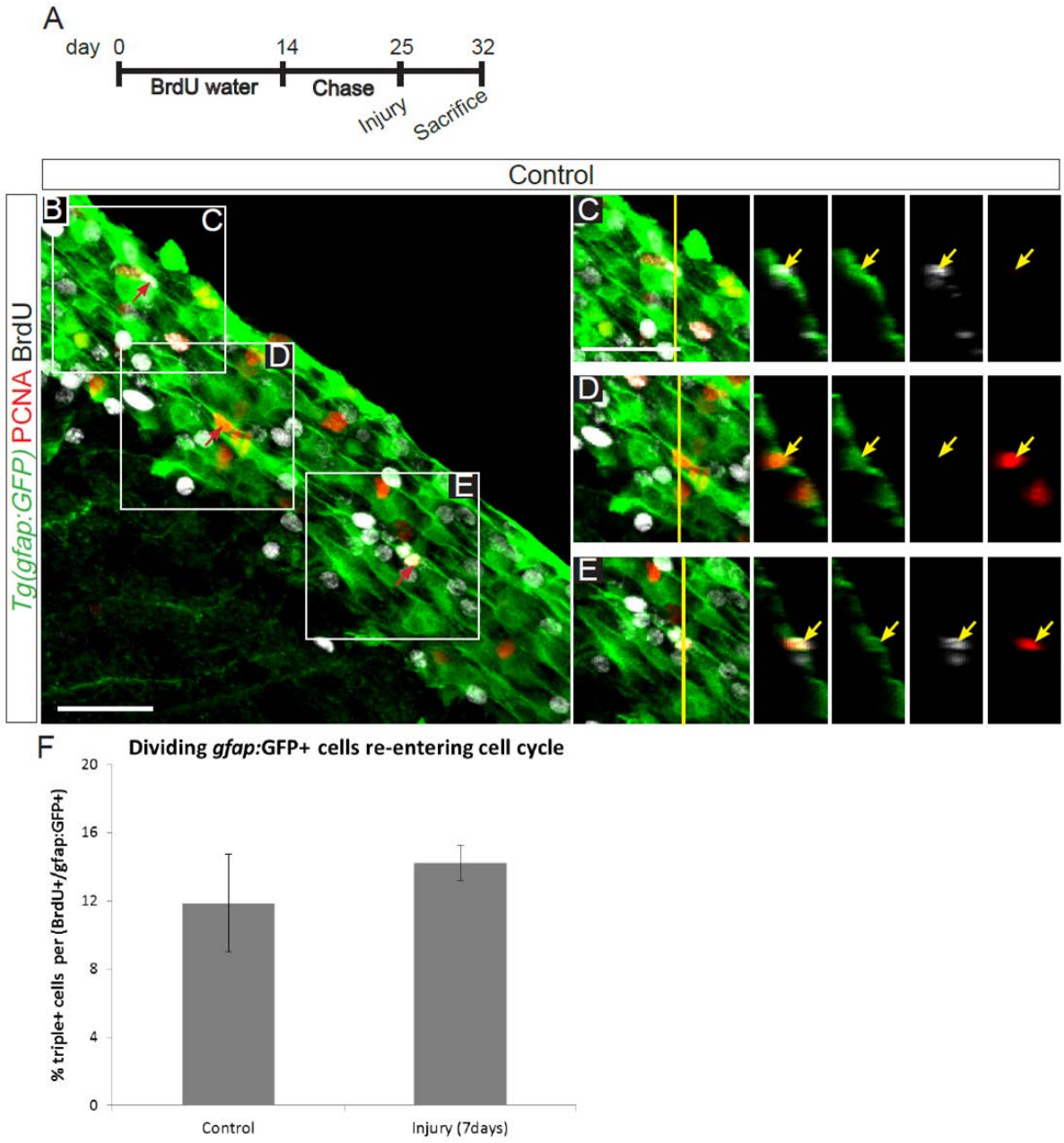

Figure 4.27: After injury there is no preferential recruitment of previously dividing or quiescent progenitors to the cell cycle. (A) Scheme of the experimental protocol used to analyze re-entry in the cell cycle. (B) Confocal picture of the dorsal area in a coronal section of the telencephalon in a control *Tg(gfap:GFP)* animal, labeled for GFP, BrdU and PCNA to identify proliferating cells. (C) Magnification of the boxed area in B, depicting an orthogonal projection of a cell positive for both *gfap:*GFP and BrdU. (D) Magnification of the boxed area in B, depicting an orthogonal projection of a cell positive for both *gfap:*GFP and PCNA. (E) Magnification of the boxed area in B, depicting an orthogonal projection of a cell positive for *gfap*:GFP, PCNA and BrdU. Yellow arrows point to double- or triple-positive cells. In all panels dorsal is up. Scale bars: B,C-20µm. (F) Quantification of the total number of *gfap:*GFP/PCNA/BrdU triple-positive cells over the total *gfap*:GFP/BrdU double-positive cells per animal in control and injured animals. Data are shown as mean +/- SEM; n=3 animals (4 sections per animal); $p>0.05$ (non-significant), Mann-Whitney test.

5 Discussion

In the present study, zebrafish was used as a model to study neural stem/progenitor cell behavior during constitutive neurogenesis and regeneration in an adult vertebrate brain.

One goal of this work was to dissect the roles of the different neural progenitor types existing in the telencephalic VZ in response to injury, namely, to distinguish the contribution of non-glial progenitors (neuroblasts and SAPs) versus RG cells. Using BrdU labeling and PSA-NCAM staining, it was shown that neuroblasts do not change proliferation after injury. However, differential labeling of non-glial progenitors and RG indicated that the former cell type contributes to regeneration by migrating to the injury site and generating neurons. The signals from the injury site were not present long enough to elicit a migration of late-generated, RG-derived, non-glial cells during the time frame of analysis, suggesting that these non-glial cells react fast to the injury, while the instructive cues are still present.

Another major aim of this study was to observe the behavior of individual adult NSCs in their niche *in vivo*, during homeostasis and after injury. Towards this purpose, an *in vivo* imaging technique was established, allowing for the first time the continuous monitoring of RG cells behavior in their natural niche in the adult vertebrate brain. This method revealed that during constitutive neurogenesis RG cells are mostly quiescent and only a small subset is enrolled in the formation of neurons. Two different modes of neuron generation were observed: cell division and direct neurogenesis. Dividing RG cells always self-renewed, generating either one RG and a more committed cell type, or two RG. In the other type of behavior, cells underwent direct conversion into neuron without a cell division step, revealing for the first time this mode of neurogenesis in the adult vertebrate brain.

After injury the proportion of dividing RG increased, whereas the direct neurogenesis events were very rare. The mode of cell division seemed to be shifted towards the production of more neurons, with the appearance of some symmetric non-gliogenic, terminally differentiating divisions and the lack of symmetric gliogenic divisions. Importantly, the imaging results could be reinforced by the *in vivo* clonal analysis. Additionally, this technique also corroborated the enhanced migration of cells from the VZ in response to injury.

5.1 Response of non-glial cells to injury

After injury in the adult zebrafish telencephalon, several events occur, that culminate in a successful regeneration. In different studies, several cell types were shown to react to injury by increasing their proliferation (Ayari et al., 2010; Baumgart et al., 2012; Kishimoto et al.,

2012; Kroehne et al., 2011; März et al., 2011). In the injury model used in the present study, RG cells start reacting at 48hpi but further increase proliferation later, interestingly, when the response of other cell types analyzed has stopped and the injury site is already restored (Baumgart et al., 2012). These observations prompted the search for the source of newborn neurons that repopulate the injury site. Obvious candidates to investigate were the non-glial progenitors at the VZ, which are part of the neurogenic lineage during homeostasis (Rothenaigner et al., 2011).

Curiously, neuroblasts marked with PSA-NCAM did not change their proliferative status in response to injury (Figure 4.1). However, after injury retrovirus-labeled progenitors were shown to migrate beyond the distance they migrate during normal neurogenesis (Figure 4.4). When combined with the absence of migration of lipofection-labeled cells (RG) (Figure 4.4), these results indicate that non-glial progenitors mediate early reactions to the injury and are important contributors to the regenerative process. Interestingly, in a different type of injury model in the zebrafish telencephalon, the distribution over time of neural progenitors labeled in the *ngn1:GFP* transgenic line, suggested that they migrate from the subpallial VZ to the injury site (Kishimoto et al., 2012). Together with the data from the present study, these results highlight the neural progenitor migration from the VZ as a common response to an insult in this brain region in zebrafish. Moreover, this reaction is conserved across species, as in rodents neuroblasts originated from the SVZ were also shown to migrate to the injury site (Arvidsson et al., 2002; Jin et al., 2003; Yamashita et al., 2006; Zhang et al., 2004). However, in contrast to the situation in zebrafish, these cells fail to survive and there is no successful neuronal regeneration in the mammalian models (Arvidsson et al., 2002; Takasawa, 2002; Thored et al., 2006). This initially conserved response of neuroblasts but distinct regeneration outcomes in the different species suggests that the injury environment may be distinct, being favorable to neuronal regeneration in the case of zebrafish, and inhibitory in the case of mammals. Therefore, searching for the molecules that constitute the regeneration-promoting environment of the zebrafish telencephalon might be a good approach to improve neuronal survival in the mammalian injury models.

In a previous study in which RG cells of the adult fish telencephalon were labeled genetically one day before injury, reporter-positive cells were shown to contribute to the generation of new neurons in the injured parenchyma (Kroehne et al., 2011). In the present study, however, no reporter-positive cells were found in the parenchyma using the lipofection labeling paradigm, which specifically labels RG (Figure 4.2, Figure 4.4). One possible explanation for this apparent inconsistency is that the smaller injury performed herein did not

release enough signals that lasted sufficiently long to elicit an activation of late-generated, RG-derived, non-glial cells, whereas in the bigger lesion from Kroehne *et al*, the inducing signals from the injury site are present for a longer time, allowing the RG to generate non-glial cells that can still sense the cues and migrate towards them. This hypothesis is supported by the observations that, both when lipofected RG are given time to generate non-glial cells before the injury (delayed paradigm, Figure 4.4) or when a larger injury was performed (Baumgart et al., 2012), reporter-positive or *gfap:GFP*-positive cells, respectively, were found in the parenchyma.

As mentioned before, the non-glial progenitors in the adult zebrafish telencephalon constitute a heterogeneous population, containing also SAPs (PSA-NCAM-negative cells) in addition to neuroblasts (Baumgart et al., 2012). It would be therefore important to distinguish the reactions of these two progenitor subtypes. In a first approach, the response of SAPs in terms of proliferation should be addressed independently of the one from neuroblasts. Since Sox2 was shown to be present in virtually all VZ progenitors (März et al., 2010a), proliferation of SAPs could be measured by quantifying Sox2+/BrdU+/PSA-NCAM-/GFAP-cells at different time-points after injury. Furthermore, a differential labeling using a retrovirus-based approach would also be interesting to further discriminate their reaction in terms of proliferation and migration. Another approach that could be explored in future studies is the observation of non-glial-cell behavior in homeostasis and after injury by *in vivo* imaging. However, all these exciting upcoming investigations highly depend on good markers/antibodies to specifically label SAPs. Upon establishment of such markers it will be possible to generate transgenic lines and/or constructs driven by SAP-specific or neuroblast-specific promoters that will facilitate the different approaches to study their behavior after injury.

One further subject to be investigated within this context is the nature of the cues that induce and guide non-glial cell migration towards the injury site. An interesting candidate is Prokineticin 2 (Prok2), a secreted protein that is involved in several physiological processes, including adult neurogenesis (Cheng et al., 2006; Ng et al., 2005). This protein is expressed in neurons of the mouse OB and acts as a chemoattractant that guides the migration of SVZ-derived neuroblasts towards the OB (Cheng et al., 2006; Ng et al., 2005; Prosser et al., 2007). Interestingly, this molecule is expressed in the constitutive neurogenic sites in the adult zebrafish brain, and an injury in the telencephalon induces a transient, ectopic expression of Prok2 at the injury site (Ayari et al., 2010), consistent with the hypothesis that it could attract neural progenitors to induce repair.

In the ischemic striatum of mammalian brains, the secretion of stromal-derived factor 1α (Sdf1α) by reactive astrocytes was shown to induce the migration of neuroblasts, that express the corresponding receptor, the C-X-C chemokine receptor type 4 (CXCR4) (Imitola et al., 2004; Liu et al., 2008; Robin et al., 2005; Thored et al., 2006; Tran et al., 2007). Curiously, this signaling pathway has been shown to control cell migration in different systems in zebrafish, such as the embryo during gastrulation (Mizoguchi et al., 2008), the germ-cells (Knaut et al., 2003) or the posterior lateral line (David et al., 2002). Considering that CXCR4 and Sdf1α are both expressed in the adult zebrafish brain (Diotel et al., 2010), they are plausible candidates to mediate migratory responses after injury.

In summary, the conservation of non-glial cells/neuroblasts responses in the zebrafish and mouse models, as well as the existence of common molecules in both systems, further validate the use of zebrafish as a model to study regeneration. Using this vertebrate model, several lines of investigation could be followed to better understand the reaction of non-glial progenitors and their role in the neuronal regeneration process in the brain. Very importantly, the *in vivo* imaging technique established here can be an important tool to pursue these investigations.

5.2 *In vivo* imaging as a tool to follow NSCs in the adult brain

To better understand the response of RG cells to injury in comparison with intact animals, an *in vivo* imaging technique using confocal and 2pLSM lasers was implemented. LSM was chosen for this purpose due to the reasonably good cellular resolution and tissue penetration (reviewed in (Fischer et al., 2011)), considering the superficial location of RG cells in the everted zebrafish telencephalon. Even though LSM has the disadvantages of causing photobleaching/damage with repetitive imaging and having a relatively slow image acquisition (Fischer et al., 2011), these limitations were not particularly relevant for the present work, since the areas of interest were imaged only once every two days,.

The implementation of this technique in the present work allowed for the first time to follow single adult NSCs in their niche in the vertebrate brain over time, revealing their behavior during homeostasis and in response to brain injury. Importantly, the clonal analysis data obtained herein supported the imaging observations, indicating that the continuous *in vivo* imaging procedure does not significantly affect the cell behavior.

Due to the sparse cell labeling used in this study, it was possible to reliably find the same cells in the different imaging sessions. In subsequent experiments, however, it would be of interest to follow cells in an uninterrupted mode to visualize particular, fast behaviors that

might be unnoticed in this paradigm. As an example, it would be interesting to follow the fast reaction of microglia to the injury and how the wound is closed without the formation of a scar. This continuous imaging with higher time resolution would also be useful to investigate mechanisms that have been shown to regulate the mode of cell division during development, such as the angle of cell division or the distribution of cell fate determinants in daughter cells (Alexandre, 2010; Chenn and McConnell, 1995; Dong et al., 2012; Konno et al., 2008; Postiglione et al., 2011; Schwamborn et al., 2009; Wilcock et al., 2007; Xie et al., 2013). However, to perform this uninterrupted type of imaging, it will be necessary to improve the fish survival, in order to allow the observation of cell behaviors for a long time. Additionally, the use of the transparent zebrafish line *casper* (White et al., 2008) could potentially increase the imaging depth and facilitate the visualization of cell behaviors closer to the injury site, in the telencephalic parenchyma.

One possible concern with the morphology-based identification of cells used in the *in vivo* imaging procedure is the wrong assignment of cell identity. On one hand, some cells could have extremely thin processes, not visible without staining and with the technical set up used here, which would lead to the wrong classification of a RG as non-glial. However, the fact that the clonal analysis, which was based on the same morphological criteria, corroborated the *in vivo* imaging results makes this wrong assignment of cell identity an unlikely possibility. On the other hand, staining of electroporated cells at 2dpl showed that there are GFAP-positive cells that do not possess RG morphology (Figure 4.5). Nonetheless, the existence of these cells should not present a concern, once they do not have a basal attachment, and therefore cannot be considered bona fide RG. Instead, these cells could be a product of a RG division, that had not yet time to downregulate the GFAP protein in the transition to a non-glial state. Alternatively they could also be RG cells that have not yet re-grown the process after a division. However, the observation of a symmetric gliogenic division by *in vivo* imaging shows that it is possible that both daughter cells have a process shortly after division (Figure 4.18).

Electroporation also revealed that there are cells with RG morphology that are negative for both the RG marker GFAP and the neuronal marker HuCD (Figure 4.5). To investigate the identity of these cells, other RG markers, such as S100β or aromatase B, should be tested. Independently of the identity of these cells, these data already demonstrate that there is heterogeneity within the RG-cell population lining the ventricle. In fact, a very recent study reported the distinct origins of two sub-populations of NSCs in the adult zebrafish pallium: one in the dorso-medial domain and another composing the lateral domain (Dirian et al.,

2014). These sub-populations of cells arise from two distinct embryonic progenitor populations that are located in different regions and activated at different stages in the developing forebrain. Therefore it is clear that adult NSCs in the zebrafish dorsal telencephalon are heterogeneous and it would be interesting to further characterize these differences and examine the biological meaning of this heterogeneity.

In summary, the *in vivo* imaging established herein allowed for the first time the visualization of adult NSCs in their natural niche in a vertebrate model, not only during homeostasis but also after brain damage. Consequently, several features of the behavior of individual adult NSCs were revealed at the single cell level, at an extent that could not be assessed by previous population-based studies. The knowledge acquired with the observation of NSC behavior in the zebrafish brain may serve as a basis to conduct studies on modulating NSC activity in the diseased brain. For the application of these findings in mammalian disease models it will be important to compare the NSC behavior in zebrafish and mammals. Hence, for a proper comparison, it is of extreme importance to implement *in vivo* imaging techniques that would allow the visualization of adult NSCs also in mammalian animal models. Such a technique could be based on the insertion of an optic probe into the brain, as it was done previously to observe neuroblasts migration (Davenne et al., 2005).

5.3 Behavior of RG cells during constitutive neurogenesis

The establishment of the *in vivo* imaging technique in the adult zebrafish telencephalon reported here allowed for the first time the visualization of adult NSCs in their intact niche in a vertebrate brain. So far, imaging of NSC behavior had only been done in embryonic stages, either in intact zebrafish embryos (Alexandre, 2010; Buckley et al., 2013; Dong et al., 2012; Lyons et al., 2003; Tawk, 2007) or mammalian and chicken embryonic brain slices (Betizeau et al., 2013; Gertz et al., 2014; Hansen et al., 2010; Noctor et al., 2001; Noctor et al., 2004; Pilz et al., 2013; Wilcock et al., 2007)

In the present work, cells were labeled by transfection of plasmids expressing a fluorescent protein driven by constitutive promoters. This method was preferred to other methods due to the lack of bias towards a particular cell type. Moreover, since the plasmid is injected in the telencephalic ventricle, it was likely to transduce mostly the cells that are directly in contact with the ventricular space, namely the RG cells. Other alternative techniques could have been the use of viruses. Simple retroviruses stably transduce dividing cells, since they can only incorporate their genetic material into the host’s DNA upon breakage of the nuclear membrane (reviewed in (Cockrell and Kafri, 2007)). A drawback of

this method, however, is that it labels a big proportion of non-glial progenitors, and it would only target a subset of RG cells, the ones undergoing division (Figure 4.3). Therefore, the quiescent RG cells, which constitute the majority of RG cell population (Chapouton et al., 2010), would not be labeled. Labeling by lentivirus transduction would be an alternative to mark also the quiescent RG (Rothenaigner et al., 2011), but it has been observed in mice that lentiviruses have a tropism for ependymal cells (Brill and Ninkovic, personal communication), which normally don't divide in physiological conditions (Carlen et al., 2009; Spassky et al., 2005). Since in the adult zebrafish telencephalon no typical ependymal cells at the brain surface have been identified (only in a separate DEL) (Lindsey et al., 2012), one cannot exclude that some RG cells may function as ependymal and therefore do not contribute to constitutive adult neurogenesis. For this reason, to avoid targeting of these putative ependymal-like cells, lentiviruses were not used.

As it had been observed before in population studies, the *in vivo* imaging data presented here confirm that only a small percentage of RG cells divide in a certain time window (Chapouton et al., 2010; Rothenaigner et al., 2011). However, these studies could not reveal the behavior of each individual cell. Herein, it was demonstrated that RG cells dividing in the intact telencephalon divide either symmetrically to produce two RG or asymmetrically, generating one RG and a non-glial daughter (summarized in

Figure 4.21). These modes of divisions of RG cells in the intact brain had previously been suggested by clonal analysis using lentivirus (Rothenaigner et al., 2011). The maintenance of RG cells in all cell divisions constitutes an important mechanism to keep the progenitor pool in the adult telencephalon, allowing the continuous neurogenesis and brain growth throughout the animal's life.

Also in agreement with the clonal analysis study (Rothenaigner et al., 2011), only one division per RG cell was observed during the time frame of analysis (Figure 4.23), demonstrating a slow proliferation rate of RG cells, a characteristic of adult NSCs. Curiously, in the asymmetric divisions, no subsequent division of the non-glial daughter was observed, in disagreement with the role of non-glial progenitors as intermediate progenitors that amplify the output from a single stem cell (Rothenaigner et al., 2011). However, it must be taken into account that the non-glial progenitors are located deeper in the telencephalon relatively to RG cells (Figure 1.4) (Ganz et al., 2010; März et al., 2010a), and therefore the technical depth limits imposed by the confocal laser might impair the visualization of the subsequent behavior of non-glial progenitors. Nevertheless, both the imaging and the clonal analysis data obtained in the present work indicate the persistent self-renewal of RG cells upon division, and the

limited progeny per activated cell. This self-renewing mode of division with a reduced cellular output per stem cell is reminiscent of the mode of neurogenesis in the adult murine hippocampus (Bonaguidi et al., 2011; Encinas et al., 2011).

A novel feature of adult neurogenesis in the adult zebrafish telencephalon uncovered by *in vivo* imaging was the direct conversion of a RG cell into a HuCD-positive neuron, without cell division (Figure 4.9,Figure 4.10). Importantly, this direct neurogenesis mode was supported by clonal analysis, in which an increase in the proportion of single non-glial cells was observed over time (Figure 4.17). Interestingly, in the previous clonal analysis performed with lentivirus, single non-glial clones were also observed at 3-4 weeks post injection (Rothenaigner et al., 2011). However these clones were neglected in this study since they were probably believed to originate from the small proportion of non-glial cells that is nonetheless targeted by lentivirus (Rothenaigner et al., 2011). Therefore, the observations made herein emphasize the importance of *in vivo* imaging as a powerful technology to reliably and accurately identify behaviors of individual cells that are difficult to notice in static methods.

Interestingly, so far this direct mode of neurogenesis had never been observed in the adult brain. This could mean either that zebrafish RG cells in the adult telencephalon possess this unique capacity, or simply that this type of cells has not yet been detected in the adult brain of other animal models due to the lack of suitable technical approaches. In the future, with the advances in the *in vivo* imaging technology in other animals or brain areas this question will certainly be resolved. Even though it has not been detected in adult brains, direct neurogenesis has been observed in embryonic systems. In the developing zebrafish hindbrain, for instance, single progenitors labeled at the neural rod stage were shown to convert into neurons directly without cell division (Lyons et al., 2003). Neurons were also shown to arise directly from RG cells after asymmetric or neurogenic cell divisions in the zebrafish forebrain (Dong et al., 2012) and hindbrain (Alexandre, 2010; Lyons et al., 2003). Moreover, NE and RG cells in the mouse embryonic cortex can also generate neurons directly without going through an intermediate progenitor state (Haubensak et al., 2004; Miyata et al., 2004; Noctor et al., 2004). Taken together, these studies and the data obtained here using the *in vivo* imaging technology reveal that the mechanism of neuron generation in the adult zebrafish telencephalon conserves features of the embryonic brain.

One relevant question that remains to be answered regarding the modes of neurogenesis in the intact zebrafish telencephalon is whether the RG cells undergoing division and the ones directly converting into neurons constitute two independent sub-populations of RG cells, or

whether they belong to the same lineage. The observation from two lineage trees of control animals that RG cells generated from an asymmetric division of a mother RG cell can undergo direct conversion into a neuron (trees E and F in Figure 4.23), strongly supports the idea that directly converting cells belong to the lineage of amplifying RG cells. Accordingly, in the zebrafish embryonic forebrain and hindbrain, and also in the mouse developing cortex, some direct neurogenesis events occur via RG cells that divide asymmetrically and generate one neuron without an intermediate progenitor step (Alexandre, 2010; Dong et al., 2012; Haubensak et al., 2004; Lyons et al., 2003; Noctor et al., 2004).

5.3.1 Molecular regulators of RG cell behavior in the intact brain

The observation of RG cell behavior in the intact zebrafish brain uncovered conserved and unique features of adult neurogenesis in vertebrates. The present findings and the technology developed in this work open new possibilities to further reveal how these cell behaviors are regulated and how they can be manipulated towards specific purposes. In this context, it will be important to identify molecular signals that are involved in the different modes of neurogenesis conducted by RG cells.

One possible candidate is the Notch signaling pathway, which has been implicated in the regulation of neural progenitor maintenance and differentiation in animals (reviewed in (Pierfelice et al., 2011)). Specifically in the zebrafish embryonic forebrain, life imaging and knock-down experiments revealed that Notch signaling within a single cell lineage controls the self-renewal or differentiation of daughter cells of an asymmetric division, with the cell that exhibits higher level of Notch remaining a progenitor, while the other differentiates (Dong et al., 2012). In this case, therefore, Notch seems to be important to maintain progenitor fate, as observed also in the zebrafish retina (Del Bene et al., 2008) and the mouse forebrain (Gaiano et al., 2000; Mizutani et al., 2007; Shitamukai et al., 2011; Yoon et al.). In contrast, in the adult telencephalon of zebrafish, Notch maintains the quiescence of RG cells, and its inhibition recruits them to the cell cycle (Chapouton et al., 2010). In a subsequent study using clonal analysis, Notch inhibition was found to increase the recruitment of RG to the cell cycle without affecting the mode of cell division (Rothenaigner et al., 2011). However it seems that Notch acts preferentially to limit the symmetric gliogenic divisions of RG cells (Alunni et al., 2013). In summary, by combining the *in vivo* imaging technology with the manipulation of this important signaling pathway it will be possible to dissect the specific role of Notch in proliferation, mode of cell division and maintenance of cell identity as well as the population(s) or sub-population(s) of adult NSCs it regulates in the adult zebrafish brain.

Components of the apical protein complex, located in the apical side of the NE/RG cell membrane, have been shown to be important to determine cell fate during development. In the mouse, partitioning defective 3 homolog (Par3), a component of this apical complex, is required to maintain apical progenitors in a self-renewing proliferative state (Bultje et al.; Costa et al., 2008). In contrast, in the developing zebrafish hindbrain, Par3 seems to be involved in neuronal fate determination (Alexandre, 2010). Likewise, atypical Protein Kinase C (aPKC), another component of the apical protein complex, was shown to induce progenitor differentiation rather than maintenance in the zebrafish retina (Baye and Link, 2007). Despite these opposite results, it is clear that proteins of the apical membrane are involved in cell fate determination in different species. Even though the expression of apical membrane components has not been investigated in the adult zebrafish brain, these observations in embryonic stages and in mice suggest that they could also play a role in the adult RG cell division mode.

5.4 Behavior of RG cells during regenerative neurogenesis

The *in vivo* imaging technique, complemented by clonal analysis, also allowed the observation of changes in RG behavior in the context of neuronal regeneration.

As had been observed in previous studies at the population level (Baumgart et al., 2012; Kroehne et al., 2011), the proportion of RG cells entering the cell cycle was increased after injury (Figure 4.13). Very importantly, the present study further uncovered a shift in the mode of cell division undergone by RG cells (Figure 4.21). Whereas during constitutive neurogenesis RG cells always self-renew, after injury some cells divided in a symmetric non-gliogenic way, depleting themselves and leading to a net increase in the production of non-glial progeny (Figure 4.22). This mode of division is a fast approach to achieve a high neuron production in less division rounds (and without changing the cell cycle length) and therefore to quickly cope with the demands of the injured brain. Despite the depletion of RG in these divisions, the NSC pool should not be affected due to the general increase in the number of dividing cells and the fact that the majority of them divide nevertheless in an asymmetric way, maintaining the RG cell pool.

Important information obtained from this data was that, also after injury, RG cells only divided once during the extent of the experiment, exhibiting a slow rate of proliferation that is comparable to the one observed in intact brains (Figure 4.24). Even though further analysis would be necessary, these results suggest that there is no change in the proliferative capacity or cell cycle length of RG cells in response to injury. However, in one single example of

asymmetric cell division after injury, the non-glial daughter cell underwent another round of proliferation (Figure 4.25), which could indicate that there is amplification of the lineage at the level of non-glial progenitors. Nevertheless, the rather low proliferative capacity of individual RG cells demonstrates that the increase in proliferation to cope with injury is achieved by the recruitment of more cells to the cell cycle rather than an increase in the rounds of division of single cells or shortening of the cell cycle. This conclusion is supported by the observation in the clonal analysis experiments that the proportion of 2-cell clones is increased at 28 days in injury conditions (Figure 4.15).

A striking feature in RG cell behavior after injury was the near absence of cells undergoing direct neurogenesis, a process that was relatively frequent in the non-injured brain (Figure 4.13). This behavior is probably not advantageous in the adverse conditions of brain damage, since it depletes the NSCs and only gives rise to one neuron per RG. Therefore it is reasonable to imagine that after injury it is more profitable for the brain to increase cell division, in order to maintain the RG cell population and generate more neurons at the same time.

In summary, the results observed using the *in vivo* imaging methodology show different behaviors of RG cells in control and injured animals. A question that could not be addressed with the experimental paradigm implemented herein is whether the same RG change their behavior following the injury, or if there are distinct RG cell sub-populations that have an intrinsic behavior profile, with one sub-population being more prominent during constitutive neurogenesis, while the other preferentially reacts to injury. In other words, are individual cells changing their mode of division after injury, or is there a specific subset of RG cells that is intrinsically programmed to divide exclusively in a symmetric terminal mode, but only gets activated in injury conditions? And are cells undergoing direct conversion not active after injury, or do they change their “internal program” and divide instead of depleting themselves? To investigate these possibilities, a different *in vivo* imaging paradigm should be employed, in which RG cells are followed for a long time in the intact brain, to identify their behavioral pattern during constitutive neurogenesis. Afterwards, the animals should be injured and the same cells should continue to be monitored for additional time after the injury.

To partially shed light on these questions, an analysis of cell cycle re-entry was made, taking advantage of the BrdU labeling methodology, in order to ascertain if cells proliferating in response to injury are the same that divide during constitutive neurogenesis (Figure 4.27). The percentage of progenitors re-entering the cell cycle was not different in injury and control conditions, indicating an equivalent contribution to the injury response of progenitors engaged

in normal neurogenesis and also quiescent cells, in a coordinated effort towards regeneration. In other regenerating systems in zebrafish, the situation seems to be different, since in the retina and the spinal cord quiescent RG-like cells that normally do not participate in constitutive neurogenesis (Müller Glia in the retina and ependymoglia in the spinal cord) are recruited to the cell cycle and actively contribute to neuronal regeneration after an insult (Fausett and Goldman, 2006; Lenkowski and Raymond, 2014; Nagashima et al., 2013; Reimer et al., 2008). It must be mentioned however, that in contrast to the telencephalon, the adult zebrafish spinal cord does not have constitutive neurogenesis (Reimer et al., 2008).

An important question regarding the behavior of stem cells in homeostasis and regeneration is whether their self-renewal is limited to a certain number of cell cycles or is unlimited. In the zebrafish caudal fin amputation paradigm it was shown that even after repeated amputations, the progenitor cells were always able to completely reconstitute the whole damaged tissue without losing efficiency (Azevedo et al., 2011; Shao et al., 2011). Interestingly, in an axonal regeneration paradigm of the zebrafish posterior lateral line, the authors observed that the latency of nerve regeneration is reduced in a second injury, suggesting that regeneration-promoting factors induced by the first cut facilitate regeneration of a second cut (Graciarena et al., 2014) and emphasizing the role of the environment in the regenerative response. Taking these findings into consideration, it would be interesting to test the self-renewal limit of adult NSCs in the zebrafish telencephalon by performing several injuries and evaluating the capacity to replace the lost neurons with the increase in the number of lesions.

5.4.1 Molecular regulators of RG cell behavior in the injured brain

Following the present description of RG cell behavioral changes in response to injury, it would be important to identify factors responsible for this difference in behavioral pattern compared to RG cells in the intact telencephalon.

One of the cellular processes that has been shown to regulate the regenerative response in the adult zebrafish telencephalon is inflammation (Kyritsis et al., 2012). In mammals, injury-induced inflammation has generally been considered to impair neurogenesis and regeneration (Ekdahl et al., 2003; Hoehn et al., 2005; Monje et al., 2003; Popovich et al., 2002). In contrast, inflammation in the zebrafish telencephalon is necessary and sufficient to induce RG cell proliferation and formation of newborn neurons. These effects were at least in part mediated by the Cysteinyl Leukotriene Receptor 1 (Cystlr1)-Leukotriene C4 (LTC4)

pathway (Kyritsis et al., 2012). Additionally, the C-X-C chemokine receptor type 5 (CXCR5) is also involved in regulating regenerative neurogenesis (Kizil et al., 2012a).

Interestingly, the transcription factor Gata3 is specifically expressed in the zebrafish telencephalon, fin and heart exclusively after injury (Kizil et al., 2012b). In the telencephalon this transcription factor is required, but not sufficient, for RG-injury induced proliferation and regenerative neurogenesis (Kizil et al., 2012b). Since this molecule is not expressed in the intact telencephalon, it is a strong candidate to modulate RG cell behavior specifically after injury.

In a study in the adult mice, Notch signaling was shown to actively maintain the quiescence of ependymal cells lining the lateral ventricles (Carlen et al., 2009). In uninjured animals ependymal cells do not produce progeny but after stroke they are activated to proliferate and generate neuroblasts and astrocytes (Carlen et al., 2009). Forced Notch signaling blocked the ependymal response to stroke, whereas inhibition of this pathway induced ependymal cells to enter cell cycle and produce neuroblasts even in control conditions, establishing the Notch pathway as a key regulator of ependymal cell activity in the mouse forebrain (Carlen et al., 2009). Reminiscent to the role of Notch in mouse ependymal cells is its function in maintaining quiescence of RG cells in the adult zebrafish telencephalon (Alunni et al., 2013; Chapouton et al., 2010). Establishing a parallel to the findings in mouse, it is conceivable that Notch signaling must be inhibited after injury so that the RG can be activated in the telencephalon. Indeed, in the zebrafish injured spinal cord, Notch signaling is a negative regulator of proliferation and motor neuron regeneration (Dias et al., 2012). However, different injury models in the adult zebrafish and newt telencephalon, revealed precisely an opposite function of Notch, since its blockade led to a reduction in the injury-induced proliferation (Kirkham et al., 2014; Kishimoto et al., 2012). These observations suggest that Notch may have a distinct role in the normal and in the injured brain as well as in different brain regions, and further highlight the dissimilarities between the constitutive and injury-induced neurogenesis.

Another signal known to play a role in regeneration is Shh. Shh signaling was shown to be important for ependymoglia proliferation and regeneration of motoneurons in the zebrafish spinal cord (Reimer et al., 2009), as well as for regeneration of midbrain dopamine neurons in the newt (Berg et al., 2010). Moreover, in the injured mouse brain, this signaling pathway is required and sufficient to induce astrocyte proliferation *in vivo* and to elicit their stem cell-like response *in vitro* (Sirko et al., 2013).

5.5 Telencephalon regeneration: two types of responses

Altogether, the results from the present work suggest that the reaction to injury in the adult zebrafish telencephalon comprises two types of responses. On one hand, non-glial progenitors from the VZ migrate to the injury site and contribute to generate newborn neurons. This conclusion is supported by the observations that only retrovirus-labeled but not lipofection-labeled cells are found in the injured parenchyma, distant from the VZ. Interestingly, the subset of non-glial cells composed of neuroblasts does not change its proliferative status. On the other hand, when the wound is already closed and some newborn neurons have been deposited in the previously injured parenchyma, RG cells located at the VZ intensify their response by increasing proliferation and changing their mode of division towards a higher net production of non-glial cells. This delayed reaction of RG was evident both in the clonal analysis and the *in vivo* imaging data, since the injury-induced RG cell divisions were also observed at late time points after injury. As at these later times no major signs of the injury are detected and the tissue appears restored (Baumgart et al., 2012), this tardy response of RG might be less associated to the reconstitution of the injured parenchyma, but more related to the replacement of non-glial cells at the VZ, that were lost during the migration at earlier stages. This “bipartite response” hypothesis and the comparison with neurogenesis during homeostasis are presented in the model in Figure 5.1.

Taken together, this work reveals the responses of different neural progenitor types to injury in the adult zebrafish telencephalon, and highlights the direct contribution of non-glial progenitors to neuron formation and the role of RG in restoring the neurogenic niche. The discovery of the distinct reactions of the different progenitor types, together with upcoming studies on the mechanisms regulating each type of progenitor may help in the development of treatments for brain injuries directed towards the net increase of the responsive endogenous progenitors. Additionally, the *in vivo* imaging technique developed herein opens new doors to the study of NSC behavior in the adult brain and will also facilitate the discovery of stem cell regulation mechanisms that can potentially be applied in future regenerative therapies.

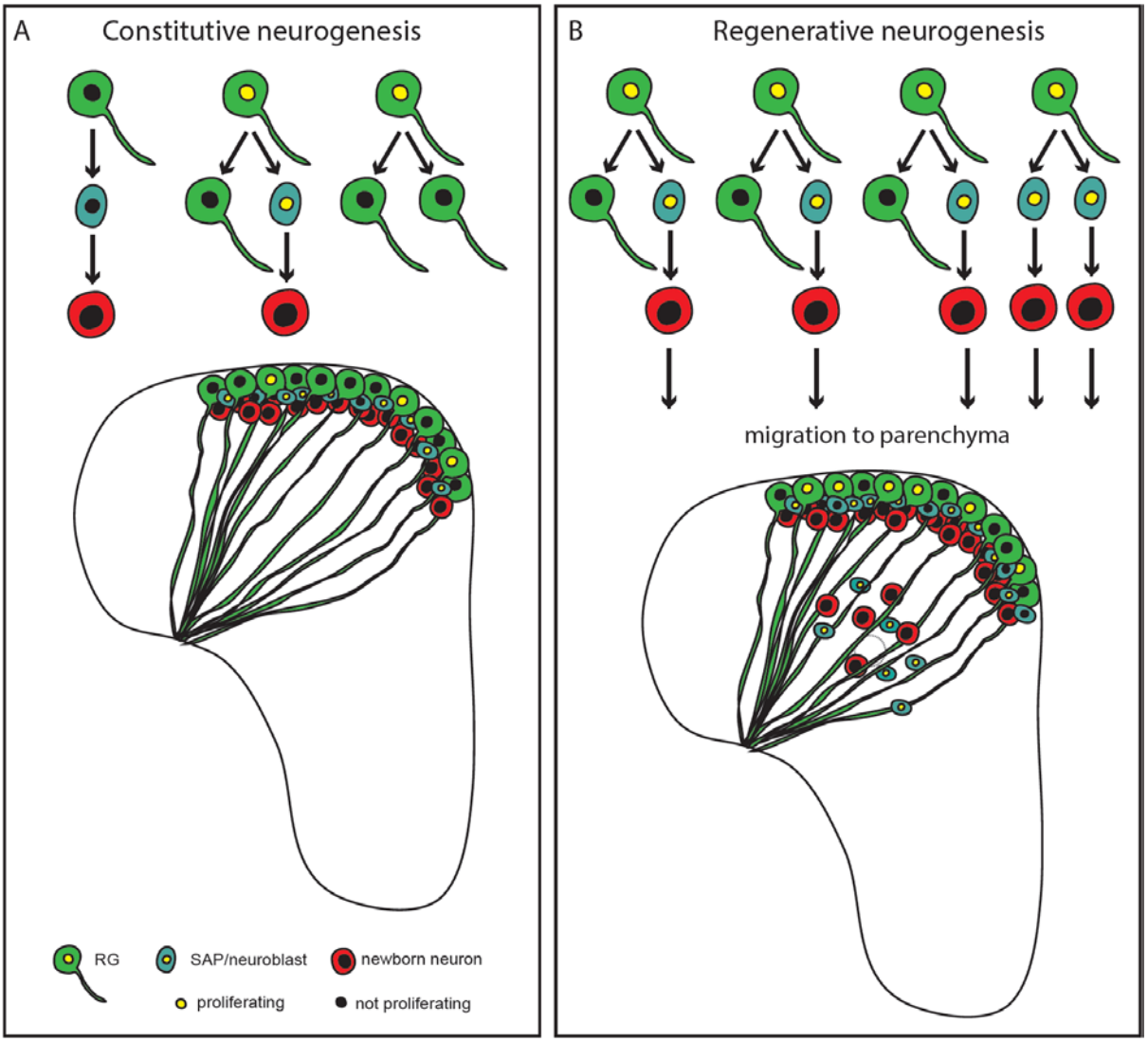

Figure 5.1: Model of neurogenesis in the adult zebrafish telencephalon in homeostasis and after injury. (A) Illustration of the modes of cell division and neuron generation during constitutive neurogenesis and the organization of the neurogenic niche in control conditions. Note the neuronal progenitor types located at the VZ and the newborn neurons deposited immediately adjacent to them. (B) Illustration of the modes of cell division during regenerative neurogenesis and the organization of the neurogenic niche in injury conditions. Note the increase in proliferating RG cells at the VZ, the change in the mode of cell division and the migration of non-glial progenitors to the injured parenchyma. Accordingly, newborn neurons are also deposited in this area, contributing to the tissue regeneration. Dimensions of cells and telencephalic hemisphere are not to scale.

6 References

Aaku-Saraste, E., Hellwig, A., and Huttner, W.B. (1996). Loss of Occludin and Functional Tight Junctions, but Not ZO-1, during Neural Tube Closure—Remodeling of the Neuroepithelium Prior to Neurogenesis. Developmental Biology *180*, 664-679.

Aaku-Saraste, E., Oback, B., Hellwig, A., and Huttner, W.B. (1997). Neuroepithelial cells downregulate their plasma membrane polarity prior to neural tube closure and neurogenesis. Mechanisms of Development *69*, 71-81.

Aboody, K., Capela, A., Niazi, N., Stern, Jeffrey H., and Temple, S. (2011). Translating Stem Cell Studies to the Clinic for CNS Repair: Current State of the Art and the Need for a Rosetta Stone. Neuron *70*, 597-613.

Adolf, B., Chapouton, P., Lam, C.S., Topp, S., Tannhauser, B., Strahle, U., Götz, M., and Bally-Cuif, L. (2006). Conserved and acquired features of adult neurogenesis in the zebrafish telencephalon. Dev Biol *295*, 278-293.

Alexandre, P.R., Alexander M; Barker, David; Blanc, Eric; Clarke, Jonathan D W (2010). Neurons derive from the more apical daughter in asymmetric divisions in the zebrafish neural tube. Nat Neurosci *13*, 673-679.

Altman, J. (1963). Autoradiographic investigation of cell proliferation in the brains of rats and cats. Anat Rec *145*, 573 - 591.

Altman, J. (1969a). Autoradiographic and histological studies of postnatal neurogenesis. 3. Dating the time of production and onset of differentiation of cerebellar microneurons in rats. J Comp Neurol *136*, 269-293.

Altman, J. (1969b). Autoradiographic and histological studies of postnatal neurogenesis. IV. Cell proliferation and migration in the anterior forebrain, with special reference to persisting neurogenesis in the olfactory bulb. The Journal of Comparative Neurology *137*, 433-457.

Altman, J., and Das, G. (1965a). Autoradiographic and histological evidence of postnatal hippocampal neurogenesis in rats. J Comp Neurol *124*, 319 - 335.

Altman, J., and Das, G.D. (1965b). Autoradiographic and histological evidence of postnatal hippocampal neurogenesis in rats. J Comp Neurol *124*, 319-335.

Altman, J., and Das, G.D. (1965c). Autoradiographic and histological evidence of postnatal hippocampal neurogenesis in rats. The Journal of Comparative Neurology *124*, 319-335.

Alunni, A., Krecsmarik, M., Bosco, A., Galant, S., Pan, L., Moens, C.B., and Bally-Cuif, L. (2013). Notch3 signaling gates cell cycle entry and limits neural stem cell amplification in the adult pallium. Development *140*, 3335-3347.

Alvarez-Buylla, A., Theelen, M., and Nottebohm, F. (1990). Proliferation “hot spots” in adult avian ventricular zone reveal radial cell division. Neuron *5*, 101-109.

Amrein, I., Dechmann, D.K.N., Winter, Y., and Lipp, H.-P. (2007). Absent or Low Rate of Adult Neurogenesis in the Hippocampus of Bats (Chiroptera). PLoS ONE *2*, e455.

Arvidsson, A., Collin, T., Kirik, D., Kokaia, Z., and Lindvall, O. (2002). Neuronal replacement from endogenous precursors in the adult brain after stroke. Nat Med *8*, 963-970.

Ayari, B., Elhachimi, K.H., Yanicostas, C., Landoulsi, A., and Soussi-Yanicostas, N. (2010). Prokineticin 2 expression is associated with neural repair of injured adult zebrafish telencephalon. J Neurotrauma *27*, 959-972.

Azevedo, A.S., Grotek, B., Jacinto, A., Weidinger, G., and Saúde, L. (2011). The Regenerative Capacity of the Zebrafish Caudal Fin Is Not Affected by Repeated Amputations. PLoS ONE *6*, e22820.

Bardehle, S., Kruger, M., Buggenthin, F., Schwausch, J., Ninkovic, J., Clevers, H., Snippert, H.J., Theis, F.J., Meyer-Luehmann, M., Bechmann, I., *et al.* (2013). Live imaging of astrocyte responses to acute injury reveals selective juxtavascular proliferation. Nat Neurosci *16*, 580-586.

Barker, J.M., Boonstra, R., and Wojtowicz, J.M. (2011). From pattern to purpose: how comparative studies contribute to understanding the function of adult neurogenesis. European Journal of Neuroscience *34*, 963-977.

Barkho, B.Z.Z., Xinyu (2011). Adult neural stem cells: response to stroke injury and potential for therapeutic applications. Curr Stem Cell Res Ther *6*, 327-338.

Batista-Brito, R., Close, J., Machold, R., and Fishell, G. (2008). The Distinct Temporal Origins of Olfactory Bulb Interneuron Subtypes. The Journal of Neuroscience *28*, 3966-3975.

Baumgart, E.V., Barbosa, J.S., Bally-Cuif, L., Götz, M., and Ninkovic, J. (2012). Stab wound injury of the zebrafish telencephalon: a model for comparative analysis of reactive gliosis. Glia *60*, 343-357.

Baye, L.M., and Link, B.A. (2007). Interkinetic Nuclear Migration and the Selection of Neurogenic Cell Divisions during Vertebrate Retinogenesis. The Journal of Neuroscience *27*, 10143-10152.

Beckervordersandforth, R., Tripathi, P., Ninkovic, J., Bayam, E., Lepier, A., Stempfhuber, B., Kirchhoff, F., Hirrlinger, J., Haslinger, A., Lie, D.C., *et al.* (2010). In vivo fate mapping and expression analysis reveals molecular hallmarks of prospectively isolated adult neural stem cells. Cell Stem Cell *7*, 744-758.

Berg, D.A., Kirkham, M., Beljajeva, A., Knapp, D., Habermann, B., Ryge, J., Tanaka, E.M., and Simon, A. (2010). Efficient regeneration by activation of neurogenesis in homeostatically quiescent regions of the adult vertebrate brain. Development *137*, 4127-4134.

Bernardos, R., and Raymond, P. (2006). GFAP transgenic zebrafish. Gene Expr Patterns *6*, 1007 - 1013.

Betizeau, M., Cortay, V., Patti, D., Pfister, S., Gautier, E., Bellemin-Ménard, A., Afanassieff, M., Huissoud, C., Douglas, Rodney J., Kennedy, H., *et al.* (2013). Precursor Diversity and Complexity of Lineage Relationships in the Outer Subventricular Zone of the Primate. Neuron *80*, 442-457.

Birse, S.C., Leonard, R.B., and Coggeshall, R.E. (1980). Neuronal increase in various areas of the nervous system of the guppy, Lebistes. The Journal of Comparative Neurology *194*, 291-301.

Blinder, P., Shih, A.Y., Rafie, C., and Kleinfeld, D. (2010). Topological basis for the robust distribution of blood to rodent neocortex. Proceedings of the National Academy of Sciences.

Bonaguidi, M.A., Wheeler, M.A., Shapiro, J.S., Stadel, R.P., Sun, G.J., Ming, G.L., and Song, H. (2011). *In vivo* clonal analysis reveals self-renewing and multipotent adult neural stem cell characteristics. Cell *145*, 1142-1155.

Bovetti, S.H., Yi-Chun; Bovolin, Patrizia; Perroteau, Isabelle;a Kazunori, Toid; Puche, Adam C. (2007). Blood vessels form a scaffold for neuroblast migration in the adult olfactory bulb. J Neuroscience *27*, 5976-5980.

Brandstätter, R., and Kotrschal, K. (1990). Brain Growth Patterns in Four European Cyprinid Fish Species (Cyprinidae, Teleostei): Roach (*Rutilus rutilus*), Bream (*Abramis brama*), Common Carp (*Cyprinus carpio*) and Sabre Carp (*Pelecus cultratus*). Brain, Behavior and Evolution *35*, 195-211.

Brill, M.S., Ninkovic, J., Winpenny, E., Hodge, R.D., Ozen, I., Yang, R., Lepier, A., Gascon, S., Erdelyi, F., Szabo, G., *et al.* (2009). Adult generation of glutamatergic olfactory bulb interneurons. Nat Neurosci *12(12)*, 1524-1533.

Buckley, C.E., Ren, X., Ward, L.C., Girdler, G.C., Araya, C., Green, M.J., Clark, B.S., Link, B.A., and Clarke, J.D.W. (2013). Mirror-symmetric microtubule assembly and cell interactions drive lumen formation in the zebrafish neural rod, Vol 32.

Buffo, A., Rite, I., Tripathi, P., Lepier, A., Colak, D., Horn, A.P., Mori, T., and Götz, M. (2008). Origin and progeny of reactive gliosis: A source of multipotent cells in the injured brain. Proc Natl Acad Sci U S A *105*, 3581-3586.

Buffo, A., Rolando, C., and Ceruti, S. (2010). Astrocytes in the damaged brain: Molecular and cellular insights into their reactive response and healing potential. Biochemical Pharmacology *79*, 77-89.

Bultje, R.S., Castaneda-Castellanos, D.R., Jan, L.Y., Jan, Y.-N., Kriegstein, A.R., and Shi, S.-H. Mammalian Par3 Regulates Progenitor Cell Asymmetric Division via Notch Signaling in the Developing Neocortex. Neuron *63*, 189-202.

Butler, A.B. (2000). Topography and topology of the teleost telencephalon: a paradox resolved. Neuroscience Letters *293*, 95-98.

Carlen, M., Meletis, K., Goritz, C., Darsalia, V., Evergren, E., Tanigaki, K., Amendola, M., Barnabe-Heider, F., Yeung, M.S.Y., Naldini, L., *et al.* (2009). Forebrain ependymal cells are Notch-dependent and generate neuroblasts and astrocytes after stroke. Nat Neurosci *12*, 259-267.

Cayouette, M., and Raff, M. (2003). The orientation of cell division influences cell-fate choice in the developing mammalian retina. Development *130*, 2329-2339.

Cayre, M.S., Colette; Strambi, Alain (1994). Neurogenesis in an adult insect brain and its hormonal control. Nature *368*, 57-59.

Chapouton, P., Adolf, B., Leucht, C., Tannhauser, B., Ryu, S., Driever, W., and Bally-Cuif, L. (2006). her5 expression reveals a pool of neural stem cells in the adult zebrafish midbrain. Development *133*, 4293-4303.

Chapouton, P., Skupien, P., Hesl, B., Coolen, M., Moore, J.C., Madelaine, R., Kremmer, E., Faus-Kessler, T., Blader, P., Lawson, N.D., *et al.* (2010). Notch Activity Levels Control the Balance between Quiescence and Recruitment of Adult Neural Stem Cells. The Journal of Neuroscience *30*, 7961-7974.

Chen, J., Magavi, S.S.P., and Macklis, J.D. (2004). Neurogenesis of corticospinal motor neurons extending spinal projections in adult mice. Proceedings of the National Academy of Sciences of the United States of America *101*, 16357-16362.

Cheng, M.Y., Leslie, F.M., and Zhou, Q.-Y. (2006). Expression of prokineticins and their receptors in the adult mouse brain. The Journal of Comparative Neurology *498*, 796-809.

Chenn, A., and McConnell, S.K. (1995). Cleavage orientation and the asymmetric inheritance of notchl immunoreactivity in mammalian neurogenesis. Cell *82*, 631-641.

Chenn, A., Zhang, Y.A., Chang, B.T., and McConnell, S.K. (1998). Intrinsic Polarity of Mammalian Neuroepithelial Cells. Molecular and Cellular Neuroscience *11*, 183-193.

Clarke, J. (2009). Live imaging of development in fish embryos. Seminars in Cell & Developmental Biology *20*, 942-946.

Clint, S.C., and Zupanc, G.K. (2001). Neuronal regeneration in the cerebellum of adult teleost fish, *Apteronotus leptorhynchus*: guidance of migrating young cells by radial glia. Brain Res Dev Brain Res *130*, 15-23.

Cockrell, A., and Kafri, T. (2007). Gene delivery by lentivirus vectors. Mol Biotechnol *36*, 184-204.

Collin, T., Arvidsson, A., Kokaia, Z., and Lindvall, O. (2005). Quantitative analysis of the generation of different striatal neuronal subtypes in the adult brain following excitotoxic injury. Experimental Neurology *195*, 71-80.

Conchello, J.-A., and Lichtman, J.W. (2005). Optical sectioning microscopy. Nat Meth *2*, 920-931.

Coskun, V., and Luskin, M.B. (2002). Intrinsic and extrinsic regulation of the proliferation and differentiation of cells in the rodent rostral migratory stream. Journal of Neuroscience Research *69*, 795-802.

Costa, M.R., Ortega, F., Brill, M.S., Beckervordersandforth, R., Petrone, C., Schroeder, T., Götz, M., and Berninger, B. (2011). Continuous live imaging of adult neural stem cell division and lineage progression *in vitro*. Development *138*, 1057-1068.

Costa, M.R., Wen, G., Lepier, A., Schroeder, T., and Götz, M. (2008). Par-complex proteins promote proliferative progenitor divisions in the developing mouse cerebral cortex. Development *135*, 11-22.

Davenne, M., Custody, C., Charneau, P., and Lledo, P.-M. (2005). *In Vivo* Imaging of Migrating Neurons in the Mammalian Forebrain. Chemical Senses *30*, i115-i116.

David, N.B., Sapède, D., Saint-Etienne, L., Thisse, C., Thisse, B., Dambly-Chaudière, C., Rosa, F.M., and Ghysen, A. (2002). Molecular basis of cell migration in the fish lateral line: Role of the chemokine receptor CXCR4 and of its ligand, SDF1. Proceedings of the National Academy of Sciences *99*, 16297-16302.

De Marchis, S., Bovetti, S., Carletti, B., Hsieh, Y.C., Garzotto, D., Peretto, P., Fasolo, A., Puche, A.C., and Rossi, F. (2007). Generation of distinct types of periglomerular olfactory bulb interneurons during development and in adult mice: implication for intrinsic properties of the subventricular zone progenitor population. J Neurosci *27*, 657-664.

Del Bene, F., Wehman, A.M., Link, B.A., and Baier, H. (2008). Regulation of Neurogenesis by Interkinetic Nuclear Migration through an Apical-Basal Notch Gradient. Cell *134*, 1055-1065.

Del Bigio, M.R. (1995). The ependyma: A protective barrier between brain and cerebrospinal fluid. Glia *14*, 1-13.

Deng, W.A., James B.; Gage, Fred H. (2010). New neurons and new memories: how does adult hippocampal neurogenesis affect learning and memory? Nat Rev Neurosci *11*, 339-350.

Dias, T.B., Yang, Y.-J., Ogai, K., Becker, T., and Becker, C.G. (2012). Notch Signaling Controls Generation of Motor Neurons in the Lesioned Spinal Cord of Adult Zebrafish. The Journal of Neuroscience *32*, 3245-3252.

Dimou, L., and Götz, M. (2014). Glial Cells as Progenitors and Stem Cells: New Roles in the Healthy and Diseased Brain, Vol 94.

Diotel, N., Vaillant, C., Gueguen, M.-M., Mironov, S., Anglade, I., Servili, A., Pellegrini, E., and Kah, O. (2010). Cxcr4 and Cxcl12 expression in radial glial cells of the brain of adult zebrafish. The Journal of Comparative Neurology *518*, 4855-4876.

Dirian, L., Galant, S., Coolen, M., Chen, W., Bedu, S., Houart, C., Bally-Cuif, L., and Foucher, I. (2014). Spatial Regionalization and Heterochrony in the Formation of Adult Pallial Neural Stem Cells. Developmental Cell.

Doetsch, F., García-Verdugo, J.M., and Alvarez-Buylla, A. (1999). Regeneration of a germinal layer in the adult mammalian brain. Proceedings of the National Academy of Sciences of the United States of America *96*, 11619-11624.

Doetsch, F., Garcia-Verdugo, J., and Alvarez-Buylla, A. (1997). Cellular composition and three-dimensional organization of the subventricular germinal zone in the adult mammalian brain. J Neurosci *17*, 5046 - 5061.

Dong, Z., Yang, N., Yeo, S.-Y., Chitnis, A., and Guo, S. (2012). Intralineage Directional Notch Signaling Regulates Self-Renewal and Differentiation of Asymmetrically Dividing Radial Glia. Neuron *74*, 65-78.

Edelmann, K., Glashauser, L., Sprungala, S., Hesl, B., Fritschle, M., Ninkovic, J., Godinho, L., and Chapouton, P. (2013). Increased Radial glia Quiescence, Decreased Reactivation upon Injury and Unaltered Neuroblast Behaviour

Underlie Decreased Neurogenesis in the Aging Zebrafish Telencephalon. Journal of Comparative Neurology *accepted on 05.03.2013*.

Ekdahl, C.T., Claasen, J.-H., Bonde, S., Kokaia, Z., and Lindvall, O. (2003). Inflammation is detrimental for neurogenesis in adult brain. Proceedings of the National Academy of Sciences *100*, 13632-13637.

Encinas, J.M., Michurina, T.V., Peunova, N., Park, J.H., Tordo, J., Peterson, D.A., Fishell, G., Koulakov, A., and Enikolopov, G. (2011). Division-coupled astrocytic differentiation and age-related depletion of neural stem cells in the adult hippocampus. Cell Stem Cell *8*, 566-579.

Enwere, E., Shingo, T., Gregg, C., Fujikawa, H., Ohta, S., and Weiss, S. (2004). Aging Results in Reduced Epidermal Growth Factor Receptor Signaling, Diminished Olfactory Neurogenesis, and Deficits in Fine Olfactory Discrimination. J Neurosci *24*, 8354-8365.

Eriksson, P.S., Perfilieva, E., Bjork-Eriksson, T., Alborn, A.M., Nordborg, C., Peterson, D.A., and Gage, F.H. (1998). Neurogenesis in the adult human hippocampus. Nat Med *4*, 1313-1317.

Ernst, A., Alkass, K., Bernard, S., Salehpour, M., Perl, S., Tisdale, J., Possnert, G., Druid, H., and Frisén, J. (2014). Neurogenesis in the Striatum of the Adult Human Brain. Cell *156*, 1072-1083.

Fausett, B.V., and Goldman, D. (2006). A Role for α1 Tubulin-Expressing Müller Glia in Regeneration of the Injured Zebrafish Retina. The Journal of Neuroscience *26*, 6303-6313.

Feng, L., Hatten, M.E., and Heintz, N. (1994). Brain lipid-binding protein (BLBP): A novel signaling system in the developing mammalian CNS. Neuron *12*, 895-908.

Fernández-Hernández, I., Rhiner, C., and Moreno, E. (2013). Adult Neurogenesis in Drosophila. Cell Reports *3*, 1857-1865.

Fischer, R.S., Wu, Y., Kanchanawong, P., Shroff, H., and Waterman, C.M. (2011). Microscopy in 3D: a biologist's toolbox. Trends in Cell Biology *21*, 682-691.

Font, E., García-Verdugo, J.M., Alcántara, S., and López-García, C. (1991). Neuron regeneration reverses 3-acetylpyridine-induced cell loss in the cerebral cortex of adult lizards. Brain Research *551*, 230-235.

Gaiano, N., Nye, J., and Fishell, G. (2000). Radial glial identity is promoted by Notch1 signaling in the murine forebrain. Neuron *26*, 395 - 404.

Ganz, J., Kaslin, J., Freudenreich, D., Machate, A., Geffarth, M., and Brand, M. (2012). Subdivisions of the adult zebrafish subpallium by molecular marker analysis. J Comp Neurol *520*, 633-655.

Ganz, J., Kaslin, J., Hochmann, S., Freudenreich, D., and Brand, M. (2010). Heterogeneity and Fgf dependence of adult neural progenitors in the zebrafish telencephalon. Glia *58*, 1345-1363.

García Verdugo, J.B.P.L.G., C (1981). Golgi and electron microscopy study of cerebral ependymocytes of the lizard *Lacerta galloti*. Trab Inst Cajal *72*, 269-278.

Gertz, C.C., Lui, J.H., LaMonica, B.E., Wang, X., and Kriegstein, A.R. (2014). Diverse Behaviors of Outer Radial Glia in Developing Ferret and Human Cortex. The Journal of Neuroscience *34*, 2559-2570.

Goldman, S., and Nottebohm, F. (1983). Neuronal production, migration, and differentiation in a vocal control nucleus of the adult female canary brain. Proc Natl Acad Sci U S A *80*, 2390 - 2394.

Götz, M., and Huttner, W.B. (2005). The cell biology of neurogenesis. Nat Rev Mol Cell Biol *6*, 777-788.

Gould, E., Tanapat, P., McEwen, B.S., Flügge, G., and Fuchs, E. (1998). Proliferation of granule cell precursors in the dentate gyrus of adult monkeys is diminished by stress. Proceedings of the National Academy of Sciences *95*, 3168-3171.

Graciarena, M., Dambly-Chaudière, C., and Ghysen, A. (2014). Dynamics of axonal regeneration in adult and aging zebrafish reveal the promoting effect of a first lesion. Proceedings of the National Academy of Sciences.

Grandel, H., and Brand, M. (2013). Comparative aspects of adult neural stem cell activity in vertebrates. Dev Genes Evol *223*, 131-147.

Grandel, H., Kaslin, J., Ganz, J., Wenzel, I., and Brand, M. (2006). Neural stem cells and neurogenesis in the adult zebrafish brain: origin, proliferation dynamics, migration and cell fate. Dev Biol *295*, 263-277.

Grupp, L., Wolburg, H., and Mack, A.F. (2010). Astroglial structures in the zebrafish brain. J Comp Neurol *518*, 4277-4287.

Gubert, F., Zaverucha-do-Valle, C., Pimentel-Coelho, P.M., Mendez-Otero, R., and Santiago, M.F. (2009). Radial glia-like cells persist in the adult rat brain. Brain Research *1258*, 43-52.

Haan, N.G., Timothy; Najdi-Samiei, Alaleh; Stratford, Christina M.; Rice, Ritva; El Agha, Elie; Bellusci, Saverio; Hajihosseini, Mohammad K. (2013). Fgf10-Expressing tanycytes add new neurons to the appetite/energy-balance regulating centers of the postnatal and adult hypothalamus. J Neuroscience *33*, 6170-6180.

Hanisch, U.-K., and Kettenmann, H. (2007). Microglia: active sensor and versatile effector cells in the normal and pathologic brain. Nat Neurosci *10*, 1387-1394.

Hansen, D.V., Lui, J.H., Parker, P.R.L., and Kriegstein, A.R. (2010). Neurogenic radial glia in the outer subventricular zone of human neocortex. Nature *464*, 554-561.

Hartfuss, E., Galli, R., Heins, N., and Götz, M. (2001). Characterization of CNS precursor subtypes and radial glia. Dev Biol *229*, 15-30.

Haubensak, W., Attardo, A., Denk, W., and Huttner, W.B. (2004). Neurons arise in the basal neuroepithelium of the early mammalian telencephalon: a major site of neurogenesis. Proc Natl Acad Sci U S A *101*, 3196-3201.

Haubst, N., Georges-Labouesse, E., De Arcangelis, A., Mayer, U., and Götz, M. (2006). Basement membrane attachment is dispensable for radial glial cell fate

and for proliferation, but affects positioning of neuronal subtypes. Development *133*, 3245-3254.

Helmchen, F., and Denk, W. (2005). Deep tissue two-photon microscopy. Nat Meth *2*, 932-940.

Hirsch, E., Gullberg, D., Balzac, F., Altruda, F., Silengo, L., and Tarone, G. (1994). αv Integrin subunit is predominantly located in nervous tissue and skeletal muscle during mouse development. Developmental Dynamics *201*, 108-120.

Hoehn, B.D., Palmer, T.D., and Steinberg, G.K. (2005). Neurogenesis in Rats After Focal Cerebral Ischemia is Enhanced by Indomethacin. Stroke *36*, 2718-2724.

Hsieh, J. (2012). Orchestrating transcriptional control of adult neurogenesis. Genes & Development *26*, 1010-1021.

Huber, A.B., Kania, A., Tran, T.S., Gu, C., De Marco Garcia, N., Lieberam, I., Johnson, D., Jessell, T.M., Ginty, D.D., and Kolodkin, A.L. (2005). Distinct Roles for Secreted Semaphorin Signaling in Spinal Motor Axon Guidance. Neuron *48*, 949-964.

Hughes, E.G., Kang, S.H., Fukaya, M., and Bergles, D.E. (2013). Oligodendrocyte progenitors balance growth with self-repulsion to achieve homeostasis in the adult brain. Nat Neurosci *16*, 668-676.

Hui, S.P., Dutta, A., and Ghosh, S. (2010). Cellular response after crush injury in adult zebrafish spinal cord. Developmental Dynamics *239*, 2962-2979.

Imitola, J., Raddassi, K., Park, K.I., Mueller, F.-J., Nieto, M., Teng, Y.D., Frenkel, D., Li, J., Sidman, R.L., Walsh, C.A., *et al.* (2004). Directed migration of neural stem cells to sites of CNS injury by the stromal cell-derived factor 1α/CXC chemokine receptor 4 pathway. Proceedings of the National Academy of Sciences *101*, 18117-18122.

Ito, Y., Tanaka, H., Okamoto, H., and Ohshima, T. (2010). Characterization of neural stem cells and their progeny in the adult zebrafish optic tectum. Developmental Biology *342*, 26-38.

Jackson, E.L., Garcia-Verdugo, J.M., Gil-Perotin, S., Roy, M., Quinones-Hinojosa, A., VandenBerg, S., and Alvarez-Buylla, A. (2006). PDGFR±-Positive B Cells Are Neural Stem Cells in the Adult SVZ that Form Glioma-like Growths in Response to Increased PDGF Signaling. *51*, 187-199.

Jászai, J.G., S; Tanaka, EM; Funk, RHW; Huttner, WB; Brand, M; Corbeil, D (2013). Spatial Distribution of Prominin-1 (CD133) – Positive Cells within Germinative Zones of the Vertebrate Brain. PLoS ONE *8*, e63457.

Jin, K., Sun, Y., Xie, L., Peel, A., Mao, X.O., Batteur, S., and Greenberg, D.A. (2003). Directed migration of neuronal precursors into the ischemic cerebral cortex and striatum. Molecular and Cellular Neuroscience *24*, 171-189.

Kálmán, M. (1998). Astroglial architecture of the carp (Cyprinus carpio) brain as revealed by immunohistochemical staining against glial fibrillary acidic protein (GFAP). Anat Embryol *198*, 409-433.

Kang, S.H., Fukaya, M., Yang, J.K., Rothstein, J.D., and Bergles, D.E. (2010). NG2+ CNS Glial Progenitors Remain Committed to the Oligodendrocyte Lineage in Postnatal Life and following Neurodegeneration. Neuron *68*, 668-681.

Kaplan, M., and Bell, D. (1984). Mitotic neuroblasts in the 9-day-old and 11-month-old rodent hippocampus. J Neurosci *4*, 1429 - 1441.

Kaslin, J., Ganz, J., and Brand, M. (2008). Proliferation, neurogenesis and regeneration in the non-mammalian vertebrate brain. Philos Trans R Soc Lond B Biol Sci *363*, 101-122.

Kaslin, J., Ganz, J., Geffarth, M., Grandel, H., Hans, S., and Brand, M. (2009). Stem cells in the adult zebrafish cerebellum: initiation and maintenance of a novel stem cell niche. J Neurosci *29*, 6142-6153.

Kassing, V., Engelmann, J., and Kurtz, R. (2013). Monitoring of Single-Cell Responses in the Optic Tectum of Adult Zebrafish with Dextran-Coupled Calcium Dyes Delivered *via* Local Electroporation. PLoS ONE *8*, e62846.

Keck, T.M.-F., Thomas D; Vaz Afonso, Miguel; Eysel, Ulf T; Bonhoeffer, Tobias; Hubener, Mark (2008). Massive restructuring of neuronal circuits during functional reorganization of adult visual cortex. Nat Neurosci *11*, 1162-1167.

Kelsh, R.N., Brand, M., Jiang, Y.J., Heisenberg, C.P., Lin, S., Haffter, P., Odenthal, J., Mullins, M.C., van Eeden, F.J., Furutani-Seiki, M., *et al.* (1996). Zebrafish pigmentation mutations and the processes of neural crest development. Development *123*, 369-389.

Kim, Y., and Szele, F. (2008). Activation of subventricular zone stem cells after neuronal injury. Cell Tissue Res *331*, 337-345.

Kirkham, M., Hameed, L.S., Berg, Daniel A., Wang, H., and Simon, A. (2014). Progenitor Cell Dynamics in the Newt Telencephalon during Homeostasis and Neuronal Regeneration. Stem Cell Reports *2*, 507-519.

Kishimoto, N., Alfaro-Cervello, C., Shimizu, K., Asakawa, K., Urasaki, A., Nonaka, S., Kawakami, K., Garcia-Verdugo, J.M., and Sawamoto, K. (2011). Migration of neuronal precursors from the telencephalic ventricular zone into the olfactory bulb in adult zebrafish. The Journal of Comparative Neurology *519*, 3549-3565.

Kishimoto, N., Shimizu, K., and Sawamoto, K. (2012). Neuronal regeneration in a zebrafish model of adult brain injury. Disease Models & Mechanisms *5*, 200-209.

Kizil, C., Dudczig, S., Kyritsis, N., Machate, A., Blaesche, J., Kroehne, V., and Brand, M. (2012a). The chemokine receptor cxcr5 regulates the regenerative neurogenesis response in the adult zebrafish brain. Neural Dev *7*, 27.

Kizil, C., Kyritsis, N., Dudczig, S., Kroehne, V., Freudenreich, D., Kaslin, J., and Brand, M. (2012b). Regenerative Neurogenesis from Neural Progenitor Cells Requires Injury-Induced Expression of Gata3. Developmental Cell *23*, 1230-1237.

Knaut, H., Werz, C., Geisler, R., The Tubingen Screen, C., and Nusslein-Volhard, C. (2003). A zebrafish homologue of the chemokine receptor Cxcr4 is a germ-cell guidance receptor. Nature *421*, 279-282.

Koke, J., Mosier, A., and Garcia, D. (2010). Intermediate filaments of zebrafish retinal and optic nerve astrocytes and Müller glia: differential distribution of cytokeratin and GFAP. BMC Research Notes *3*, 50.

Konno, D., Shioi, G., Shitamukai, A., Mori, A., Kiyonari, H., Miyata, T., and Matsuzaki, F. (2008). Neuroepithelial progenitors undergo LGN-dependent planar divisions to maintain self-renewability during mammalian neurogenesis. Nat Cell Biol *10*, 93-101.

Kornack, D.R., and Rakic, P. (1999). Continuation of neurogenesis in the hippocampus of the adult macaque monkey. Proceedings of the National Academy of Sciences *96*, 5768-5773.

Kowalczyk, T., Pontious, A., Englund, C., Daza, R.A., Bedogni, F., Hodge, R., Attardo, A., Bell, C., Huttner, W.B., and Hevner, R.F. (2009). Intermediate neuronal progenitors (basal progenitors) produce pyramidal-projection neurons for all layers of cerebral cortex. Cereb Cortex *19*, 2439-2450.

Kriegstein, A., and Alvarez-Buylla, A. (2009). The glial nature of embryonic and adult neural stem cells. Annu Rev Neurosci *32*, 149-184.

Kroehne, V., Freudenreich, D., Hans, S., Kaslin, J., and Brand, M. (2011). Regeneration of the adult zebrafish brain from neurogenic radial glia-type progenitors. Development *138*, 4831-4841.

Kuge, A., Takemura, S., Kokubo, Y., Sato, S., Goto, K., and Kayama, T. (2009). Temporal profile of neurogenesis in the subventricular zone, dentate gyrus and cerebral cortex following transient focal cerebral ischemia. Neurological Research *31*, 969-976.

Kyritsis, N., Kizil, C., Zocher, S., Kroehne, V., Kaslin, J., Freudenreich, D., Iltzsche, A., and Brand, M. (2012). Acute inflammation initiates the regenerative response in the adult zebrafish brain. Science *338*, 1353-1356.

Lam, C.S., März, M., and Strähle, U. (2009). gfap and nestin reporter lines reveal characteristics of neural progenitors in the adult zebrafish brain. Developmental Dynamics *238*, 475-486.

Lazarini, F., and Lledo, P.-M. (2011). Is adult neurogenesis essential for olfaction? Trends in Neurosciences *34*, 20-30.

Lee, D.A., Bedont, J.L., Pak, T., Wang, H., Song, J., Miranda-Angulo, A., Takiar, V., Charubhumi, V., Balordi, F., Takebayashi, H., *et al.* (2012). Tanycytes of the hypothalamic median eminence form a diet-responsive neurogenic niche. Nat Neurosci *15*, 700-702.

Lenkowski, J.R., and Raymond, P.A. (2014). Müller glia: Stem cells for generation and regeneration of retinal neurons in teleost fish. Progress in Retinal and Eye Research *40*, 94-123.

Li, L., Lundkvist, A., Andersson, D., Wilhelmsson, U., Nagai, N., Pardo, A., Nodin, C., Stahlberg, A., Aprico, K., and Larsson, K. (2008). Protective role of reactive astrocytes in brain ischemia. J Cereb Blood Flow Metab *28*, 468 - 481.

Lindsey, B.W., Darabie, A., and Tropepe, V. (2012). The cellular composition of neurogenic periventricular zones in the adult zebrafish forebrain. The Journal of Comparative Neurology *520*, 2275-2316.

Liu, X.S., Chopp, M., Santra, M., Hozeska-Solgot, A., Zhang, R.L., Wang, L., Teng, H., Lu, M., and Zhang, Z.G. (2008). Functional response to SDF1α through over-expression of CXCR4 on adult subventricular zone progenitor cells. Brain Research *1226*, 18-26.

Lledo, P.M., Merkle, F.T., and Alvarez-Buylla, A. (2008). Origin and function of olfactory bulb interneuron diversity. Trends Neurosci *31*, 392-400.

Lois, C., and Alvarez-Buylla, A. (1994). Long-distance neuronal migration in the adult mammalian brain. Science *264*, 1145-1148.

Lois, C., García-Verdugo, J.-M., and Alvarez-Buylla, A. (1996). Chain Migration of Neuronal Precursors. Science *271*, 978-981.

López-Garcia, C.T., PL; Del Corral, J (1984). Increase of the neuron number in some cerebral cortical areas of a lizard, *Podarcis hispanica*, (Steind., 1870), during postnatal periods of life. Journal of Hirnforsch *25*, 255-259.

Lugert, S., Basak, O., Knuckles, P., Haussler, U., Fabel, K., Götz, M., Haas, C.A., Kempermann, G., Taylor, V., and Giachino, C. (2010). Quiescent and Active Hippocampal Neural Stem Cells with Distinct Morphologies Respond Selectively to Physiological and Pathological Stimuli and Aging. Cell Stem Cell *6*, 445-456.

Lyons, D.A., Guy, A.T., and Clarke, J.D.W. (2003). Monitoring neural progenitor fate through multiple rounds of division in an intact vertebrate brain. Development *130*, 3427-3436.

Magavi, S.S., Leavitt, B.R., and Macklis, J.D. (2000). Induction of neurogenesis in the neocortex of adult mice. Nature *405*, 951-955.

Malatesta, P., Hartfuss, E., and Götz, M. (2000). Isolation of radial glial cells by fluorescent-activated cell sorting reveals a neuronal lineage. Development *127*, 5253 - 5263.

Manabe, N., Hirai, S.-I., Imai, F., Nakanishi, H., Takai, Y., and Ohno, S. (2002). Association of ASIP/mPAR-3 with adherens junctions of mouse neuroepithelial cells. Developmental Dynamics *225*, 61-69.

Marcus, R.C., Delaney, C.L., and Easter, S.S. (1999). Neurogenesis in the visual system of embryonic and adult zebrafish (*Danio rerio*). Visual Neuroscience *16*, 417-424.

März, M., Chapouton, P., Diotel, N., Vaillant, C., Hesl, B., Takamiya, M., Lam, C.S., Kah, O., Bally-Cuif, L., and Strähle, U. (2010a). Heterogeneity in progenitor cell subtypes in the ventricular zone of the zebrafish adult telencephalon. Glia *58*, 870-888.

März, M., Schmidt, R., Rastegar, S., and Strähle, U. (2010b). Expression of the transcription factor Olig2 in proliferating cells in the adult zebrafish telencephalon. Developmental Dynamics *239*, 3336-3349.

März, M., Schmidt, R., Rastegar, S., and Strähle, U. (2011). Regenerative response following stab injury in the adult zebrafish telencephalon. Developmental Dynamics *240*, 2221-2231.

Maslov, A.Y., Barone, T.A., Plunkett, R.J., and Pruitt, S.C. (2004). Neural Stem Cell Detection, Characterization, and Age-Related Changes in the Subventricular Zone of Mice. The Journal of Neuroscience *24*, 1726-1733.

Megason, S.G., and Fraser, S.E. (2003). Digitizing life at the level of the cell: high-performance laser-scanning microscopy and image analysis for in toto imaging of development. Mechanisms of Development *120*, 1407-1420.

Menn, B., Garcia-Verdugo, J.M., Yaschine, C., Gonzalez-Perez, O., Rowitch, D., and Alvarez-Buylla, A. (2006). Origin of Oligodendrocytes in the Subventricular Zone of the Adult Brain. J Neurosci *26*, 7907-7918.

Mensinger, A.F., and Powers, M.K. (1999). Visual function in regenerating teleost retina following cytotoxic lesioning. Visual Neuroscience *16*, 241-251.

Merkle, F.T., Mirzadeh, Z., and Alvarez-Buylla, A. (2007). Mosaic organization of neural stem cells in the adult brain. Science *317*, 381-384.

Miller, F.D., and Gauthier-Fisher, A. (2009). Home at Last: Neural Stem Cell Niches Defined. Cell Stem Cell *4*, 507-510.

Mirzadeh, Z., Merkle, F.T., Soriano-Navarro, M., Garcia-Verdugo, J.M., and Alvarez-Buylla, A. (2008). Neural Stem Cells Confer Unique Pinwheel Architecture to the Ventricular Surface in Neurogenic Regions of the Adult Brain. *3*, 265-278.

Misgeld, T.K., Martin (2006). *In vivo* imaging of the diseased nervous system. Nat Rev Neurosci *7*, 449-463.

Miyata, T., Kawaguchi, A., Saito, K., Kawano, M., Muto, T., and Ogawa, M. (2004). Asymmetric production of surface-dividing and non-surface-dividing cortical progenitor cells. Development *131*, 3133-3145.

Mizoguchi, T., Verkade, H., Heath, J.K., Kuroiwa, A., and Kikuchi, Y. (2008). Sdf1/Cxcr4 signaling controls the dorsal migration of endodermal cells during zebrafish gastrulation. Development *135*, 2521-2529.

Mizutani, K.-i., Yoon, K., Dang, L., Tokunaga, A., and Gaiano, N. (2007). Differential Notch signalling distinguishes neural stem cells from intermediate progenitors. Nature *449*, 351-355.

Monje, M.L., Toda, H., and Palmer, T.D. (2003). Inflammatory Blockade Restores Adult Hippocampal Neurogenesis. Science *302*, 1760-1765.

Mosimann, C., Kaufman, C.K., Li, P., Pugach, E.K., Tamplin, O.J., and Zon, L.I. (2011). Ubiquitous transgene expression and Cre-based recombination driven by the ubiquitin promoter in zebrafish. Development *138*, 169-177.

Mueller, T., and Wullimann, M.F. (2009). An Evolutionary Interpretation of Teleostean Forebrain Anatomy. Brain, Behavior and Evolution *74*, 30-42.

Mumm, J.S., Williams, P.R., Godinho, L., Koerber, A., Pittman, A.J., Roeser, T., Chien, C.-B., Baier, H., and Wong, R.O.L. (2006). *In Vivo* Imaging Reveals Dendritic Targeting of Laminated Afferents by Zebrafish Retinal Ganglion Cells. Neuron *52*, 609-621.

Nagashima, M., Barthel, L.K., and Raymond, P.A. (2013). A self-renewing division of zebrafish Müller glial cells generates neuronal progenitors that require N-cadherin to regenerate retinal neurons. Development *140*, 4510-4521.

Nakatomi, H., Kuriu, T., Okabe, S., Yamamoto, S.-i., Hatano, O., Kawahara, N., Tamura, A., Kirino, T., and Nakafuku, M. (2002). Regeneration of Hippocampal Pyramidal Neurons after Ischemic Brain Injury by Recruitment of Endogenous Neural Progenitors. *110*, 429-441.

Ng, K.L., Li, J.-D., Cheng, M.Y., Leslie, F.M., Lee, A.G., and Zhou, Q.-Y. (2005). Dependence of Olfactory Bulb Neurogenesis on Prokineticin 2 Signaling. Science *308*, 1923-1927.

Noctor, S., Flint, A., Weissman, T., Dammerman, R., and Kriegstein, A. (2001). Neurons derived from radial glial cells establish radial units in neocortex. Nature *409*, 714 - 720.

Noctor, S.C., Martinez-Cerdeno, V., Ivic, L., and Kriegstein, A.R. (2004). Cortical neurons arise in symmetric and asymmetric division zones and migrate through specific phases. Nat Neurosci *7*, 136-144.

Noctor, S.C., Martinez-Cerdeno, V., and Kriegstein, A.R. (2007). Contribution of Intermediate Progenitor Cells to Cortical Histogenesis. Arch Neurol *64*, 639-642.

Northcutt, R.G., and Braford, M., Jr. (1980). New Observations on the Organization and Evolution of the Telencephalon of Actinopterygian Fishes. In Comparative Neurology of the Telencephalon, S.E. Ebbesson, ed. (Springer US), pp. 41-98.

Ohab, J.J.F., Sheila; Blesch, Armin; Carmichael, S. Thomas (2006). A neurovascular niche for neurogenesis after stroke. J Neuroscience *26*, 13007-13016.

Ortega, F.G., Sergio; Masserdotti, Giacomo; Deshpande, Aditi; Simon, Christiane; Fischer, Judith; Dimou, Leda; Chichung Lie, D; Schroeder, Timm; Berninger, Benedikt (2013). Oligodendrogliogenic and neurogenic adult subependymal zone neural stem cells constitute distinct lineages and exhibit differential responsiveness to Wnt signalling. Nat Cell Biol *15*, 602-613.

Ory, D.S., Neugeboren, B.A., and Mulligan, R.C. (1996). A stable human-derived packaging cell line for production of high titer retrovirus/vesicular stomatitis virus G pseudotypes. Proceedings of the National Academy of Sciences *93*, 11400-11406.

Paez-Gonzalez, P., Abdi, K., Luciano, D., Liu, Y., Soriano-Navarro, M., Rawlins, E., Bennett, V., Garcia-Verdugo, Jose M., and Kuo, Chay T. Ank3-Dependent SVZ Niche Assembly Is Required for the Continued Production of New Neurons. Neuron *71*, 61-75.

Paquet, D., Bhat, R., Sydow, A., Mandelkow, E.-M., Berg, S., Hellberg, S., xE, lting, J., Distel, M., xF, *et al.* (2009). A zebrafish model of tauopathy allows *in vivo* imaging of neuronal cell death and drug evaluation. The Journal of Clinical Investigation *119*, 1382-1395.

Park, H.-C., Kim, C.-H., Bae, Y.-K., Yeo, S.-Y., Kim, S.-H., Hong, S.-K., Shin, J., Yoo, K.-W., Hibi, M., Hirano, T., *et al.* (2000). Analysis of Upstream Elements in the HuC Promoter Leads to the Establishment of Transgenic Zebrafish with Fluorescent Neurons. Developmental Biology *227*, 279-293.

Pellegrini, E., Mouriec, K., Anglade, I., Menuet, A., Le Page, Y., Gueguen, M.-M., Marmignon, M.-H., Brion, F., Pakdel, F., and Kah, O. (2007). Identification of aromatase-positive radial glial cells as progenitor cells in the ventricular layer of the forebrain in zebrafish. The Journal of Comparative Neurology *501*, 150-167.

Peretto, P., Merighi, A., Fasolo, A., and Bonfanti, L. (1997). Glial Tubes in the Rostral Migratory Stream of the Adult Rat. Brain Research Bulletin *42*, 9-21.

Peri, F., and Nüsslein-Volhard, C. (2008). Live Imaging of Neuronal Degradation by Microglia Reveals a Role for v0-ATPase a1 in Phagosomal Fusion *In Vivo*. Cell *133*, 916-927.

Pfeifer, A., Brandon, E.P., Kootstra, N., Gage, F.H., and Verma, I.M. (2001). Delivery of the Cre recombinase by a self-deleting lentiviral vector: Efficient gene targeting *in vivo*. Proceedings of the National Academy of Sciences *98*, 11450-11455.

Pierce, A.A.X., Allison W. (2010). De novo neurogenesis in adult hypothalamus as a compensatory mechanism to regulate energy balance. J Neuroscience *30*, 723-730.

Pierfelice, T., Alberi, L., and Gaiano, N. (2011). Notch in the Vertebrate Nervous System: An Old Dog with New Tricks. Neuron *69*, 840-855.

Pilz, G.A., Shitamukai, A., Reillo, I., Pacary, E., Schwausch, J., Stahl, R., Ninkovic, J., Snippert, H.J., Clevers, H., Godinho, L., *et al.* (2013). Amplification of progenitors in the mammalian telencephalon includes a new radial glial cell type. Nat Commun *4*, 2125.

Ponti, G., Obernier, K., Guinto, C., Jose, L., Bonfanti, L., and Alvarez-Buylla, A. (2013). Cell cycle and lineage progression of neural progenitors in the ventricular-subventricular zones of adult mice. Proceedings of the National Academy of Sciences *110*, E1045-E1054.

Popovich, P.G., Guan, Z., Mcgaughy, V., Fisher, L., Hickey, W.F., and Basso, D.M. (2002). The Neuropathological and Behavioral Consequences of Intraspinal Microglial/Macrophage Activation. Journal of Neuropathology & Experimental Neurology *61*, 623-633.

Portavella, M., Torres, B., and Salas, C. (2004). Avoidance Response in Goldfish: Emotional and Temporal Involvement of Medial and Lateral Telencephalic Pallium. The Journal of Neuroscience *24*, 2335-2342.

Postiglione, Maria P., Jüschke, C., Xie, Y., Haas, Gerald A., Charalambous, C., and Knoblich, Juergen A. (2011). Mouse Inscuteable Induces Apical-Basal Spindle Orientation to Facilitate Intermediate Progenitor Generation in the Developing Neocortex. Neuron *72*, 269-284.

Prosser, H.M., Bradley, A., and Caldwell, M.A. (2007). Olfactory bulb hypoplasia in Prokr2 null mice stems from defective neuronal progenitor migration and differentiation. Eur J Neurosci *26*, 3339-3344.

Reimer, M.M., Kuscha, V., Wyatt, C., Sorensen, I., Frank, R.E., Knuwer, M., Becker, T., and Becker, C.G. (2009). Sonic hedgehog is a polarized signal for motor neuron regeneration in adult zebrafish. J Neurosci *29*, 15073-15082.

Reimer, M.M., Sorensen, I., Kuscha, V., Frank, R.E., Liu, C., Becker, C.G., and Becker, T. (2008). Motor neuron regeneration in adult zebrafish. J Neurosci *28*, 8510-8516.

Rice, A.C., Khaldi, A., Harvey, H.B., Salman, N.J., White, F., Fillmore, H., and Bullock, M.R. (2003). Proliferation and neuronal differentiation of mitotically active cells following traumatic brain injury. Experimental Neurology *183*, 406-417.

Richter, W. (1965). Regeneration in the tectum opticum of Leucaspius delineatus (Heckel 1843). Z Mikrosk Anat Forsch *74*, 46-68.

Richter, W. (1970). Regeneration im telencephalon von juvenilen und adulten Lebistes reticulates (Teleostei). Z Mikrosk Anat Forsch *81*, 345-358.

Robel, S., Berninger, B., and Götz, M. (2011). The stem cell potential of glia: lessons from reactive gliosis. Nature Reviews Neuroscience *12(2)*, 88-104.

Robin, A.M., Zhang, Z.G., Wang, L., Zhang, R.L., Katakowski, M., Zhang, L., Wang, Y., Zhang, C., and Chopp, M. (2005). Stromal cell-derived factor 1[alpha] mediates neural progenitor cell motility after focal cerebral ischemia. J Cereb Blood Flow Metab *26*, 125-134.

Robins, S.C., Stewart, I., McNay, D.E., Taylor, V., Giachino, C., Goetz, M., Ninkovic, J., Briancon, N., Maratos-Flier, E., Flier, J.S., *et al.* (2013). alpha-Tanycytes of the adult hypothalamic third ventricle include distinct populations of FGF-responsive neural progenitors. Nat Commun *4*, 2049.

Rodríguez, F., López, J.C., Vargas, J.P., Gómez, Y., Broglio, C., and Salas, C. (2002). Conservation of Spatial Memory Function in the Pallial Forebrain of Reptiles and Ray-Finned Fishes. The Journal of Neuroscience *22*, 2894-2903.

Rothenaigner, I., Krecsmarik, M., Hayes, J.A., Bahn, B., Lepier, A., Fortin, G., Götz, M., Jagasia, R., and Bally-Cuif, L. (2011). Clonal analysis by distinct viral vectors identifies bona fide neural stem cells in the adult zebrafish telencephalon and characterizes their division properties and fate. Development *138*, 1459-1469.

Saito, K., Kawaguchi, A., Kashiwagi, S., Yasugi, S., Ogawa, M., and Miyata, T. (2003). Morphological asymmetry in dividing retinal progenitor cells. Development, Growth & Differentiation *45*, 219-229.

Sauer, F.C. (1935). Mitosis in the neural tube. The Journal of Comparative Neurology *62*, 377-405.

Sawamoto, K., Wichterle, H., Gonzalez-Perez, O., Cholfin, J.A., Yamada, M., Spassky, N., Murcia, N.S., Garcia-Verdugo, J.M., Marin, O., Rubenstein, J.L.R., *et al.* (2006). New Neurons Follow the Flow of Cerebrospinal Fluid in the Adult Brain. Science *311*, 629-632.

Schwamborn, J.C., Berezikov, E., and Knoblich, J.A. (2009). The TRIM-NHL Protein TRIM32 Activates MicroRNAs and Prevents Self-Renewal in Mouse Neural Progenitors. Cell *136*, 913-925.

Seri, B., García-Verdugo, J.M., Collado-Morente, L., McEwen, B.S., and Alvarez-Buylla, A. (2004). Cell types, lineage, and architecture of the germinal zone in the adult dentate gyrus. The Journal of Comparative Neurology *478*, 359-378.

Seri, B.G.V., Jose Manuel; McEwen, Bruce S.; Alvarez Buylla, Arturo (2001). Astrocytes give rise to new neurons in the adult mammalian hippocampus. J Neuroscience *21*, 7153-7160.

Shaner, N.C., Lin, M.Z., McKeown, M.R., Steinbach, P.A., Hazelwood, K.L., Davidson, M.W., and Tsien, R.Y. (2008). Improving the photostability of bright monomeric orange and red fluorescent proteins. Nat Meth *5*, 545-551.

Shao, J., Chen, D., Ye, Q., Cui, J., Li, Y., and Li, L. (2011). Tissue regeneration after injury in adult zebrafish: The regenerative potential of the caudal fin. Developmental Dynamics *240*, 1271-1277.

Shen, Q., Wang, Y., Kokovay, E., Lin, G., Chuang, S.M., Goderie, S.K., Roysam, B., and Temple, S. (2008). Adult SVZ stem cells lie in a vascular niche: a quantitative analysis of niche cell-cell interactions. Cell Stem Cell *3*, 289-300.

Sherpa, T., Fimbel, S.M., Mallory, D.E., Maaswinkel, H., Spritzer, S.D., Sand, J.A., Li, L., Hyde, D.R., and Stenkamp, D.L. (2008). Ganglion cell regeneration following whole-retina destruction in zebrafish. Developmental Neurobiology *68*, 166-181.

Shibata, T., Yamada, K., Watanabe, M., Ikenaka, K., Wada, K., Tanaka, K., and Inoue, Y. (1997). Glutamate Transporter GLAST Is Expressed in the Radial Glia–Astrocyte Lineage of Developing Mouse Spinal Cord. The Journal of Neuroscience *17*, 9212-9219.

Shitamukai, A., Konno, D., and Matsuzaki, F. (2011). Oblique radial glial divisions in the developing mouse neocortex induce self-renewing progenitors outside the germinal zone that resemble primate outer subventricular zone progenitors. J Neurosci *31*, 3683-3695.

Shook, B.A., Manz, D.H., Peters, J.J., Kang, S., and Conover, J.C. (2012). Spatiotemporal changes to the subventricular zone stem cell pool through aging. J Neurosci *32*, 6947-6956.

Simmons, A.M., Tanyu, L.H., Horowitz, S.S., Chapman, J.A., and Brown, R.A. (2008). Developmental and Regional Patterns of GAP-43 Immunoreactivity in a Metamorphosing Brain. Brain, Behavior and Evolution *71*, 247-262.

Simon, C., Dimou, L., and Götz, M. (2011). Progenitors in the adult cerebral cortex - cell cycle properties and regulation by physiological stimuli and injury Glia *59(6)*, 869-881.

Sirko, S., Behrendt, G., Johansson, P.A., Tripathi, P., Costa, M., Bek, S., Heinrich, C., Tiedt, S., Colak, D., Dichgans, M., *et al.* (2013). Reactive glia in the injured brain acquire stem cell properties in response to sonic hedgehog. [corrected]. Cell Stem Cell *12*, 426-439.

Sofroniew, M.V. (2009). Molecular dissection of reactive astrogliosis and glial scar formation. Trends in Neurosciences *32*, 638-647.

Spalding, Kirsty L., Bergmann, O., Alkass, K., Bernard, S., Salehpour, M., Huttner, Hagen B., Boström, E., Westerlund, I., Vial, C., Buchholz, Bruce A.,

et al. (2013). Dynamics of Hippocampal Neurogenesis in Adult Humans. Cell *153*, 1219-1227.

Spassky, N., Merkle, F.T., Flames, N., Tramontin, A.D., Garcia-Verdugo, J.M., and Alvarez-Buylla, A. (2005). Adult Ependymal Cells Are Postmitotic and Are Derived from Radial Glial Cells during Embryogenesis. J Neurosci *25*, 10-18.

Stensaas, L., and Stensaas, S. (1968). Light microscopy of glial cells in turtles and birds. ZZellforsch *91*, 315-340.

Stichel, C.C., and Müller, H.W. (1998). The CNS lesion scar: new vistas on an old regeneration barrier. Cell Tissue Res *294*, 1-9.

Suh, H., Consiglio, A., Ray, J., Sawai, T., D'Amour, K.A., and Gage, Fred H. (2007). *In Vivo* Fate Analysis Reveals the Multipotent and Self-Renewal Capacities of Sox2+ Neural Stem Cells in the Adult Hippocampus. Cell Stem Cell *1*, 515-528.

Sundholm-Peters, N.L., Yang, H.K., Goings, G.E., Walker, A.S., and Szele, F.G. (2005). Subventricular zone neuroblasts emigrate toward cortical lesions. J Neuropathol Exp Neurol *64*, 1089-1100.

Takasawa, K.-i.K., Kazuo; Yagita, Yoshiki; Sasaki, Tsutomu; Tanaka, Shigeru; Matsushita, Kohji; Ohstuki, Toshiho; Miyata, Takaki; Okano, Hideyuki; Hori, Masatsugu; Matsumoto, Masayasu (2002). Increased Proliferation of Neural Progenitor Cells but Reduced Survival of Newborn Cells in the Contralateral Hippocampus After Focal Cerebral Ischemia in Rats. J Cereb Blood Flow Metab *22*, 299-307.

Tatsumi, K., Takebayashi, H., Manabe, T., Tanaka, K.F., Makinodan, M., Yamauchi, T., Makinodan, E., Matsuyoshi, H., Okuda, H., Ikenaka, K., *et al.* (2008). Genetic fate mapping of Olig2 progenitors in the injured adult cerebral cortex reveals preferential differentiation into astrocytes. J Neurosci Res *86*, 3494-3502.

Tavazoie, M., Van der Veken, L., Silva-Vargas, V., Louissaint, M., Colonna, L., Zaidi, B., Garcia-Verdugo, J.M., and Doetsch, F. (2008). A Specialized Vascular Niche for Adult Neural Stem Cells. Cell Stem Cell *3*, 279-288.

Tawk, M.A., Claudio; Lyons, Dave A.; Reugels, Alexander M.; Girdler, Gemma C.; Bayley, Philippa R.; Hyde, David R.; Tada, Masazumi; Clarke, Jonathan D. W. (2007). A mirror-symmetric cell division that orchestrates neuroepithelial morphogenesis. Nature *446*, 797-800.

Thored, P., Arvidsson, A., Cacci, E., Ahlenius, H., Kallur, T., Darsalia, V., Ekdahl, C.T., Kokaia, Z., and Lindvall, O. (2006). Persistent production of neurons from adult brain stem cells during recovery after stroke. STEM CELLS *24*, 739-747.

Thored, P., Wood, J., Arvidsson, A., Cammenga, J., Kokaia, Z., and Lindvall, O. (2007). Long-term neuroblast migration along blood vessels in an area with transient angiogenesis and increased vascularization after stroke. Stroke *38*, 3032-3039.

Tonchev, A.B., Yamashima, T., Sawamoto, K., and Okano, H. (2005). Enhanced proliferation of progenitor cells in the subventricular zone and limited

neuronal production in the striatum and neocortex of adult macaque monkeys after global cerebral ischemia. Journal of Neuroscience Research *81*, 776-788.

Trachtenberg, J.T.C., Brian E.; Knott, Graham W; Feng, Guoping; Sanes, Joshua R; Welker, Egbert; Svoboda, Karel (2002). Long-term *in vivo* imaging of experience-dependent synaptic plasticity in adult cortex. Nature *420*, 788-794.

Tran, P.B., Banisadr, G., Ren, D., Chenn, A., and Miller, R.J. (2007). Chemokine receptor expression by neural progenitor cells in neurogenic regions of mouse brain. The Journal of Comparative Neurology *500*, 1007-1034.

Tropepe, V., Craig, C.G., Morshead, C.M., and van der Kooy, D. (1997). Transforming Growth Factor-α Null and Senescent Mice Show Decreased Neural Progenitor Cell Proliferation in the Forebrain Subependyma. The Journal of Neuroscience *17*, 7850-7859.

Vargas, J.P., Rodríguez, F., López, J.C., Arias, J.L., and Salas, C. (2000). Spatial learning-induced increase in the argyrophilic nucleolar organizer region of dorsolateral telencephalic neurons in goldfish. Brain Research *865*, 77-84.

W. Köster, R., and Fraser, S.E. (2004). Time-Lapse Microscopy of Brain Development. In Methods in Cell Biology, M.W. H. William Detrich Iii, and I.Z. Leonard, eds. (Academic Press), pp. 207-235.

Weigmann, A., Corbeil, D., Hellwig, A., and Huttner, W.B. (1997). Prominin, a novel microvilli-specific polytopic membrane protein of the apical surface of epithelial cells, is targeted to plasmalemmal protrusions of non-epithelial cells. Proceedings of the National Academy of Sciences *94*, 12425-12430.

Weiner, L. (2008). Definitions and Criteria for Stem Cells. In Neural Stem Cells, L. Weiner, ed. (Humana Press), pp. 3-8.

Westerfield, M. (2000). The zebrafish book. A guide for the laboratory use of zebrafish (Danio rerio), 4th ed. edn (Univ. of Oregon Press, Eugene).

White, R.M., Sessa, A., Burke, C., Bowman, T., LeBlanc, J., Ceol, C., Bourque, C., Dovey, M., Goessling, W., Burns, C.E., *et al.* (2008). Transparent Adult Zebrafish as a Tool for *In Vivo* Transplantation Analysis. Cell Stem Cell *2*, 183-189.

Widestrand, Å., Faijerson, J., Wilhelmsson, U., Smith, P.L.P., Li, L., Sihlbom, C., Eriksson, P.S., and Pekny, M. (2007). Increased Neurogenesis and Astrogenesis from Neural Progenitor Cells Grafted in the Hippocampus of GFAP−/−Vim−/− Mice. STEM CELLS *25*, 2619-2627.

Wilcock, A.C., Swedlow, J.R., and Storey, K.G. (2007). Mitotic spindle orientation distinguishes stem cell and terminal modes of neuron production in the early spinal cord. Development *134*, 1943-1954.

Williams, B.P., and Price, J. (1995). Evidence for multiple precursor cell types in the embryonic rat cerebral cortex. Neuron *14*, 1181-1188.

Wu, S.X., Goebbels, S., Nakamura, K., Kometani, K., Minato, N., Kaneko, T., Nave, K.A., and Tamamaki, N. (2005). Pyramidal neurons of upper cortical layers generated by NEX-positive progenitor cells in the subventricular zone. Proc Natl Acad Sci U S A *102*, 17172-17177.

Wullimann, M.F., and Rink, E. (2002). The teleostean forebrain: a comparative and developmental view based on early proliferation, Pax6 activity and catecholaminergic organization. Brain Res Bull *57*, 363-370.

Xie, Y., Jüschke, C., Esk, C., Hirotsune, S., and Knoblich, Juergen A. (2013). The Phosphatase PP4c Controls Spindle Orientation to Maintain Proliferative Symmetric Divisions in the Developing Neocortex. Neuron *79*, 254-265.

Xu, H.-T.P., Feng; Yang, Guang; Gan, Wen-Biao (2007). Choice of cranial window type for *in vivo* imaging affects dendritic spine turnover in the cortex. Nat Neurosci *10*, 549-551.

Yamashita, T., Ninomiya, M., Hernández Acosta, P., García-Verdugo, J.M., Sunabori, T., Sakaguchi, M., Adachi, K., Kojima, T., Hirota, Y., Kawase, T., *et al.* (2006). Subventricular Zone-Derived Neuroblasts Migrate and Differentiate into Mature Neurons in the Post-Stroke Adult Striatum. The Journal of Neuroscience *26*, 6627-6636.

Yoon, K.-J., Koo, B.-K., Im, S.-K., Jeong, H.-W., Ghim, J., Kwon, M.-c., Moon, J.-S., Miyata, T., and Kong, Y.-Y. Mind Bomb 1-Expressing Intermediate Progenitors Generate Notch Signaling to Maintain Radial Glial Cells. Neuron *58*, 519-531.

Young, K.M., Fogarty, M., Kessaris, N., and Richardson, W.D. (2007). Subventricular zone stem cells are heterogeneous with respect to their embryonic origins and neurogenic fates in the adult olfactory bulb. J Neurosci *27*, 8286-8296.

Zhang, R., Zhang, Z., Wang, L., Wang, Y., Gousev, A., Zhang, L., Ho, K.-L., Morshead, C., and Chopp, M. (2004). Activated Neural Stem Cells Contribute to Stroke-Induced Neurogenesis and Neuroblast Migration Toward the Infarct Boundary in Adult Rats. J Cereb Blood Flow Metab *24*, 441-448.

Zupanc, G.K. (1999). Neurogenesis, cell death and regeneration in the adult gymnotiform brain. Journal of Experimental Biology *202*, 1435-1446.

Zupanc, G.K., and Ott, R. (1999a). Cell proliferation after lesions in the cerebellum of adult teleost fish: time course, origin, and type of new cells produced. Exp Neurol *160*, 78-87.

Zupanc, G.K., and Zupanc, M.M. (1992). Birth and migration of neurons in the central posterior/prepacemaker nucleus during adulthood in weakly electric knifefish (Eigenmannia sp.). Proceedings of the National Academy of Sciences *89*, 9539-9543.

Zupanc, G.K.H., and Ott, R. (1999b). Cell Proliferation after Lesions in the Cerebellum of Adult Teleost Fish: Time Course, Origin, and Type of New Cells Produced. Experimental Neurology *160*, 78-87.

Appendix I

Stab Wound Injury of the Zebrafish Telencephalon: A Model for Comparative Analysis of Reactive Gliosis

EMILY VIOLETTE BAUMGART,[1] JOANA S. BARBOSA,[1,2] LAURE BALLY-CUIF,[3] MAGDALENA GÖTZ,[1,4]* AND JOVICA NINKOVIC[1,4]

[1]*Institute for Stem Cell Research, Helmholtz Center Munich, German Research Center for Environmental Health, Neuherberg, Germany*

[2]*PhD Programme in Biomedicine and Experimental Biology (BEB), Center for Neuroscience and Cell Biology, University of Coimbra, Coimbra, Portugal*

[3]*Zebrafish Neurogenetics Group, Laboratory of Neurobiology and Development (N&D), CNRS UPR 3294, Institute of Neurobiology Alfred Fessard, Gif-sur-Yvette cédex, France*

[4]*Department of Physiological Genomics, Institute of Physiology, Ludwig-Maximilians University Munich, Munich, Germany*

KEY WORDS

regeneration in the CNS; ependymoglia; oligodendrocyte progenitors; brain injury; glia scar

ABSTRACT

Reactive glia, including astroglia and oligodendrocyte progenitors (OPCs) are at the core of the reaction to injury in the mammalian brain with initially beneficial and later partially adverse functions such as scar formation. Given the different glial composition in the adult zebrafish brain with radial ependymoglia but no parenchymal astrocytes, we examined the glial response to an invasive stab wound injury model in the adult zebrafish telencephalon. Strikingly, already a few days after injury the wound was closed without any scar tissue. Similar to mammals, microglia cells reacted first and accumulated close to the injury site, while neither GFAP+ radial ependymoglia nor adult OPCs were recruited to the injury site. Moreover, OPCs failed to increase their proliferation after this injury, while the number of proliferating GFAP+ glia was increased until 7 days after injury. Importantly, neurogenesis was also increased after injury, generating additional neurons recruited to the parenchyma which survived for several months. Thus, these data suggest that the specific glial environment in the adult zebrafish telencephalon is not only permissive for long-term neuronal survival, but avoids scar formation. Invasive injury in the adult zebrafish telencephalon may therefore provide a useful model to untangle the molecular mechanisms involved in these beneficial glial reactions.

INTRODUCTION

Glial cells mediate the wound reaction in the brain after any type of injury or inflammation (for review see Hanisch and Kettenmann, 2007; Pekny and Nilsson, 2005; Ridet et al., 1997; Robel et al., 2011; Silver and Miller, 2004; Sofroniew, 2009). For example, after invasive injury the reaction of glial cells (reactive gliosis) is important to limit the injury size and inflammatory reaction, but also contributes to scar formation, with deleterious consequences on neuronal survival and axonal growth (Hanisch and Kettenmann, 2007; Pekny and Nilsson, 2005; Ridet et al., 1997; Robel et al., 2011; Silver and Miller, 2004; Sofroniew, 2009). In the mammalian CNS, reactive gliosis is mediated by three major cell types: the microglia, the astrocytes and the NG2+ or Olig2+ glial progenitors, also referred to as oligodendrocyte progenitors (OPCs) (Hanisch and Kettenmann, 2007; Robel et al., 2011; Sofroniew, 2009). Microglial cells are of mesodermal origin and are involved in phagocytosis and in cytokine communication in a highly specific manner (Hanisch and Kettenmann, 2007). Astroglial cells are crucial to limit the size of the wound as well as inflammation and are also thought to play an important role in reestablishing the blood–brain barrier (Buffo et al., 2010; Robel et al., 2011; Sofroniew, 2009). Interestingly, attenuated reactive astrogliosis resulting from deletion of the intermediate filaments GFAP and Vimentin initially leads to increased inflammatory reaction and injury size, but also reduces scar formation (Pekny and Pekna, 2004; Robel et al., 2011), suggesting initially beneficial but later disadvantageous effects of reactive astrogliosis.

Important insights into the role of astrogliosis may be gained by analysis of the injury reaction in brains lacking astrocytes, as is the case for most bony fish. In contrast to rays and sharks, which possess some astroglia-like cells in the expanded forebrain parenchyma, most bony fish lack parenchymal astrocytes in the grey matter (GM) and white matter (WM) of the brain and spinal cord (Ari and Kálmán, 2008; Hui et al., 2010; Kálmán, 2002), while the optic nerve comprises a specialized set

Note added in Proof: Note the difference in glial cell reactivity when stab wound injury is performed through the skull (as recently published in März et al., 2011; Kishimoto et al., 2012) versus injury via the nostrils (this paper, and the recently published work by Kraehlin et al., 2011, where injury affects almost half of the telencephalic hemisphere). Injuries through the skull damage the VZ and allow CSF entry into the brain parenchyma, which may account for the observed differences.

Additional Supporting Information may be found in the online version of this article.

Grant sponsors: DFG including the SFB596, SFB870, the BMBF, the Bavarian Ministry for Science (For NeuroCell), the EU (EUTRACC and EduGlia) and Foundation for Science and Technology, Portugal (to J.B.).

*Correspondence to: Magdalena Götz or Jovica Ninkovic, Helmholtz Zentrum Munchen, Institute of Stem Cell Research, Ingolstädter Landstr. 1, 85764 Neuherberg, Germany. E-mail: magdalena.goetz@helmholtz-muenchen.de or ninkovic @helmholtz-muenchen.de

Received 21 April 2011; Accepted 21 October 2011

DOI 10.1002/glia.22269

Published online in Wiley Online Library (wileyonlinelibrary. com).

of reticular astrocytes expressing cytokeratins (Maggs and Scholes, 1990). Instead, GFAP- and S100β-expressing glial cells are located at the ventricle with their processes spanning the entire parenchyma in most brain regions and in the spinal cord of zebrafish (Adolf et al., 2006; Chapouton et al., 2006; Ganz et al., 2010; Grandel et al., 2006; Kaslin et al., 2009; März et al., 2010a; Reimer et al., 2008, 2009). Accordingly, these cells are referred to as radial glia, tanycytes, or ependymoglia (Grupp et al., 2010; Robel et al., 2011), and likely combine the function of mammalian ependymal cells and astroglia. Thus, the absence of parenchymal protoplasmic astrocytes prompts the question as to how an invasive injury would be shielded off and if so by which set of glial cells. Would the radial ependymoglia leave their ventricular location and migrate to the site of injury or would other glial cells, such as the NG2 glia, perform this function in the zebrafish? Notably radial glia/ependymocytes continue to generate neurons in the adult zebrafish telencephalon (Adolf et al., 2006; Ganz et al., 2010; Kaslin et al., 2008), prompting the idea that, if emigrating GFAP+ cells are present upon lesion, they may simultaneously serve two functions: wound closure and neuronal repair.

The response of microglia cells has been documented after injury in the zebrafish spinal cord (Becker and Becker, 2001), but not yet upon lesion in the brain. Likewise, ependymoglia can up-regulate Olig2 and newly generate spinal cord motoneurons after injury (Reimer et al., 2008, 2009), but the reaction of parenchymal Olig2+ cells (März et al., 2010b; Park et al., 2007) to invasive injury has not yet been examined in the zebrafish adult brain. Interestingly, NG2+/Olig2+/PDGFRα+ progenitors in the adult mammalian brain were recently identified as life-long progenitors that self-renew and also generate mature oligodendrocytes (Dimou et al., 2008; Kang et al., 2010; Rivers et al., 2008). In the mouse brain, these cells potently react to injury by increasing their proliferation and thereby generating more of themselves as well as mature oligodendrocytes (Dimou et al., 2008; Kang et al., 2010; Simon et al., 2011). As the transcription factor Olig2 is crucially involved in development of oligodendrocytes and specific types of neurons in both zebrafish and mice (Kim et al., 2008; McFarland et al., 2008; Shin et al., 2003; Takebayashi et al., 2002a,b; Zannino and Appel, 2009; Zhou and Anderson, 2002), the role of Olig2+ cells in the adult zebrafish brain may also resemble their counterparts in the mammalian brain. Indeed, proliferation of Olig2+ cells followed by differentiation into oligodendrocytes has recently also been shown in the adult zebrafish telencephalon (März et al., 2010b). Notably, however, the contribution of Olig2+ cells to wound closure and/or scar formation given the high expression of the proteoglycan NG2 on these cells is not clear even in the mammalian brain. Moreover, these cells transform into reactive astrocytes in some rodent brain injury models (Fawcett and Asher, 1999; Hampton et al., 2004; Levine et al., 2001; Tatsumi et al., 2008; Zhao et al., 2009) (see however Komitova et al., 2011), leading to the idea that they may serve as a possible source of reactive astrocytes in the zebrafish brain.

Therefore, here we set out to examine the glial reactivity to an invasive stab wound injury in the adult zebrafish telencephalon as recently described (Ayari et al., 2010). The stab wound injury can be performed by inserting a syringe through the nostril of an adult zebrafish thereby causing a circumscribed injury in the parenchyma of the telencephalon without injuring ventricular lining (Ayari et al., 2010). This results in increased neurogenesis in this region, consistent with the profound regenerative capacity of the zebrafish found also in other parts of the CNS and in other organs (Becker and Becker, 2008; Brignull et al., 2009; DeLaurier et al., 2010; Poss et al., 2003; Raya et al., 2004). Restorative neurogenesis can be elicited in the zebrafish CNS both in regions that normally stop neurogenesis at the adult stage, such as the spinal cord (Reimer et al., 2008, 2009), and in regions that maintain ongoing neurogenesis in the adult, such as the telencephalon (Adolf et al., 2006; Ayari et al., 2010; Ganz et al., 2010; März et al., 2010a). In mammals, an injury in the vicinity of neurogenic sites results in emigration of progenitors and the generation of young neurons (Arvidsson et al., 2002; Brill et al., 2009; Collin et al., 2005; Kim and Szele, 2008; Sundholm-Peters et al., 2005; Thored et al., 2007), but most of them fail to survive (Thored et al., 2007), except in injury conditions where neurons die by apoptosis, which avoids a strong reactive gliosis (Chen et al., 2004). This prompted us to examine the glia response to injury, and the long-term survival of neurons settling at the former injury site, in the brain parenchyma of the adult zebrafish.

MATERIALS AND METHODS

Fish Maintenance and Strains

Fish were kept under standard conditions as previously described (Westerfield, 2000). Adult 3- to 4-month-old wild-type zebrafish (*Danio rerio*) of the AB strain, or of the transgenic lines *Tg(fli1aEGFP)y1* (Lawson and Weinstein, 2002), *Tg(gfap:gfp)mi2001* (Bernardos and Raymond, 2006), and *Tg(olig2:gfp)* (Shin et al., 2003) were used for all experiments. All experiments were performed according to the animal handling guidelines of the EU and the state of Bavaria (license number 55.2.-1-54-2531-100-10).

Stab Wound Injury of the Adult Zebrafish Telencephalon

As described in the Results section, the small telencephalic injuries in 3- to 4-month-old adult zebrafish were made using a 100 × 0.9 mm glass capillary needle (KG01, A. Hartenstein). All needles were pulled on a Narishige Puller (model PC-10) using a "One-stage" pull setting at a heater level of 63.5°C. The resulting dimensions of the needle used to make the telencephalic injury were 5 mm in length and 0.1 mm in diameter. For larger injuries, a Braun Omnican® 50 single-use in-

sulin syringe was used (8 mm in length and 0.3 mm in diameter).

Before injury, fish were anesthetized in 0.02% Tricaine for 30 to 45 s. Fish were placed in a Tricaine-soaked sponge to keep them firmly in place for the procedure, yet allowing accessibility to the head. With the visual aid of a dissecting microscope, the glass capillary needle was inserted into the zebrafish nose holes. In the adult zebrafish, the telencephalon is easily visible under a transparent section of the skull, which imitates the shape of the underlying brain, consistently allowing for control of the lesion track location and endpoint. After injury, fish were placed in fresh fish water with ample circulation, to insure complete recovery from the anesthetics.

BrdU Labeling

To label cells in S phase, fish were injected intraperitoneally with 50 μL/g body weight of the thymidine analog bromo-deoxy-uridine (BrdU) diluted in 110 mM NaCl pH 7.0 as previously described (Adolf et al., 2006).

Tissue Preparation

Fish were euthanized with 0.2% Tricaine. Brains were fixed in the skull for 1 h at 4°C and then dissected and fixed for an additional 3 h at 4°C in 4% paraformaldehyde (PFA) in phosphate-buffered saline (PBS). Brains were then washed twice with PBS and processed immediately for sectioning. For immunofluorescent stainings, whole brains were embedded in 3% agarose in PBS and cut serially at 100 μm thickness using a vibrating microtome (HM 650 V, Microm). All sections were stored at −20°C in storage buffer (0.25 M NaH_2PO_4; 30% ethylene glycol; 30% glycerol) until further processing.

Immunohistochemistry

We used rat anti-5-bromo-2-deoxyuridine (BrdU) (MCA2060, 1:200, Serotec), chick anti-Green Fluorescent Protein (GFP) (GFP-1020, 1:1,500, Aves Labs), anti-Human Neuronal Protein HuC/HuD (HuCD) (A-21271, 1:600, Invitrogen/Molecular Probes), anti-GFAP (Z0334, 1:200, DAKO), anti-S100β (CB1040, 1:500, Millipore), anti-fish leukocytes (4C4) (92092321, 7.4.C4, 1:500, Health Protection Agency Culture Collections), anti-PSA-NCAM (MAB5324, 1:100, Millipore), and rabbit anti-MCM5 (gift from Soojin Ryu) (1:1,000) antibodies. Primary antibodies were detected by subclass-specific secondary antibodies labeled with FITC (1:200, Jackson ImmunoResearch Laboratories), Cy3 (1:700, Jackson ImmunoResearch Laboratories), Alexa 488 (1:1,000, Invitrogen), or Alexa 546 (1:1,000, Invitrogen). Nuclear staining was performed with 4′,6-diamidino-2-phenylindole dihydrochloride (DAPI) (Sigma). All sections were embedded in Aqua Polymount (Polyscience). Immunodetection of BrdU required a pretreatment with 2 N HCl followed by washes with borate buffer and PBS before the sections were immersed in the anti-BrdU antibody. The detection of 4C4 required a postfixation with 4% PFA for 20 min before BrdU pretreatment. All antibodies were dissolved in 0.5% Triton X and 10% normal goat serum (NGS), except for PSA-NCAM where no Triton X was used. All sections were photographed and analyzed under an Olympus Fluoview confocal microscope with FV10-ASW 2.1 software or a Zeiss Axioplan 2 microscope.

Quantification

All quantitative results are represented as averages with standard error of the mean. The unpaired ANOVA test was performed to test for statistical significance.

RESULTS

Establishing a Stab Wound Injury Model in the Adult Zebrafish Telencephalon

In order to test the glial reaction to invasive injury in the GM of the zebrafish brain, we first developed a technique to generate reproducible stab wound injuries in the zebrafish telencephalon. We based our technique on the previously described model (Ayari et al., 2010), but chose in average younger fish (3–4 months old) and accordingly used a smaller sized injury device, a glass capillary (5 mm in length and 0.1 mm in diameter, compared with a 26G needle (0.457 mm in diameter) (Ayari et al., 2010)) to avoid any damage in the radial glial cell layer lining the ventricle. The easily visible nasal holes of the adult zebrafish (* in Fig. 1A) were used as a point-of-entry to reproducibly injure the same brain areas. Indeed, the injury track, as marked by the carbocyanine dye, DiI, was visible as extension through the dorsal cellular layers of the olfactory bulb which continued into the telencephalon parenchyma and ended before the diencephalon (red bar in Fig. 1A and arrows in Fig. 1B) in all animals ($n = 6$) used in these test experiments. As intended, the injury paths were found in the telencephalic parenchyma avoiding the progenitor region located in the ventricular zone (VZ) (Fig. 1B). Often the stab wound injury is located in the subpallium, i.e. the ventral region of the telencephalon (Fig. 1B; white arrows), but sometimes also in the dorsolateral region (Fig. 6B, asterisk).

Lack of Scar Formation After Stab Wound Injury of the Adult Zebrafish Telencephalon

To follow the injury size over time, we performed DAPI counterstaining on consecutive coronal sections at different time points following stab wound injury (Fig. 1C–V). At 1 day post-injury (dpi), the injury was clearly visible as a site of high DAPI signal due to a large mass of cells (red arrows in Fig. 1H–L and data not shown; $n = 25$ animals examined), in agreement with previous reports where sites of brain injury were filled with erythrocytes, phagocytes, and other cells shortly after the injury (Bernstein, 1967). By 2 dpi, the injury site appeared already smaller in diameter (arrows in Fig. 1M–P, $n = 23$ animals examined) and injury sites were

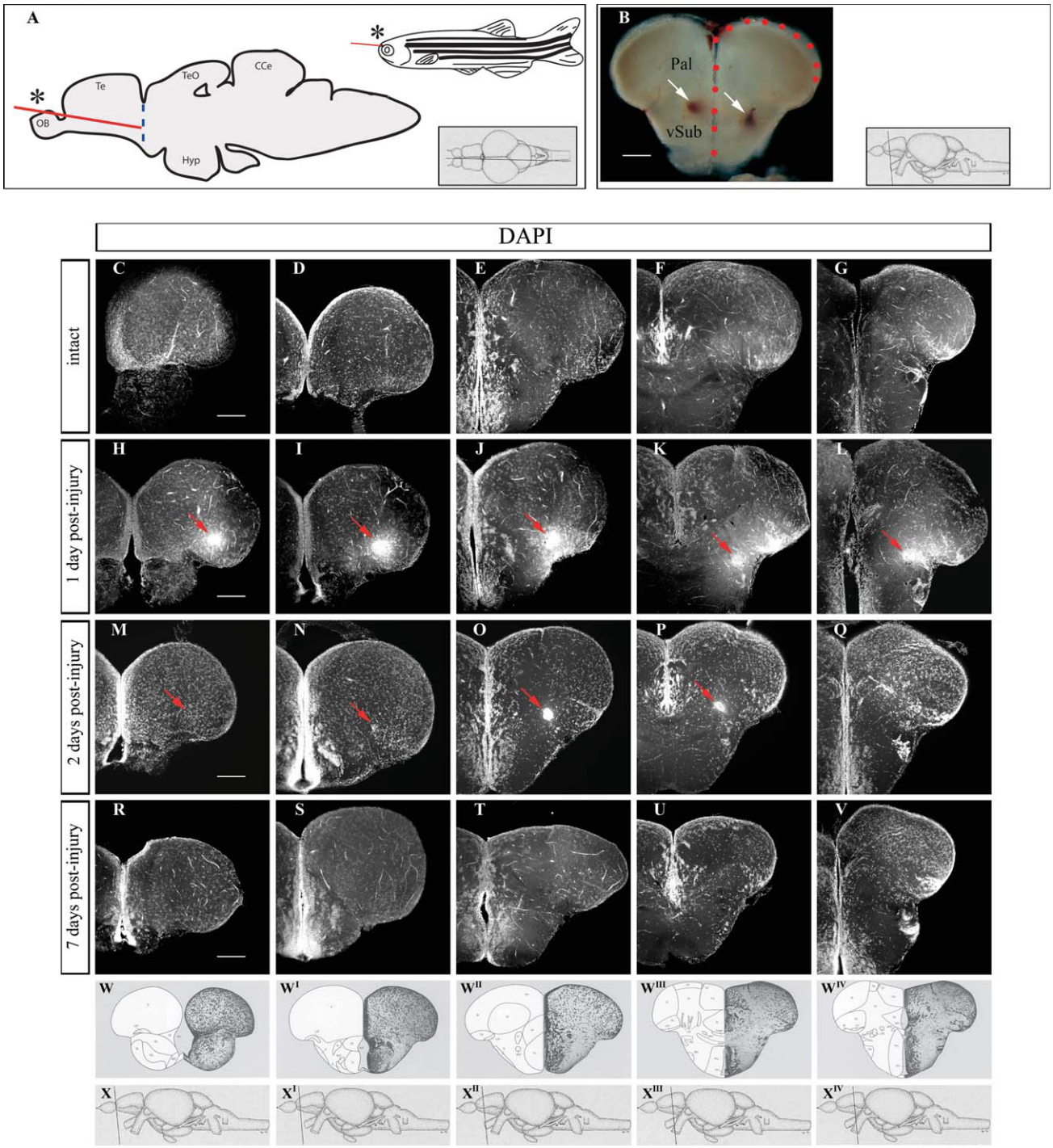

Fig. 1. The adult zebrafish telencephalon has a tremendous wound healing capacity. (**A**) Scheme depicting the stab wound paradigm in the adult zebrafish telencephalon. The red line indicates point-of-entry through the nasal holes (asterisk) and subsequent injury track created through the telencephalon. The blue dashed line indicates the end point of the injury track in the adult telencephalon. (**B**) Representative micrograph of coronal cross-section through zebrafish telencephalon depicting DiI-labeled bilateral injury tracks (white arrows) in the parenchyma of the telencephalic subpallium in a 4-month-old adult zebrafish. The level of cross-section is indicated in the inset. Note that the injury tracks are distant from progenitors (indicated with red dots) in the zebrafish neurogenic zones. (**C–V**) Wound healing capacity in the adult zebrafish telencephalon following stab wound injury. Micrographs representing single optical sections through the telencephalic hemisphere, dorsal up, with the nuclear stain (DAPI) labeling all cells at the given post-injury time points and rostrocaudal levels as indicated in panels **W–X**^{IV}. Note that following the stab wound injury, the injured area is infiltrated with a high number of cells (red arrow in H–P) and the injury site is no longer visible at 7 days post-injury (dpi) (R–V). (W–X) Schematic representation of adult zebrafish brain after Wullimann et al. (1996). CCe: corpus cerebellaris, dSub: dorsal subpallium, Hyp: hypothalamus, OB: olfactory bulb, Pal: pallium, Te: telencephalon, TeO: tectum opticum, vSub: ventral subpallium. Scale bars = 100 μm.

no longer discernible in all consecutive sections, suggesting that wound healing and restoration of parenchymal tissue had already begun (Fig. 1M,Q). Strikingly, by 7 dpi, the site of damage or a histological scar was no longer detectable in the majority of injured brains (75%, $n = 24$). Moreover, in cases where the injury site was visible, the injury track could only be observed in a few consecutive sections per brain, while the tissue morphology of the remaining sections was indistinguishable from that of the intact control telencephalon (Fig. 1R–V). When the injured telencephalon was observed at even later time points, ranging from 1.5 to 2.5 months post-injury, we were unable to visualize the site of injury, with the parenchyma being cleared of injury indicators such as debris, clusters of nucleated cells, or dense regions of blood vessels (Fig. 7A,B and data not shown). Taken together, our observations further support the wound healing capacity in the adult zebrafish, revealing the complete tissue restoration and lack of scar formation in the stab wound injured telencephalon. There is a gradual disappearance of the injury tract at progressive post-injury time points, leaving the injured loci unidentifiable several weeks post-injury.

Microglia Reactivity After Stab Wound Injury in the Adult Zebrafish Telencephalon

Given the fast and complete healing response, rendering injured and uninjured hemispheres undistinguishable, we typically performed bilateral injuries to avoid confusion between injured and uninjured sites. As the first cell type reacting to injury in the mouse telencephalon is the microglia, we first examined their reaction by immunostaining for 4C4, which was previously used to label microglial cells in the zebrafish (Becker and Becker, 2001). Few nicely branched and hence not activated microglia were detected in the intact telencephalon (Fig. 2A,A') and virtually none of the microglia located in the parenchyma were found to proliferate and hence to incorporate BrdU (Fig. 2A',C, Supp. Info. Fig. 1). Within 1 to 2 days after injury, however, many more microglial cells were observed in the injured brain (Fig. 2B,C) accumulating around the injury site (Supp. Info. Fig. 2). The morphology of these 4C4-positive microglia cells had also changed to a phagocytotic type of activated microglia (Fig. 2B', Supp. Info. Fig. 2) as described in other injury conditions in the zebrafish (Kassen et al., 2007; Vihtelic and Hyde, 2000). Moreover, consistent with their increase in number, many of these activated microglia stained positive for BrdU incorporation (2× intraperitoneal BrdU injections with 2 h after each injection, Fig. 2B',C, Supp. Info. Fig. 1). This may reflect their active proliferation following injury, or, as microglia cells are highly phagocytotic, accumulation of cellular debris, including BrdU-labeled DNA fragments, in their cytoplasm. To distinguish between these hypotheses, we performed two sets of experiments. First, we examined BrdU in combination with DAPI. If microglia had engulfed BrdU-positive cells, they might display

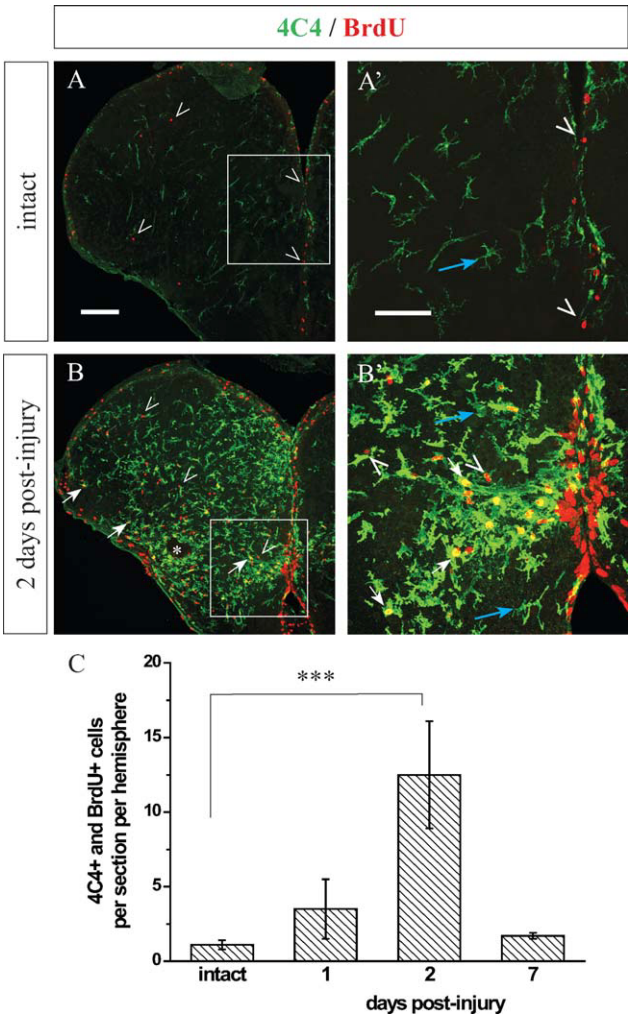

Fig. 2. Microglia response in the injured adult zebrafish telencephalon. (**A–C**) Injury in the adult zebrafish telencephalon causes an innate immune reaction indicated by increased numbers of proliferating microglia marked by 4C4. Confocal images depicting cells immunoreactive for microglia marker 4C4 (green) and BrdU (red) in the intact control (A, **A**′) and injured adult telencephalon at 2 dpi (B, **B**′). A′ and B′ are magnifications of the boxed areas in A and B respectively. (C) Histogram depicting the proliferating microglia cells at different time points following injury in the zebrafish telencephalon. Data are shown as mean ± SEM. Note the increase in number of proliferating 4C4-positive microglia throughout the parenchyma (sevenfold increase when compared with the intact control tissue, $n = 3$ animals per time point examined, $^{***}P < 0.001$) and their hypertrophy, shown by increase in size and immunoreactivity to 4C4 following injury. All micrographs are maximum intensity projections of optical z-stacks, coronal cross-sections, dorsal up, white arrows indicate colabeled BrdU-positive/4C4-positive cells, white arrowheads mark BrdU single-positive cells, blue arrows indicate 4C4-single-positive cells and white asterisk indicates the site of injury when visible. Scale bars = 80 μm in A, B, and 40 μm in A′, B′.

additional BrdU-positive debris in vesicles in the cytoplasm or even more than one nucleus. However, we could not observe any BrdU-positive and 4C4-positive cell with an additional nucleus, BrdU always colocalized to the single nucleus of a cell and BrdU was not found in fragments in the cytoplasm (data not shown). Second, we used a different marker for proliferating cells, immunostaining for MCM-5, a nuclear antigen present in the proliferating cells (Ryu et al., 2005). This analysis

revealed a substantial number of proliferating cells with microglia identity (~20% of all MCM5+ cells at 2 dpi, Supp. Info. Fig. 2). Moreover, the presence of MCM5- and 4C4-double immunopositive cells in the brain parenchyma suggests that the increased number of microglia is at least in part due to their proliferation in the brain parenchyma. However, the high number of cells infiltrating into the lesion track observed at 1 dpi (Fig. 1H–L) suggests that this increase might be partially caused by an infiltration or immigration of microglia cells. Notably, already at 7 dpi microglial cells had ceased to proliferate (Fig. 2C and Supp. Info. Fig. 1) and resumed a branched and less activated morphology.

Olig2 Glia Reactivity After Stab Wound Injury in the Adult Zebrafish Telencephalon

In the rodent stab wound injured forebrain, Olig2-expressing glial progenitors are also amongst the first glial cells to react and increase their proliferation within 2 days (Buffo et al., 2005; Simon et al., 2011; Zhao et al., 2009). As these glial progenitors constantly proliferate in the healthy adult mouse forebrain (Dimou et al., 2008; Simon et al., 2011), we first examined Olig2+ cells after two consecutive BrdU injections with a 2 h interval in the healthy adult zebrafish telencephalon. Typically, very few BrdU-labeled cells were detected in the brain parenchyma in the intact adult brain (Figs. 3A,A',C and 6F). However, most of these indeed co-localized with Olig2 (data not shown) or with GFP in the *olig2*:gfp transgenic line (Park et al., 2007; Shin et al., 2003) (Fig. 3A',C and Supp. Info. Fig. 1B,C), consistent with a recent report (März et al., 2010b). Surprisingly, and in profound contrast to the situation in the rodent brain, these cells did not increase their proliferation after stab wound injury (Fig. 3B,B',C; Supp. Info. Fig. 1), and accordingly their overall number remained unchanged upon injury (Fig. 3A–C, Supp. Info. Fig. 1C). Also after longer BrdU labeling over the course of 3 days no increase in the number of BrdU-incorporating Olig2+ cells was detectable (data not shown). Thus, despite the ongoing proliferation of Olig2+ cells in the normal zebrafish brain parenchyma, these cells fail to increase their proliferation in our stab wound injury paradigm.

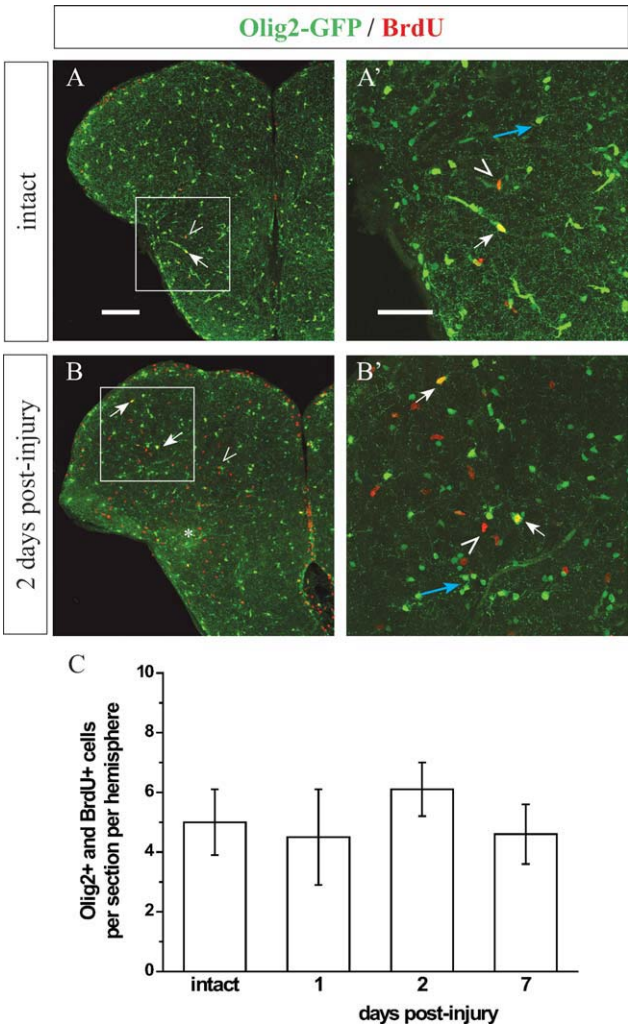

Fig. 3. Oligodendrocyte progenitors do not react to the stab wound injury in the adult zebrafish telencephalon. (**A** and **B**) Confocal images showing cells immunoreactive for Olig2-GFP (green) and BrdU (red) in the intact control (A) and injured adult telencephalon 2 dpi (B) in olig2:gfp transgenic line [Tg(Olig2:gfp)]. **A′** and **B′** are magnifications of the boxed areas in A and B, respectively. (**C**) Histogram depicting the number of proliferating Olig2-GFP positive cells following injury. Note that comparable numbers of Olig2+ cells proliferate in the intact and injured adult telencephalon ($n > 3$ animals examined per time point). All micrographs are maximum intensity projections of optical z-stacks, coronal cross-sections, dorsal up, white arrows indicate colabeled BrdU-positive/GFP-positive cells, white arrowheads mark BrdU single-positive cells, blue arrows GFP-positive only cells, and white asterisk indicate site of injury when visible. Scale bars = 80 μm in A, B and 40 μm in A′, B′.

Ependymoglia Reactivity After Stab Wound Injury in the Adult Zebrafish Telencephalon

Next we examined the reaction of GFAP-expressing ependymoglia/radial glia cells at the ventricle (Ganz et al., 2010; März et al., 2010a) after the stab wound injury. Toward this end we used Tg(*gfap*:GFP) transgenic fish, expressing GFP under control of zebrafish *gfap* regulatory elements (Bernardos and Raymond, 2006). Consistent with previous work (Bernardos and Raymond, 2006; Ganz et al., 2010; März et al., 2010a), we also observed reliable colocalization of GFP with GFAP immunoreactivity in the radial glia cells at the VZ and the processes extending into the parenchyma prior to injury and at all post-injury time points examined (Fig. 4A,B and data not shown).

When we examined these cells after injury, we often observed that the injury track disrupted GFAP-GFP-positive radial glial fibers (Fig. 4C,D, $n = 13$ animals examined). Notably, however, there was no obvious increase in GFAP-GFP expression at the ventricular surface or in the processes extending into the parenchyma (Fig. 4A,B). The disruption of GFAP-GFP-positive radial glial fibers by cellular debris was still visible at 2 dpi (Fig. 4D, $n = 14$ animals examined). Importantly, cells sur-

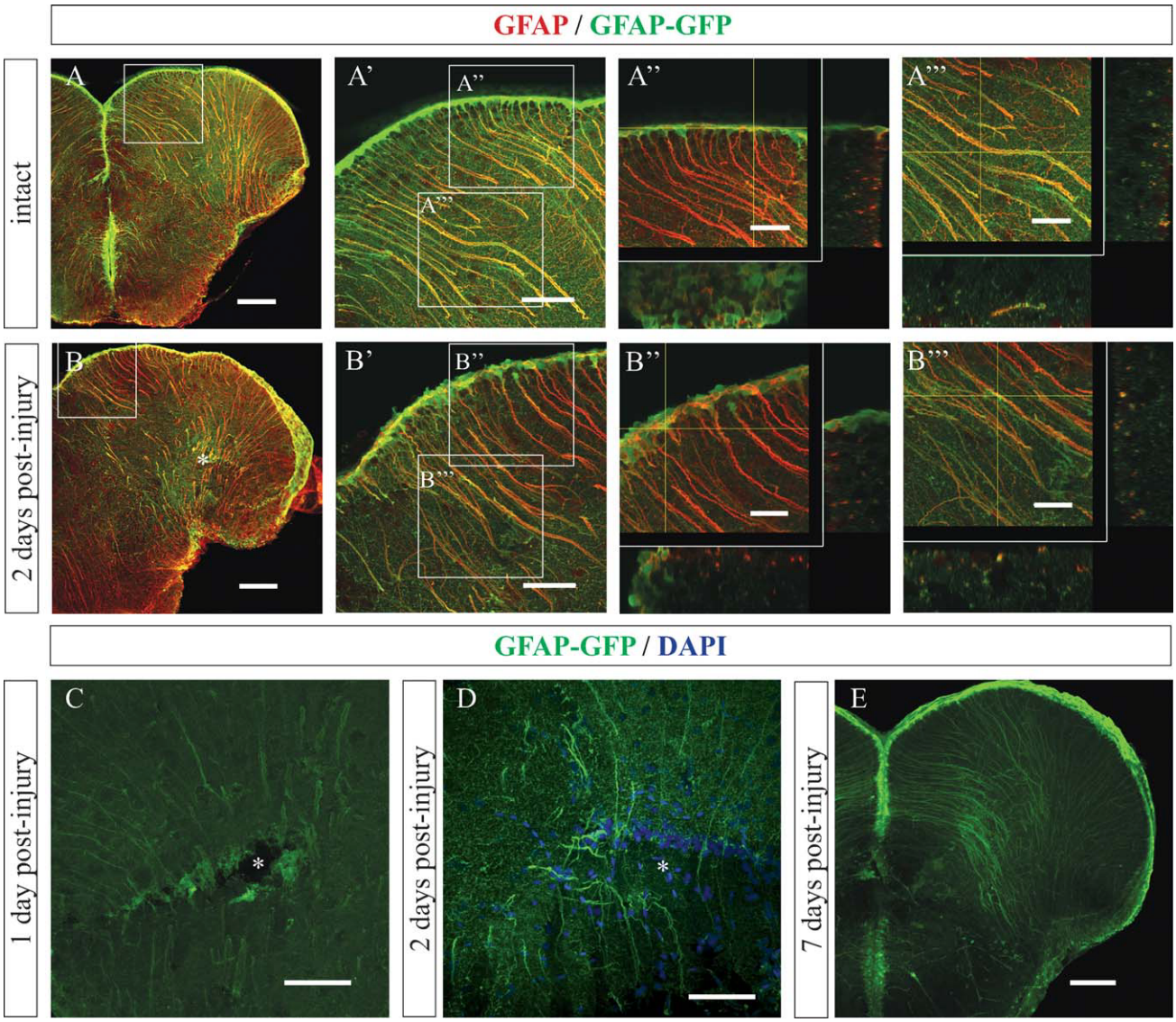

Fig. 4. Astrogliosis in the injured adult zebrafish telencephalon. (**A** and **B**) Micrographs comparing GFP (green) and endogenous GFAP (red) immunoreactivity in the intact control (A) and the injured (B) telencephalon of the adult Tg[gfap:gfp] zebrafish. **A**′ and **B**′ are close-ups of the boxed areas in A and B, respectively. **A**″, **A**‴, **B**″, and **B**‴ are representative orthogonal projections of boxed areas in A′ and B′. Note the extensive overlap of GFP and endogenous GFAP signals in both intact (A–A‴) and injured (B–B‴) telencephalon ($n > 3$ animals per time point examined). (**C–E**) Micrographs representing GFP immunoreactivity (green) in the Tg[gfap:gfp] adult zebrafish brain in response to stab wound injury 1 dpi (C), 2 dpi (D), and 7 dpi (E). Asterisk indicates the injury site in (B–D). Note a failure of glial scar formation as shown through the absence of accumulating GFP-positive glia near the vicinity of the injured areas (C–E). In contrast, GFP-positive radial glia cell bodies remain at the VZ with only processes extending into the parenchyma (E). All micrographs are maximum intensity projections of optical z-stacks, coronal cross-sections, dorsal up. Scale bars = 20 μm in A″, A‴, B″, and B‴; 40 μm in A′, B′, C, D, and 80 μm in A, B, E.

rounding the injury track were never GFP-positive in the Tg(*gfap*:GFP) transgenic fish at any post-injury time point analyzed (Fig. 4C,D and data not shown). Moreover, we did not observe any increase in the density of the GFAP-GFP positive fibers in the proximity of the lesion track or at a more distant location in the injured hemisphere when compared with the noninjured brain (Supp. Info. Fig. 3A,B). The absence of an increase in density of GFAP-GFP fibers at 1 dpi and 2 dpi is reminiscent of results observed after cerebellum injury in the brown ghost, where the density of GFAP-positive radial glial fibers only increased starting at 8 dpi (Clint and Zupanc, 2001). In our model we could not detect any increase in GFAP-GFP signal at 1, 2, or 7 dpi (Fig. 4, $n = 13$ animals examined). Likewise, at none of these time points (1, 2, and 7 dpi) were GFAP-GFP-positive somata detectable that had entered the parenchyma and surrounded the injury site (Fig. 4 and data not shown), suggesting that cells with radial glia/ependymoglial identity do not accumulate and form a scar in this injury model. However, it may be possible that GFAP only detects a subset of ependymoglial cells. Therefore, we also stained for BLBP, Nestin, and S100β, which are all expressed in ependymoglia/radial glia in the intact

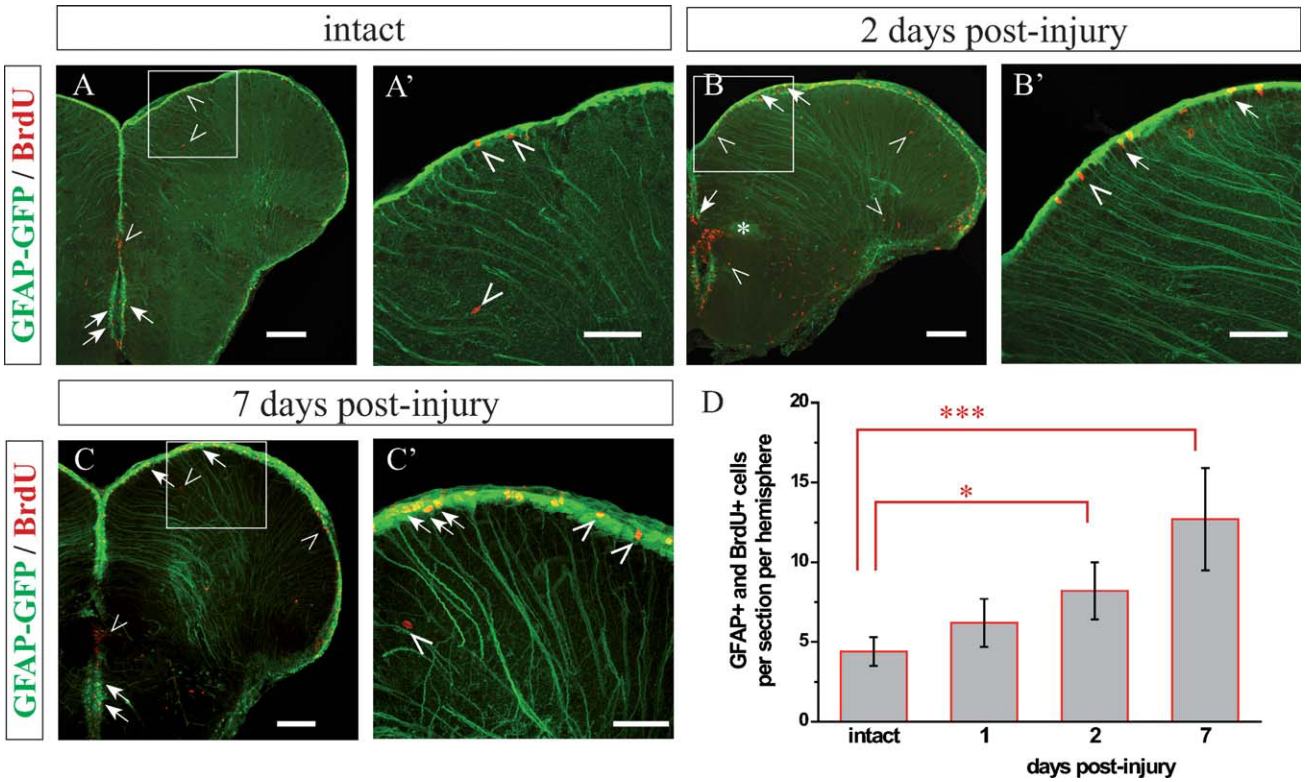

Fig. 5. Proliferation of ependymoglia cells in response to injury. (**A–C**) Micrographs depicting double immunodetection of GFAP-GFP (green) and BrdU (red) in the intact control (A) and injured adult telencephalon 2 dpi (B) and 7 dpi (C). **A′**, **B′**, and **C′** are magnifications of the boxed areas in A, B, and C, respectively. White arrows indicate colabeled cells and white arrowheads mark BrdU single-positive cells. The injury site in (B) is indicated by an asterisk. (**D**) Histogram depicting the proliferative response of ependymoglial cells following injury. Note that GFP-positive ependymoglial cells do not migrate toward injury site, but increase their proliferation as early as 48 dpi ($P < 0.05$, $n > 3$ animals per time point examined, data shown as mean ± SEM). All micrographs are maximum intensity projections of optical z-stacks, coronal cross-sections, dorsal up. Scale bars = 80 μm in A, B, C, and 40 μm in A′, B′, C′.

zebrafish telencephalon and do not label any cell bodies in the intact brain parenchyma (Ganz et al., 2010; März et al., 2010a). Notably, we could not detect expression of these markers near the injury site (Supp. Info. Fig. 3 and data not shown). The absence of OPCs and astroglial accumulation around the injury site could be due to the absence of a recruitment signal from the injured parenchyma. Therefore, we tested if an increased injury size may be sufficient to elicit the migration of glial cells, as the size of injury is a key parameter for the glial cell reaction (Robel et al., 2011). Following larger injuries (see Materials and Methods section) which affected about 1/6 of the total telencephalic parenchyma we could detect some degree of radial glia somata accumulation in the vicinity of the site of injury, reminiscent of the glia scar formation in mammals (Supp. Info. Fig. 4B,C). However, even in this case, the larger injury could heal and the lesion track could be detected in only 70% of analyzed animals at 7 dpi without scar formation (Supp. Info. Fig. 4C, $n \geq 4$ animals examined).

In the mammalian brain, many astroglial cells resume proliferation after injury (for review see Robel et al., 2011). We therefore examined whether the GFAP-GFP-positive ependymoglia/radial glia cells in the VZ would increase their proliferation in reaction to stab wound injury. Indeed, already at 2 dpi (small injury) the number of proliferating GFAP-GFP-positive radial glial cells was clearly increased at the ventricle (Fig. 5, Supp. Info. Fig.1A) and the increased proliferation was even more pronounced at 7 dpi (2.5-fold increase in GFAP-GFP+/BrdU+ at the VZ; Fig. 5C,D, Supp. Info. Fig. 1A). Thus, the proliferative response of ependymoglia/radial glia persists beyond the time of microglia activation in the adult zebrafish telencephalon, reminiscent of the timing of reactive astrocyte proliferation in the mouse telencephalon (Buffo et al., 2008; Simon et al., 2011). However, no GFAP-GFP+/BrdU+ cells could be observed in the brain parenchyma at any time point after small (injury induced with small needle—5 mm in length and 0.1 mm in diameter) stab wound injury (Fig. 5, Supp. Info. Figs. 1 and 3), in profound difference to the astrogliosis around a stab wound injury in the mammalian brain.

Type III Cell Reactivity After Stab Wound Injury in the Adult Zebrafish Telencephalon

Given the normal contribution of the VZ to neurogenesis, we next examined the reaction of other VZ proliferating progenitor subtypes after stab wound injury, such as the Type III cells, an intermediate type of progenitor that no longer expresses radial glia markers but is not yet positive for the markers of mature neurons (see Cha-

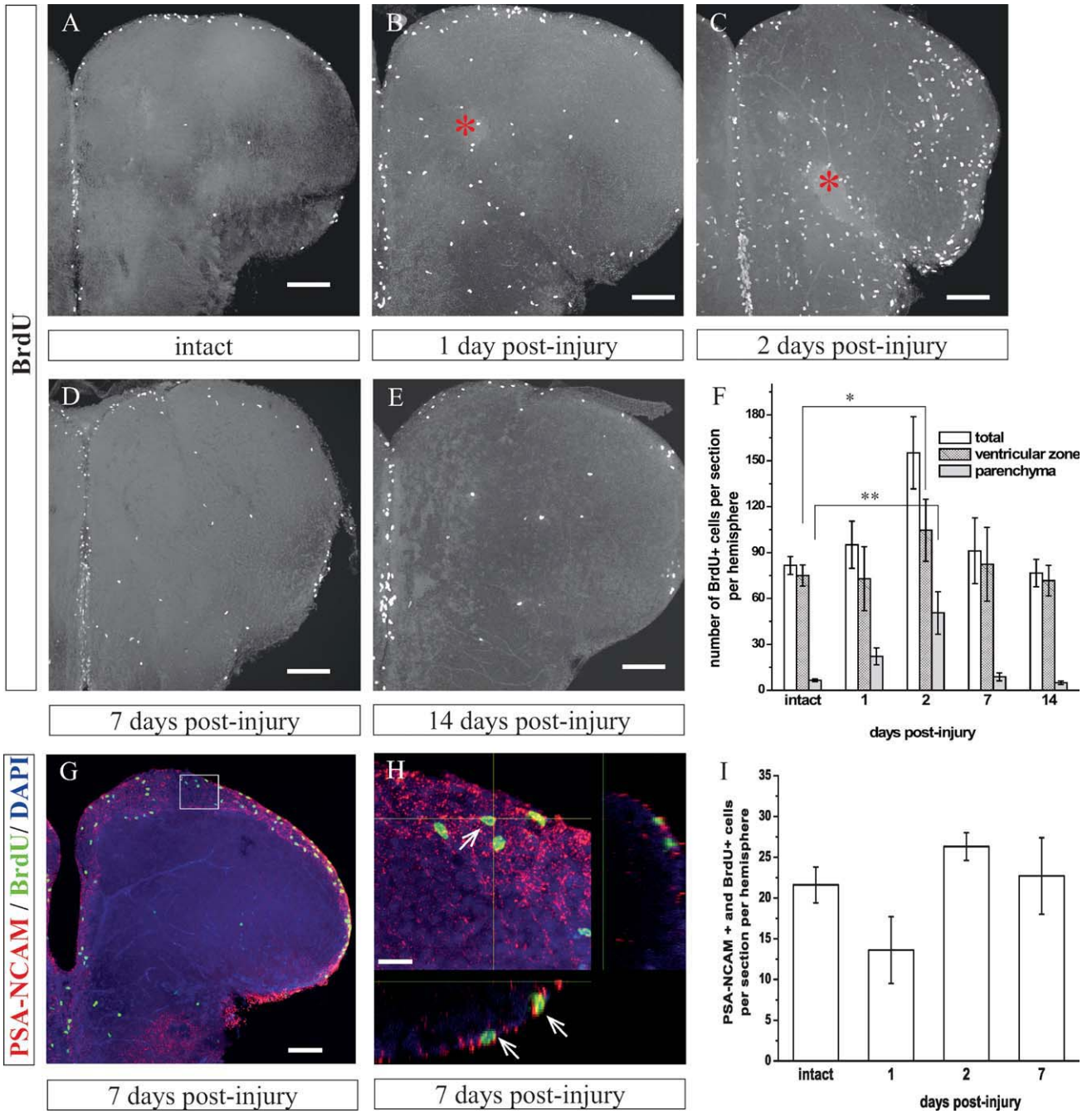

Fig. 6. The lesion-induced proliferative response of the adult zebrafish telencephalon does not involve Type III progenitors. The injury was introduced as depicted in Fig. 1A,B and two consecutive BrdU pulses were administered. (**A**–**E**) Micrographs representing BrdU immunolabeling (white) on brain sections, dorsal up, of a 3-month-old adult zebrafish in the intact brain (A) and following stab wound injury (B–E, sacrificial post-injury time points as labeled). Note the dramatic increase in the number of proliferating cells as early as 2 days after injury (compare A and C). Images are maximum intensity projections of optical z-stacks. The injury site is indicated by an asterisk when visible. Scale bars 80 μm. (**F**) Histogram showing the total number of proliferating progenitors (open bars), number of progenitors proliferating in the VZ (patterned bars), and brain parenchyma (grey bars) following the stab wound injury. Note the peak of proliferation at 2 dpi with a tremendous increase of BrdU-incorporating cells in the brain parenchyma (eightfold increase when compared with the intact control tissue). Interestingly, the number of BrdU-incorporating cells returns to basal levels after 7 dpi (**$P < 0.01$, *$P < 0.05$; $n > 3$ animals examined per time point). (**G**–**I**) Type III progenitors do not increase their proliferation in response to the stab wound injury. (G, H) Micrographs representing immunolabeling for BrdU and PSA-NCAM to identify proliferating Type III cells at 7 dpi. Scale bars 50 μm in (G) and 20 μm in (H). (I) Histogram depicting the proliferation of Type III cells following injury ($n = 3$ animals examined per time point).

pouton et al., 2010; Ganz et al., 2010; März et al., 2010a). When comparing the overall proliferative response along the ventricle and in the parenchyma (Fig. 6), we noted that proliferation increased first in the parenchyma with a 3.4-fold increase already at 1 dpi (Fig. 6A,B,F), while an increase in VZ proliferation was only detectable by 2 dpi (Fig. 6C,F). The peak of the overall proliferative response occurred at this stage

(Fig. 6C–F), which was also the maximal response in the VZ, although the proliferative response was weaker in the VZ (25%, Fig. 6C,F) than in the parenchyma (eightfold, Fig. 6C,F). Finally, the proliferative reaction of the VZ to the stab wound injury had already almost vanished by 7 dpi and was undetectable by 14 dpi (Fig. 6D–F), even though the peak of proliferating GFAP+ radial glia in the VZ was reached at 7 dpi (Fig. 5C,D). Importantly, a proliferative response with the same kinetics was observed following unilateral lesion where the contralateral, uninjured side was used as a control (Supp. Info. Fig. 5).

We showed previously that the peak of proliferation for ependymoglial cells at the VZ takes place at late post-lesion stages, suggesting that neural progenitors may account for the majority of proliferating VZ cells in the injured telencephalon during the early reaction phase (around 2 dpi). To assess the identity of these progenitors, we co-stained sections for BrdU and PSA-NCAM, which marks neuroblasts (März et al., 2010a). Indeed, this cell type is the most abundant proliferative cell type in the VZ (Supp. Info. Fig. 1C). However, we did not see any further proliferative response of VZ Type III cells to the stab wound injury at any analyzed time point (Fig. 6G–I and Supp. Info. Fig. 1C, $n = 3$ animals per time point examined). As these cells may also migrate into the brain parenchyma and contribute to neurogenesis, we next examined their contribution to the proliferative pool in the brain parenchyma. There again we could not see any increase in the number of PSA-NCAM+ and BrdU+ cells at any time point examined. In addition, Fli-eGFP-positive endothelial cells (Supp. Info. Fig. 6), Olig2-GFP+ and 4C4+ cells account only for about 50% of all cells proliferating in the injured telencephalic parenchyma at 2 dpi (Supp. Info. Fig. 1C). Together, these findings suggest the presence of an additional set of progenitors in the injured telencephalic ventricular zone and parenchyma at this stage. These might correspond to a progenitor stage that down-regulated radial glia markers, but still did not start expressing neuronal commitment markers such as PSA-NCAM.

Increased Neurogenesis Results in Long-Term Surviving Neurons in the Parenchyma After Stab Wound Injury

We next examined to which extent those progenitors reactivated upon lesion contribute to long-lasting neuro-

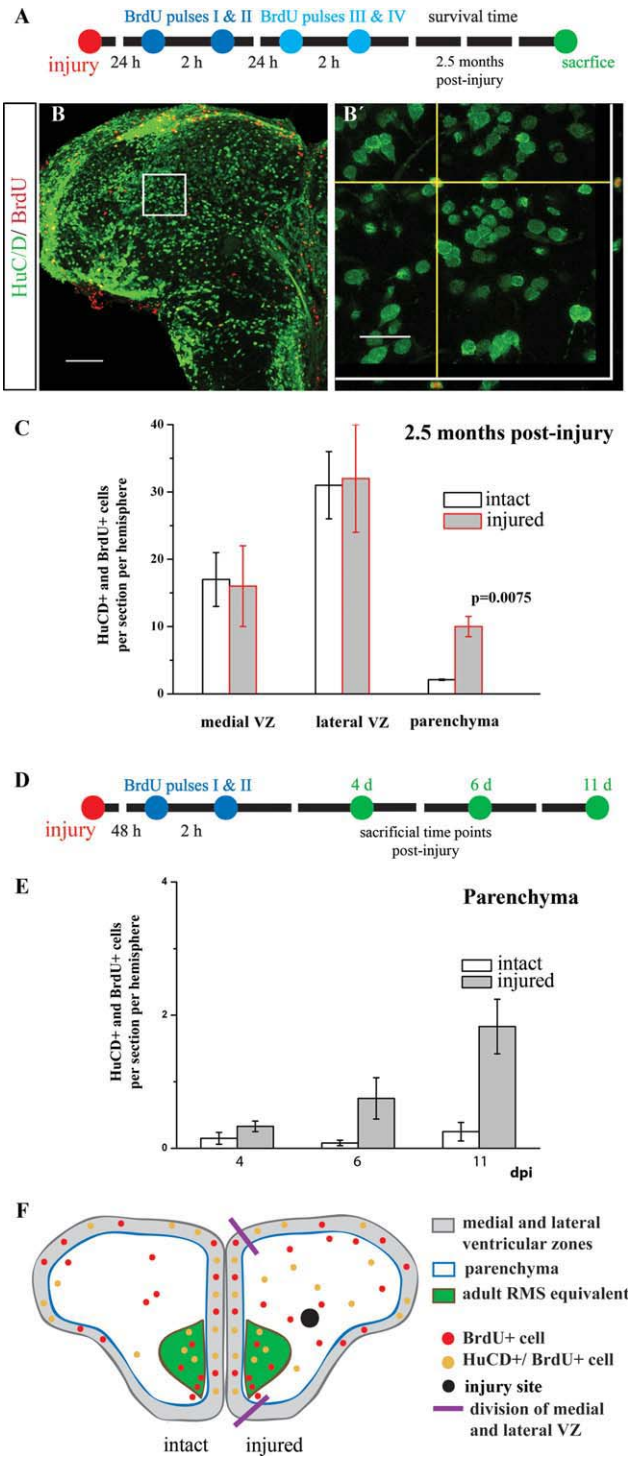

Fig. 7. Stab wound injury induces *de novo* neurogenesis in the brain parenchyma outside of neurogenic zones. (**A**) Scheme of the experimental design to assess neurogenesis in the adult telencephalon following brain injury. (**B**) Micrograph depicting BrdU-positive (red) and HuC/D-positive (green) neuron in the parenchyma of the adult zebrafish telencephalon 2.5 months post-injury. (**B′**) An orthogonal projection of the area boxed in (B), confirming colocalization of HuC/D and BrdU immunoreactivity. (**C**) Histogram depicting the number of dual HuC/D-positive and BrdU-positive cells 2.5 months after injury and BrdU labeling in the neurogenic areas (medial and lateral VZ) and parenchyma in the intact (open bars) and injured zebrafish telencephalon (grey bars). Note a significant increase ($P = 0.0075$; $n \geq 3$ animals) in the number of double-positive cells in the brain parenchyma following injury, while there is no difference in the neurogenic areas. Data are represented as mean ± SEM and $n \geq 3$ animals examined per time point. (**D**) Scheme depicting the experimental design to distinguish DNA repair from *de novo* neurogenesis. (**E**) Histogram showing the number of BrdU and HuCD-positive cells in the telencephalic parenchyma in the intact (open bars) and injured telencephalon (grey bars). Data are shown as mean ± SEM, $n \geq 3$ animals per time point. Note the gradual increase of dual positive cells scattered throughout the injured parenchyma from 6 dpi onwards. (**F**) Scheme depicting neurogenesis in the intact (left hemisphere) and injured (right hemisphere) adult zebrafish telencephalon 2.5 months after BrdU administration. Micrographs are maximum intensity projections of optical z-stacks, coronal cross-sections, dorsal up. Scale bars = 80 μm in B and 20 μm in B′.

genesis. We therefore performed BrdU injections twice at 1 and 2 dpi and examined the number of BrdU-labeled cells that had differentiated into neurons (as indicated by HuC/D-immunostaining) and survived 2.5 months later (Fig. 7A–C). When these cells were quantified close to the ventricular zone (either medially or laterally) where neurons normally settle, their numbers were not changed after brain injury (Fig. 7C), suggesting that the normally occurring neurogenesis in the adult zebrafish telencephalon is not much altered in our stab wound injury model. In contrast to the VZ, however, we noted a profound and statistically significant fivefold increase of BrdU and HuC/D-positive cells in the telencephalic parenchyma 2.5 months after stab wound injury when compared to the intact controls (Fig. 7C). While these results suggest increased neurogenesis in the stab wound injured parenchyma, cells undergoing DNA-repair also incorporate BrdU (Cooper-Kuhn and Kuhn, 2002) and damaged neurons often initiate the S phase of the cell cycle but do not further complete the cell cycle (Copani et al., 2007; Hoozemans et al., 2002; Wang et al., 2006). To examine whether the BrdU-labeling of HuC/D+ neurons is due to proliferation or DNA repair, we gave BrdU pulses to the injured animals at the peak of proliferation, and then sacrificed them at 4, 6, and 11 dpi (Fig. 7D). We reasoned that, in the case of DNA repair, we would detect comparable numbers of BrdU-positive neurons residing in the brain parenchyma shortly after the labeling and after 2.5 months. In stark contrast, we observed a gradual increase in the number of newly generated neurons as marked by the coexpression of HuCD and BrdU within the parenchyma (Fig. 7E; $n \geq 3$ animals examined per time point), throughout the observation period. Importantly, the number of BrdU-labeled neurons at 11 dpi was still fivefold lower than after 2.5 months, clearly demonstrating that BrdU-labeled neurons observed at 2.5 months after injury are not due to DNA repair, but that most of them appeared at later stages post-injury as a result of *de novo* neurogenesis.

Taken together, our data suggest that the zebrafish telencephalon has the capacity to *de novo* generate additional neurons in response to injury in the brain parenchyma where newly generated neurons normally do not settle in the intact, noninjured brain.

DISCUSSION

Here we established a stab wound injury model of the adult zebrafish telencephalon with a limited and reproducible injury size, avoiding injury of the ependymoglia and allowing complete healing without scar formation within about 1 week. In addition, increased neurogenesis contributed neurons to the brain parenchyma, which survived for several months, revealing a beneficial environment for wound healing and neural repair in this model. Interestingly, we discovered major differences in cellular reactivity in this model compared with other injury models in zebrafish or in the mammalian telencephalon. While microglia reactivity is comparable to other models, the major differences consist of the lack in Olig2+ cell proliferation and astrogliosis around the injury site (Table 1). These exciting data may therefore be a suitable model for dissecting beneficial and detrimental aspects of the glia response after injury (see also Robel et al., 2011).

TABLE 1. Comparison of the Cellular Responses to Injury in the Mouse and Zebrafish Telencephalon

	Mammals	Zebrafish
Wound healing	+, Scar	+, No scar (only sparse cells following large injuries)
Proliferative response	+	+
In parenchyma	+	+
At ventricle	− (except in SEZ)	+
Microglia reaction	+	+
Endothelial proliferation	+	+
OPC reaction	+	−
Astrogliosis	+	− (Only sparse cells following large injuries)
GFAP upregulation	+	−
Proliferation	+	−
Type III cell reaction	− (only in neurogenic sites)	−
Neurogenesis	− (only in neurogenic sites)	+
Long-term survival of regenerating neurons	− (only in special injury paradigms)	+

Gliosis in the Adult Zebrafish Telencephalon Following Stab Wound Injury

As in the mammalian brain (Hanisch and Kettenmann, 2007; Simon et al., 2011), the first cell type to react to the stab wound injury in the adult zebrafish telencephalon is microglia (Peri and Nüsslein-Volhard, 2008; Reimer et al., 2009). Microglial cells become hypertrophic as fast as 24 h following injury, increasing proliferation and accumulating around the injury site within 2 dpi. The microglial reaction not only starts fast, but is also transient and disappears in the injured parenchyma within 1 week. Interestingly, the peak of microglia activation at 2 dpi also correlates with the closure of the injury track, consistent with a role of microglia in the clearance of damaged cells and cellular debris (Hanisch and Kettenmann, 2007). Indeed, the activation and accumulation of microglia with beneficial effects on neurogenesis after stroke has recently been described (Thored et al., 2009). After the injury track and necrotic tissue are no longer detectable, microglial hypertrophy and proliferation returns to basal levels with only a few 4C4+ cells in the telencephalon parenchyma by 7 dpi.

In the mouse telencephalon adult oligodendrocyte progenitors (OPCs) react almost simultaneously with microglia (Buffo et al., 2005; Simon et al., 2011). As Olig2+ cells also constitute the major (though small) population of parenchymal progenitors in the intact zebrafish adult telencephalon (März et al., 2010b) this may indicate also a continuous generation of new oligodendrocytes e.g. to myelinate the constantly newly generated neurons (März et al., 2010b). In zebrafish as in mice, there are profound region-specific differences with pronounced

oligodendrogliogenesis in the adult telencephalon, but not in the spinal cord (Dimou et al., 2008; Kang et al., 2010; Reimer et al., 2008, 2009; Rivers et al., 2008). Interestingly, after spinal cord transection there is little proliferation in the WM (Hui et al., 2010) and it is rather radial glia lining the ventricle that prominently increase their proliferation, up-regulate Olig2 and Sox11b, and regenerate motoneurons (Guo et al., 2011; Reimer et al., 2008, 2009) as well as other types of interneurons (Hui et al., 2010). The lack of reaction of Olig2-expressing parenchymal cells to injury in the spinal cord, however, is well consistent with the lack of increased proliferation and/or migration to the injury site in the telencephalon as observed in our study. This is of particular interest, as this population carries the NG2 proteoglycan in the mammalian CNS, one of the chondroitin sulfate proteoglycans contributing to inhibition of axonal outgrowth (see e.g. Alilain et al., 2011). Thus, the enormous proliferation of this population and their accumulation around the injury site in the mouse CNS (Dimou et al., 2008; Lytle et al., 2009; Simon et al., 2011) may not only inhibit neurite outgrowth but also be an important contributor to scar formation.

The last glial cell type to react to injury in the mouse telencephalon is the astrocyte (for recent reviews see Buffo et al., 2010; Robel et al., 2011; Sofroniew, 2009). Activated astrocytes become hypertrophic within a few days and also up-regulate the intermediate filaments GFAP, Nestin, and Vimentin as well as chondroitin sulfate proteoglycans, Tenascin C and other ECM (extracellular matrix) components (Buffo et al., 2010; Robel et al., 2011; Sofroniew, 2009). In our injury paradigm in the zebrafish telencephalon, we could not detect up-regulation of GFAP by immunocytochemistry, in contrast to the massive increase in GFAP-immunoreactivity after stab wound injury in the mouse telencephalon (Buffo et al., 2005; Simon et al., 2011). However, larger injuries induced not only GFAP up-regulation in the zebrafish telencephalon (Supp. Info. Fig. 4), but also the accumulation of ependymoglia and their processes in the vicinity of the injury site, suggesting that the reaction of ependymoglia in zebrafish telencephalon depends on the size of injury, as it is the case in the mammalian CNS (Sofroniew, 2009). However, despite the low changes in GFAP or S100β expression following a small injury, proliferation of GFAP+ cells at the ventricle was increased in reaction to injury, being most pronounced at 7 dpi when other cells had already ceased their reaction. Interestingly, reactive astroglia in the mouse telencephalon show the same delayed increase in proliferation reaching a peak at 7 days after stab wound injury (Simon et al., 2011). Notably, however, zebrafish radial glia-like ependymal cells are already proliferating before injury, which is in contrast to astrocytes in the intact mouse telencephalon (Buffo et al., 2008). Moreover, radial glia-like cells did not assemble around the injury site after the small injury in profound contrast to the strong astrogliosis surrounding a stab wound injury in the rodent telencephalon (see e.g. Buffo et al., 2008). We also observed that even larger injury triggered only sparse ependymoglial cells to surround the injury site. These data suggest the existence of dual signals for the ependymoglial reaction. While the small lesion would be sufficient to provide the proliferation cues for the ependymoglia, the larger injury is necessary to generate the additional signals eliciting their migration and accumulation in the parenchyma. Importantly, the larger injury might also allow the entry of cerebrospinal fluid into the brain parenchyma, causing the altered glia response including the migration of ependymoglia toward the injury site.

Astrogliosis was suggested to play an important role for re-establishing the blood–brain barrier and limiting the entry, spread, and persistence of inflammatory cells in the injured brain parenchyma (Sofroniew, 2009). These functions in zebrafish must be performed by other cells surrounding the injury site, e.g. the microglia or the population of proliferating cells lacking glial markers. Such a reaction may also help to provide the metabolic support performed by astrocytes in the mammalian brain (Brown and Ransom, 2007). Furthermore, it is important to consider the profound difference in glial reactivity in the teleost white and grey matter regions. Astrogliosis appears to occur in white matter regions as observed in the cerebellum (Clint and Zupanc, 2001) and optic nerve (Koke et al., 2010). This difference may be due to the presence of specific sets of astrocytes in the white matter, such as the reticular astrocytes positive for cytokeratins in the optic nerve (Koke et al., 2010).

Gliosis and Repair

Besides microglial cells transiently surrounding the injury site in the stab wound-injured zebrafish telencephalon, none of the other glial cell types present in the adult zebrafish grey matter accumulate around the injury site. Instead, we observed a pronounced proliferation of non-glia progenitors or dedifferentiated cells negative for glial markers. Interestingly, in the crush-injured spinal cord GFAP is first down-regulated, indicative of a dedifferentiation reaction, and the largest population of proliferating cells are such dedifferentiated progenitors (see Fig. 5 in Hui et al., 2010). In our study, we observed a considerable proportion of proliferating cells in the VZ as well as in the parenchyma to be negative for glial markers or PSA-NCAM. Interestingly, also in the mouse telencephalon such marker-negative cells have been observed following injury (Buffo et al., 2005). At the VZ, radial glial cells may have proceeded in increased number or faster to the neuronal fate committed progenitors (Rothenaigner et al., 2011) that did not yet reach the Type III stage and are therefore negative for PSA-NCAM. Alternatively, increased proliferation of this progenitor type may be a direct response to the injury. In the parenchyma, the number of marker-negative cells started increasing at 1 dpi, with a peak of proliferation at 2 dpi, also implying these cells as a possible source of the newly generated neurons. Indeed, given that long-term surviving neurons detected 2.5 months

after the injury are generated at 2 dpi, i.e. before the peak of radial glia proliferation, it is likely that they originate from these marker-negative progenitors.

While further studies have to examine the exact contribution of these different progenitors to the additional neurogenesis observed here, the important findings of our work in regard to neurogenesis are that (a) it is increased upon stab wound injury beyond the normal rate of neurogenesis and (b) these additionally generated neurons survive for a long time. Notably, neurogenic sites in the rodent telencephalon also react to a neighboring injury with increased proliferation, neurogenesis (Arvidsson et al., 2002; Kim and Szele, 2008; Rice et al., 2003), and an initial differentiation into the adequate type of neurons which were affected at the site of injury (Arvidsson et al., 2002; Brill et al., 2009; Collin et al., 2005; Kim and Szele, 2008; Magavi et al., 2000; Sundholm-Peters et al., 2005). However, these neurons fail to survive and are eventually eliminated from the brain (Battista and Rutishauser, 2010; Thored et al., 2006, 2007, 2009). In contrast, our data show that in the zebrafish telencephalon newly generated neurons survive for long periods of time, highlighting the profound difference between the environments that new neurons encounter after injury in the adult zebrafish and mouse telencephalon. Therefore, this injury model provides an exciting new system to dissect the signals allowing not only a complete wound repair in the absence of scar formation in the brain, but also the recruitment and long-term survival of newly generated neurons.

It is obviously tempting to speculate that the lack of accumulation of glial cells (astrocytes and Olig2+ glia) around the injury site may contribute to creating a beneficial environment in the adult zebrafish brain, while they may have adverse effects on neuroblast survival in the adult mouse telencephalon. This concept is supported by the observation that mouse models with attenuated gliosis exhibit improved survival of neural cell transplants (Pekny and Nilsson, 2005; Pekny and Pekna, 2004; Widestrand et al., 2007) and that long-term survival of newly generated neurons has been observed only in lesion models with neurons dying by apoptosis virtually avoiding reactive gliosis (Magavi et al., 2000). Thus, minimizing the number of astroglia and Olig2+ glia around the injury site or altering the signals mediated by these cells (as in the GFAP/Vimentin double knock-out mice (Pekny and Nilsson, 2005; Pekny and Pekna, 2004; Widestrand et al., 2007)) may help to promote the survival of new neurons from exogenous and endogenous sources.

Moreover, our findings also imply that the reaction of microglial cells, Olig2+ and GFAP+ glial cells can be separated, at least in the zebrafish telencephalon. Microglia in the zebrafish telencephalon, despite being activated, may fail to release recruitment signals for Olig2+ and ependymoglia, or the latter populations may lack the relevant receptors in zebrafish while having these receptors in the mammalian brain. Alternatively, damaged neurons may release signals recruiting astroglia and Olig2+ glia in the mouse telencephalon but not in zebrafish, such as e.g. IL-6 or BMP—potent factors eliciting reactive astrogliosis (Fuller et al., 2007; Xiao et al., 2010). Thus, after having characterized the key cellular reactions taking place upon stab wound injury in the present work, it will now be important to elucidate the differences in the molecular signature of the cells reacting to injury in the zebrafish brain, involving mostly the microglia, and how their expression profile may differ from the activated microglia in the mammalian system. This will further our understanding of how reactive gliosis differs in animal models with profound regenerating capacity of complex structures, such as teleost or amphibians (Becker and Becker, 2007, 2008; Bernhardt et al., 1996; Brignull et al., 2009; Brockes and Kumar, 2002; Campbell and Crews, 2008; DeLaurier et al., 2010; Endo et al., 2007; Hui et al., 2010; Kimmel et al., 2010; Reimer et al., 2008, 2009; Stenkamp and Kwang, 2007; Tal et al., 2009), creating a beneficial environment in these animal models as opposed to an adverse environment created in the mammalian brain. It is now clear that neurogenesis is well possible in the adult mammalian CNS, also after injury (Buffo et al., 2005, 2008; Nakatomi et al., 2002; Ohori et al., 2006). Hence, the key to eliciting long-lasting repair now lies in understanding the environment created after injury, such that one may create a beneficial environment for these young neurons, allowing them to survive and integrate. The direct comparison of stab wound injury in the adult mouse and zebrafish telencephalon provides an excellent comparison to dissect harmful and beneficial reactions after injury.

Note added in Proof: Note the difference in glial cell reactivity when stab wound injury is performed through the skull (as recently published in März et al., 2011; Kishimoto et al., 2012) versus injury via the nostrils (this paper, and the recently published work by Kraehlin et al., 2011, where injury affects almost half of the telencephalic hemisphere). Injuries through the skull damage the VZ and allow CSF entry into the brain parenchyma, which may account for the observed differences.

ACKNOWLEDGMENTS

The authors thank Alexandra Lepier for help in 4C4 antibody production and David Traver for Fli1 transgenic fish.

REFERENCES

Adolf B, Chapouton P, Lam CS, Topp S, Tannhauser B, Strahle U, Gotz M, Bally-Cuif L. 2006. Conserved and acquired features of adult neurogenesis in the zebrafish telencephalon. Dev Biol 295:278–293.

Alilain WJ, Horn KP, Hu H, Dick TE, Silver J. 2011. Functional regeneration of respiratory pathways after spinal cord injury. Nature 475:196–200.

Ari C, Kálmán M. 2008. Glial architecture of the ghost shark (*Callorhinchus milii, Holocephali, Chondrichthyes*) as revealed by different immunohistochemical markers. J Exp Zool B Mol Dev Evol 310:504–519.

Arvidsson A, Collin T, Kirik D, Kokaia Z, Lindvall O. 2002. Neuronal replacement from endogenous precursors in the adult brain after stroke. Nat Med 8:963–970.

Ayari B, Elhachimi KH, Yanicostas C, Landoulsi A, Soussi-Yanicostas N. 2010. Prokineticin 2 expression is associated with neural repair of injured adult zebrafish telencephalon. J Neurotrauma 27:959–972.

Battista D, Rutishauser U. 2010. Removal of polysialic acid triggers dispersion of subventricularly derived neuroblasts into surrounding CNS tissues. J Neurosci 30:3995–4003.

Becker CG, Becker T. 2007. Growth and pathfinding of regenerating axons in the optic projection of adult fish. J Neurosci Res 85:2793–2799.

Becker CG, Becker T. 2008. Adult zebrafish as a model for successful central nervous system regeneration. Restor Neurol Neurosci 26:71–80.

Becker T, Becker CG. 2001. Regenerating descending axons preferentially reroute to the gray matter in the presence of a general macrophage/microglial reaction caudal to a spinal transection in adult zebrafish. J Comp Neurol 433:131–147.

Bernardos R, Raymond P. 2006. GFAP transgenic zebrafish. Gene Expr Patterns 6:1007–1013.

Bernhardt R, Tongiorgi E, Anzini P, Schachner M. 1996. Increased expression of specific recognition molecules by retinal ganglion cells and by optic pathway glia accompanies the successful regeneration of retinal axons in adult zebrafish. J Comp Neurol 376:253–264.

Bernstein JJ. 1967. The regenerative capacity of the telencephalon of the goldfish and rat. Exp Neurol 17:44–56.

Brignull HR, Raible DW, Stone JS. 2009. Feathers and fins: Non-mammalian models for hair cell regeneration. Brain Res 1277:12–23.

Brill MS, Ninkovic J, Winpenny E, Hodge RD, Ozen I, Yang R, Lepier A, Gascon S, Erdelyi F, Szabo G, Parras C, Guillemot F, Frotscher M, Berninger B, Hevner RF, Raineteau O, Gotz M. 2009. Adult generation of glutamatergic olfactory bulb interneurons. Nat Neurosci 12:1524–1533.

Brockes JP, Kumar A. 2002. Plasticity and reprogramming of differentiated cells in amphibian regeneration. Nat Rev Mol Cell Biol 3:566–574.

Brown AM, Ransom BR. 2007. Astrocyte glycogen and brain energy metabolism. Glia 55:1263–1271.

Buffo A, Rite I, Tripathi P, Lepier A, Colak D, Horn AP, Mori T, Gotz M. 2008. Origin and progeny of reactive gliosis: A source of multipotent cells in the injured brain. Proc Natl Acad Sci USA 105:3581–3586.

Buffo A, Rolando C, Ceruti S. 2010. Astrocytes in the damaged brain: Molecular and cellular insights into their reactive response and healing potential. Biochem Pharmacol 79:77–89.

Buffo A, Vosko MR, Erturk D, Hamann GF, Jucker M, Rowitch D, Gotz M. 2005. Expression pattern of the transcription factor Olig2 in response to brain injuries: Implications for neuronal repair. Proc Natl Acad Sci USA 102:18183–18188.

Campbell L, Crews C. 2008. Molecular and cellular basis of regeneration and tissue repair. Cell Mol Life Sci 65:73–79.

Chapouton P, Adolf B, Leucht C, Tannhauser B, Ryu S, Driever W, Bally-Cuif L. 2006. her5 expression reveals a pool of neural stem cells in the adult zebrafish midbrain. Development 133:4293–4303.

Chapouton P, Skupien P, Hesl B, Coolen M, Moore JC, Madelaine R, Kremmer E, Faus-Kessler T, Blader P, Lawson ND, Bally-Cuif L. 2010. Notch activity levels control the balance between quiescence and recruitment of adult neural stem cells. J Neurosci 30:7961–7974.

Chen J, Magavi SSP, Macklis JD. 2004. Neurogenesis of corticospinal motor neurons extending spinal projections in adult mice. Proc Natl Acad Sci USA 101:16357–16362.

Clint SC, Zupanc GK. 2001. Neuronal regeneration in the cerebellum of adult teleost fish, *Apteronotus leptorhynchus*: Guidance of migrating young cells by radial glia. Brain Res Dev Brain Res 130:15–23.

Collin T, Arvidsson A, Kokaia Z, Lindvall O. 2005. Quantitative analysis of the generation of different striatal neuronal subtypes in the adult brain following excitotoxic injury. Exp Neurol 195:71–80.

Cooper-Kuhn CM, Kuhn HG. 2002. Is it all DNA repair? Methodological considerations for detecting neurogenesis in the adult brain. Brain Res Dev Brain Res 134:13–21.

Copani A, Caraci F, Hoozemans JJM, Calafiore M, Angela Sortino M, Nicoletti F. 2007. The nature of the cell cycle in neurons: Focus on a "non-canonical" pathway of DNA replication causally related to death. Biochim Biophys Acta 1772:409–412.

DeLaurier A, Eames BF, Blanco-Sanchez B, Peng G, He X, Swartz ME, Ullmann B, Westerfield M, Kimmel CB. 2010. Zebrafish sp7:EGFP: A transgenic for studying otic vesicle formation, skeletogenesis, and bone regeneration. Genesis 48:505–511.

Dimou L, Simon C, Kirchhoff F, Takebayashi H, Gotz M. 2008. Progeny of Olig2-expressing progenitors in the gray and white matter of the adult mouse cerebral cortex. J Neurosci 28:10434–10442.

Endo T, Yoshino J, Kado K, Tochinai S. 2007. Brain regeneration in anuran amphibians. Dev, Growth Diff 49:121–129.

Fawcett JW, Asher RA. 1999. The glial scar and central nervous system repair. Brain Res Bull 49:377–391.

Fuller ML, DeChant AK, Rothstein B, Caprariello A, Wang R, Hall AK, Miller RH. 2007. Bone morphogenetic proteins promote gliosis in demyelinating spinal cord lesions. Ann Neurol 62:288–300.

Ganz J, Kaslin J, Hochmann S, Freudenreich D, Brand M. 2010. Heterogeneity and Fgf dependence of adult neural progenitors in the zebrafish telencephalon. Glia 58:1345–1363.

Grandel H, Kaslin J, Ganz J, Wenzel I, Brand M. 2006. Neural stem cells and neurogenesis in the adult zebrafish brain: Origin, proliferation dynamics, migration and cell fate. Dev Biol 295:263–277.

Grupp L, Wolburg H, Mack AF. 2010. Astroglial structures in the zebrafish brain. J Comp Neurol 518:4277–4287.

Guo Y, Ma L, Cristofanilli M, Hart RP, Hao A, Schachner M. 2011. Transcription factor Sox11b is involved in spinal cord regeneration in adult zebrafish . Neuroscience 172:329–341.

Hampton DW, Rhodes KE, Zhao C, Franklin RJM, Fawcett JW. 2004. The responses of oligodendrocyte precursor cells, astrocytes and microglia to a cortical stab injury, in the brain. Neuroscience 127:813–820.

Hanisch U-K, Kettenmann H. 2007. Microglia: active sensor and versatile effector cells in the normal and pathologic brain. Nat Neurosci 10:1387–1394.

Hoozemans JJM, Brückner MK, Rozemuller AJM, Veerhuis R, Eikelenboom P, Arendt T. 2002. Cyclin D1 and cyclin E are co-localized with cyclo-oxygenase 2 (COX-2) in pyramidal neurons in Alzheimer disease temporal cortex. J Neuropathol Exp Neurol 61: 678–688.

Hui SP, Dutta A, Ghosh S. 2010. Cellular response after crush injury in adult zebrafish spinal cord. Dev Dyn 239:2962–2979.

Kálmán M. 2002. GFAP expression withdraws—A trend of glial evolution? Brain Res Bull 57:509–511.

Kang SH, Fukaya M, Yang JK, Rothstein JD, Bergles DE. 2010. NG2+ cns glial progenitors remain committed to the oligodendrocyte lineage in postnatal life and following neurodegeneration. Neuron 68:668–681.

Kaslin J, Ganz J, Brand M. 2008. Proliferation, neurogenesis and regeneration in the non-mammalian vertebrate brain. Philos Trans R Soc Lond B Biol Sci 363:101–122.

Kaslin J, Ganz J, Geffarth M, Grandel H, Hans S, Brand M. 2009. Stem cells in the adult zebrafish cerebellum: Initiation and maintenance of a novel stem cell niche. J Neurosci 29:6142–6153.

Kassen SC, Ramanan V, Montgomery JE, T. Burket C, Liu C-G, Vihtelic TS, Hyde DR. 2007. Time course analysis of gene expression during light-induced photoreceptor cell death and regeneration in albino zebrafish. Dev Neurobiol 67:1009–1031.

Kim H, Shin J, Kim S, Poling J, Park H-C, Appel B. 2008. Notch-regulated oligodendrocyte specification from radial glia in the spinal cord of zebrafish embryos. Dev Dyn 237:2081–2089.

Kim Y, Szele F. 2008. Activation of subventricular zone stem cells after neuronal injury. Cell Tissue Res 331:337–345.

Kimmel CB, DeLaurier A, Ullmann B, Dowd J, McFadden M. 2010. Modes of developmental outgrowth and shaping of a craniofacial bone in zebrafish. PLoS One 5:e9475.

Koke J, Mosier A, Garcia D. 2010. Intermediate filaments of zebrafish retinal and optic nerve astrocytes and Muller glia: Differential distribution of cytokeratin and GFAP. BMC Res Notes 3:50.

Komitova M, Serwanski DR, Richard Lu Q, Nishiyama A. 2011. NG2 cells are not a major source of reactive astrocytes after neocortical stab wound injury. Glia 59:800–809.

Lawson ND, Weinstein BM. 2002. In vivo imaging of embryonic vascular development using transgenic zebrafish. Dev Biol 248:307–318.

Levine JM, Reynolds R, Fawcett JW. 2001. The oligodendrocyte precursor cell in health and disease. Trends Neurosci 24:39–47.

Lytle JM, Chittajallu R, Wrathall JR, Gallo V. 2009. NG2 cell response in the CNP-EGFP mouse after contusive spinal cord injury. Glia 57:270–285.

Magavi SS, Leavitt BR, Macklis JD. 2000. Induction of neurogenesis in the neocortex of adult mice. Nature 405:951–955.

Maggs A, Scholes J. 1990. Reticular astrocytes in the fish optic nerve: macroglia with epithelial characteristics form an axially repeated lacework pattern, to which nodes of Ranvier are apposed. J Neurosci 10:1600–1614.

März M, Chapouton P, Diotel N, Vaillant C, Hesl B, Takamiya M, Lam CS, Kah O, Bally-Cuif L, Strähle U. 2010a. Heterogeneity in progenitor cell subtypes in the ventricular zone of the zebrafish adult telencephalon. Glia 58:870–888.

März M, Schmidt R, Rastegar S, Strähle U. 2010b. Expression of the transcription factor Olig2 in proliferating cells in the adult zebrafish telencephalon. Dev Dyn 239:3336–3349.

McFarland KA, Topczewska JM, Weidinger G, Dorsky RI, Appel B. 2008. Hh and Wnt signaling regulate formation of olig2+ neurons in the zebrafish cerebellum. Dev Biol 318:162–171.

Nakatomi H, Kuriu T, Okabe S, Yamamoto S-i, Hatano O, Kawahara N, Tamura A, Kirino T, Nakafuku M. 2002. Regeneration of hippocampal pyramidal neurons after ischemic brain injury by recruitment of endogenous neural progenitors. Cell 110:429–441.

Ohori Y, Yamamoto S, Nagao M, Sugimori M, Yamamoto N, Nakamura K, Nakafuku M. 2006. Growth factor treatment and genetic manipulation stimulate neurogenesis and oligodendrogenesis by endogenous neural progenitors in the injured adult spinal cord. J Neurosci 26:11948–11960.

Park HC, Shin J, Roberts RK, Appel B. 2007. An olig2 reporter gene marks oligodendrocyte precursors in the postembryonic spinal cord of zebrafish. Dev Dyn 236:3402–3407.

Pekny M, Nilsson M. 2005. Astrocyte activation and reactive gliosis. Glia 50:427–434.

Pekny M, Pekna M. 2004. Astrocyte intermediate filaments in CNS pathologies and regeneration. J Pathol 204:428–437.

Peri F, Nüsslein-Volhard C. 2008. Live imaging of neuronal degradation by microglia reveals a role for v0-ATPase a1 in phagosomal fusion in vivo. Cell 133:916–927.

Poss KD, Keating MT, Nechiporuk A. 2003. Tales of regeneration in zebrafish. Dev Dyn226202–22610.

Raya A, Consiglio A, Kawakami Y, Rodriguez-Esteban C, Izpisua-Belmonte JC. 2004. The zebrafish as a model of heart regeneration. Cloning Stem Cells 6:345–351.

Reimer MM, Kuscha V, Wyatt C, Sorensen I, Frank RE, Knuwer M, Becker T, Becker CG. 2009. Sonic hedgehog is a polarized signal for motor neuron regeneration in adult zebrafish. J Neurosci 29:15073–15082.

Reimer MM, Sorensen I, Kuscha V, Frank RE, Liu C, Becker CG, Becker T. 2008. Motor neuron regeneration in adult zebrafish. J Neurosci 28:8510–8516.

Rice AC, Khaldi A, Harvey HB, Salman NJ, White F, Fillmore H, Bullock MR. 2003. Proliferation and neuronal differentiation of mitotically active cells following traumatic brain injury. Exp Neurol 183:406–417.

Ridet JL, Malhotra SK, Privat A, Gage FH. 1997. Reactive astrocytes: Cellular and molecular cues to biological function. Trends Neurosci 20:570–577.

Rivers LE, Young KM, Rizzi M, Jamen F, Psachoulia K, Wade A, Kessaris N, Richardson WD. 2008. PDGFRA/NG2 glia generate myelinating oligodendrocytes and piriform projection neurons in adult mice. Nat Neurosci 11:1392–1401.

Robel S, Berninger B, Götz M. 2011. The stem cell potential of glia: Lessons from reactive gliosis. Nature Reviews Neuroscience 12:88–104.

Rothenaigner I, Krecsmarik M, Hayes JA, Bahn B, Lepier A, Fortin G, Gotz M, Jagasia R, Bally-Cuif L. 2011. Clonal analysis by distinct viral vectors identifies bona fide neural stem cells in the adult zebrafish telencephalon and characterizes their division properties and fate. Development 138:1459–1469.

Ryu S, Holzschuh J, Erhardt S, Ettl A-K, Driever W. 2005. Depletion of minichromosome maintenance protein 5 in the zebrafish retina causes cell-cycle defect and apoptosis. Proc Natl Acad Sci USA 102:18467–18472.

Shin J, Park HC, Topczewska JM, Mawdsley DJ, Appel B. 2003. Neural cell fate analysis in zebrafish using olig2 BAC transgenics. Methods Cell Sci 25:7–14.

Silver J, Miller JH. 2004. Regeneration beyond the glial scar. Nat Rev Neurosci 5:146–156.

Simon C, Dimou L, Gotz M. 2011. Progenitors in the adult cerebral cortex—cell cycle properties and regulation by physiological stimuli and injury Glia 59:869–881.

Sofroniew MV. 2009. Molecular dissection of reactive astrogliosis and glial scar formation. Trends Neurosci 32:638–647.

Stenkamp DL, Kwang WJ. 2007. Neurogenesis in the fish retina. International Review of Cytology: Academic Press. pp 173–224.

Sundholm-Peters NL, Yang HK, Goings GE, Walker AS, Szele FG. 2005. Subventricular zone neuroblasts emigrate toward cortical lesions. J Neuropathol Exp Neurol 64:1089–1000.

Takebayashi H, Nabeshima Y, Yoshida S, Chisaka O, Ikenaka K. 2002a. The basic helix-loop-helix factor olig2 is essential for the development of motoneuron and oligodendrocyte lineages. Curr Biol 12:1157–1163.

Takebayashi H, Ohtsuki T, Uchida T, Kawamoto S, Okubo K, Ikenaka K, Takeichi M, Chisaka O, Nabeshima Y. 2002b. Non-overlapping expression of Olig3 and Olig2 in the embryonic neural tube. Mech Dev 113:169–174.

Tal TL, Franzosa JA, Tanguay RL. 2009. Molecular signaling networks that choreograph epimorphic fin regeneration in zebrafish—A minireview. Gerontology 56:231–240.

Tatsumi K, Takebayashi H, Manabe T, Tanaka KF, Makinodan M, Yamauchi T, Makinodan E, Matsuyoshi H, Okuda H, Ikenaka K, Wanaka A. 2008. Genetic fate mapping of Olig2 progenitors in the injured adult cerebral cortex reveals preferential differentiation into astrocytes. J Neurosci Res 86:3494–3502.

Thored P, Arvidsson A, Cacci E, Ahlenius H, Kallur T, Darsalia V, Ekdahl CT, Kokaia Z, Lindvall O. 2006. Persistent production of neurons from adult brain stem cells during recovery after stroke. Stem Cells 24:739–747.

Thored P, Heldmann U, Gomes-Leal W, Gisler R, Darsalia V, Taneera J, Nygren JM, Jacobsen S-EW, Ekdahl CT, Kokaia Z, Lindvall O. 2009. Long-term accumulation of microglia with proneurogenic phenotype concomitant with persistent neurogenesis in adult subventricular zone after stroke. Glia 57:835–849.

Thored P, Wood J, Arvidsson A, Cammenga J, Kokaia Z, Lindvall O. 2007. Long-term neuroblast migration along blood vessels in an area with transient angiogenesis and increased vascularization after stroke. Stroke 38:3032–3039.

Vihtelic TS, Hyde DR. 2000. Light-induced rod and cone cell death and regeneration in the adult albino zebrafish (*Danio rerio*) retina. J Neurobiol 44:289–307.

Wang Y, Du D, Fang L, Yang G, Zhang C, Zeng R, Ullrich A, Lottspeich F, Chen Z. 2006. Tyrosine phosphorylated Par3 regulates epithelial tight junction assembly promoted by EGFR signaling. EMBO J 25:5058–5070.

Westerfield M. 2000. The zebrafish book. A guide for the laboratory use of zebrafish (*Danio rerio*). Eugene: University of Oregon Press:.

Widestrand Å, Faijerson J, Wilhelmsson U, Smith PLP, Li L, Sihlbom C, Eriksson PS, Pekny M. 2007. Increased neurogenesis and astrogenesis from neural progenitor cells grafted in the hippocampus of GFAP−/−Vim−/− mice. Stem Cells 25:2619–2627.

Wulliman M, Rupp B, Reichert H. 1996. Neuroanatomy of the zebrafish brain: A topological atlas. Basel: Birkhäuser Verlag. pp1–144.

Xiao Q, Du Y, Wu W, Yip HK. 2010. Bone morphogenetic proteins mediate cellular response and, together with Noggin, regulate astrocyte differentiation after spinal cord injury. Exp Neurol 221:353–366.

Zannino DA, Appel B. 2009. Olig2+ precursors produce abducens motor neurons and oligodendrocytes in the zebrafish hindbrain. J Neurosci 29:2322–2333.

Zhao J-W, Raha-Chowdhury R, Fawcett JW, Watts C. 2009. Astrocytes and oligodendrocytes can be generated from NG2+ progenitors after acute brain injury: Intracellular localization of oligodendrocyte transcription factor 2 is associated with their fate choice. Eur J Neurosci 29:1853–1869.

Zhou Q, Anderson DJ. 2002. The bHLH transcription factors OLIG2 and OLIG1 couple neuronal and glial subtype specification. Cell 109:61–73.